

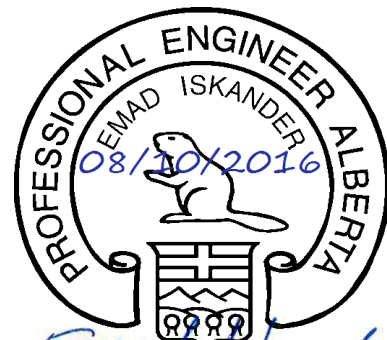


CANADIAN HYDROTECH
C O R P O R A T I O N

LONG TERM FLOOD MITIGATION MEASURES COUGAR CREEK

DESIGN REPORT

ISSUED FOR PERMITTING



Emad Iskander

APEGA PERMIT NUMBER: 13440

Prepared by: Canadian Hydrotech Corp.

Edition: June 30, 2016

Doc. No.: LTMM CC - REP - DES-01

Distribution: ToC: 1 digital copy

Canadian Hydrotech Corporation: 1 digital copy; 1 hardcopy: project file

Preparation:

MSc/EIs

April 18, 2016

Review:

MSc/JIa/AHe/DPo

June 30, 2016

Approved:

EIs

August 10, 2016

This page is intentionally left blank

Revision Log

Revision No.:	Description	Date
01	Update of the 60% Design Report for Issue for Permitting	April 18, 2016

00 DIRECTORIES

00.01 Table of Contents

00 Directories4

00.01 Table of Contents4

00.02 Figures9

00.03 Tables.....16

00.04 Acronyms and Technical Terms20

00.05 Appendices24

00.06 List of Drawings25

01 Executive Summary29

02 Limitations31

03 Introduction.....32

03.01 Project Background32

03.02 Project Area32

03.03 Location of the proposed Retention Structure33

03.04 Current Situation at the Location of the proposed Structure33

03.05 Current Situation downstream of the Location of the proposed Structure.....34

04 Design Basis36

04.01 Project and Design History36

04.02 Geology.....37

04.02.01 General Geologic and Geotechnical Setting37

04.02.02 Bedrock Geology.....37

04.02.03 Surficial Geology38

04.02.04 Geological and Geotechnical Site Conditions.....38

04.03 Seismic Site Conditions44

04.04 Climatic Site Conditions45

04.05 Frost Penetration Depth47

04.06 Hydraulic Situation at the existing Channel50

04.06.01 Durability of Existing Channel Reinforcement.....50

04.06.02 Hydraulic Limitations at Culverts.....51

04.07 Gravel Debris Volumes52

04.08 Flood Hydrology.....52

04.09 Surveys.....53

04.09.01	Bare Earth LiDAR Data, Province of Alberta	53
04.09.02	Bare Earth UAV LiDAR Data, Survey 2014, Town of Canmore.....	53
04.09.03	Channel Survey as built 2013, ISL-Engineering Ltd.....	53
04.09.04	Quality Control	53
04.10	Site Access	54
05	Design Criteria and Requirements.....	55
05.01	Selection of Dam Construction Concept	55
05.01.01	Main functional Criteria.....	55
05.01.02	Selected Construction Type.....	55
05.01.03	Investigation of alternative Concepts.....	56
05.01.04	Examples of recent Flood and Debris Retention Structures	57
05.02	Dam Performance Criteria.....	60
05.03	Geotechnical Design Criteria and Requirements	61
05.03.01	Slope Stability including Seismic Design Criteria	61
05.03.02	Design Criteria for Grading	62
05.04	Structural Design Criteria and Requirements.....	64
05.04.01	Design Codes	64
05.04.02	Materials.....	64
05.04.03	Loads and Load Factors	64
05.04.04	Reinforced Concrete Design	64
05.04.05	Structural Analysis	64
05.04.06	Environmental Conditions and Durability	65
05.05	Hydraulic Design Criteria and Requirements	65
05.06	Codes and Standards	65
06	Design Requirements	67
06.01	Design Approach.....	67
06.01.01	Hazard Mitigation and Level of Protection.....	67
06.01.02	Structure Type	67
06.01.03	Complementary Grade Control	67
06.01.04	Design Life	67
06.01.05	Dam Classification	67
06.02	Design Assumptions and Loadings	69
06.02.01	Geotechnical Design Parameters	69

06.02.02	Loadings.....	72
06.03	Site Requirements	74
06.04	Operating Requirements and Maintenance.....	74
06.05	Public Safety	74
06.06	Regulatory Compliance.....	74
07	Preliminary Risk Assessment	76
08	Facility Description	77
08.01	General Dam Construction Concept.....	77
08.02	Brief Description of Elements.....	77
09	Hydrotechnical Design.....	79
09.01	Flood Hydrology.....	79
09.02	Storage Capacity and Throttle Setting.....	80
09.03	Bottom Outlet Structure, Throttle and Ventilation.....	89
09.04	Overflow Section, Spillway	89
09.05	Stilling Basin.....	90
09.06	Scaled Physical Modelling of Inflow Structure and Gravel Rake	91
10	Geotechnical Design	92
10.01	Detailed Construction Concept	92
10.02	Seepage	93
10.02.01	Seepage Calculations.....	93
10.02.02	Seepage Control Measures.....	93
10.03	Grading Design of Filters	94
10.03.01	General	94
10.03.02	Design Criteria for Grading.....	95
10.03.03	Preliminary Grading Bands.....	95
10.03.04	Permeability Estimates.....	100
10.04	Dam Stability.....	102
10.04.01	Software Description	102
10.04.02	Theory and Numerical Approaches for Seepage Calculations	102
10.04.03	Applied Failure Models.....	105
10.04.04	Geotechnical Design Parameters	108
10.04.05	Results of Dam Stability Analysis.....	108
10.05	Dam Deformation, Forces and Moments acting on the Cut-Off Wall.....	156

10.05.01	Abstraction of the Structure for FEA	156
10.05.02	Deformation Analysis	157
10.05.03	Acting Forces and Moments on the Cut-Off Wall	167
11	Structural Design	176
11.01	Bottom Outlet Structure.....	176
11.01.01	External loading for Load Case G – Spillway Flood.....	177
11.01.02	Internal Forces from structural 2D Analysis	180
11.01.03	Internal Forces by 1D Model	185
11.01.04	Acting Forces and Moments.....	186
11.01.05	Structural Design of Critical Sections.....	186
11.02	Cut-Off Wall	188
11.02.01	Secant Pile Wall	188
11.03	Lining of the Downstream Slope	189
11.04	Spillway Training Walls	189
11.05	Intake Box.....	190
11.05.01	Loads, Acting Forces and Moments.....	190
11.05.02	Design of Critical Sections	196
12	Dam Instrumentation and Data Transmission.....	197
12.01	Site Command Post (SCP)	197
12.02	Permanent Survey Points for Tachymeter Survey.....	197
12.03	Inclinometer Gauges.....	197
12.04	Piezometers inside the Dam Structure.....	197
12.05	Piezometer for Detection of Height of Impoundment.....	197
12.06	Flow Height Gauge at the Outlet Structure.....	197
12.07	Discharge Monitoring at all Drainage Pipes	197
12.08	Web Camera	197
13	Access Ramp	198
14	Operation and Service Facilities	199
15	Investigation of Freezing	200
15.01	Purpose of Investigation of Freezing	200
15.02	Methodology	200
15.03	Basic Data	202
15.04	Calculation Results.....	204

15.04.01	Mean Annual Air Temperature of 3.374°C.....	205
15.04.02	Sequence of Mean Weekly Air Temperatures varying according to Records in Winter 2016	205
15.04.03	Air Temperatures at -40°C for seven Days followed by mean annual air Temperature	209
16	Construction	217
16.01	Preliminary and rough Construction Staging Concept	217
16.02	Description of Grout Works and Deep Foundation Works	217
16.02.01	Deep Foundation	217
16.02.02	Rock Grouting	219
16.03	Description of Earthworks	221
16.03.01	Footprint.....	221
16.03.02	Embankment Fill.....	222
16.03.03	Construction Equipment.....	222
16.03.04	Quality Control	222
17	Testing and Commissioning.....	224
18	Creek Slope Stability Assessment	225
18.01	General	225
18.01.01	Purpose of the Analysis	225
18.01.02	Summary.....	226
18.02	Geomorphic Phenomena.....	227
18.03	Kinematic Analysis	227
18.03.01	Methodology	227
18.03.02	Results and Assessment	228
18.04	Sliding Wedge Analysis	229
18.04.01	Methodology	229
18.04.02	Results	230
19	References	235

00.02 Figures

Figure 1: Location of the Cougar Creek Watershed. The outline represents the extension of the watershed (basemap source: ESRI, unspecified scale).....	32
Figure 2: Debris-Net at the intended location of the debris-flood retention structure as part of short-term mitigation measures (CHT 2015).....	33
Figure 3: Cougar Creek directly upstream of the proposed structure; viewing upstream (CHT 2015).....	34
Figure 4: Cougar Creek approximately 1.5km upstream of the proposed structure; viewing upstream (CHT 2015).....	34
Figure 5: Kame-Terrace forming the right bank of No Man’s Land.....	35
Figure 6: Reinforced downstream channel	35
Figure 7: Downstream channel and culvert of Bow Valley Trail with houses next to Cougar Creek channel	35
Figure 8: Geological Cross Sections according to GSCmap Nr. 1265a (1970) – Sections, showing the general tectonic and stratigraphic setting.....	37
Figure 9: Geological cross section (Thurber Engineering Ltd., 2015b).....	39
Figure 10: Rock outcrop at the left abutment (Photo: ALPINFRA 2014).....	39
Figure 11: Rock outcrop at the right abutment (Photo: ALPINFRA 2014).....	40
Figure 12: Geological Map from Thurber Engineering (2015b).....	41
Figure 13: Length section along the creek axis (Thurber Engineering Ltd., 2015b)	43
Figure 14: Climate diagram for the Kananaskis climate station at 1,391.1 MASL. Mean monthly values from 1940 to 2013.....	46
Figure 15: Kananaskis climate station, Snow on Ground frequency analysis - Gumbel distribution.....	46
Figure 16: Thermal conductivity of frozen coarse-grained soil (Kersten, 1949)	48
Figure 17: mean (normal) freezing Index map of Canada (Dow Chemical Canada ULC, 2008)	49
Figure 18: Lambda (λ) coefficient for the modified Breggen equation (Sanger & Sayles, 1978)	49
Figure 19: Frost penetration for different soils (Dow Chemical Canada ULC, 2008)	50
Figure 20: Design of the channel reinforcement (ISL Engineering Ltd., 2013).....	51
Figure 21: Access to the construction site by paved and unpaved roads	54
Figure 22: Dam construction concept of the Sösetalsperre (Campen, 2002)	56
Figure 23: Non-linear shear function based on reduced shear data from Lafarge material below 64mm	70
Figure 24: Non-linear shear function based on reduced shear data from Stoneworks Creek material	71
Figure 25: Non-linear shear function based on reduced shear data from Stewart Creek material.....	71
Figure 26: IDF-hydrographs for precipitation scenarios with a return period of 100 years	80
Figure 27: IDF-hydrographs for precipitation scenarios with a return period of 300 years	80
Figure 28: IDF-hydrographs for precipitation scenarios with a return period of 1,000 years	80
Figure 29: Storage curve at the selected location for retention structure	82

Figure 30: Discharge curve for the planned retention structure height82

Figure 31: Inflow and outflow hydrographs for a 100 year return period related scenario with 2 hours of rainfall duration85

Figure 32: Inflow and outflow hydrographs for a 100 year return period related scenario with 9 hours of rainfall duration86

Figure 33: Inflow and outflow hydrographs for a 300 year return period related scenario with 4 hours of rainfall duration87

Figure 34: Inflow and outflow hydrographs for the back calculated June 2013 storm event88

Figure 35: Dam construction concept according to drawing LTMM-CC-DAM-50392

Figure 36: Cut-off measures and grout curtain according to drawing LTMM-CC-DAM-50593

Figure 37: Design Grading Band, Dam Zone 1 – Outer Support Body; the red line indicates the upper limit, the blue one the lower limit.95

Figure 38: Design Grading Band, Dam Zone 2 – Inner Support Body; the red line indicates the upper limit, the blue one the lower limit.96

Figure 39: Design Grading Band, Dam Zone 3 – Deceleration Zone; the red line indicates the upper limit, the blue one the lower limit.97

Figure 40: Design Grading Band, Dam Zone 6; the red line indicates the upper limit, the blue one the lower limit.97

Figure 41: Design Grading Band, Dam Zone 7 – Drainage Prism and Drainage Layer; the red line indicates the upper limit, the blue one the lower limit.98

Figure 42: Preliminary Design Grading Band, Transition Layer A; the red line indicates the upper limit, the blue one the lower limit.99

Figure 43: Preliminary Design Grading Band, Transition Layer B; the red line indicates the upper limit, the blue one the lower limit.100

Figure 44: Slide 7.0 steady state FEA seepage calculation, triangular elements, LC-E103

Figure 45: Slide 7.0 steady state boundary conditions, LC-E103

Figure 46: Slide 7.0, Rapid drawdown boundary conditions, B-Bar method104

Figure 47: WinTube steady state FEA seepage calculation, quadrilateral elements, piezometric head boundary conditions105

Figure 48: Static scheme - Spencer Method105

Figure 49: Groundwater, STL-A111

Figure 50: Seepage calculation for ground water flow only, potentials [m] and free surface, WinTube, STL-A 111

Figure 51: LC-A, circular surface, GLE, FoS = 1.68112

Figure 52: LC-A, circular surface, GLE, FoS ≥ 1.88112

Figure 53: LC-A circular surface with at least 6 m depth, GLE, FoS = 2.12113

Figure 54: LC-A, non-circular surface, GLE, FoS = 1.64113

Figure 55: LC-A, non-circular surface, GLE, FoS ≥ 1.88 114
Figure 56: LC-A, non-circular surface with at least 5 m depth, GLE, FoS = 2.00.....114
Figure 57: LC-A, phi-c reduction, nodal displacement vector [mm], FoS = 1.62115
Figure 58: LC-A-1, 0.5*PGA, 5,000yr return period, $e_v = + 2/3 e_{h_r}$, circular surface, GLE, FoS = 1.38116
Figure 59: LC-A-1, 0.5*PGA, 5,000yr return period, $e_v = - 2/3 e_{h_r}$, circular surface, GLE, FoS = 1.38117
Figure 60: LC-A-1, 0.5*PGA, 5,000yr return period, $e_v = + 2/3 e_{h_r}$, circular surface, GLE, FoS ≥ 1.55 117
Figure 61: LC-A-1, 0.5*PGA, 5,000 yr return period, $e_v = - 2/3 e_{h_r}$, circular surface, GLE, FoS ≥ 1.51 117
Figure 62: LC-A-1, 0.5*PGA, 5,000 yr return period, $e_v = + 2/3 e_{h_r}$, circular surface with at least 5 m depth, GLE, FoS ≥ 1.72 118
Figure 63: LC-A-1, 0.5*PGA, 5,000 yr return period, $e_v = - 2/3 e_{h_r}$, circular surface with at least 5 m depth, GLE, FoS ≥ 1.70 118
Figure 64: LC-A-1, 0.5*PGA, 5,000 yr return period, $e_v = + 2/3 e_{h_r}$, non-circular surface, GLE, FoS = 1.36.....119
Figure 65: LC-A-1, 0.5*PGA, 5,000 yr return period, $e_v = - 2/3 e_{h_r}$, non-circular surface, GLE, FoS = 1.35.....119
Figure 66: LC-A-1, 0.5*PGA, 5,000 yr return period, $e_v = + 2/3 e_{h_r}$, non-circular surface, GLE, FoS ≥ 1.58120
Figure 67: LC-A-1, 0.5*PGA, 5,000 yr return period, $e_v = - 2/3 e_{h_r}$, non-circular surface, GLE, FoS ≥ 1.54120
Figure 68: LC-A-1, 0.5*PGA, 5,000 yr return period, $e_v = + 2/3 e_{h_r}$, non-circular surface with at least 5 m depth, GLE, FoS = 1.62121
Figure 69: LC-A-1, 0.5*PGA, 5,000 yr return period, $e_v = - 2/3 e_{h_r}$, non-circular surface with at least 5 m depth, GLE, FoS = 1.61121
Figure 70: Impoundment level at approximately 1/3 dam height STL-B,122
Figure 71: LC-B, circular surface, GLE, FoS = 1.67122
Figure 72: LC-B, circular surface, GLE, FoS ≥ 1.88123
Figure 73: LC-B, circular surface with at least 4 m depth, GLE, FoS = 2.05123
Figure 74: LC-B, non-circular surface, GLE, FoS = 1.63124
Figure 75: LC-B, non-circular surface, GLE, FoS ≥ 1.88 124
Figure 76: LC-B, non-circular surface with at least 4 m depth, GLE, FoS = 2.01125
Figure 77: impoundment level at approximately 1/2 dam height, STL-C.....125
Figure 78: LC-C, circular surface, GLE, FoS = 1.67126
Figure 79: LC-C, circular surface, GLE, FoS ≥ 1.88126
Figure 80: LC-C circular surface with at least 3 m depth, GLE, FoS = 2.10127
Figure 81: LC-C, non-circular surface, GLE, FoS = 1.62127
Figure 82: LC-C, non-circular surface, GLE, FoS ≥ 1.88 128
Figure 83: LC-C, non-circular surface with at least 4 m depth, GLE, FoS = 2.06128
Figure 84: impoundment level at approximately 2/3 dam height, STL-D129

Figure 85: LC-D, circular surface, GLE, FoS = 1.66129

Figure 86: LC-D, circular surface, GLE, FoS ≥ 1.88130

Figure 87: LC-D circular surface with at least 6 m depth, GLE, FoS = 2.21130

Figure 88: LC-D, non-circular surface, GLE, FoS = 1.61131

Figure 89: LC-D, non-circular surface, GLE, FoS ≥ 1.87131

Figure 90: LC-D non-circular surface with at least 6 m depth, GLE, FoS = 2.14.....132

Figure 91: full impoundment, Slide 7.0, STL-E.....132

Figure 92: Seepage calculation for full impoundment, potentials [m] and free surface, WinTube, LC-E133

Figure 93: LC-E, circular surface, GLE, FoS = 1.65133

Figure 94: LC-E, circular surface, GLE, FoS ≥ 1.88134

Figure 95: LC-E, circular surface with at least 8 m depth, GLE, FoS = 2.44.....134

Figure 96: LC-E, non-circular surface, GLE, FoS = 1.60135

Figure 97: LC-E, non-circular surface, GLE, FoS ≥ 1.96135

Figure 98: LC-E, non-circular surface with at least 8 m depth, GLE, FoS = 2.41136

Figure 99: LC-E, phi-c reduction, nodal displacement vector [mm], FoS = 1.61136

Figure 100: Overtopping, STL-F137

Figure 101: LC-F, circular surface, GLE, FoS = 1.63137

Figure 102: LC-F, circular surface, GLE, FoS ≥ 1.89138

Figure 103: LC-F, circular surface with at least 5 m depth, GLE, FoS = 2.53.....138

Figure 104: LC-F, non-circular surface, GLE, FoS = 1.58.....139

Figure 105: LC-F, non-circular surface, GLE, FoS ≥ 1.93.....139

Figure 106: LC-F, non-circular surface with at least 8 m depth, GLE, FoS = 2.39140

Figure 107: Seepage, Slide 7.0, STL-G.....141

Figure 108: seepage, rapid drawdown after 10 days full impoundment, WinTube, LC-G141

Figure 109: LC-G, B-Bar = 1.0 for Zone 3, circular surface with at least 5 m depth, GLE, FoS = 2.08142

Figure 110: LC-G, B-Bar = 1.0 for Zone 2 and 3, circular surface with at least 5 m depth, GLE, FoS = 1.60142

Figure 111: LC-G, B-Bar = 1.0 for Zone 2, 3 and the Cougar Creek Alluvium, circular surface with at least 5 m depth, GLE, FoS = 1.37143

Figure 112: LC-G, B-Bar = 1.0 for Zone 3, non-circular surface with at least 5 m depth, GLE, FoS = 1.95143

Figure 113: LC-G, B-Bar = 1.0 for Zone 2 and 3, non-circular surface with at least 5 m depth, GLE, FoS = 1.55.144

Figure 114: LC-G, B-Bar = 1.0 for Zone 2, 3 and the Cougar Creek Alluvium, non-circular surface with at least 5 m depth, GLE, FoS = 1.34.....144

Figure 115: LC-G, phi-c reduction, rapid drawdown after 10 days full impoundment, nodal displacement vector [mm], FoS = 1.57.....145

Figure 116: critical seismic coefficient, empty retention structure, circular surface, GLE, $k_h = 0.286$146

Figure 117: critical seismic coefficient, empty retention structure, circular surface, GLE, $FoS = 1.00$ 146

Figure 118: critical seismic coefficient, empty retention structure, circular surface, GLE, $k_h = 0.312$147

Figure 119: critical seismic coefficient, empty retention structure, circular surface with at least 5.0 m depth, GLE, $k_h = 0.402$ 147

Figure 120: critical seismic coefficient, empty retention structure, circular surface with at least 5.0 m depth, GLE, $FoS = 1.00$ 148

Figure 121: critical seismic coefficient, empty retention structure, non-circular surface, GLE, $k_h = 0.275$ 148

Figure 122: critical seismic coefficient, empty retention structure, non-circular surface, GLE, $k_h = 0.312$ 149

Figure 123: critical seismic coefficient, empty retention structure, non-circular surface with at least 6.0 m depth, GLE, $k_h = 0.372$ 149

Figure 124; critical seismic coefficient, empty retention structure, non-circular surface with at least 6.0 m depth, GLE, $FoS = 1.00$150

Figure 125: critical seismic coefficient, empty retention structure, circular surface, GLE, $k_h = 0.266$151

Figure 126: critical seismic coefficient, empty retention structure, circular surface, GLE, $FoS = 1.00$ 151

Figure 127: critical seismic coefficient, empty retention structure, circular surface, GLE, $k_h = 0.188$152

Figure 128: critical seismic coefficient, empty retention structure, circular surface with at least 6.0 m depth, GLE, $k_h = 0.280$152

Figure 129: critical seismic coefficient, empty retention structure, circular surface with at least 6.0 m depth, GLE, $FoS = 1.00$ 153

Figure 130: critical seismic coefficient, empty retention structure, non-circular surface, GLE, $k_h = 0.257$ 153

Figure 131: critical seismic coefficient, empty retention structure, non-circular surface, GLE, $k_h = 0.203$ 154

Figure 132: critical seismic coefficient, empty retention structure, non-circular surface with at least 6.0 m depth, GLE, $k_h = 0.283$ 154

Figure 133; critical seismic coefficient, empty retention structure, non-circular surface with at least 6.0 m depth, GLE, $FoS = 1.01$155

Figure 134: Dam Zones and Material156

Figure 135: considered construction stages in WinTube157

Figure 136: LC-A, dam deformation, nodal displacement u [mm] for $1/3$ of ϕ for wall-soil interaction.....158

Figure 137: LC-A, horizontal nodal displacement u_x [mm] for $1/3$ of ϕ for wall-soil interaction.....159

Figure 138: LC-A, vertical nodal displacement u_y [mm] for $1/3$ of ϕ for wall-soil interaction159

Figure 139: LC-E, dam deformation, nodal displacement u [mm] for $1/3$ of ϕ for wall-soil interaction160

Figure 140: LC-E, horizontal nodal displacement u_x [mm] for $1/3$ of ϕ for wall-soil interaction.....160

Figure 141: LC-E, vertical nodal displacement u_y [mm] for $1/3$ of ϕ for wall-soil interaction.....161

Figure 142: LC-H, dam deformation, nodal displacement u [mm] for $1/3$ of ϕ for wall-soil interaction.....161

Figure 143: LC-H horizontal nodal displacement u_x [mm] for 1/3 of ϕ for wall-soil interaction.....162

Figure 144: LC-H, vertical nodal displacement u_y [mm] for 1/3 of ϕ for wall-soil interaction162

Figure 145: Vertical displacements [mm] of the BOS with jet-grouted columns with an E-Modulus of 1GPa, arranged as in the base design.166

Figure 146: Vertical displacements [mm] of the BOS with jet-grouted columns with E=1GPa, sparing 4 columns at the intake and outlet.....167

Figure 147: Simplification of the cross section of the bottom outlet structure for structural analyses.....176

Figure 148: Phase2 model to calculate lateral earth pressure on walls.....178

Figure 149: Horizontal stress S_{xx} [kPa] and stress trajectories showing arching in the embankment around the bottom outlet179

Figure 150: Vertical stress S_{yy} [kPa] and stress trajectories showing arching in the embankment around the bottom outlet180

Figure 151: External pressures on the bottom outlet structure181

Figure 152: Abaqus model and in-plane shear stresses for $K_o = 1.0$ 182

Figure 153: Deformed shape and distribution of displacements u_1 & u_2 for $K_o = 1.0$ [m]183

Figure 154: Normal stresses S_{11} & S_{22} for $K_o = 1.0$ [kPa]184

Figure 155: Critical sections for reinforced concrete design of the BOS.....184

Figure 156: Stress distribution from the 2D model on the BOS base slab and deck slab sections184

Figure 157: Stress distribution from the 2D model on the BOS sidewall sections.....184

Figure 158: Internal forces and moments from the frame model185

Figure 159: Construction scheme of the secant pile wall and adjacent support piles for the BOS (see Drawing LTMM CC-DFG-404 R00).....188

Figure 160: Detail of downstream lining and spillway-training walls (section is normal to the slope - see Drawing LTMM CC-DAM-506)190

Figure 161: Cross section of the intake box191

Figure 162: Longitudinal section of the intake box192

Figure 163: Shell model of the northern half, utilizing symmetry192

Figure 164: Finite element mesh.....193

Figure 165: Deformed shape and contour lines of u_1 displacement in longitudinal direction [m]193

Figure 166: Deformed shape and contour lines of u_2 displacement in transverse direction [m]194

Figure 167: Membrane force SF_2 in transverse direction [kN/m]194

Figure 168: Transverse bending moment SM_2 [kN.m/m].....195

Figure 169: Longitudinal bending moment SM_1 [kN.m/m]195

Figure 170: Idealized variation of soil temperature with time for various depths (Hillel, 1982)201

Figure 171: Example of a soil temperature profile as it varies from season to season (Hillel, 1982)201

Figure 172: Recorded air temperature and water temperature at the well TP14-3 at Cougar Creek202

Figure 173: Example of mean weekly air and water temperature during winter, based on the temperature log at Cougar Creek (see Figure 172)202

Figure 174: Extreme minimum temperature zones of parts of Central and Western Canada (NRC, 2014)203

Figure 175: stationary temperature analysis in °C, mean annual air temperature 3.374 °C205

Figure 176: transient temperature analysis in °C mean weekly temperature -10.9 ° C.....205

Figure 177: transient temperature analysis in °C mean weekly temperature -8.70 ° C.....206

Figure 178: transient temperature analysis in °C mean weekly temperature 0.10 ° C.....206

Figure 179: transient temperature analysis in °C mean weekly temperature -5.00 ° C.....207

Figure 180: transient temperature analysis in °C mean weekly temperature 0.50 ° C.....207

Figure 181: transient temperature analysis in °C mean weekly temperature -1.20 ° C.....208

Figure 182: transient temperature analysis in °C mean weekly temperature -0.10 ° C.....208

Figure 183: transient temperature analysis in °C, extreme minimum -40.0 ° C for 7 days.....209

Figure 184: transient temperature analysis in °C, 14 days after extreme minimum, 3.375 ° C.....209

Figure 185: transient temperature analysis in °C, 28 days after extreme minimum, 3.375 ° C.....210

Figure 186: stationary temperature analysis in °C, mean annual air temperature 3.374 °C210

Figure 187: transient temperature analysis in °C mean weekly temperature -10.9 ° C.....211

Figure 188: transient temperature analysis in °C mean weekly temperature -8.70 ° C.....211

Figure 189: transient temperature analysis in °C mean weekly temperature -6.30 ° C.....212

Figure 190: transient temperature analysis in °C mean weekly temperature 0.10 ° C.....212

Figure 191: transient temperature analysis in °C mean weekly temperature -5.00 ° C.....213

Figure 192: transient temperature analysis in °C mean weekly temperature 0.50 ° C.....213

Figure 193: transient temperature analysis in °C mean weekly temperature 1.30 ° C.....214

Figure 194: transient temperature analysis in °C mean weekly temperature -1.20 ° C.....214

Figure 195: transient temperature analysis in °C mean weekly temperature -0.10° C.....215

Figure 196: transient temperature analysis in °C, extreme minimum -40.0 ° C, 7 days215

Figure 197: transient temperature analysis in °C, 14 days after extreme minimum, 3.375 ° C.....216

Figure 198: transient temperature analysis in °C, 28 days after extreme minimum, 3.375 ° C.....216

Figure 199: Slope gradient map with selected sectors for the kinematic and sliding wedge analysis, according to drawing LTMM CC-CSSA-110 R01226

Figure 200: Example of the stereo plot with the critical zone for planar sliding (red).....228

Figure 201: Example of the stereo plot with the primary (red) and secondary (yellow) critical zones for wedge sliding.....228

Figure 202: Typical wedge geometry for the Sliding Wedge analysis (Rocscience Inc., 2016)229

00.03 Tables

Table 1: List of available Documents as Design Basis.....	36
Table 2: Statistical summary of bedding planes and joint Sets recorded by (Thurber Engineering Ltd., 2015a) .40	
Table 3: Ground water levels according to table 7 – report on the Phase 2A geotechnical investigation (Thurber Engineering Ltd., 2015a).....	42
Table 4: Summary of Aquifer Parameter Estimates (Waterline Resources Inc, 2015).....	42
Table 5: Overview of the Kananaskis Climate Station	45
Table 6: thermal parameters based on Canadian climate normal station Kananaskis	48
Table 7: Cougar Creek Soil Parameter	48
Table 8: Resulting parameters from the frost penetration depth calculation	50
Table 9: Scenarios supplied by BGC Engineering.....	52
Table 10: Specifications of NAD 83 (CSRS) / UTM Zone 11N.....	53
Table 11: Specifications of NAD 83 / Alberta 3TM 114W.....	53
Table 12: Suggested Design Earthquake Levels according to CDA Guidelines Table 1 (CDA, 2007)	60
Table 13: Factors of Safety for Slope Stability	61
Table 14: Factors of Safety for Slope Stability	61
Table 15: Factors of Safety for Slope Stability	61
Table 16: Accepted Factors of Safety for Slope Stability for BC.....	62
Table 17: Filter Criteria according to Terzaghi (1922)	62
Table 18: Criteria for Base soil categories according to the U.S. Army Corps of Engineers (2004) based on Sherard & Dunnigan (1985)	62
Table 19: Gradation limits for prevention of segregation for coarse filters according to the U.S. Army Corps of Engineers (2004).....	63
Table 20: Resulting and relevant filter criteria for dam zones and on site material.....	63
Table 21: Relevant and applicable design codes and guidelines.....	65
Table 22: Dam Classification according to Table 2-1 CDA Dam Safety Guidelines (2007)	68
Table 23: Characteristic design values for material parameters – part 1	69
Table 24: Characteristic design values for material parameters - part 2	69
Table 25: Normal operating impoundment levels (STL and SL)	73
Table 26: Unusual impoundment levels and ground movement (STL and SL).....	73
Table 27: Seismic Load Cases (SL) for the stability analysis.....	74
Table 28: Load Case Combinations (LC).....	74
Table 29: Peak discharges for rainfall durations ranging from 2 hours to 12 hours and return periods of 100 years, 300 years and 1,000 years	79

Table 30: Characteristic storage and discharge data of the retention structure83

Table 31: Height and volume of impoundment, outflow and spillway utilization for 100-yr return period IDF’s84

Table 32: Height and volume of impoundment, outflow and spillway utilization for 300-yr return period IDF’s84

Table 33: Height and volume of impoundment, outflow and spillway utilization for 1,000-yr return period IDF’s84

Table 34: Height and volume of impoundment, outflow and spillway utilization for the back calculated June 2013 event84

Table 35: Height and volume of impoundment, outflow and spillway utilization for worst case LDOF scenarios84

Table 36: Summary of estimated PMF peak flows according to Appendix J – Hydrological Assessment.....90

Table 37: Results and Parameters from dimensioning of the stilling basin90

Table 38: Dam fill zones, alluvial deposits and their interfaces95

Table 39: Preliminary Design Grading Band, Outer Support Body – Dam Zone 1.....95

Table 40: Preliminary Design Grading Band, Inner Support Body - Dam Zone 296

Table 41: Preliminary Design Grading Band, Deceleration Zone - Zone 3.....97

Table 42: Preliminary Design Grading Band, Protection Layer, Zone 6.....98

Table 43: Preliminary Design Grading Band, Drainage Layer, Zone 798

Table 44: Summary of fulfilled filter criteria and required transition layers.....99

Table 45: Preliminary Design Grading Band, Transition Layer A99

Table 46: Preliminary Design Grading Band, Transition Layer B100

Table 47: Methods to estimate hydraulic conductivity.....101

Table 48: Estimated permeability for the different dam zones101

Table 49: Summary of minimum Factors of Safety of the slope stability analysis109

Table 50: critical seismic coefficient k_h for LC-A and its estimated return period109

Table 51: critical seismic coefficient k_h for LC-E and its estimated return period.....110

Table 52: Seismic hazard values according to the NBCC Site Class B and C110

Table 53: LC-A, Factor of Safety, Method: GLE/Morgenstern - Price110

Table 54: LC-A-1, $e_v = + 2/3 e_h$, Factor of Safety, Method: GLE/Morgenstern - Price115

Table 55: LC-A-1, $e_v = - 2/3 e_h$, Factor of Safety, Method: GLE/Morgenstern - Price115

Table 56: LC-B, Factor of Safety, Method: GLE/Morgenstern - Price122

Table 57: LC-C, Factor of Safety, Method: GLE/Morgenstern - Price125

Table 58: LC-D, Factor of Safety, Method: GLE/Morgenstern - Price.....129

Table 59: LC-E, Factor of Safety, Method: GLE/Morgenstern - Price132

Table 60: LC-F, Factor of Safety, Method: GLE/Morgenstern - Price137

Table 61: LC-G, Factor of Safety, Method: GLE/Morgenstern – Price and B-Bar140

Table 62: critical seismic coefficient, empty retention structure.....145

Table 63: critical seismic coefficient, full impoundment.....150

Table 64: nodal displacement, $\delta = 1/3 * \varphi$ 157

Table 65: nodal displacement, $\delta = 2/3 * \varphi$ 158

Table 66: horizontal nodal displacement u_x [mm], groundwater, LC-A.....163

Table 67: horizontal nodal displacement u_x [mm], full impoundment, LC-E.....164

Table 68: horizontal nodal displacement u_x [mm], drawdown following full impoundment, LC-H165

Table 69: Vertical displacements at the BOS and the seal wall versus quality of ground improvement at full impoundment.....166

Table 70: Normal forces at the seal wall and pile wall, N_x [kN], groundwater, LC-A167

Table 71: Normal forces at the seal wall and pile wall, N_x [kN], full impoundment, LC-E.....168

Table 72: Normal forces at the seal wall and pile wall, N_x [kN], , drawdown following full impoundment, LC-H169

Table 73: Shear forces at the seal wall and pile wall, V_z [kN], groundwater, LC-A170

Table 74: Shear forces at the seal wall and pile wall, V_z [kN], full impoundment, LC-E171

Table 75: Shear forces at the seal wall and the pile wall, V_z [kN], drawdown following full impoundment, LC-H172

Table 76: Bending moments at the seal wall and pile wall, M_y [kNm], groundwater, LC-A.....173

Table 77: Bending moments at the seal wall and pile wall, M_y [kNm], full impoundment, LC-E.....174

Table 78: Bending moments at the seal wall and the pile wall, M_y [kNm], drawdown following full impoundment, LC-H175

Table 79: Acting forces and moments on the bottom outlet structure186

Table 80: Parameter used for the thermal analysis, (Hillel, 1982)204

Table 81: Frost penetration depth, Frost lenses [m], groundwater no impoundment.....204

Table 82: Frost penetration depth, Frost lenses [m], 2m impoundment, ice204

Table 83: Overview of chapters and drawings for the Creek Slope Stability Assessment225

Table 84: Results from the Kinematic Analysis for Planar and Wedge Sliding (No. of Entries: 642).....228

Table 85: Input Data for Sliding Wedge Analysis.....230

Table 86: Sliding Wedge Analysis and resulting Factor of Safety for Sector 1230

Table 87: Sliding Wedge Analysis and resulting Factor of Safety for Sector 2231

Table 88: Sliding Wedge Analysis and resulting Factor of Safety for Sector 3231

Table 89: Sliding Wedge Analysis and resulting Factor of Safety for Sector 4231

Table 90: Sliding Wedge Analysis and resulting Factor of Safety for Sector 5232

Table 91: Sliding Wedge Analysis and resulting Factor of Safety for Sector 6232

Table 92: Sliding Wedge Analysis and resulting Factor of Safety for Sector 7233

Table 93: Sliding Wedge Analysis and resulting Factor of Safety for Sector 8233

Table 94: Sliding Wedge Analysis and resulting Factor of Safety for Sector 9234

00.04 Acronyms and Technical Terms

Acronym/Variable	Unit	Description
μ	m ² /s	dynamic viscosity
a	m	width of the throttle
A	m ²	cross-sectional area
ABBC	-	Alberta Building Code
AEP	1/years	annual exceedance probability
API	-	American Petroleum Institute
ASTM	-	American Society for Testing and Materials
b	m	height of the throttle
β	-	thermal ratio parameter
c	kN/m ²	cohesion
C	-	sorting coefficient
C _i	kJ/m ³ °C	specific heat of ice
c _p	Ws/K kg	specific thermal capacity
C _s	kJ/m ³ °C	specific heat of dry soil
C _u	-	number of unconformity
C _v	kJ/m ³ °C	volumetric heat capacity of the soil
CSA	-	Canadian Standards Association
CDA	-	Canadian Dam Association
CGS	-	Canadian Geotechnical Society
δ	°	structure – soil friction angle
D ₁₀	mm	diameter of particles of 10 percent cumulative weight passed
D _{10F}	mm	diameter of particles of 10 percent cumulative weight passed (filter)
d _{15B}	mm	diameter of particles of 15 percent cumulative weight passed (drained material)
D _{15F}	mm	diameter of particles of 15 percent cumulative weight passed (filter)
D ₆₀	mm	diameter of particles of 60 percent cumulative weight passed
d _{85B}	mm	diameter of particles of 85 percent cumulative weight passed (drained material)
D _{90F}	mm	diameter of particles of 90 percent cumulative weight passed (filter)
d _e	mm	effective grain diameter
DTM	-	digital terrain model
E	m	energy head
ε	-	targeted degree of impoundment
E _{50,ref}	MN/m ²	secant modulus at a certain reference pressure
EGDM	-	earthquake design ground motion
e _h	-	horizontal seismic load coefficient (=k _h)
E _i , E _{i+1}	kN	forces exerted by neighboring blocks; inclined from a horizontal plane by angle δ
E _{s,ref}	MN/m ²	stiffness modulus at a certain reference pressure
E _{u-r,ref}	MN/m ²	unloading-reloading modulus at a certain reference pressure
e _v	-	vertical seismic coefficient (=k _v)

Acronym/Variable	Unit	Description
f(n)	-	porosity function
f _c	MPa	compressive strength
F _{ef}	kN	effective external load vector
F _i (u)	kN	internal reaction forces as functions of the displacement u
F _i (σ _{plc})	kN	internal reaction forces resulting from the primary stress state
FEMA	-	Federal Emergency Management Agency, US Department of Homeland Security
FoS	-	factor of safety
Fr	-	Froude-number
F _{x_i} , F _{y_i}	kN	horizontal and vertical forces
f _y	MPa	yield stress
g	m/s ²	gravitational acceleration
gradT	K/m	temperature gradient
H	m	resulting flow-height
h ₀	m	height of the relating water level
h ₁	m	depth of inflow water jet
h ₂	m	conjugated water depth
h _c	m	flow height
h _s	m	height of counter sill (selected)
h _u	m	targeted depth of tailing-water
h _{u-min}	m	minimum depth of tail-water
I	%	inclination of the spillway
I _d	°C days	design freezing index
I _m	°C days	mean (normal) freezing index
I _s	°C-days	surface freezing index
IDF	m ³ /s	inflow design flood
ISRM	-	International Society for Rock Mechanics
K	m/s	hydraulic conductivity
k _f	W/mK	thermal conductivity of the freezing soil
k _h	-	horizontal seismic coefficient
K _O	kN/m ²	earth pressure at-rest
k _{st}	m ^{1/3} /s	coefficient of roughness according to Strickler
Kt	W/K m	tensor of conductivity with conductivity being dependant on flow direction
k _v	-	vertical seismic coefficient
L	kJ/kg	latent heat of fusion of water to ice
λ	-	dimensionless coefficient that is a function of the temperature gradient, the volumetric latent heat of the soil and the volumetric heat capacity of the soil
LC	-	load case combination
LDOF	-	landslide dam outbreak flood
LiDAR	-	light detection and ranging
L _s	kJ/m ³	volumetric latent heat of the soil
L _T	m	length of the stilling basin

Acronym/Variable	Unit	Description
M	kN.m	moment
M_{1i}		moment of forces f_{xi} , f_{yi} , rotation about point M, which is the center of the i^{th} segment of the slip surface
MAAT	°C	mean annual air temperature
MASL	m	metres above sea level
MDE	-	maximum design earthquake
MPSP	-	multiple packer sleeved pipe
N	kN/m	force
n	-	empirical factor to determine the soil freezing index i_s from the air freezing index i_d
N_i	kN	normal forces on the slip surface
NRC	-	National Research Council Canada
NBC	-	National Building Code of Canada
OBE	-	operating basis earthquake
ONR	-	Austrian Design Code
P	-	external load vector
PGA	g	peak ground acceleration
PMF	m^3/s	probable maximum flood
PMP	mm	probable maximum precipitation
Q	m^3/s	discharge
q	W/m	power of sources or sinks
Q_{air}	m^3/s	air flux
RP	years	return period
S	J/K m^3	specific storage coefficient
SL	-	seismic load
SLS	-	serviceability limit state
STL	-	storage level load case
S_{xx} & S_{yy}	-	stress components
t	days	duration of the freezing period
T_i	kN	shear forces on the slip surface
UAV	-	unmanned aerial vehicle
U_i	Pa	pore pressure resultant on the i^{th} segment of slip surface
ULS	-	ultimate limit state
\underline{v}	W/ m^2	vector of heat fluxes
v_1	m/s	cross sectional flow velocity
v_c	m/s	flow velocity of water discharged through the throttle
w	-	gravimetric water content of the soil
W_i	N	block weight, including the influence of the coefficient of vertical earthquake k_v
X	m	depth of frost penetration
γ	kN/ m^3	unit weight
γ'	kN/ m^3	unit weight under buoyancy
γ_d	kg/ m^3	dry unit weight

Acronym/Variable	Unit	Description
ρ	kg/m ³	fluid (water) density, specific weight
ϕ	°	friction angle
Ψ	°	angle of dilatancy
β_{so}	-	air requirement coefficient
μ	-	discharge coefficient
ν	m ² /s	kinematic viscosity

00.05 Appendices and complementary Documents

Title of Document	Document No.
Geotechnical Design Basis Memorandum	LTMM CC - M - GTDB-01
Appendix D - Seismic Hazard Assessment	LTMM CC - REP - AP-D-01
Appendix E - Dam Breaching and Inundation Analysis	LTMM CC - REP - AP-E-01
Emergency Preparedness Plan	LTMM CC - REP - EPP-00
Emergency Response Plan	LTMM CC - REP - ERP-00
Operation, Maintenance and Surveillance Plan	LTMM CC - REP - OMS-00
Appendix J - Hydrological Assessment	LTMM CC - REP - AP-J-01
Appendix K - Calculation Reports of Structural and Geotechnical Analysis	LTMM CC - REP - AP-K-00

00.06 List of Drawings

Drawing No.	Type	Content	Scale
LTMM CC-GEN-001 R00	Plan View	Project Area	1:75,000
LTMM CC-GEN-002 R00	Plan View	Current Site Situation - Overview Contour Lines and Shaded Relief	1:10,000
LTMM CC-GEN-010 R00	Plan View, Longitudinal Section	Location of Proposed Structure General Overview 60% Design Stage	1:10,000
LTMM CC-GEN-011 R00	Plan View	Site Access General Overview	1:10,000
LTMM CC-GEN-020 R00	Plan View	Geomorphic Map General Overview Issued for Permitting	1:5,000
LTMM CC-GTDB-101 R00	Plan View	Location of Test Pits and Drillings Overall Investigation Campaign Construction Site Cougar Creek	1:750
LTMM CC-CSSA-110 R00	Plan View	Slope Gradient Map Construction Site Creek Slope Stability Assessment	1:2,500
LTMM CC-CSSA-111 R00	Stereo Plot	Kinematic Analysis Sector 1 Creek Slope Stability Assessment	N/A
LTMM CC-CSSA-112 R00	Stereo Plot	Kinematic Analysis Sector 2 Creek Slope Stability Assessment	N/A
LTMM CC-CSSA-113 R00	Stereo Plot	Kinematic Analysis Sector 3 Creek Slope Stability Assessment	N/A
LTMM CC-CSSA-114 R00	Stereo Plot	Kinematic Analysis Sector 4 Creek Slope Stability Assessment	N/A
LTMM CC-CSSA-115 R00	Stereo Plot	Kinematic Analysis Sector 5 Creek Slope Stability Assessment	N/A
LTMM CC-CSSA-116 R00	Stereo Plot	Kinematic Analysis Sector 6 Creek Slope Stability Assessment	N/A
LTMM CC-CSSA-117 R00	Stereo Plot	Kinematic Analysis Sector 7 Creek Slope Stability Assessment	N/A
LTMM CC-CSSA-118 R00	Stereo Plot	Kinematic Analysis Sector 8 Creek Slope Stability Assessment	N/A
LTMM CC-CSSA-119 R00	Stereo Plot	Kinematic Analysis Sector 9 Creek Slope Stability Assessment	N/A
LTMM CC-CSSA-120 R00	Stereo Plot	Wedge Stability Analysis Sector 1 Creek Slope Stability Assessment	N/A
LTMM CC-CSSA-121 R00	Stereo Plot	Wedge Stability Analysis Sector 2 Creek Slope Stability Assessment	N/A
LTMM CC-CSSA-122 R00	Stereo Plot	Wedge Stability Analysis Sector 3 Creek Slope Stability Assessment	N/A
LTMM CC-CSSA-123 R00	Stereo Plot	Wedge Stability Analysis Sector 4 Creek Slope Stability Assessment	N/A

Drawing No.	Type	Content	Scale
LTMM CC-CSSA-124 R00	Stereo Plot	Wedge Stability Analysis Sector 5 Creek Slope Stability Assessment	N/A
LTMM CC-CSSA-125 R00	Stereo Plot	Wedge Stability Analysis Sector 6 Creek Slope Stability Assessment	N/A
LTMM CC-CSSA-126 R00	Stereo Plot	Wedge Stability Analysis Sector 7 Creek Slope Stability Assessment	N/A
LTMM CC-CSSA-127 R00	Stereo Plot	Wedge Stability Analysis Sector 8 Creek Slope Stability Assessment	N/A
LTMM CC-CSSA-128 R00	Stereo Plot	Wedge Stability Analysis Sector 9 Creek Slope Stability Assessment	N/A
LTMM CC-AP-D-201 R00	Map	Tectono-Seismic Situation South West Canada - Alberta	1:5,000,000
LTMM CC-AP-D-202 R00	Map	Tectono-Seismic Situation Canmore Region	1:1,500,000
LTMM CC-AP-E-301 R00	Map	Dam Breach and Inundation Calculation Overview of Discharge Readouts and POIs	1:10,000
LTMM CC-AP-E-302 R00	Map	Dam Breach and Inundation Calculation Flood Water Depth after 1 hour	1:10,000
LTMM CC-AP-E-303 R00	Map	Dam Breach and Inundation Calculation Flood Water Depth after 2 hours	1:10,000
LTMM CC-AP-E-304 R00	Map	Dam Breach and Inundation Calculation Flood Water Depth after 3 hours	1:10,000
LTMM CC-AP-E-305 R00	Map	Dam Breach and Inundation Calculation Flood Water Depth after 5 hours	1:10,000
LTMM CC-AP-E-306 R00	Map	Dam Breach and Inundation Calculation Flood Water Depth after 10 hours	1:10,000
LTMM CC-AP-E-307 R00	Map	Dam Breach and Inundation Calculation Flood Water Depth after 15 hours	1:10,000
LTMM CC-DFG-401 R00	Plan View	Ground Improvement and Cut-Off Measures Rock Grouting, Pile Arrangement, Ground Improvement Issued for Permitting	1:500
LTMM CC-DFG-402 R00	Plan View	Trench Excavation For Abutments and Capping Beam Issued for Permitting	1:500
LTMM CC-DFG-403 R00	Longitudinal Section	Growthhole Arrangement Longitudinal Section 1 DC Issued for Permitting	1:500
LTMM CC-DFG-404 R00	Detail	Pile Arrangement Detail in Plan Issued for Permitting	1:50
LTMM CC-DAM-501 R00	Plan View	Access and Retention Structure Site Overview Issued for Permitting	1:1,250
LTMM CC-DAM-502 R00	Plan View	Retention Structure	1:750

Drawing No.	Type	Content	Scale
		Site Overview Issued for Permitting	
LTMM CC-DAM-503 R00	Cross Section	Dam Construction Concept Cross Section 11 D Issued for Permitting	1:500
LTMM CC-DAM-504 R00	Cross Section	Intake, Bottom Outflow and Stilling Basin Cross Section 10 D Issued for Permitting	1:500
LTMM CC-DAM-505 R00	Longitudinal Section	Seal Wall, Cut Off and Grout Curtain Longitudinal Section 1 DC Issued for Permitting	1:500
LTMM CC-DAM-506 R00	Sections and Detail	Spillway Shell Section CS2-D and Detail CS3-D Issued for Permitting	1:500/1:50
LTMM CC-DAM-507 R00	Cross Section	Intake Cross Section 12-IN Issued for Permitting	1:100
LTMM CC-DAM-508 R00	Cross Section	Intake Cross Section 13-IN and 16-IN Issued for Permitting	1:100
LTMM CC-DAM-509 R00	Cross Section	Intake Cross Section 14-IN Issued for Permitting	1:150
LTMM CC-DAM-510 R00	Cross Section	Emergency Bypass Cross Section 15-D Issued for Permitting	1:500
LTMM CC-DAM-511 R00	Details	Emergency Bypass Conceptual Design Issued for Permitting	1:500
LTMM CC-DAM-520 R00	Plan View	Instrumentation Scheme Concept Design Issued for Permitting	1:500
LTMM CC-DAM-521 R00	Sections	Instrumentation Scheme Concept Design Issued for Permitting	1:100
LTMM CC-DAM-601 R00	Cross Section	Bottom Outlet Structure Reinforcement Scheme Issued for Permitting	1:50
LTMM CC-DAM-602 R00	Longitudinal Section	Bottom Outlet Structure Reinforcement and Jointing Scheme Issued for Permitting	1:50
LTMM CC-DAM-603 R00	Longitudinal Section	Bottom Outlet Structure Joint Details Issued for Permitting	1:10
LTMM CC-ACC-702 R00	Longitudinal	Access Road	1:1,000

Drawing No.	Type	Content	Scale
	Section	Longitudinal Section 3 AR Issued for Permitting	
LTMM CC-ACC-703 R00	Cross Sections	Access Road Cross Section 1 AR, 2 AR, 3 AR Issued for Permitting	1:200
LTMM CC-ACC-704 R00	Cross Sections	Access Road Cross Section 4 AR, 5 AR Issued for Permitting	1:200
LTMM CC-ACC-705 R00	Cross Sections	Access Road Cross Section 6 AR, 9 AR Issued for Permitting	1:200
LTMM CC-ACC-706 R00	Cross Sections	Access Road Cross Section 7 AR, 8 AR Issued for Permitting	1:200

01 EXECUTIVE SUMMARY

Due to recurring flood events, the Town of Canmore is establishing long-term mitigation measures at Cougar Creek in Canmore, Alberta. The construction of a debris-flood retention structure at the apex of the Cougar Creek alluvial fan is envisioned.

Because of the June 2013 flood, the Town of Canmore (ToC) has retained BGC Engineering Ltd. to conduct a hazard and risk assessment, as well as a hydro-climatic analysis in 2013 and 2014. Thurber Engineering Ltd. performed geotechnical investigations in 2014 and 2015. ALPINFRA Consulting and Engineering GmbH was retained by the Town to evaluate several mitigation options. The Town selected Option A, a debris-flood retention embankment dam.

Subsequently, the Town of Canmore retained Canadian Hydrotech Corp. to design the retention structure and to prepare application documents for the Town to obtain the necessary regulatory approval, agreements and authorization from Alberta Environment and Parks (AEP), prior to commencement of construction works.

Canadian Hydrotech Corp. concluded the design for application and approval including the appendices, reports and corresponding memorandums as listed in chapter 00.04. Design drawings are listed in chapter 00.06.

The selected mitigation option, a debris-flood retention structure, consists of an earth and rock-fill embankment dam with a reinforced monolithic concrete seal wall, cut-off measures in the water saturated alluvial deposits below the structure, as well as of flood flow-control structures. Flood discharge from the Cougar Creek catchment is retained by the structure and the remaining discharge is controlled by a throttle that is installed at the inflow section of a box-shaped bottom outlet structure. The remaining design discharge at full impoundment is $45\text{m}^3/\text{s}$.

Considering full impoundment, and referring to the dam safety technical bulletin of the Canadian Dam Association (CDA, 2007), the proposed retention structure would be classified as a “very high consequence dam”. However, full impoundment is very rare. This could happen approximately every 100 years, or even less frequently. Considering a dry dam and an empty retention basin, the structure should not be considered as a water retaining or water storing structure, but as a water diversion structure.

The target level of flood protection is governing the hydrological design and the storage capacity. The structure shall provide protection against floods, resulting from storm events with return periods of up to 1,000 years. Because of the narrow situation at the downstream embankment slope, resulting from local topography, the complete dam structure is designed to resist overtopping.

For relevant load cases, which are related to certain impoundment levels, seepage and stability analyses were conducted. CHT investigated the stability of the structure for normal operating conditions, for overtopping and rapid drawdown, as well as under consideration of seismic loading. The obtained factors of safety are in accordance with criteria listed in the technical bulletin of the CDA: “Geotechnical Considerations for Dam Safety” (CDA, 2007). Because impoundment is very rare, the geotechnical and structural dam design in terms of seismic loading and stability is based on peak ground acceleration values ($0.5\times\text{PGA}$) resulting from earthquakes with a return period of 5,000 years for the empty (dry) structure. For the dry, as well as for the fully impounded structure, the seismic yield acceleration was analyzed.

Dam fill zones, drainages and collectors are designed according to requirements for the capabilities of drainage and filter-stability. Quality control during dam construction (deep foundation, grouting, concreting, gradation of granular fill material, compaction, lift thicknesses and construction sequences) is essential for a safe structure and shall be guaranteed by the owner. Flow control structures are designed according to hydraulic conditions for different operating states. Physical scaled modelling was conducted to supplement the hydraulic design.

The inflow of the bottom outlet structure is protected against blockage from gravel and wooden debris by means of a steel rake structure. An emergency bypass outside the intake structure is provided for emptying the reservoir in case of blockage at the intake.

Because flood events are accompanied by significant bedload transport, gravel debris and wooden debris will accumulate upstream of the structure. Although the debris-rake design is optimized for self-clearing of accumulated gravel, clearance of the reservoir from gravel will be required from time to time. For maintenance purpose, and for access during construction, public paved roads to Cougar Creek are available. A gravel road along the creek will be used for the remaining distance to the construction site and to the structure. A permanent access road to the crest of the structure will be constructed by cutting into the creek slopes following standard forestry practices. Slope stabilization will be done as required.

An observation, service and maintenance platform will be established at the orographic right side, above the crest, directly above the access road, safe from floodwater. Monitoring data from dam instrumentation will be collected and transmitted to a Town of Canmore server.

02 LIMITATIONS

The dam design is mainly based on geotechnical design parameters. These parameters were developed by CHT based on results from the geotechnical investigation program performed by others. These parameters are best estimate parameters but subject to confirmation ahead of construction.

The stability analyses are based on geotechnical investigation results. The outcomes of these analyses govern the dam construction concept and, in consequence, the structural design. The design values derived from the geotechnical investigation program are based on established engineering practice; however, conditions in the field may differ from assumed models and predictions. Therefore, CHT is using the appropriate safety factors in its design to account for potential variability. In case the geotechnical design parameters, as determined during construction, are substantially different from current assumptions, amendments to the design may be required.

Because of time constraints, the minimum required geotechnical investigation program for the current design was conducted. Supplementary geotechnical detail investigations at the higher rock abutments ahead of construction are therefore necessary. Preparation of the abutments and construction of the abutment trench, for keying in the seal wall, need to be executed according to observed conditions and under the guidance of the geotechnical site engineer. Local measures for rock slope stabilization may be required and need to be decided onsite during construction of the access ramps, the rock abutments, as well as of the associated rock excavation for the stilling basin and the emergency bypass. During the preparation of the dam footprint, supplementary plate loading tests are required to determine loading capacity and stiffness. Soil exchange might be required for areas at the footprint that are not according to specifications.

Canadian Hydrotech Corp. prepared this report for the Town of Canmore. The assumptions and the design rely heavily on third party data and information available to Canadian Hydrotech Corp. at the time of report preparation. The confidence level of the design presented herein is in accordance with the confidence level of the available input data.

Any use a third party makes of this report or any reliance on decisions based on it, is done within the responsibility of such a third party. In terms of protection to our client, the public, and Canadian Hydrotech Corp., the Town of Canmore and/or firms, retained by the Town for this particular project, may use this report. Authorization outside of this use needs our approval.

03 INTRODUCTION

03.01 Project Background

Due to recurring floods, the Town of Canmore is establishing long-term mitigation measures at Cougar Creek in Canmore, Alberta. A protection structure at the apex of the Cougar Creek alluvial fan shall protect the Town by retaining floods and debris floods. The maximum remaining peak discharge to the lower channel is $45\text{m}^3/\text{s}$. Because of the June 2013 flood, a forensic study, a hazard and risk assessment, as well as a hydro-climatic analysis were conducted. As basis for the option analysis, geotechnical investigations were conducted in 2014. Those investigations have been refined for detail design in 2015. Mitigation strategies and options were investigated and evaluated in 2014. Option A, a debris-flood retention structure, was selected.

The Town of Canmore retained Canadian Hydrotech Corp. to design the retention structure and to create application documents for the Town to obtain the necessary regulatory approval from Alberta Environment and Parks (AEP) prior to commencement of construction works.

03.02 Project Area

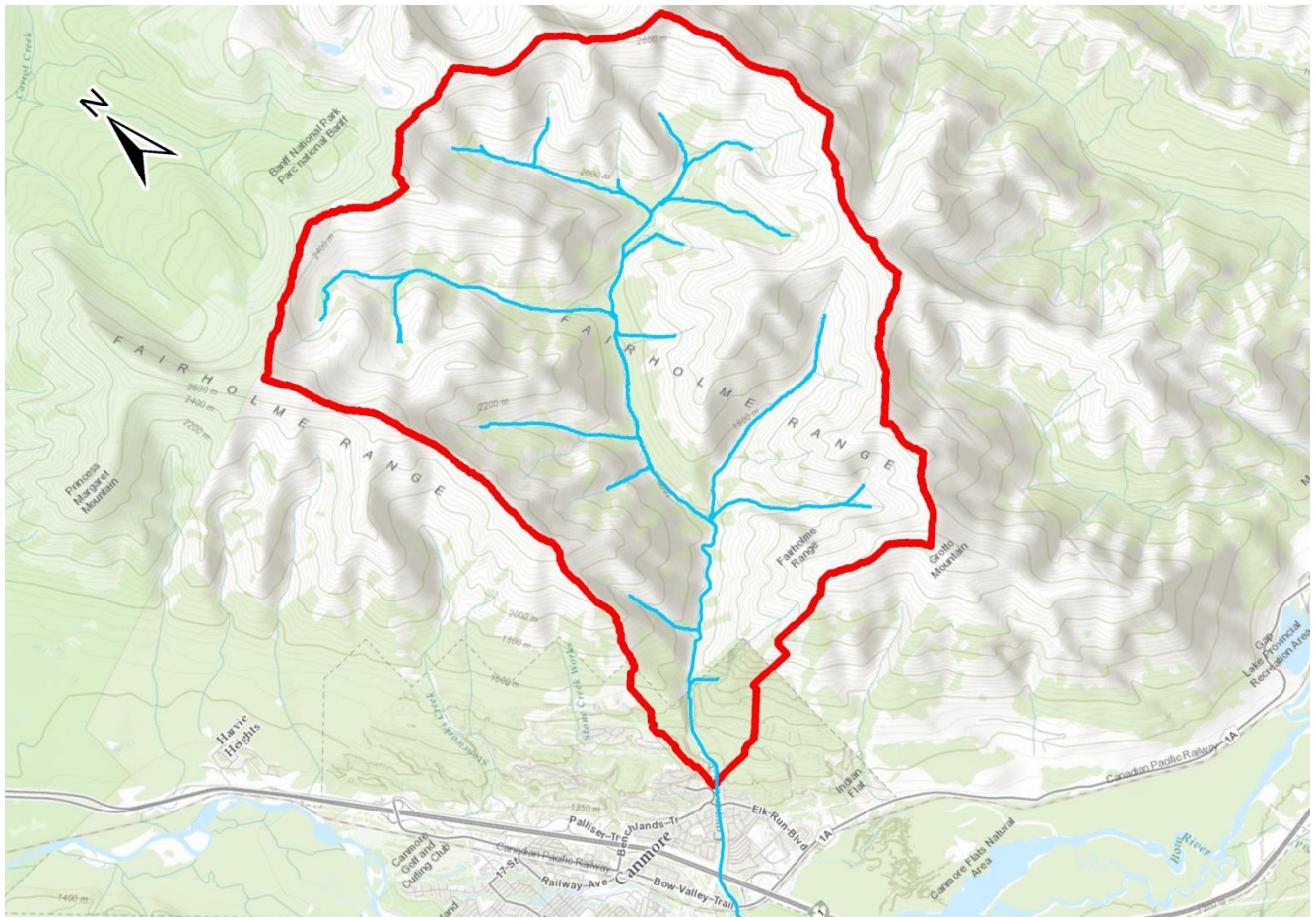


Figure 1: Location of the Cougar Creek Watershed. The outline represents the extension of the watershed (basemap source: ESRI, unspecified scale)

Cougar Creek is a mountain creek in the Fairholme Mountain Range, discharging into the Bow River. The watershed is located to the northeast of the Town of Canmore. The southeastern suburban area of Canmore is built onto the alluvial fan of Cougar Creek. The watershed, 42km^2 in total, reaches from Mt. Townsend (2,820 MASL) in the northeast to Mt. Fable (2,702 MASL) in the east, Grotto Mountain (2,730 MASL) in the south as well as Mt. Lady MacDonald (2,606 MASL) and Mt. Charles Stewart (2,797 MASL) in the west. From the highest

altitudes down to approximately 2,050 MASL, the slopes are bare of any vegetation and dominated by rockfall detachments and rockfall deposits. The rock formations primarily consist of carbonates and siliciclastic rocks. A detailed description of the geology of Cougar Creek watershed is given in the Debris Flood Hazard Assessment by BGC Engineering Ltd. (2014b).

The valley section inside the watershed is covered by dense coniferous forest. A total of 23 partially inactive tributaries discharge into Cougar Creek before it reaches the fan apex and flows through No Man's Land and the armoured channel through Canmore. Through time, these tributaries have carved multiple erosional scars into the landscape, indicating that the watershed has been affected by mass movement and debris flows. The Cougar Creek watershed is shown in Figure 1.

03.03 Location of the proposed Retention Structure

The retention structure is placed at the Cougar Creek fan apex, directly upstream of No Man's Land. The downstream embankment of the retention structure is supported by bedrock walls, forming a bottleneck as shown in the design drawing LTMM CC-DAM-501. A wider overview, indicating the location of the retention structure is shown in drawing LTMM CC-GEN-010.

03.04 Current Situation at the Location of the proposed Structure

A debris net is currently installed at the intended location of the retention structure, spanning across the creek. The debris net is part of the short-term mitigation measures and retains gravel and wooden debris, which can potentially block existing culverts (see Figure 2). The foundation of the debris net is constructed with concrete well rings and four micro-piles for each net post. Construction details are shown in drawings by BGC Engineering Inc. and Gygax Engineering Associates Ltd.



Figure 2: Debris-Net at the intended location of the debris-flood retention structure as part of short-term mitigation measures (CHT 2015)

The creek upstream of the proposed structure is of natural character, formed by steep bedrock walls and a creek bed consisting of well graded alluvial deposits, washed out from fines at the creek bed surface. Tributary creeks discharge sediments originating from rock-fall deposits and debris flows into Cougar Creek.



Figure 3: Cougar Creek directly upstream of the proposed structure; viewing upstream (CHT 2015)



Figure 4: Cougar Creek approximately 1.5km upstream of the proposed structure; viewing upstream (CHT 2015)

03.05 Current Situation downstream of the Location of the proposed Structure

Downstream of the proposed retention structure expands an area called “No Man’s Land”. No Man’s Land is a transition area between the creek and the fan, formed of bedrock at the orographic left bank and inhomogeneous cemented glacial-fluvial deposits in form of the Kame-Terrace on the orographic right bank (see Figure 5). Downstream of No Man’s Land an artificial channel was constructed and armoured with articulated concrete mats (see Figure 6 and Figure 7).

The assessment of the hydraulic discharge capacity of the downstream channel, as well as of existing culverts, considering clear water discharge, as well as bedload transport, was subject of a separate channel improvement design project issued for permit in May of 2016 (CHT 2016). This investigation shows that a clear water discharge of $45\text{m}^3/\text{s}$, including bedload transport, can be hydraulically safely discharged through the channel and the culvert at the Elk Run Blvd. crossing. Considering a minimum required update of the inflow of the culvert at highway 1, impoundment of Highway 1 can be avoided almost completely. The nominal discharge capacity at Highway 1 of $64\text{m}^3/\text{s}$ cannot be confirmed by the hydraulic assessment mentioned above considering bedload. More details are available in the design report (Doc. No.: CC CHU - REP - DES-00 - 2016-05-04, CHT 2016). The results outlined in this report are underpinning the selected design discharge through the bottom outlet structure of $45\text{m}^3/\text{s}$ for full impoundment.



Figure 5: Kame-Terrace forming the right bank of No Man's Land



Figure 6: Reinforced downstream channel



Figure 7: Downstream channel and culvert of Bow Valley Trail with houses next to Cougar Creek channel

04 DESIGN BASIS

04.01 Project and Design History

Reports and materials as listed in Table 1 from previous investigations and design projects were made available as a basis for the design presented herein:

Table 1: List of available Documents as Design Basis

Prepared by	Document No.	Content	Date
Reports			
CH2M Hill Engineering Ltd.	CGY\25182\999.R	Cougar Creek Flood Risk Mapping Study	1994/03
M. J. O'Connor & Associates Ltd.	10-038	Geotechnical Evaluation Proposed Canmore Residential Subdivision and Highway Commercial Area	1980-07-04
BGC Engineering Ltd.	TC13-004	Cougar Creek, 2013 Forensic Analysis and Short-Term Debris Flood Mitigation	2013-12-04
BGC Engineering Ltd.	TC13-005	Cougar Creek Forensic Analysis, Hydroclimatic Analysis of the June 2013 Storm	2014-01-10
BGC Engineering Ltd.	TC13-010	Cougar Creek Debris Flood Hazard Assessment	2014-03-07
BGC Engineering Ltd.	TC14-001	Cougar Creek Debris Flood Risk Assessment	2014-06-11
ALPINFRA Consulting & Engineering GmbH	16494_REP03_R03_20141213	Option Analysis, Mountain Creek Hazard Mitigation Measures, Design of Mitigation Measures Cougar Creek Including design drawings.	2014-12-14
Town of Canmore		Option Analysis Summary Report, Cougar Creek Long Term Mitigation	2015-01-13
Thurber Engineering Ltd.	19-598-440A	Cougar Creek Long Term Debris Flood Mitigation, Initial Geotechnical Field Investigation	2014-08-18
Thurber Engineering Ltd.	19-598-440	Cougar Creek Long Term Debris Flood Mitigation, Geotechnical Investigation for Phase 1 Option Analysis	2015-11-09
Thurber Engineering Ltd.	19-598-440B	Cougar Creek Long Term Mitigation Project Phase 2A Geotechnical Investigation	2015-12-22
Thurber Engineering Ltd.	14-264-2	Cougar Creek Long Term Mitigation Project Phase 2B Geotechnical Investigation, Thurber Engineering Ltd.	2015-12-24
Canadian Hydrotech Corp.	LTMM CC – DBM-02 – 2015/05/21	LONG TERM MITIGATION MEASURES COUGAR CREEK - Design Basis Memorandum	2015-05-21
Canadian Hydrotech Corp.	CC CHU - REP - DES-00 - 2016-05-04	Cougar Creek - Update of Grade Control Design Report - Issued for Permit	2016-05-04
Drawings only			
ISL Engineering Ltd.	344 SO	Cross Sections for Channel Bank Protection	2013-09-09

04.02 Geology

04.02.01 General Geologic and Geotechnical Setting

The Debris Flood Hazard Report (BGC Engineering Ltd., 2014b) summarizes the regional geological frame as follows: *“The Canadian Rocky Mountains (CRM) are a fold and thrust belt, where thick units of more erosion resistant Paleozoic carbonates were folded and thrust progressively in a north-westerly direction over more friable Mesozoic sandstones and shales. Four main sequences of rocks can be characterized in the Canmore region. The oldest unit at the base is referred to as the basement rocks of the North American cratonic plate (30 – 50 km thick), which bears no relevance to this present study. The next unit is the Pre-Cambrian to Lower-Cambrian clastic and minor carbonate rock unit (~10 km thick) composed of weathered rock from the Canadian Shield (further east). The ~6.5 km thick, middle carbonate unit (Middle-Cambrian to Upper Jurassic, 540 – 155 Ma) consists of marine carbonates (limestone and dolostone) and shale. The upper unit (~ 5 km thick) is composed of a young Jurassic to Tertiary (155 – 1.9 Ma) unit of sandstone, shale, conglomerate and coal. This final unit consists of eroded sediments from an uplifting landscape into a foreland basin to the east (Gadd, 1995; Henderson et al, 2009). Osborn et al. (2006) describe the final stages of the mountain building stage as being associated with differential erosion of various units. The softer Mesozoic rocks led to rounded mountain tops exposing the underlying Paleozoic and Proterozoic rocks that can support steeper and higher slopes.”*

A more detailed description also focusing on relationships between lithological - structure geological setting and erosion is available and thoroughly explained in the Debris Flood Hazard Assessment (BGC Engineering Ltd., 2014b).

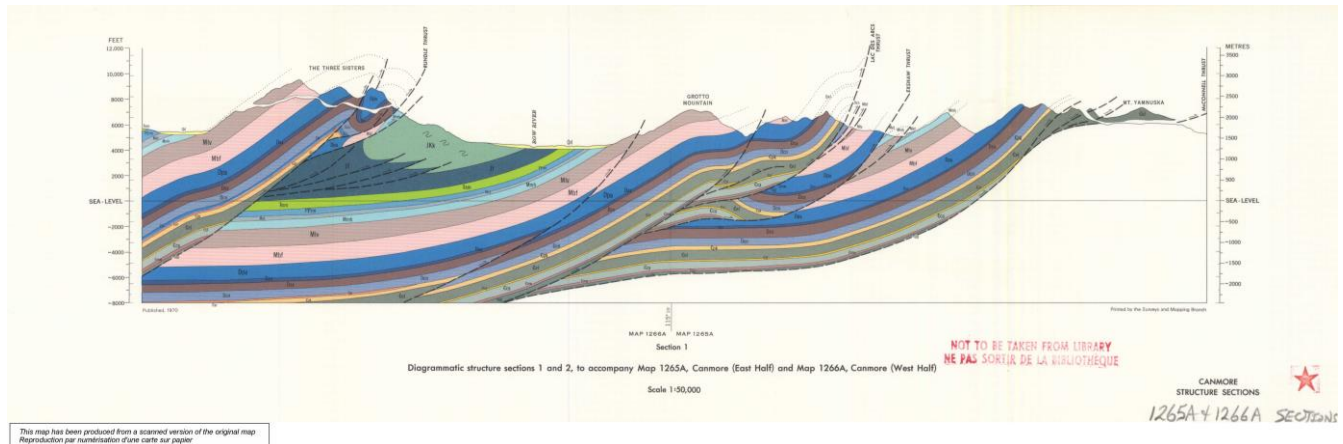


Figure 8: Geological Cross Sections according to GSCmap Nr. 1265a (1970) – Sections, showing the general tectonic and stratigraphic setting

The geotechnical investigation report Phase 2A (Thurber Engineering Ltd., 2015a) refers to the Map 1266A, published by the Geological Survey of Canada (GSC) in 1970, and to the Map 236, published by the Alberta Geological Survey (AGS) (see Figure 8), as well as to its own surficial mapping conducted within the investigation. Thurber identified bedrock formation and surficial geology as summarized in chapter 04.02.02.

04.02.02 Bedrock Geology

04.02.02.01 Mississippian Etherington Formation (Met)

Consists of light grey limestone, cherty limestone and calcarenitic limestone, dolomite, cherty dolomite, green and red shale, siltstone and breccia.

04.02.02.02 Permian and Pennsylvanian Rocky Mountain Group (PPrm)

Consists of light grey quartz sandstone, dolomitic sandstone, silty dolomite and chert.

04.02.02.03 Triassic Sulphur Mountain Formation (Trsm)

Consists of dark grey and brown, thin bedded siltstone, silty mudstone, shale and dolomitic siltstone.

04.02.03 Surficial Geology

04.02.03.01 Modern Cougar Creek Alluvium (Qma)

Granulometric, consists of moderately well to well-sorted gravels, cobbles and boulders, typically sub-rounded to rounded. Petrologically, mainly consist of quartzite, carbonates and quartz-rich sandstone.

04.02.03.02 Cougar Creek Colluvium/Alluvium – Lower and Upper Bench (Qc/a-l and Qc/a-u)

According to the geotechnical report on Phase 2A (Thurber Engineering Ltd., 2015a): *“This material is found within “lower” benches straddling both sides of the creek and situated one to two meters above the modern flood plain, and an “upper” bench five to seven meters higher than the lower benches. This unit is highly variable, consisting mostly of a poorly sorted diamict but with lenses of sorted gravels. Clast content is up to 70% and clast sizes range from gravel to boulder. There is some cementation, but not sufficient to provide significant mechanical strength. In the upper bench, there are fewer exposures of the unit but available indications are that the sediment there is similar to that in the lower benches.”*

04.02.03.03 Till (Qt)

A massive, unsorted diamict unit, overlying the bedrock on the upper slopes of Cougar Creek is described in the geotechnical investigation report Phase 2A (Thurber Engineering Ltd., 2015a). The diamict is (per definition) matrix-supported with approximately 40% clast content. The matrix is identified as silty fine sand with low to moderate cementation and indications of high calcite content. Petrologically, the clasts mainly consist of quartzite, granulometric of coarse sand to cobble, angular to sub-rounded.

A more detailed lithology is outlined in the reports mentioned above.

04.02.04 Geological and Geotechnical Site Conditions

The geotechnical investigation Phase 2A report (Thurber Engineering Ltd., 2015a) contains a cross section along the proposed dam axis as shown in Figure 9 (for orientation only). For a more detailed view, refer to the geotechnical investigation report.

Figures and Maps as well as cross sections presented herein originate from the geotechnical investigation reports from Thurber and are for orientation purposes only. More detailed figures and maps are available in the referenced reports.

The cross section shows that the bedrock, belonging to the Rocky Mountain Group (predominantly sandstone, some siltstone and limestone), reaches up to the preliminary set crest of the proposed retention structure. The bedrock forms a round shaped creek bed filled with modern alluvium.

The approximate shape of the bedrock surface was determined by means of drilling four vertical test holes and geophysical investigations. Drillings as well as geophysical investigations indicate a glacially imprinted valley. The valley slopes above ground indicate the orientation of discontinuities characterizing the bedrock structure and are without any major soil cover except for the till/colluvium cover above the creek walls.

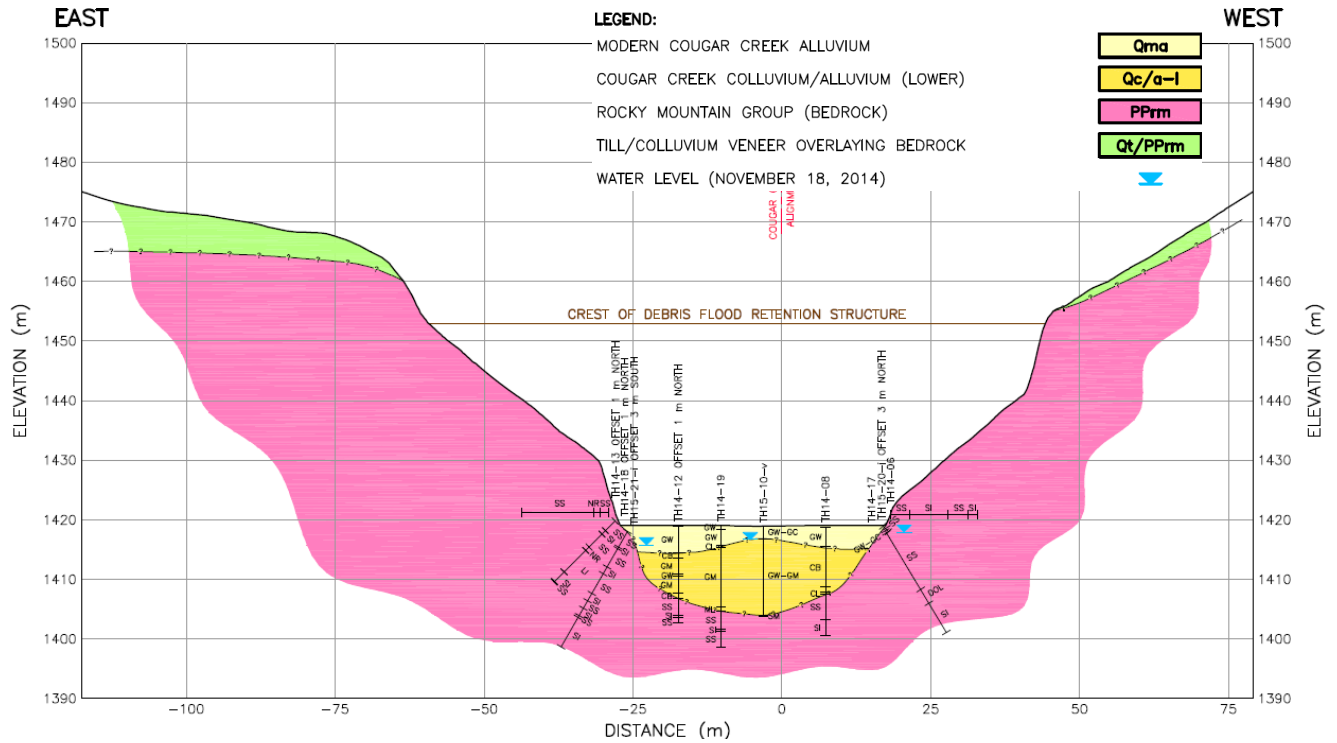


Figure 9: Geological cross section (Thurber Engineering Ltd., 2015b)

04.02.04.01 Left abutment

According to the available drill logs, the left abutment is characterized by sandstone and siltstone, faintly weathered, fine grained and strong to very strong. It appears intensively fractured and joints are planar and vary from smooth to very rough. Water pressure tests indicate medium transmissivity with Lugeon values of up to 30l/min/m.



Figure 10: Rock outcrop at the left abutment (Photo: ALPINFRA 2014)

04.02.04.02 Right abutment

According to available drill logs, the right abutment is characterized predominantly by sandstone with some siltstone layers, and as recorded in the 45° inclined Drilling TH14-18 (Thurber 2014), limestone occurs beyond 7m. Fine-grained infills, either of joint or of faults, are recorded as well. In general, the drill records and observations lead to the impression that some open fractures at the right abutment, which indicates high water permeability, in particular at the contact between sandstone and limestone, need to be taken into account. The general appearance of the sand and siltstone is similar to the left abutment except the joint infills observed there. The limestone appears fresh, finely grained, strong and with very close to medium fracture spacing. Water pressure tests indicate medium to very high transmissivity with Lugeon values of up to 150l/min/m.



Figure 11: Rock outcrop at the right abutment (Photo: ALPINFRA 2014)

04.02.04.03 Discontinuities

The geotechnical investigation Phase 2A report (Thurber Engineering Ltd., 2015a) contains the following data for orientation of discontinuities:

Table 2: Statistical summary of bedding planes and joint Sets recorded by (Thurber Engineering Ltd., 2015a)

Discontinuity Type	Number of Observations	Dip (°) (Min/Max/Mean Vector)			Dip Direction (°) (Min/Max/Mean Vector)		
		Min	Max	Mean	Min	Max	Mean
Bedding	50	20	49	35	208	258	237
Joint Set 1	59	74/72	90/90	87	124/313	165/336	142
Joint Set 2	27	41	84	61	57	90	75

Thurber mapped a fault as indicated in Figure 5 of Appendix A of the Phase 2A geotechnical investigation report (Thurber Engineering Ltd., 2015a) and Figure 3 in the Investigation Report Phase 2B, as a vertical element crossing the Cougar Creek Valley approximately 25m upstream of the proposed dam axis (see Figure 12). Figure 5 in the investigation report Phase 2B indicates this fault as an oblique fault, which appears to be plausible referring to the regional tectonic setting.

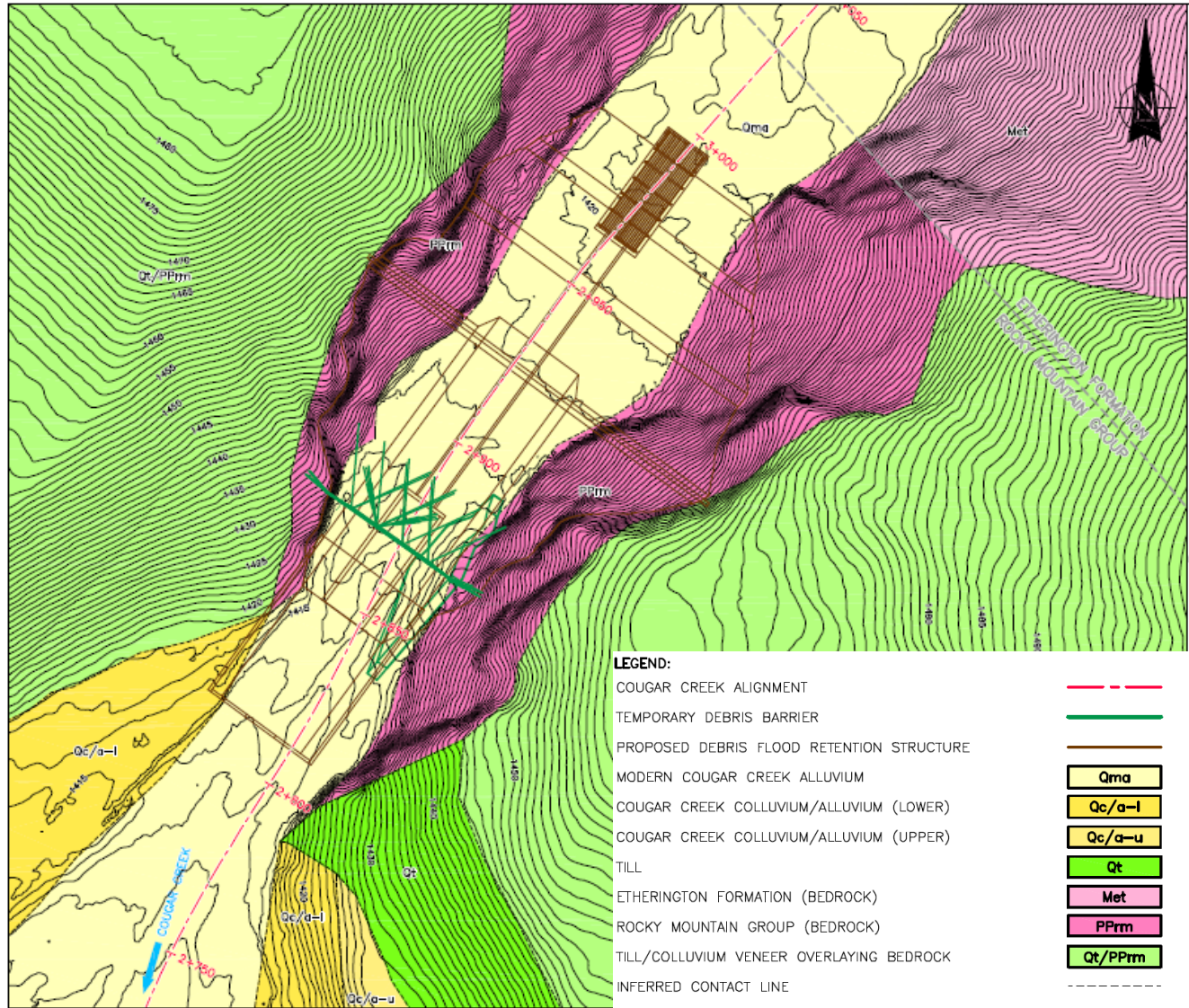


Figure 12: Geological Map from Thurber Engineering (2015b)

04.02.04.04 Footprint

The footprint of the proposed structure is characterized by modern alluvium. According to the Phase 2A and Phase 2B geotechnical investigation reports, the alluvium consists of well-graded gravel in the uppermost layers and silty gravel containing some thin layers of lean clay and well graded gravel in the floor. Groundwater observation during drilling indicated a ground water level of some 3m to 3.5m below surface (Table 3). Slug tests conducted in 2014 and pumping tests in 2015 indicate water permeability coefficients within the alluvium reaching from approximately 2×10^{-4} m/s to 4×10^{-5} m/s, indicating the potential of a high groundwater flow velocity in the current state and emphasizing the need of reliable seepage cut-off measures (see Table 3 and Table 4).

Water pressure tests, conducted in the lower abutments and the footprint, indicate medium to high transmissivity, emphasizing the need of a grout curtain to limit seepage to a safe level.

The alignment of the bedrock face along the creek axis is similar to the inclination of the creek bed. The layers within the modern alluvium vary in thickness, lateral distribution and shape.

Table 3: Ground water levels according to table 7 – report on the Phase 2A geotechnical investigation (Thurber Engineering Ltd., 2015a)

Test Hole ID	Ground Elevation (m)	Screen Depth (m)	Soil Unit in Response Zone	Depth to Groundwater (m)	Groundwater Elevation (m)
TH14-07	1,419.6	8.9 – 14.9	Silt, sandy Gravel	3.1	1,416.5
TH14-09	1,419.1	8.9 – 14.9	Silt, sandy Gravel	2.9	1,416.1
TH14-5A	1,413.2	4.0 – 5.8	Gravel and Cobbles	3.6	1,409.6
TH14-5B	1,413.2	11.0 – 14.2	Clay (Till), Gravel	4.4	1,408.9

Table 4: Summary of Aquifer Parameter Estimates (Waterline Resources Inc, 2015)

Well Name	Solution	Time Interval	Transmissivity (m ² /d)	Storativity (unitless)	Specific Yield	β	Hydraulic Conductivity (m/s)
TH14-09	Cooper-Jacob (1946)	Early-Time Drawdown	215	7E-04	NA	NA	4E-05
	Agarwal (1980)	Early-Time Recovery	110	3E-03	NA	NA	2E-05
	Neuman (1974)	All Data	215	3E-03	0.3	0.006	4E-05
TH15-11-v	Cooper-Jacob (1946)	Early-Time Drawdown	225	2E-04	NA	NA	5E-05
	Agarwal (1980)	Early-Time Recovery	120	1E-03	NA	NA	2E-05
	Neuman (1974)	All Data	225	1E-03	0.3	0.008	5E-05
TH14-07	Cooper-Jacob (1946)	Early-Time Drawdown	210	1E-04	NA	NA	4E-05
	Agarwal (1980)	Early-Time Recovery	113	4E-04	NA	NA	2E-05
	Neuman (1974)	All Data	210	7E-04	0.3	0.0037	4E-05
TH15-22-v	Cooper-Jacob (1946)	Early-Time Drawdown	170	3E-05	NA	NA	3E-05
	Agarwal (1980)	Early-Time Recovery	112	5E-05	NA	NA	2E-05
	Neuman (1974)	All Data	170	1E-04	0.2	0.007	3E-05
TH14-5B	Cooper-Jacob (1946)	Early-Time Drawdown	900	3E-05	NA	NA	2E-04
	Agarwal (1980)	Early-Time Recovery	700	4E-05	NA	NA	1E-04
	Neuman (1974)	All Data	790	4E-05	0.2	0.01	2E-04
TH14-5A	Cooper-Jacob (1946)	Early-Time Drawdown	1,800	1E-04	NA	NA	4E-04
	Agarwal (1980)	Early-Time Recovery	1,800	1E-04	NA	NA	3E-04
	Neuman (1974)	All Data	1,760	1E-04	0.2	0.006	4E-04
TH15-10-v (Source Well)	Cooper-Jacob (1946)	Early-Time Drawdown	230	NA	NA	NA	5E-05
	Agarwal (1980)	Early-Time Recovery	125	NA	NA	NA	3E-05

Notes: 'NA' indicates the parameter is not applicable to the solution.

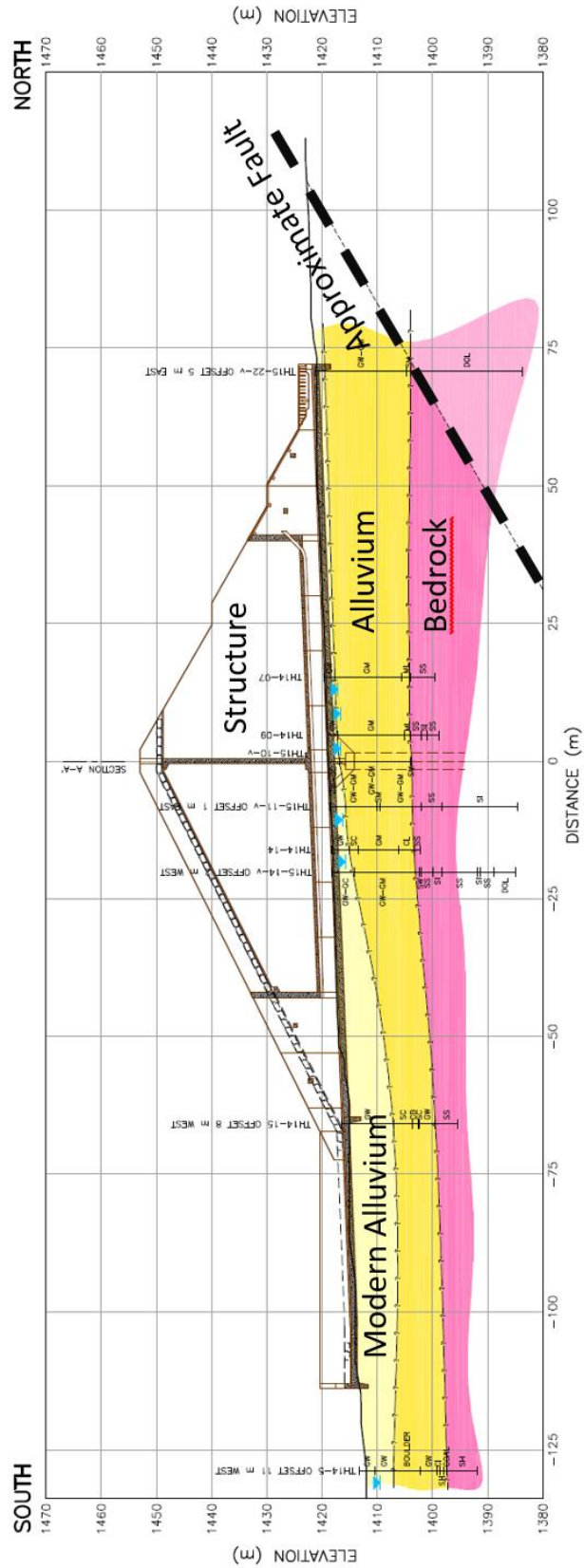


Figure 13: Length section along the creek axis (Thurber Engineering Ltd., 2015b)

04.03 Seismic Site Conditions

The seismic situation is investigated in detail in the Appendix D – Seismic Hazard Assessment. A brief summary is presented herein as follows:

Data from the Geological Survey of Canada (GSC), the United States Geological Survey (USGS) and the Incorporated Research Institutions for Seismology (IRIS), as well as stress tensors, currently published by the World Stress Map project (Reiter, 2014) were processed and visualized in the maps LTMM CC-AP-D-201 and LTMM CC-AP-D-202.

In the region of Canmore, the following recent Earthquakes were recorded:

- (1) Magnitude of 2.1 earthquake on April 22, 2008, located approximately 13km southeast of Canmore.
- (2) Magnitude of 2.1 earthquake on February 24, 2002, located approximately 14km east of Canmore.
- (3) Magnitude of 2.2 earthquake on March 25, 2008, located approximately 21km ENE of Canmore.
- (4) Magnitude 3.3 to 3.6 earthquake on July 28, 2002, located approximately 22km SSE of Canmore.
- (5) Magnitude 3.1 earthquake on October 16, 2014, located approximately 19.2 km northwest of Canmore near Banff.

Considering the magnitudes from these earthquakes, the estimated local peak ground accelerations range from 0.005g to 0.01g (spatially referred to the epicenters). In general, the area around Canmore is of low seismicity.

04.04 Climatic Site Conditions

The Town of Canmore is located in the Rocky Mountain Natural Region that experiences cold winters and short summers. The Kananaskis climate station (AB3053600) is located approximately 20 km ESE of Canmore at 1,391.1 MASL and possess high quality daily data records back to 1939. Because of the proximity to Canmore and the comparable sea level, this climate station is a good indicator for trends in the Canmore Region.

Nevertheless, based on microclimate and the topography, the climatic conditions at the location of the proposed retention structure may differ slightly compared to the averages from the Kananaskis climate station.

Table 5: Overview of the Kananaskis Climate Station

Kananaskis Climate Station	
Station Name	Kananaskis
Province	Alberta
Climate Identifier	3053600
Latitude	51.03
Longitude	-115.03
Altitude	1,391.1 MASL
Temperature Records	1939/08 - 2013/07
Precipitation Records	1939/08 – 2013/07
Snow on Ground Records	1981/04 – 2013/07

Analyzing the mean monthly temperature and precipitation at Kananaskis, the temperatures drop below 0°C from November to March with precipitation at or below 40mm. Weather is dominated by the dry and cold continental polar air mass, which is formed over central Canada and the north of the USA. Intense cold weather is sometimes triggered by continental arctic air mass from the far North. The majority of precipitation originates from maritime polar air masses from the pacific north, which is cold and moist, but is mostly blocked by topographic barriers (mountain ranges between the coast and Canmore). Therefore, the winter season in the Canmore region is cold and arid.

In April, when the mean temperature starts to climb above the freezing point, the air gets more humid and precipitation increases, peaking in June at 110 mm per month. This short spring season is the wettest period in the area, as maritime tropical air masses from the Gulf of Mexico travel through the USA and supply the area with moist air. The summer/autumn season from July to October is cool with mean temperatures from 5 to 15 °C and again fairly arid with monthly precipitation of 60-70 mm from July to September and hardly 40 mm in October.

Characteristic monthly mean temperature and precipitation for the Canmore region, based on the Kananaskis climate station, is shown in Figure 14.

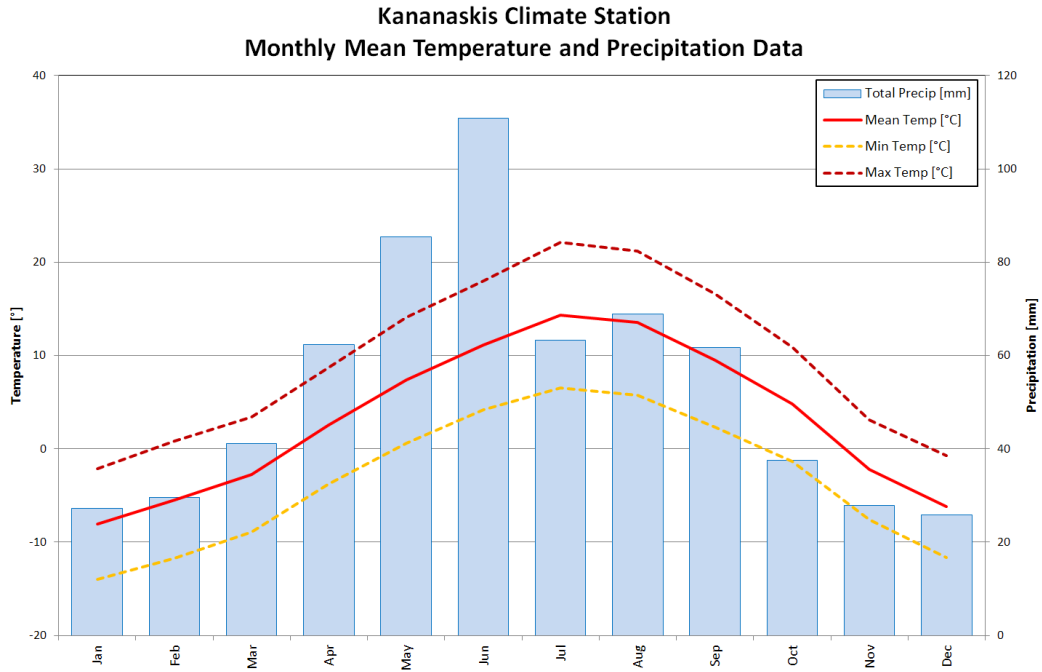


Figure 14: Climate diagram for the Kananaskis climate station at 1,391.1 MASL. Mean monthly values from 1940 to 2013.

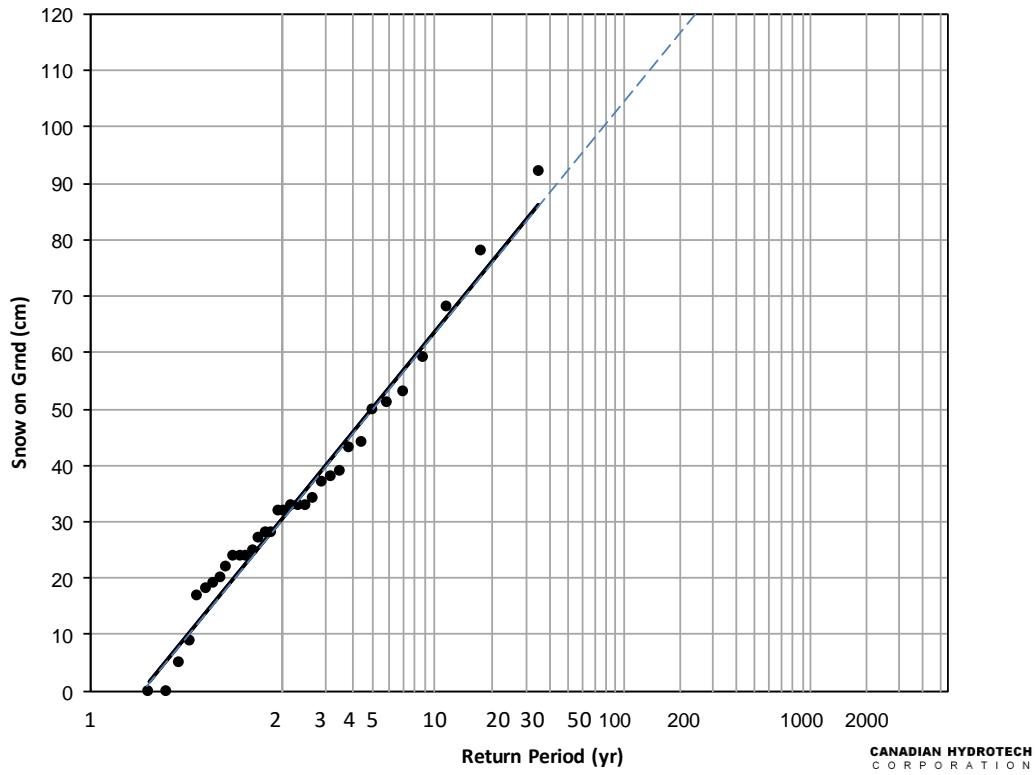


Figure 15: Kananaskis climate station, Snow on Ground frequency analysis - Gumbel distribution

04.05 Frost Penetration Depth

According to the Foundation Engineering Manual - part 13 (CGS, 2006), the design depth of frost penetration for the structure is estimated by the modified Berggren equation, described in Section 13.4.2 of the manual mentioned above. This approach may be used to determine the design depth of frost penetration and can be used to establish the minimum depth of soil cover over a footing.

For Canmore the freezing map of Canada indicates a normal freezing index of 2500 degree-days Fahrenheit, based on the period from 1931 to 1960. (Division of Building Research, National Research Council, and the Atmospheric Environment Service, Dept. of the Environment, Canada).

For determining the frost penetration depth, the simplified approach without the consideration of frost heave (modified Berggren method without considering frost Heave) according to (Sanger & Sayles, 1978).

$$X = \lambda \cdot \sqrt{\frac{2 \cdot k_f \cdot I_s}{L_s}} \quad \text{Equation 1}$$

$$I_d = 100 + 1.29 \cdot I_m \quad \text{Equation 2}$$

$$I_s = n \cdot I_d \quad \text{Equation 3}$$

$$L_s = \gamma_d \cdot w \cdot L \quad \text{Equation 4}$$

$$\beta = \frac{\text{MAAT} \cdot t}{I_s} \quad \text{Equation 5}$$

$$\mu = \frac{C_v \cdot I_s}{L_s \cdot t} \quad \text{Equation 6}$$

$$C_v = \gamma_d \cdot (C_s + C_i \cdot w) \quad \text{Equation 7}$$

where

X	depth of frost penetration [m]
I _s	surface freezing index [°C-days]
k _f	thermal conductivity of the freezing soil [W/mK]
L _s	volumetric latent heat of the soil [kJ/m ³]
λ	dimensionless coefficient that is a function of the temperature gradient, the volumetric latent heat of the soil and the volumetric heat capacity of the soil.
I _d	design freezing Index [°C days]
I _m	mean (normal) freezing Index [°C days], [°F days]/1.8 = [°C days]
n	empirical factor to determine the soil freezing index I _s from the air freezing index I _d
γ _d	dry unit weight [kg/m ³]
w	gravimetric water content of the soil
L	latent heat of fusion of water to ice, L=334 [kJ/kg]
β	thermal ratio parameter
MAAT	mean annual air temperature [°C]
t	duration of the freezing period [days]
C _v	volumetric heat capacity of the soil [kJ/m ³ °C]
C _s	specific heat of dry soil, C _s = 0.71 [kJ/kg°C]
C _i	specific heat of ice, C _i = 2.1 [kJ/kg°C]

The following parameters were used for the calculation of frost penetration depth, based on the Kananaskis climate station data (see chapter 04.04).

Table 6: thermal parameters based on Canadian climate normal station Kananaskis

Parameter	Value
t [days]	182
MAAT [°C]	3.375

The sieving test results performed on the Cougar Creek alluvium by Golder Associates (2015a) were used to determine the soil parameters. The arithmetic mean value was determined from each of the three examined soil samples.

The thermal conductivity of the soil is derived from Figure 16.

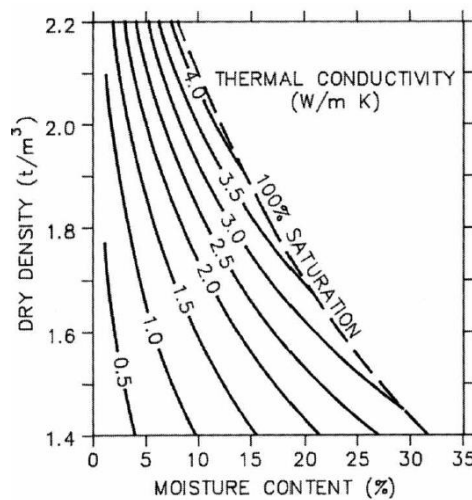


Figure 16: Thermal conductivity of frozen coarse-grained soil (Kersten, 1949)

Table 7: Cougar Creek Soil Parameter

Parameter	Value
γ_d [kg/m ³]	2,185
w [-]	0.041
kf [W/mK]	1.5

For Canmore the freezing map of Canada indicates a normal freezing index of 2,500 degree-days Fahrenheit, based on the period from 1931 to 1960. (Division of Building Research, National Research Council, and the Atmospheric Environment Service, Dept. of the Environment, Canada). To calculate the surface freezing Index the value of factor-n for the most probable value of 0.9 for the gravel-surface type based on (Johnston, 1981) was used.

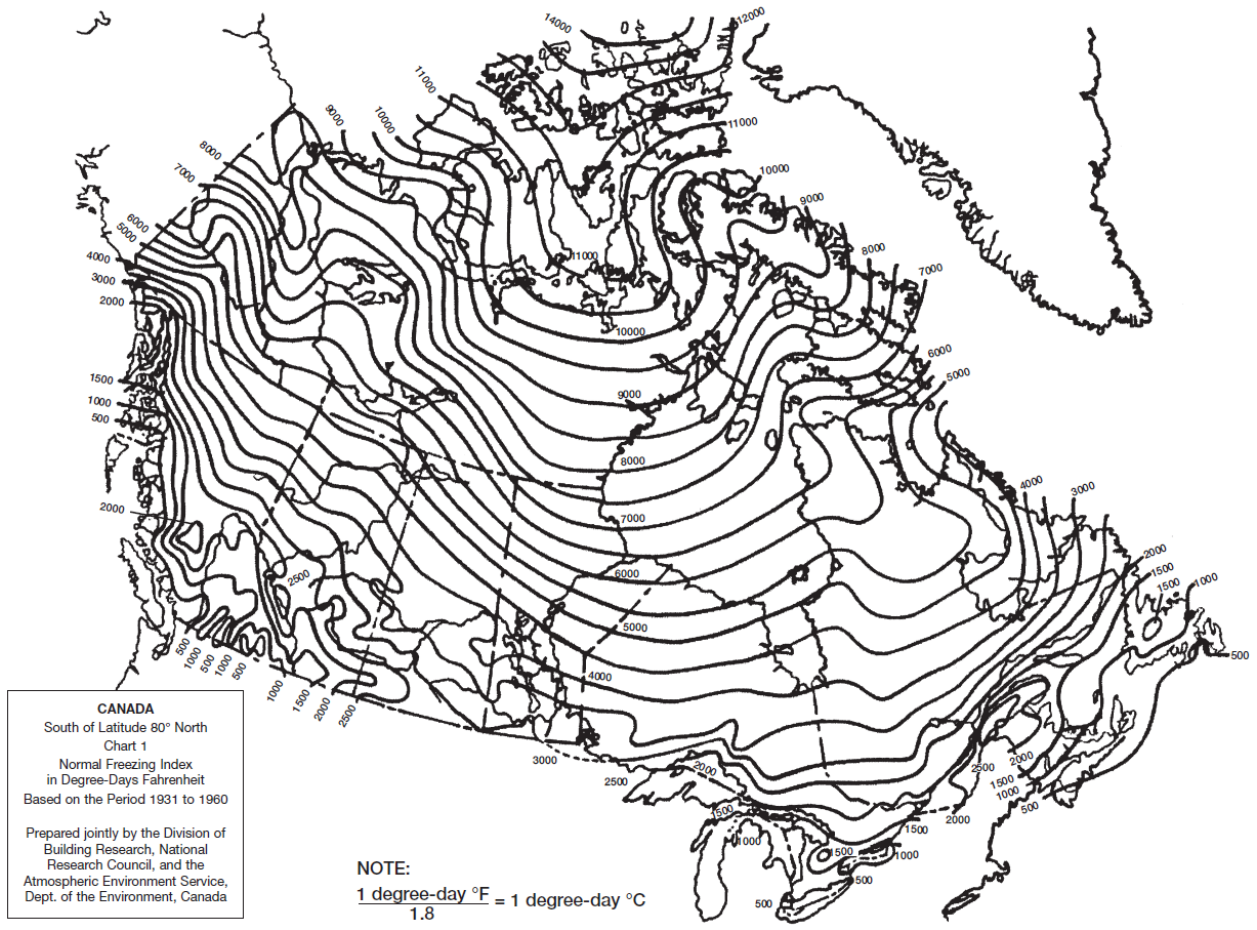


Figure 17: mean (normal) freezing Index map of Canada (Dow Chemical Canada ULC, 2008)

The dimensionless coefficient λ is a function of the temperature gradient, the volumetric latent heat of the soil and the volumetric heat capacity of the soil. The coefficient is determined from the relationship developed by (Sanger & Sayles, 1978) shown in Figure 18.

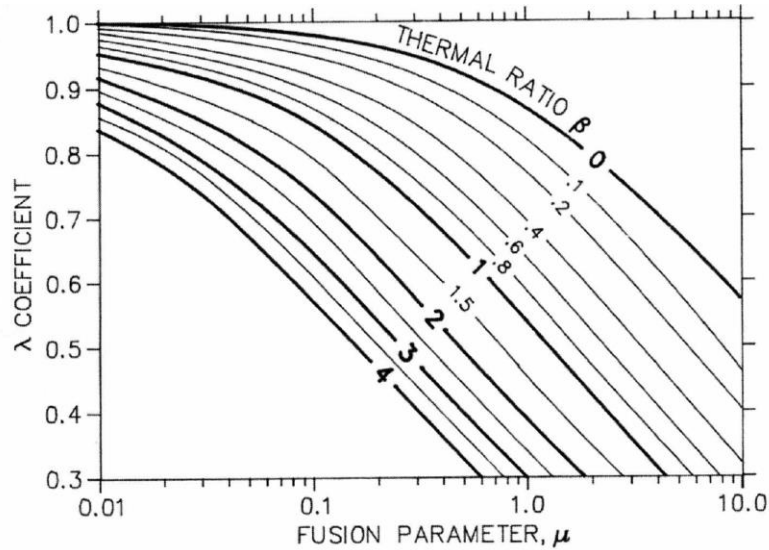


Figure 18: Lambda (λ) coefficient for the modified Breggen equation (Sanger & Sayles, 1978)

Based on Equation 5, Equation 6 and Figure 18 the coefficient λ results in 0.76. Therefore, the frost penetration depth based on the modified Breggen method is $X=2.88\text{m}$.

Table 8: Resulting parameters from the frost penetration depth calculation

Parameter	Value
λ	0.76
X (frost penetration depth)	2.88

The Dow Chemical Company provides frost penetration estimates based on the normal freezing index (see Figure 19) which results in frost penetration of approximately 7 feet / 2.15m for Canmore.

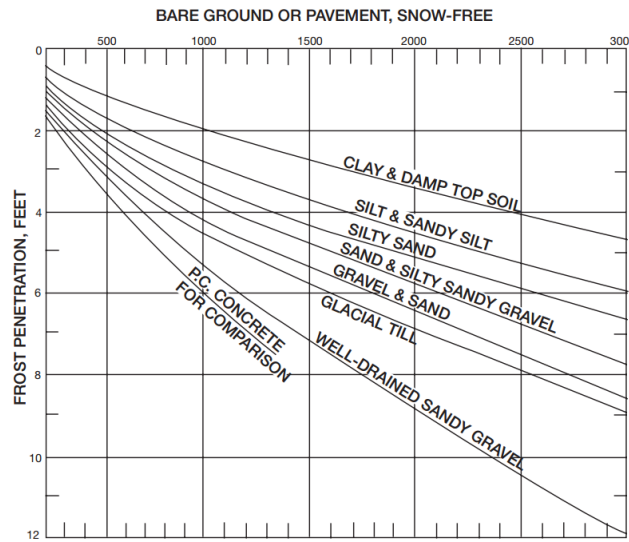


Figure 19: Frost penetration for different soils (Dow Chemical Canada ULC, 2008)

04.06 Hydraulic Situation at the existing Channel

04.06.01 Durability of Existing Channel Reinforcement

For short-term mitigation measures, established after the flood event 2013, the Town installed articulated concrete mats at the channel banks for slope protection as shown in the design drawings of ISL (2013) (see Figure 20).

Steel-cables connect single concrete-bodies forming a mat. The technical documents enclosed with the drawings show a design flow depth of 0.7 m referring to a design discharge of $64\text{m}^3/\text{s}$, based upon the maximum and limiting discharge capacity of the culverts at Highway 1 and Bow Valley Trail. According to the design drawings, the maximum design water level at Elk Run Boulevard is 3.4m due to backwater effects. A more comprehensive analysis of the hydraulic capacity was conducted within the design of complementary grade control measures by Canadian Hydrotech in May 2016 (CHT 2016).

Under consideration of substantial bedload transport processes taking place in case of flood events, a limited resistance of the channel banks against abrasion needs to be considered. Low stability of the channel bed as well as high likeliness of flow concentration on the outside bends could overstress the cable-concrete mats and limit the capacity and overall stability of the channel. Complementary grade control at critical sections is therefore recommended.

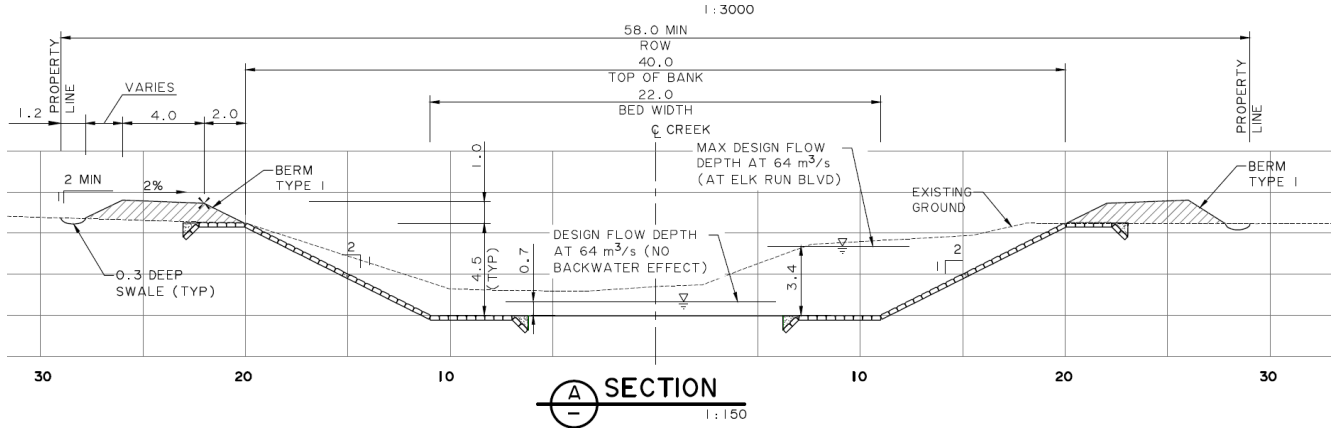


Figure 20: Design of the channel reinforcement (ISL Engineering Ltd., 2013)

04.06.02 Hydraulic Limitations at Culverts

BGC Engineering Ltd. collected available data on types and hydraulic design capacities of existing culverts for road crossings at the Cougar Creek Channel (BGC Engineering Ltd., 2013). All culverts are designed for a discharge capacity of at least 64m³/s. In 2016 the CPR Crossing was replaced with a clear-span bridge construction.

Crossing	Description
Elk Run Boulevard (Photo 2-1)	<ul style="list-style-type: none"> elliptical, multi-plated steel culvert design drawings by Engineering Associates Canada (1982) show the culvert is approximately 6.45 m high, 9.5 m wide and 29 m long with a gradient of 5% capacity = 160 m³/s (CH2M HILL, 1993a) concrete wingwalls at 45° are located at both the inlet and outlet, and extend out about 5 m concrete cutoff wall extends about 1.4 m below the culvert invert. The culvert was rehabilitated in 2012. Design drawings by Associated Engineering (2012) show the installation of an invert protection plate, repairs to the cutoff wall and placement of a concrete liner at the base of the culvert.
Highway 1 (Photo 2-2)	<ul style="list-style-type: none"> three concrete box culverts: 2.44 m wide x 2.75 m high x 64 m long constructed in 1967 capacity = 64 m³/s (CH2M HILL, 1993a) culverts installed with a concrete apron and wingwalls
Highway 1A (Photo 2-3)	<ul style="list-style-type: none"> three concrete box culverts: 2.44 m wide x 2.75 m high x 20 m long constructed in 1967 capacity = 64 m³/s (CH2M HILL, 1993a) culverts installed with a concrete apron and wingwalls
CP Railway	<ul style="list-style-type: none"> three concrete box culverts: 3 m wide x 1.55 m high x 5.8 m long (Hydroconsult, 1999) 2 x 900 mm CSP culverts¹

04.07 Gravel Debris Volumes

Within the Debris Flood Hazard Assessment (BGC Engineering Ltd., 2014b), return period-related debris-volumes were estimated by assigning a certain sediment concentration to event magnitudes. This data was derived by means of investigation of past events as well as from indications identified in the catchment area.

Table 9: Scenarios supplied by BGC Engineering

Return Period (yrs)	Volume Estimate (m ³)	Sediment concentration (%)	Peak* Flow (m ³ /s)	Hydro-Geomorphic Processes	ID	Model Runs and Assumptions
< 10	< 6,000	0	-	Flooding		No run
10 to 30	30,000	10	30	Flooding/ Debris flood	1	ERBC performs to capacity
30-100	40,000	20	50	Debris flood	2	ERBC performs to capacity
100 to 300	60,000	20	60	Debris flood/LDOF	3a	ERBC performs to capacity
					3b	ERBC is blocked
300 to 1000	160,000	30	700	LDOF	4	ERBC is blocked
1000 to 3000	260,000	30	1000	LDOF	5	ERBC is blocked
No mitigation ¹	90,000	20	80	Debris flood	6	ERBC performs as it is kept open artificially

LDOF = landslide dam outbreak flood, ERBC = Elk Run Boulevard culvert, ¹ represents June 2013 event, * Peak flow as reported here is the total discharge including the sediment in transport.

04.08 Flood Hydrology

The Flood Hydrology is comprehensively discussed in Appendix J. Relevant hydrological parameters and design values, as well as design hydrographs, are listed in chapter 09 - Hydrotechnical Design.

04.09 Surveys

04.09.01 Bare Earth LiDAR Data, Province of Alberta

On June 28, 2013, the company LSI LiDAR Services International Inc. conducted an airborne LiDAR survey of the Town of Canmore and Bow River valley covering a total area of 53 km². The data was recorded with an average ground sampling distance of 0.42m and delivered as a set of LAS- and ASCII-files. Further details are listed in the LiDAR survey report by LSI Inc. Different to the data specifications in the corresponding report, the spatial reference of the point clouds delivered is NAD83 (CSRS) / UTM Zone 11N rather than NAD83 / Alberta 3TM 114W:

Table 10: Specifications of NAD 83 (CSRS) / UTM Zone 11N

Specifications of NAD83 (CSRS) / UTM Zone 11N	
EPSG Code:	2955
WGS84 Bounds:	Longitude: -120.0000° to -114.0000°; Latitude: 49.0000° to 79.0000°
Central Meridian:	117° W
False Easting:	50,0000.0m
False Northing:	0.0 m
Area Used:	Canada: 120° W to 114° W

A map with topographical details is shown in the design drawing LTMM CC-GEN-002)

04.09.02 Bare Earth UAV LiDAR Data, Survey 2014, Town of Canmore

On June 19, 2014, the company Postflight Terra 3D conducted a LiDAR survey via an UAV to generate a high-resolution terrain model of the lower Cougar Creek channel section. The survey covered an area of 2.0167 km² with an average ground sampling distance of 0.0655m. Further details are listed in the quality report by Postflight Terra 3D. The spatial reference for the data is NAD83 (CSRS) / UTM Zone 11N. The data was used to compile a detailed topographical dataset, which was used as design basis.

04.09.03 Channel Survey as built 2013, ISL-Engineering Ltd.

From August 10 – 11, 2013, ISL Ltd. conducted a topographic survey of the lower Cougar Creek channel section available as AutoCAD drawing with contour lines with an interval of 0.5 m.

The spatial reference for the data is NAD83 / Alberta 3TM 114W (reference meridian):

Table 11: Specifications of NAD 83 / Alberta 3TM 114W

Specifications of NAD83 / Alberta 3TM 114W	
EPSG Code:	3776
WGS84 Bounds:	Longitude: -115.5000° to -112.5000°; Latitude: 49.0000° to 60.0000°
Central Meridian:	114° W
False Easting:	0.0 m
False Northing:	0.0 m
Area Used:	Canada: 115.5° W to 112.5° W

04.09.04 Quality Control

For a quality assessment within the design project, the digital terrain models that were generated from the LiDAR data were compared to the recorded ground control points (GCP) from the UAV LiDAR survey. Therefore, the location heights at the locations of the GCP were taken from the digital terrain models (DTM)

and compared to corresponding GCP, that are listed in the survey report with longitude, latitude and height [MASL]. The spatial reference for the data is NAD83 (CSRS) / UTM Zone 11N.

A maximum divergence between ground control points and the terrain model data of -0,099m was found and the digital model is to be classified as sufficiently precise for the design. Regardless of that, ahead of construction, a detailed site survey will be required.

04.10 Site Access

Access to the construction site is on paved roads up to Cougar Creek. The rest of the access to the site is on a gravel road along the creek. A permanent access road to the crest of the structure will be constructed, mainly by cutting into the creek embankment slopes following standard forestry practices.

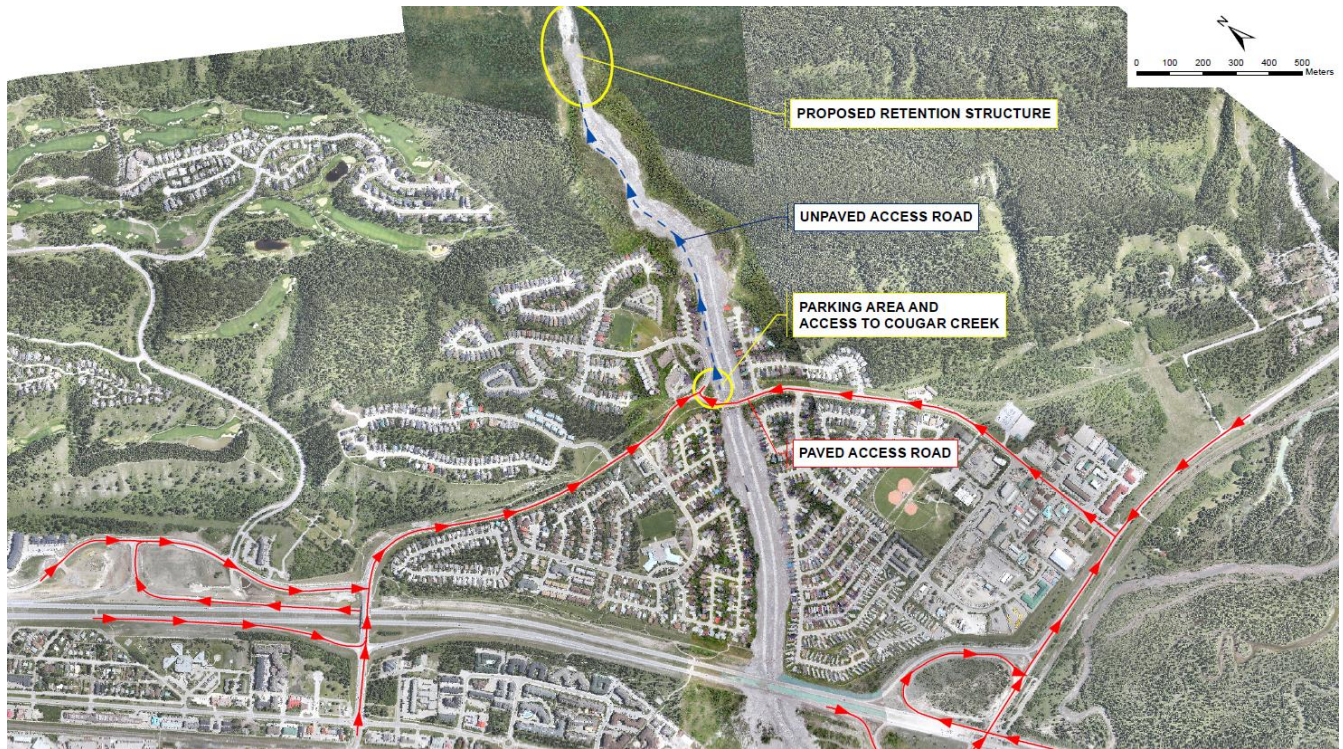


Figure 21: Access to the construction site by paved and unpaved roads

05 DESIGN CRITERIA AND REQUIREMENTS

05.01 Selection of Dam Construction Concept

05.01.01 Main functional Criteria

The proposed structure is a debris-flood retention structure for retention and controlled discharge of inflowing floodwater. If impoundment takes place, gravel debris starts to aggrade at the apex of the retention basin and wooden debris could potentially float towards the retention structure. The wooden debris is retained by the debris rake to keep the bottom outlet, in particular the throttle, clear of obstruction for discharge. At full impoundment, the throttle allows for a discharge rate of 45m³/s. Alternative discharge rates can be realized by adjusting the mounting position of the throttle at a different installation height. However, the throttle is not adjustable during a flood event.

Because impoundment is comparatively rare, the long-term behavior of the structure under loading conditions cannot be observed accordingly. Therefore, all elements need to be robust even though, contrary to dam structures for hydroelectric generation, no permanent loading is given. In addition, the bottom outlet structure has to allow for a comparatively high discharge for the normal operating conditions. This requires an opening in the impervious core of the structure, normally avoided for dam structures.

If flood retention is intended, a certain level of protection needs to be defined. All floods within this level of protection will be retained and all floods exceeding this level will utilize the spillway and the stilling basin. As the length of the dam crest is comparatively short, the full width of the structure is designed for overtopping. Therefore a separate spillway has not been designed.

Addressing specific constraints and functional criteria, a number of structure types have been considered within recent mitigation projects. For occasionally impounded retention structures, a rock or earth fill embankment dam with a reinforced concrete seal wall and a reinforced bottom outlet, structurally connected to the seal wall, turned out to be the most suitable solution. In many cases, the concrete seal wall forms a trapezoidal overflow section for the spillway. The thickness of the seal wall depends on the structure height and on the stress-strain behaviour of adjacent fill material.

05.01.02 Selected Construction Type

The selected construction is a type “Lankowitzbach” structure (Scheikl, Fieger, & Ribitsch, 2015). It is based on the general concept of the well investigated embankment dam “Bockhartsee”, a hydropower embankment dam in Salzburg, Austria (Schober, 1987) and on the Sösetalsperre (Campen, 2002), an embankment dam for another hydropower plant in Germany. Both structures as well as type Lankowitzbach are zoned rock and earth fill embankment dams with a central concrete core wall. The core wall of the Lankowitzbach flood retention structure is tied into abutment trenches, which are cut into the pre-treated, grouted bedrock. The Bockhartsee structure, as well as Lankowitzbach and Sösetalsperre, are equipped with a vertical drainage layer downstream of the concrete seal wall, which is connected to a horizontal drainage layer at the footprint of the downstream embankment. At the Lankowitzbach structure, a vertical layer of impervious soil is placed upstream of the concrete seal wall and a bottom outlet structure feeds through the embankment structure and the concrete seal wall, similar as to the situation at the Sösetalsperre (Franke, 2001).

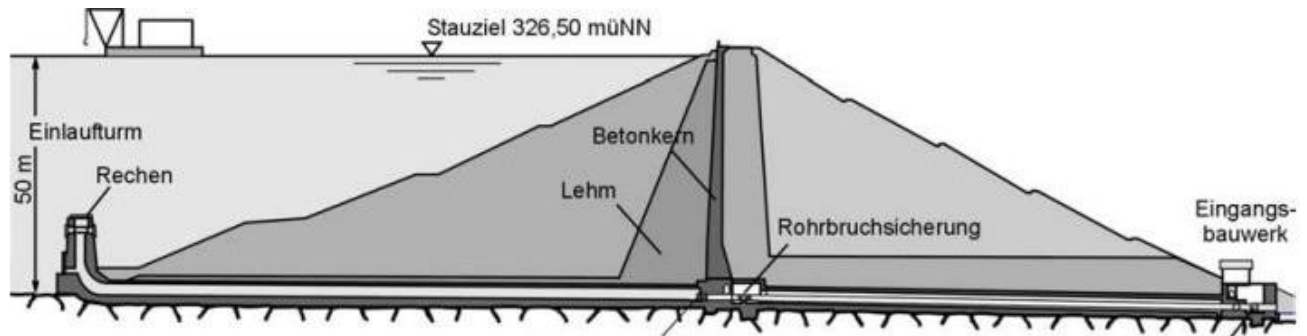


Figure 22: Dam construction concept of the Sösetalsperre (Campen, 2002)

05.01.03 Investigation of alternative Concepts

In the course of the detailed design, alternatives for the seal wall, as well as for the bottom outlet structure, have been investigated. The outcome of this investigation is presented in the memorandum on the investigation of alternatives for the bottom outlet structure and the seal wall design.

The following options for the bottom outlet structure were investigated:

- The base design, a segmental, box-shaped, reinforced cast-in-place bottom outlet structure aligned straight in the creek centerline, which feeds through the seal wall of the retention structure. It is placed on the alluvium, which is treated with ground improvement measures such as jet grouting to reduce differential settlements.
- Option 1, a segmental, box-shaped, reinforced cast-in-place bottom outlet structure placed on a rock-slope-cut at the orographic left (southeastern) abutment of the retention structure, aligned along the rock face with curves.
- Option 2, a mined diversion tunnel around the southeastern side of the retention structure.

The left abutment was selected for the optional alignment of the bottom outlet structure, because it appears to be more stable.

The following options for the cut-off in the alluvium and the seal wall in the embankment dam were discussed:

- The base design, a combination of a secant pile wall with reinforced secondary piles intersecting primary piles, socketed into bedrock with a minimum of 1m, and a segmented reinforced, cast-in-place concrete wall with expansion joints and flexible water stops between wall segments.
- Option 1, a mixed in place wall using a double cutter hydro-phrease and cement slurries for seepage cut-off in the alluvium and for establishing the seal wall core of the embankment dam. The construction would be performed top-down from the dam crest. This option requires the BOS in a diversion tunnel.
- Option 2, an asphalt concrete core placed on a special formed and pretreated plinth which is structurally connected to the secant pile wall. At the abutments, a steep plinth is tied into a pre-grouted bedrock trench.

With respect to the cut-off wall, after review and evaluation of all technical aspects, including value engineering and cost comparison, the selection of the base design, including an adjustment of the structural layout (such as eliminating the expansion joints and using shrinkage compensating concrete), was recommended.



With respect to the bottom outlet structure, the evaluation of alternatives shows that both options, the tunnel and the bottom outlet structure at the abutment, would increase the project cost.




Therefore, the base design, considering the optimization of joint details, as well as of ground improvement as shown in the corresponding sections of the memorandum and supported by calculations in Appendix B of the memorandum, was recommended.


However, it is believed that there may be a benefit for the Town of Canmore to take advantage of the current slowdown in mining and thus receive competitive pricing for the tunnel option as well. Therefore, including the tunnel option in the bid documents, and letting Contractors bid on both options was recommended.

05.01.04 Examples of recent Flood and Debris Retention Structures

Structure and Description of Elements	Photos
<p>Flood Retention Structure Lankowitzbach, Austria.</p> <p>Earth and rock fill embankment dam with a reinforced concrete seal core and a bottom outlet structure feeding through the concrete core. The spillway consists of a trapezoidal section at the crest, an armored channel at the downstream slope and a stilling basin at the toe of the downstream slope.</p>	
<p>Flood Retention Structure Lankowitzbach, Austria.</p> <p>Backfill at an immediate construction stage at the upstream embankment.</p>	

Structure and Description of Elements	Photos
<p>Flood Retention Structure Lankowitzbach, Austria.</p> <p>Intake of the bottom outlet structure with a debris rake, which is partly finished.</p>	 A photograph showing the intake of a bottom outlet structure. The structure consists of several parallel, angled metal debris rakes supported by concrete pillars. The structure is situated in a rocky, excavated area with a concrete channel leading away. The background shows a grassy hillside under a clear blue sky.
<p>Flood Retention Greinbach, Austria.</p> <p>Construction of the spillway with a stone armored shell (lining) placed on reinforced concrete, adjacent to the reinforced concrete seal wall.</p>	 A photograph showing the construction of a spillway. A large, rectangular area of reinforced concrete is visible, with a grid of steel rebar exposed. A stone armored shell (lining) is being placed on top of the concrete. The structure is adjacent to a reinforced concrete seal wall. The background shows a rural landscape with yellow flowers and buildings.

Structure and Description of Elements	Photos
<p>Flood Retention Greinbach, Austria.</p> <p>Intake of the bottom outlet structure with a debris rake.</p>	
<p>Flood Retention Greinbach, Austria.</p> <p>Throttle opening upstream of the baffle plate, protected by the debris rake.</p>	
<p>Debris Flood Retention Gstocketbach, Austria.</p> <p>Outflow structure with baffle plate (throttle behind piled-up riprap is not visible) and reinforced concrete seal wall partly refilled.</p>	

Structure and Description of Elements	Photos
<p>Debris Flood Retention Gstocketbach, Austria.</p> <p>Backfilling of the reinforced concrete seal wall with cement and lime stabilized soil.</p>	

05.02 Dam Performance Criteria

Design earthquake levels according to Chapter 7 - Table 1, CDA - Dam Safety Guidelines (CDA, 2007) are listed in Table 12. Assuming a very high consequence class dam, an earthquake design ground motion with a return period of 5,000 years would need to be applied for normal operating conditions, which is steady state full impoundment. This is to be applied for structures with permanent storage such as power generation or water supply storage structures. Because a flood retention structure is not impounded permanently, but empty for most of the time, this criterion for ground motion has been applied to the dry dam only. Additionally, the critical seismic coefficient was analyzed for the dry as well as for the fully impounded structure. Details regarding dam stability are listed in chapter 10.04.

Table 12: Suggested Design Earthquake Levels according to CDA Guidelines Table 1 (CDA, 2007)

Dam Class	AEP EDGM [Note 1]
Low	1/500
Significant	1/1,000
High	1/2,500
Very High	1/5,000 [Note 2]
Extreme	1/10,000 [Note 2]
<p>Acronyms: AEP, annual exceedance probability; EDGM, earthquake design ground motion</p> <p>Note 1. AEP levels for EDGM are to be used for mean rather than median estimates of the hazard</p> <p>Note 2. The EDGM value must be justified to demonstrate conformance to societal norms of acceptable risk. Justification can be provided with the help of failure modes analysis focused on the particular modes that can contribute to failure initiated by a seismic event. If the justification cannot be provided, the EDGM should be 1/10,000.</p>	

05.03 Geotechnical Design Criteria and Requirements

05.03.01 Slope Stability including Seismic Design Criteria

The National Building Code of Canada (NRC, 2010) suggests earthquakes with a probability of exceedance of 2% in 50 years (annual probability of exceedance of 1/2,475) for seismic slope stability analysis. This criterion would be applicable for the dry embankment dam slopes.

The Highway Bridge Design Code (S6-14) (CSA, 2014) proposes the same annual probability for a pseudo-static limit-equilibrium slope stability analysis. In addition, the Highway Bridge Design Code requires for the application of seismic loads as horizontal and vertical seismic coefficients. These shall not be lower than one-half of the corresponding peak ground acceleration.

The selected design criterion (annual probability of exceedance of 1/5,000) is above the mentioned criterion, appearing reasonable because of greater consequences in case of an earthquake induced dam breach.

05.03.01.01 Required Factors of Safety (FoS) according to the CDA Guidelines

Table 13: Factors of Safety for Slope Stability

Loading conditions	Minimum factor of Safety [Note 1]	Slope
End of construction before reservoir filling. For a retention structure the normal and "dry condition"	1.3	Upstream and Downstream
Long-term (steady state seepage, normal reservoir level)	1.5	Downstream
Full or partial rapid drawdown	1.2 – 1.3 [Note 2]	Upstream
Note 1: Factor of safety is the factor required to reduce operational shear strength parameters in order to bring a potential sliding mass into a state of limiting equilibrium, using generally accepted methods of analysis. Note 2: Higher factors of safety may be required if drawdown occurs relatively frequently during normal operation.		

Table 14: Factors of Safety for Slope Stability

Loading conditions	Minimum factor of Safety	Slope
Pseudo static	1.0	Upstream and Downstream
Post-earthquake	1.2-1.3	Upstream and Downstream

05.03.01.02 FoS According to Engineering Guidelines for Evaluation of Hydro-Power Projects

The required factors of safety for slope stability of embankment dams are defined in the Engineering Guidelines for Evaluation of Hydro-Power Projects (Federal Energy Regulatory Commission (FERC), 2006) as listed in Table 15.

Table 15: Factors of Safety for Slope Stability

Loading conditions	Minimum factor of Safety	Slope
End of construction condition	1.3	Upstream and Downstream
Sudden drawdown from maximum pool	> 1.1	Upstream
Sudden drawdown from spillway crest or top of gates	1.2	Upstream
Steady seepage with maximum storage pool	1.5	Upstream and Downstream

Loading conditions	Minimum factor of Safety	Slope
Steady seepage with surcharge pool	1.4	Downstream
Earthquake (for steady seepage conditions with seismic loading using a pseudo static lateral force coefficient)	> 1.0	Upstream and Downstream

05.03.01.03 FoS according to Landslide Assessment Guidelines in British Columbia

The guidelines for Legislated Landslide Assessments for Proposed Residential Development in British Columbia are listing required factors of safety according to Table 16.

Table 16: Accepted Factors of Safety for Slope Stability for BC

Loading conditions	Minimum factor of Safety	Slope
Static Condition	1.5	Upstream and Downstream
Newly Constructed Slopes under Pseudo-Static Seismic Analysis	1.1	Downstream

05.03.02 Design Criteria for Grading

Depending on the general fill material characteristics and the material characteristic of the footprint, the grading of dam zones needs to meet the requirements according to Table 17, Table 18 and Table 19, resulting in particular basic filter criteria for the proposed dam zones and on site material as listed in Table 20.

The filter criteria introduced by Terzaghi (1922) is generally more relevant for interfaces between coarse-grained materials, whereas Sherard & Dunnigan (1985) address stability aspects relevant for fine grained material. It has to be noted, that the criteria introduced by Terzaghi (1922) address filter stability and permeability. Filter stability is of primary importance for the grading design of fill material. For the design of the filter layer both criteria are relevant and need to be fulfilled because the dam construction concept of proposed retention structure contains coarse-grained and highly permeable fill material to assure slope stability for rapid drawdown as well as for fine grained material used in the embankment.

Table 17: Filter Criteria according to Terzaghi (1922)

No.	Design Criteria	D15F
1	Filter Stability Criteria	$D_{15F} < 4 * d_{15B}$
2	Permeability Criteria	$D_{15F} > 4 * d_{15B}$

Table 18: Criteria for Base soil categories according to the U.S. Army Corps of Engineers (2004) based on Sherard & Dunnigan (1985)

Base Soil Category	% finer than 0.075 mm	Design Criteria
1	≥ 85 %	$D_{15F} \leq 9 * d_{85B}$ but not less than 0.2 mm
2	40 – 85 %	$D_{15F} \leq 0.7$ mm
3	15 – 40%	$D_{15F} \leq 0.7 \text{ mm} + \frac{(40 - A) * 4 * d_{85B} - 0.7 \text{ mm}}{25}$ $A = \% \text{ passing } 0.075 \text{ sieve after regrading}$ $(4 * d_{85B} \geq 0.7 \text{ mm})$
4	< 15 %	$D_{15F} \leq 4 * d_{85B}$ of base soil after regrading

¹ Category designation for soil containing particles larger than 4.75 mm is determined from a gradation curve of the base soil, which has been adjusted to 100% passing the No. 4 (4.75 mm) sieve.

² Filters are to have a maximum particle size of 3 in. (75 mm) and a maximum of 5% passing the No. 200 (0.075 mm) sieve with the plasticity index (PI) of the fines equal to zero. PI is determined on the material passing the No. 40 (0.425 mm) sieve in accordance with EM 1110-2-1906.

Base Soil Category	% finer than 0.075 mm	Design Criteria
³ To ensure sufficient permeability, filters are to have a D ₁₅ size equal to or greater than 4 x D ₁₅ but no smaller than 0.1 mm.		

Table 19: Gradation limits for prevention of segregation for coarse filters according to the U.S. Army Corps of Engineers (2004)

Minimum D _{10F} [mm]	Maximum D _{90F} [mm]
< 0.5	20
0.5 – 1.0	25
1.0 – 2.0	30
2.0 – 5.0	40
5.0 – 10	50
10 - 50	60

To prevent gap graded fill material from segregation during transport and compaction, a certain limit of unconformity must not be exceeded as defined by Equation 8.

$$C_u = \frac{D_{60}}{D_{10}} \leq 6 \quad \text{Equation 8}$$

where

- C_u Number of unconformity
- D₆₀ Diameter of particles of 60 percent cumulative weight passed
- D₁₀ Diameter of particles of 10 percent cumulative weight passed

Table 20: Resulting and relevant filter criteria for dam zones and on site material

Base Soil	Dam Zone	Terzaghi Design Criteria	% finer than 0.075 mm	Base Soil Category	Sherard Design Criteria
Lafarge	1 - Outer Support Body	2.4 ≥ D _{15F} ≥ 72 mm 20 ≥ D _{15F} ≥ 560 mm	11.0	4	D _{15F} ≤ 18 mm
Stoneworks Creek	2 - Inner Support Body	0.72 ≥ D _{15F} ≥ 56 mm 20 ≥ D _{15F} ≥ 300 mm	17.0	3	D _{15F} ≤ 16.83 mm
Stewart Creek	3 – Deceleration Zone	0.004 ≥ D _{15F} ≥ 2 mm 0.012 ≥ D _{15F} ≥ 28 mm	63.0	2	D _{15F} ≤ 0.7 mm
-	6 – Protection Layer	1.0 ≥ D _{15F} ≥ 18 mm 2.04 ≥ D _{15F} ≥ 60 mm	6.41	4	D _{15F} ≤ 8,4 mm
Cougar Creek Alluvium	On Site Material	0.072 ≥ D _{15F} ≥ 56 mm 20 ≥ D _{15F} ≥ 300 mm	17.0	3	D _{15F} ≤ 16.83 mm

05.04 Structural Design Criteria and Requirements

05.04.01 Design Codes

- Reinforced concrete design is according to CAN/CSA A23.3-14, "Design of Concrete Structures".
- Durability requirements for reinforced concrete structures are according to ACI 350-01, "Code Requirements for Environmental Engineering Concrete Structures".
- Structural steel design is according to CAN/CSA S16.1-09, "Design of Steel Structures".

05.04.02 Materials

- Concrete with compressive strength $f'_c = 35$ MPa after 28 days.
- Steel reinforcement of deformed high tensile steel bars grade 400 to CAN/CSA G30.18 (yield stress $f_y = 400$ MPa).
- Structural Steel shapes to CAN/CSA G40.2/G40.21 grade 350W for rolled shapes and grade 350W class H for HSS sections.
- Steel bolts are of high tensile steel conforming to ASTM A325M.
- Anchor bolts are to ASTM A307M.

05.04.03 Loads and Load Factors

Structures are designed to carry the governing cases of loading under the most onerous load combinations. Acting loads include the self-weight, internal and external water and earth pressure with the following basic assumptions:

- Unit weight of reinforced concrete = 25 kN/m^3 .
- Unit weight of dry fill = 23 kN/m^3 .
- Unit weight of saturated fill = 25 kN/m^3 .

Load factors are according to CSA A23.3-14, Annex C. The governing load combinations are:

- Serviceability Limit State (SLS) = $1.0 \times D + 1.0 \times H + 1.0 \times F$
- Ultimate Limit State (ULS) = $1.25 \times D + 1.5 \times H + 1.5 \times F$

05.04.04 Reinforced Concrete Design

- Reinforced concrete design is governed by the durability requirements for the SLS. All sections are checked for crack width limitations according to code requirement.
- The ULS will be automatically satisfied if the service steel stress is below the following limit:
- Maximum service steel stress = (yield stress 400 MPa) \times (capacity reduction factor 0.85) / (maximum load factor 1.5) = 226 MPa
- Otherwise, the ULS is checked using factored loads and interaction diagrams.

05.04.05 Structural Analysis

All analyses have been carried out using service loads and all structures are analyzed using 1D or 2D models and an elastic material model.

The following software was used for structural analysis:

- Phase2 v6.0 by Rocscience Inc.
- Plaxis 2D v2016 by Plaxis B.V.
- Abaqus v6.13 by Dassault Systèmes.
- PCAcol v3.0 by Portland Cement Association.
- Excel spreadsheets to check the service stresses in rectangular concrete sections at the Serviceability Limit State for crack control.

05.04.06 Environmental Conditions and Durability

- Groundwater salinity for the Canmore Dam site is minimal according to the chemical analysis as listed in the geotechnical investigation report (Thurber Engineering Ltd., 2015b).
- Clear concrete cover to reinforcement is 50 mm.
- Maximum allowable crack width is 0.27mm, corresponding to the normal sanitary exposure category of ACI 350-01.
- There is no waterproofing of reinforced concrete structures necessary unless otherwise noted.

05.05 Hydraulic Design Criteria and Requirements

The Dam Safety Guidelines (CDA, 2007) do not list mandatory design criteria for flow control structures. Therefore, the flow control for the proposed retention structure was exclusively based on best engineering practice as well as experience gained by the physical modeling tests.

As outlined in the part 6 of the Dam Safety Guidelines (CDA, 2007), spillway design should be in accordance with the declarations of the USBR (1987) and based on best engineering practice.

05.06 Codes and Standards

Table 21 lists relevant codes and guidelines applied for the design of the structure.

Table 21: Relevant and applicable design codes and guidelines

Subject	Nr.	Title	Issue
Structural Loads			
ONR	24800	Austrian Design Code Protection Works for Torrent Control – Terms and their definitions as well as classification	2009-02-15
ONR	24801	Austrian Design Code Protection Works for torrent control – Static and dynamic actions on structures	2013-08-15
Design of Concrete and Steel Structures			
NRC	NBC	National Building Code of Canada	2010
NRC	ABBC	Alberta Building Code Volume 1 and 2	2014
CSA	A23.3-14	Design of Concrete Structures	2014
CSA	S16-14	Canadian Highway Bridge Design Code	2014
CSA	A23.1-14	Concrete materials and methods of concrete construction	2014
CSA	A23.2-14	Test methods and standard practices for concrete	2014
CAN/CSA	S269.3-M92	Concrete Formwork	2013
ONR	24802	Protection Works for torrent control – Design of structures	2011 01 01

Dam Design and Design of Foundations			
CDA		Technical Bulletins of the CDA	2006/2013
CGS		Canadian Foundation Engineering Manual and actual Errata	2006
T10-99		Foundation Design, Ministry of Transportation of BC	
ATC-49		Recommendations LRFD Guidelines for the Seismic Design of Highway Bridges, BC Ministry of Transportation	
		Manual of Control of Erosion and Shallow Slope Movement, BC Ministry of Transportation	1997
CAN/CSA	S6-06	CSA S6-06 and the BC supplement to CSA S6-06	
Grouting			
ISRM		Report on the Commission on Rock Grouting	1996
U.S. Army Corps of Engineers	EM 1110-2-3506	Grouting Technology	1984
API	SP 13B-1	Recommended Practice for Field Testing Water-Based Drilling Fluids	1997
ASTM	C109	Standard Test Method for Compressive Strength of Hydraulic Cement Mortars	
ASTM	C150	Standard Specification for Portland Cement	
ASTM	C191	Standard Test Method for Time of Setting of Hydraulic Cement by Vicat Needle	
ASTM	C494	Standard Specification for Chemical Admixtures for Concrete	
ASTM	C595	Standard Specifications for Blended Hydraulic Cements	
ASTM	C939	ASTM C939 Standard Test Method for Flow of Grout for Preplaced- Aggregate Concrete	
ASTM	C940	Standard Test Method for Expansion and Bleeding of Freshly Mixed Grouts for Preplaced-Aggregate Concrete in the Laboratory	
ASTM	C1602	Standard Specification for Mixing Water Used in the Production of Hydraulic Cement Concrete	
ASTM	D2113	Standard Practice for Diamond Core Drilling for Site Investigation	
ASTM	D4044	Standard Test Method (Field Procedure) for Instantaneous Change in Head (Slug) Tests for Determining Hydraulic Properties of Aquifers	
ASTM	D4380	Standard Test Method for Density of Bentonitic Slurries	
ASTM	D6910	Standard Test Method for Marsh Funnel Viscosity of Clay Construction Slurries	

06 DESIGN REQUIREMENTS

06.01 Design Approach

06.01.01 Hazard Mitigation and Level of Protection

The structure is for mitigating storm related debris-floods and landslide dam outbreak floods from the Cougar Creek catchment. The level of protection is defined by the accepted residual risk, resulting from frequencies of floods, not retained by the structure. This determination has been done by BGC Engineering Ltd. within risk assessments (BGC Engineering Ltd., 2014, 2015). Input data, including flood discharges and related frequencies, which are based on the hydrological analysis (Appendix J), are provided by CHT.

06.01.02 Structure Type

The selection of the structure type is part of the design process and the main functional criteria are listed in section 05.01. Addressing specific constraints and functional criteria, a number of structure types have been constructed for comparable mitigation projects. For occasionally impounded retention structures, a rock or earth fill embankment dam with a reinforced concrete seal wall and a reinforced bottom outlet, feeding through the concrete seal wall, turned out to be the most suitable and robust solution. The thickness of the seal wall depends on the height and on the characteristics of adjacent fill material. The spillway is armored for protection against erosion.

06.01.03 Complementary Grade Control

To increase the capability of the existing channel, in particular of the culverts capacity to discharge flood water, containing bedload, the inflow situation and critical sections of the channel shall be updated in the long-term.

06.01.04 Design Life

The design life of the structure is at least 500 years, regardless of the level of protection provided. The design life is considered in the general design approach and the longevity of the structure will be assured by means of subsequent and ongoing inspection and maintenance. In general, the proposed construction type of an earth and rock-fill dam is of high robustness and durability. Sealing measures and seepage cut-off measures are proposed to be constructed with reinforced concrete, which are buried and not exposed to the environment. Because the very long-term durability of concrete is not well understood, recurring checks are required and if indicated, rehabilitation has to be done. An impervious earth-fill material upstream of the monolithic joint-less concrete seal wall is incorporated in the design. This layer is durable and normally maintenance free. Freestanding concrete structures, which are exposed to the environment, need to be inspected more frequently.

06.01.05 Dam Classification

Assuming full impoundment as a normal operating state and applying the classification scheme given by the guidelines of the CDA, the proposed retention structure would be classified as a "very high consequence dam". However, full impoundment is very rare and is expected to occur with an estimated return period of approximately 100 years or more. Considering a dry dam, the structure should not be considered as a water retaining or water storing, but as a water diversion structure. Nevertheless, a detailed analysis of the dam stability and dam deformation under consideration of ground movement needs to be performed and earthquake assessment is obligatory. The classification scheme of the CDA is listed in Table 22.

Table 22: Dam Classification according to Table 2-1 CDA Dam Safety Guidelines (2007)

Dam Class	Population at risk [Note 1]	Incremental losses		
		Loss of life [Note 2]	Environmental and cultural values	Infrastructure and economics
Low	None	0	Minimal short-term loss No long-term loss	Low economic losses; area contains limited infrastructure of services
Significant	Temporary only	Unspecified	No significant loss or deterioration of fish or wildlife habitat Loss of marginal habitat only Restoration or compensation in kind highly possible	Losses to recreational facilities, seasonal workplaces, and infrequently used transportation routes
High	Permanent	10 or fewer	Significant loss or deterioration of important fish or wildlife habitat Restoration or compensation in kind highly possible	High economic losses affecting infrastructure, public transportation, and commercial facilities
Very high	Permanent	100 or fewer	Significant loss or deterioration of critical fish or wildlife habitat Restoration or compensation in kind possible but impractical	Very high economic losses affecting important infrastructure of services (e.g., highway, industrial facility, storage facilities for dangerous substances)
Extreme	Permanent	More than 100	Major loss of critical fish or wildlife habitat Restoration or compensation in kind impossible	Extreme losses affecting critical infrastructure or services (e.g., hospital, major industrial complex, major storage facilities for dangerous substances)

Note 1. Definitions for population at risk:

None – There is no identifiable population at risk, so there is no possibility of loss of life other than through unforeseeable misadventure.

Temporary – People are only temporarily in the dam-breach inundation zone (e.g., seasonal cottage use, passing through on transportation routes, participating in recreational activities).

Permanent – The population at risk is ordinarily located in the dam-breach inundation zone (e.g., as permanent residents); three consequence classes (high, very high, extreme) are proposed to allow for more detailed estimates of potential loss of life (to assist in decision-making if the appropriate analysis is carried out).

Note 2. Implications for loss of life:

Unspecified – The appropriate level of safety required at a dam where people are temporarily at risk depends on the number of people, the exposure time, the nature of their activity, and other conditions. A higher class could be appropriate, depending on the requirements. However, the design flood requirement, for example, might not be higher if the temporary population is not likely to be present during the flood season.

06.02 Design Assumptions and Loadings

06.02.01 Geotechnical Design Parameters

The geotechnical design baseline is presented in detail in the Geotechnical Design Basis Memorandum (LTMM CC - M - GTDB-01). The characteristic mechanical and geo-hydraulic material parameters are listed in Table 23. Parameters are based on information, derived from third reports and test results, provided by Thurber Engineering Ltd. (2014 and 2015), from Waterline Resources Inc. (2015), Century Wireline Services (2015), as well as from Golder Associates (2015a). One point loading stiffness parameters were derived from preliminary triaxial-tests performed by Golder Associates (2015b). Further, Canadian Hydrotech Corp. performed plate-loading tests, to obtain stiffness parameters for loading and unloading sequences required for the application of hyperbolic stress strain models. The listed characteristic parameters are for structural and geotechnical FE analysis and for limit state stability analysis if materials are not specified by nonlinear shear functions. With availability of further test results, parameters might possibly change and adjustment might be required. For limit state stability analysis the angle of dilatancy was neglected.

Table 23: Characteristic design values for material parameters – part 1

Fill Material	Zone 01	Zone 02	Zone 03	Zone 06 and 07
	Lafarge	Stoneworks Creek	Stewart Creek	Filter Material
$E_{50,ref}$ [MN/m ²]	95	88	45	88
$E_{s,ref}$ [MN/m ²]	85	79	41	79
$E_{u-r,ref}$ [MN/m ²]	300	278	145	278
M	0.35	0.35	0.35	0.35
γ [kN/m ³]	24	23	22	20
γ' [kN/m ³]	14	13	12	10
ϕ [°]	41	36	33	36
c [kN/m ²]	10	5	0	5
K [m/s]	$\approx 2 \cdot 10^{-5}$	$\approx 2,5 \cdot 10^{-5}$	$\approx 5 \cdot 10^{-7}$	$\approx 5 \cdot 10^{-3}$
Ψ [°]*	$\varphi/2$	$\varphi/2$	$\varphi/2$	$\varphi/2$
ν	0.25	0.3	0.3	0.3
Specific Storage Capacity	0.2	0.2	0.1	0.15

Table 24: Characteristic design values for material parameters - part 2

On Site Material	Alluvium	Sand/Silt Lenses	Rock	Grouted Rock
	Cougar Creek	Cougar Creek	Cougar Creek	Cougar Creek
$E_{50,ref}$ [MN/m ²]	95	45	-	-
$E_{s,ref}$ [MN/m ²]	85	41	-	-
$E_{u-r,ref}$ [MN/m ²]	300	145	-	-
M	0.35	0.35	-	-
E Young's [MN/m ²]			6,000	8,000
γ [kN/m ³]	23	23	26,5	27
γ' [kN/m ³]	13	13	16,5	17
ϕ' [°]	35	33	42	42
c' [kN/m ²]	2	0	50	100

On Site Material	Alluvium	Sand/Silt Lenses	Rock	Grouted Rock
	Cougar Creek	Cougar Creek	Cougar Creek	Cougar Creek
K [m/s]	$3 \cdot 10^{-5}$	$5 \cdot 10^{-6}$	$3 \cdot 10^{-6}$ (anisotropic)	$1 \cdot 10^{-6}$ (anisotropic)
Ψ [°]*	$\varphi/2$	$\varphi/2$	-	-
ν	0.3	0.3	0.15	0.1
Specific Storage Capacity	0.2	0.2	0.05	0.025

To account for stress dependent shear resistance of granular fill material, nonlinear shear functions for limit state stability analysis are applied. The derivation of these functions is presented in the Geotechnical Design Basis Memorandum (CHT 2016). Applied shear functions are the following:

Zone 1 Material

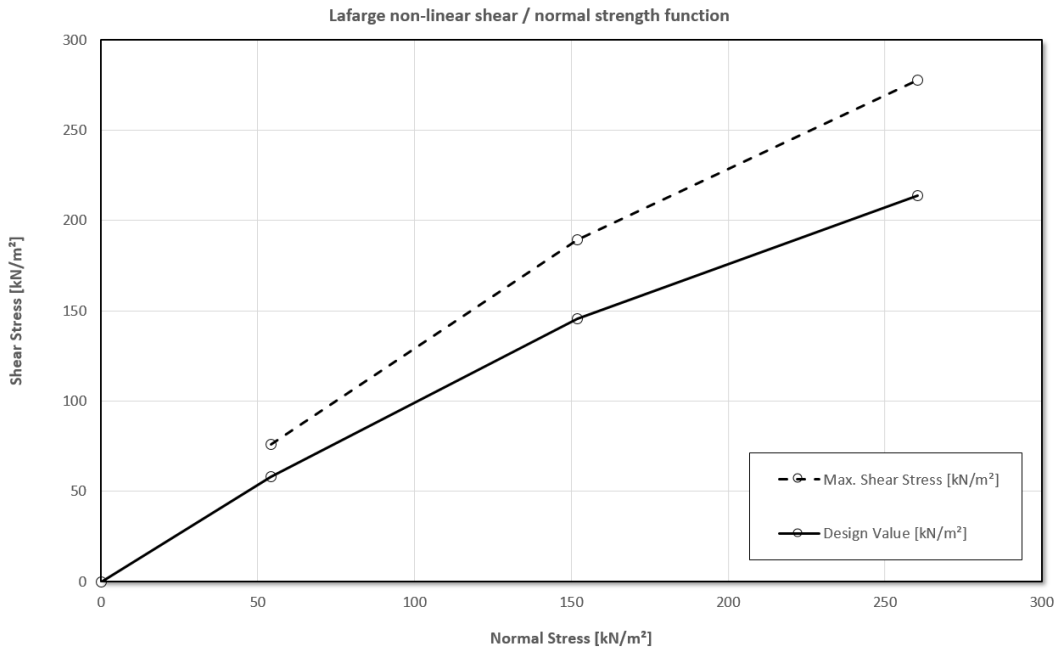


Figure 23: Non-linear shear function based on reduced shear data from Lafarge material below 64mm

Zone 2 Material and Cougar Creek Alluvium

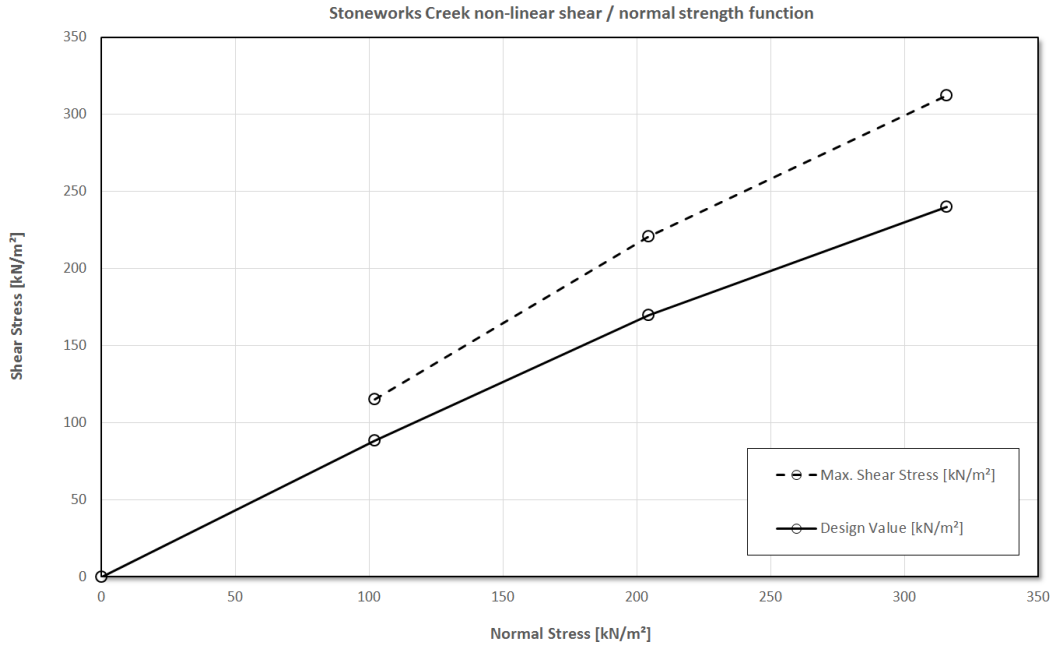


Figure 24: Non-linear shear function based on reduced shear data from Stoneworks Creek material

Zone 3 Material

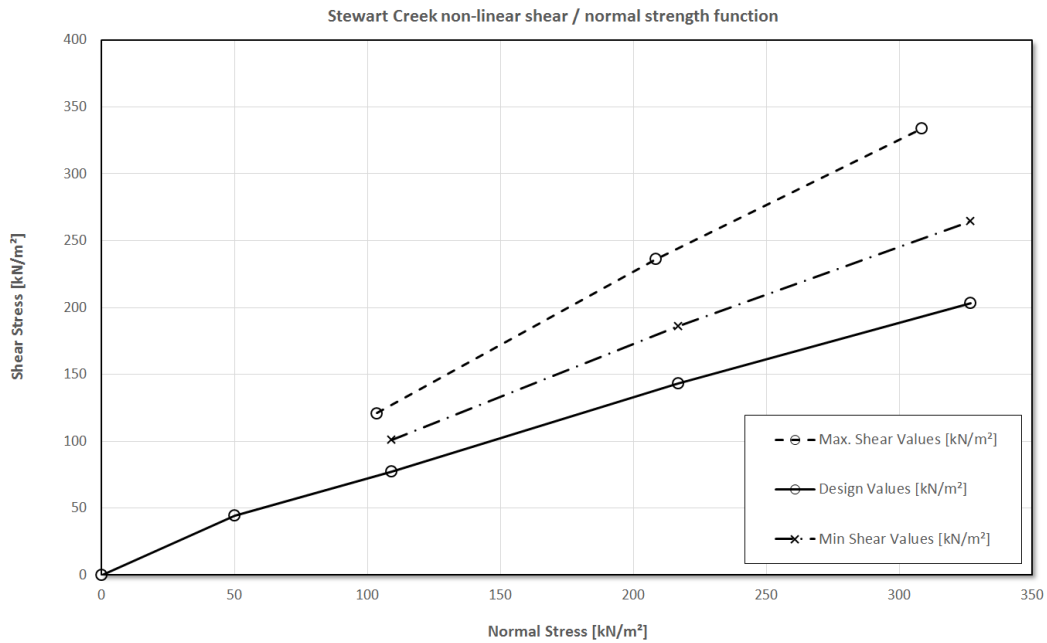


Figure 25: Non-linear shear function based on reduced shear data from Stewart Creek material

06.02.02 Loadings

06.02.02.01 Inflow Design Floods and Probable Maximum Flood

According to the Dam Safety Guidelines 2007 (Edition 2013) from the Canadian Dam Association, the probable maximum flood has to be assessed as basis for the design of a dam and water diversion structures. "Hydrological safety hazards include extreme rainfall and snowmelt events that can lead to natural floods of variable magnitude. The maximum flood for which the dam is to be designed or evaluated for is termed the Inflow Design Flood (IDF); the IDF should be selected on the basis of the potential consequences of failure." (Canadian Dam Association, 2013).

In the current design project, which is for a flood retention structure, IDF's are to be understood as a normal loading condition in a range for which the retention structure is dimensioned. Because the retention structure is not designed to retain all possible floods, the PMF needs to be estimated as a basis for the hydraulic design of the spillway and the stilling basin. The design value for the spillway flood is discussed in chapter 09.

06.02.02.02 Loading Conditions according to the CDA Guidelines

According to the Dam Safety Guidelines (CDA, 2007), all loading conditions a dam can be exposed to in its lifetime need to be defined and categorized with respect to the likeliness of occurrence. The level of conservatism used to establish acceptance criteria should reflect the probability of occurrence as well as the degree of variability, relative to the soil engineering properties selected for the analysis.

The following general loading conditions for assessing the stability of embankment dams can be listed:

Normal Loading Conditions

Normal loading conditions are those for which the structure is expected to experience during normal operations.

Unusual Loading Conditions

Unusual loading conditions may occur on an exceptional basis. In specific ways, they exert more stress onto the structure compared to normal loading conditions. Since these loads do not occur on an ongoing basis, a factor of safety lower than for the normal loading conditions is considered acceptable. Minor damage such as crest settlement, minor transverse cracking and small, permanent deformations can be accepted. However, the structure should continue to behave in a satisfactory and safe manner.

Extreme Loading Conditions

Extreme loading conditions are those that correspond to highly improbable events, which, if they occur, would be considered as emergency cases. The structure should be able to resist extreme loading conditions without failing, although the factors of safety may be low and the structure may be close to its ultimate limits. The functionality of the structure may be compromised and major repairs required, up to and including replacement. A detailed discussion and guidance on strength parameters relative to each loading case can be found in the Dam Safety Guidelines (CDA, 2007). In general, the geotechnical parameters used are preferably derived from laboratory tests that are most representative of the conditions involved in the analysis.

06.02.02.03 Considered Loading Conditions and Load Cases

Following load cases are currently considered:

Construction Conditions

These include all load cases that can occur during all stages of construction.

- Wind load on the free standing concrete core wall
- Uneven compaction of up- and downstream fill
- Uneven layer heights up- and downstream of the seal wall during filling
- Acting stresses on concrete parts due to confinement during filling and compaction

Normal Operating Conditions

As normal operating conditions, following impoundment levels and ground movement are considered:

Table 25: Normal operating impoundment levels (STL and SL)

Impoundment Level - Load Cases (STL)	Description
STL-A	Groundwater, End of construction
STL-B	Impoundment 1/3 of structure height
STL-C	Impoundment 1/2 of structure height
STL-D	Impoundment 2/3 of structure height
STL-E	full impoundment level
STL-H	STL-A after draw down
Seismic Load (SL)	Description
OBE / SL-1	1/1,000 – PGA (or 1/2,475) slope stability (Soil Class B according to DTM Report for the upper 30m below the structure)

Unusual Operating Conditions

As unusual operating conditions, following impoundment levels are considered:

Table 26: Unusual impoundment levels and ground movement (STL and SL)

Impoundment Level related Load Cases (STL)	Description
STL-F	overtopping
STL-G	Rapid Draw Down
Seismic Load (SL)	Description
-	-

Extreme Operating Conditions

As extreme operating conditions, the dry dam and earthquake induced ground movement for pseudo static analysis is considered as following:

Table 27: Seismic Load Cases (SL) for the stability analysis

Seismic Load (SL)	Description
SL-1	Serviceability Criteria: 1/5,000 (Soil Class B according to DTM Report for the upper 30m below the structure)

Load Combinations

The following load case combinations are considered:

Table 28: Load Case Combinations (LC)

Load Case Combination (LC)	Impoundment Level related Load case (STL)	Seismic Load (SL)	Operation Condition
A	A	-	normal
A-1	A	1	unusual
B	B	-	normal
C	C	-	normal
D	D	-	normal
E	E	-	normal
F	F	-	unusual
G	G	-	unusual
H	A	-	normal

06.03 Site Requirements

Site access will be established ahead of structure construction within pre construction works. A description of site access is given in chapter 04.10 and shown in drawing no. LTMM CC-GEN-011. Details of access ramps are shown in drawings LTMM CC-DAM-702 to LTMM CC-DAM-706.

A service, maintenance and observation area is located above the right abutment, accessible from the downstream access ramp.

06.04 Operating Requirements and Maintenance

The Operation, Maintenance and Surveillance (OMS) Manual has been prepared according to the Dam Safety Guidelines by the Canadian Dam Association (CDA, 2007). The document provides the operating staff with the required information to safely operate the structure and ensure its proper management.

06.05 Public Safety

Public safety issues are discussed in the Emergency Preparedness Plan (ERP), which is to be used as a guide to assist Emergency Planners in developing local response plans to deal with a major flood and/or dam breach at Cougar Creek debris flood retention structure. Local Authorities should use this plan as a guide to developing annexes to their existing Municipal Emergency Plans (MEP) that deal specifically with their response to a major flood and/or dam breach.

The plan specifically addresses what would happen downstream of the Cougar Creek debris flood retention structure, generally how people and property would be affected, and how emergency responders would be notified of any emergency involving a large flood, potential and/or imminent dam breach.

06.06 Regulatory Compliance

The design was carried out under consideration of the following regulatory guidelines:

- Dam Safety Guidelines by the Canadian Dam Association (CDA 2007 – 2013 Edition);

- Technical Bulletin of the Dam Safety Guidelines by the Canadian Dam Association (CDA 2007)
- Dam and Canal Safety Guidelines – Water Act – Water (ministerial) Regulation Part 6 of the Dam Safety and Water Projects Branch of Alberta Environment and Parks.

07 PRELIMINARY RISK ASSESSMENT

The Cougar Creek debris-flood retention structure is a protection structure to reduce flood risks for the Town of Canmore. However, it is a complex embankment dam construction of considerable height, associated with geotechnical challenges. In case of substantial impoundment or overtopping, loads lead to stresses, dam deformation and substantial loading of flow control equipment.

Generally, the design was done based on comprehensively acquired geotechnical and hydrological data under consideration of up-to date design codes, standards and engineering practice by a design team highly experienced with embankment dam and flood protection structures. Dam stability and grading design, as the most substantial aspects regarding dam failures, are discussed in chapter 09.

Regardless of aspects mentioned above the structure is related to following general risks:

- Unexpected geotechnical subsurface information and/or insufficient interpretation of ground conditions. This could lead to unexpected response of the ground to loading and structure deformation respectively, causing overstressing of the structure and failure.
- Insufficient information about hydrological data and incorrect derivation of the spillway flood causing overstressing of the spillway and erosion of abutments at the downstream slope.
- Very unlikely superposition of full impoundment and seismic events with ground movement greater than the analyzed seismic yield acceleration (critical seismic coefficient).
- Unobserved long term related disintegration of flow control equipment in particular at the spillway and subsequent loss of functional reliability.

The Emergency Response Plan provides all information required to handle incidences outside of usual operating conditions.

08 FACILITY DESCRIPTION

08.01 General Dam Construction Concept

The proposed dam construction concept consists of a zoned earth-rock fill dam with an impervious reinforced concrete seal wall. The concrete seal wall is structurally connected with a secant pile wall that cuts off seepage in the alluvium. The abutments of the concrete seal wall and the secant pile wall are keyed into the bedrock. Bedrock will be grouted ahead of dam construction to a remaining Lugeon value of 10 [l/m/min at a reference pressure of 10bar]. Structural grouting shall seal interfaces between improved bedrock and concrete structures as well as between the secant pile wall and the seal wall.

The structure is designed for very long durability and for minimizing maintenance. Therefore, all inaccessible joints, such as in the seal-wall, have been removed and shrinkage compensating concrete is used for a monolithic structure design. Expansion joints required for the bottom outlet structure are protected with stainless steel covers and are equipped with a system of three water-stops: a flexible outside water-stop, an internal water-stop and a maintainable omega seal at the inside of the bottom outlet structure. The base slab of the bottom outlet structure is designed with hinges at joints without allowing for expansion. This joint, reinforcement and waterproofing scheme is shown in the design drawing LTMM CC-DAM-602. The complete bottom outlet structure is supported by ground improvement to reduce vertical displacements, under loading conditions, to a minimum.

08.02 Brief Description of Elements

a) Embankment Dam Structure

The proposed embankment dam construction concept consists of a zoned earth-rock fill dam with an impervious reinforced concrete seal wall and seepage cut-off measures.

b) Seepage Control Measures

The design of seepage control measures is based on rock and soil characteristics examined within the geotechnical investigation campaigns, permeability data for the alluvial deposits and the results from water pressure tests in bedrock (Thurber Engineering Ltd., 2015b). The following system is provided for seepage control:

- A secant pile wall for seepage cut-off in the alluvial deposits consisting of primary piles and reinforced secondary piles. Secondary piles are cutting a secant section of the primary piles. The piles are bored through the alluvium and tied into the bedrock with sufficient depth to assure a sufficient structural connection.
- A grout curtain for reducing seepage through the bedrock to an acceptable limit. The design and construction objective is to sufficiently treat the bedrock by means of cement based grouting such that the remaining transmissivity is below or equal to 10 Lugeon. The spatial extent of the grout curtain is designed to obtain a phreatic line and seepage quantities suitable for a safe and stable embankment dam structure. The contact between the secant pile wall and grouted bedrock is grouted as well.
- An impervious reinforced monolithic concrete seal wall tied into the grouted bedrock by means of rock trenches and additionally sealed at the interface by means of structural grouting, using sleeve hoses. The concrete seal wall is structurally attached to the secant pile wall and the interface is sealed by means of structural grouting.
- Drainage layers in the downstream embankment for discharging remaining seepage.

c) Flow Control Structures

The flow control structures are the following:

- Tunnel shaped bottom outlet structure constructed in reinforced cast in-place concrete, feeding through the concrete seal wall;
- Throttle made out of a steel plate stiffened by means of H-beams, welded onto the throttle-plate;
- Intake wing walls;
- Intake gravel rake;
- Outlet structure;
- Armored dam crest and downstream embankment slope designed as spillway;
- Spillway training walls for the protection of the abutments of the overflowable downstream embankment slope as described in section d) below.
- Stilling basin constructed in reinforced cast in-place concrete with piers and baffles for a controlled hydraulic jump and energy dissipation;

d) Spillway

The spillway is formed by the downstream embankment slope. It has a reinforced concrete lining that is additionally covered by a layer of grouted stone pitching. The complete structure is fully overtoppable. The overflow-section at the dam crest is approximately 100m wide.

e) Emergency Bypass

The emergency bypass is located at the toe of the upstream embankment slope on the right. It consists of an intake structure of reinforced concrete protected with a small debris rake, a stainless steel pipe feeding through the core wall to a separate outlet structure. It is equipped with a valve for opening the emergency bypass, if required. The opening in the core wall is designed as a watertight pipe gland based on stainless steel flanges and a bitumen infill in the ring-space of the opening.

09 HYDROTECHNICAL DESIGN

09.01 Flood Hydrology

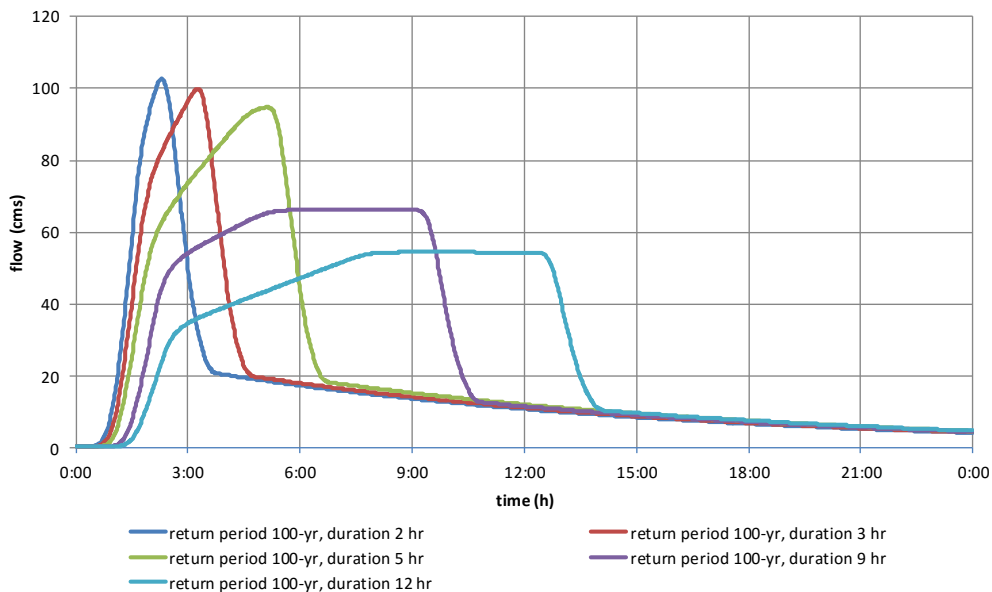
In order to estimate representative design floods and maximum probable floods, the flood hydrology for the Cougar Creek mitigation project was investigated in detail in Appendix J - Hydrological Assessment (LTMM CC - REP - AP-J). Relevant aspects are summarized in the following sections herein. It must be underlined that the normal operating state and purpose of the structure is flood retention. The term “inflow design flood” (IDF) is used herein for scenarios, utilizing the structure in terms of a normal operating state. The purpose of a flood retention structure is to assure a certain level of protection. The structure must be capable of reducing flood discharges to a certain maximum value. Inflow scenarios exceeding the IDF are utilizing the spillway and are herein referred to as “spillway floods”. The hydraulic design of the spillway is discussed in chapter 09.04. The IDF for the spillway design is discussed in Appendix J.

For the hydrotechnical design of the structure, in particular for dimensioning of the storage capacity for normal operating conditions (no overtopping), flood discharges resulting from precipitation scenarios, according to Table 29, were considered.

Table 29: Peak discharges for rainfall durations ranging from 2 hours to 12 hours and return periods of 100 years, 300 years and 1,000 years

Rainfall Durations	Peak Discharges for RP of 100-yr [m ³ /s]	Peak Discharges for RP of 300-yr [m ³ /s]	Peak Discharges for RP of 1,000-yr [m ³ /s]
2 hours	102.7	135.7	167.8
3 hours	99.9	131.1	159.4
5 hours	94.8	114.8	135.7
9 hours	66.3	79.8	93.6
12 hours	54.5	64.8	75.7

IDF hydrographs considered for the determination of the required storage capacity and structure height are shown in Figure 26, Figure 27 and Figure 28.



CANADIAN HYDROTECH CORPORATION

Figure 26: IDF-hydrographs for precipitation scenarios with a return period of 100 years

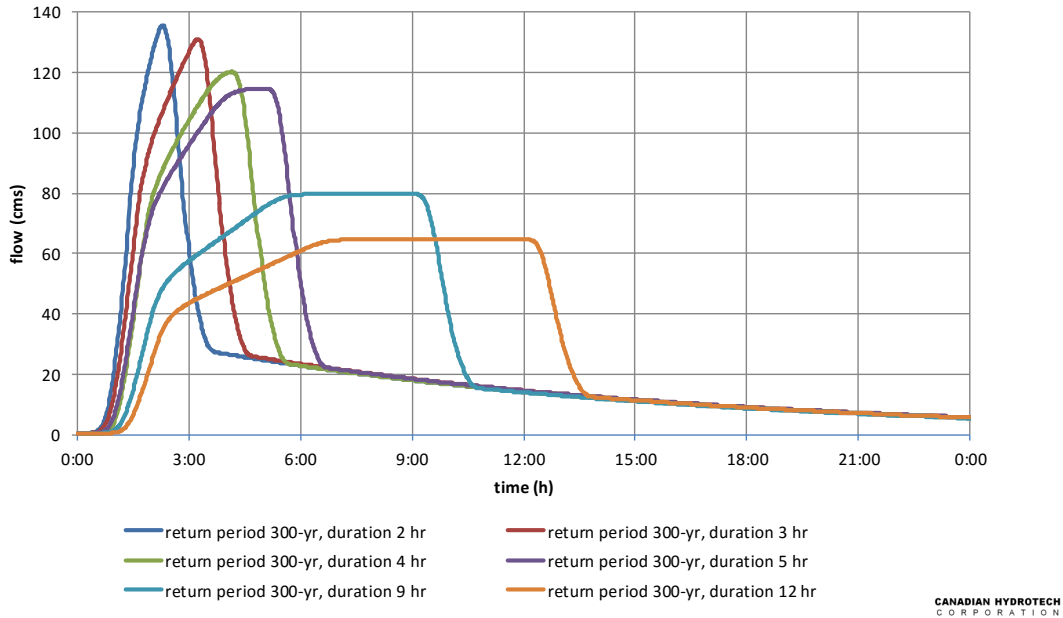


Figure 27: IDF-hydrographs for precipitation scenarios with a return period of 300 years

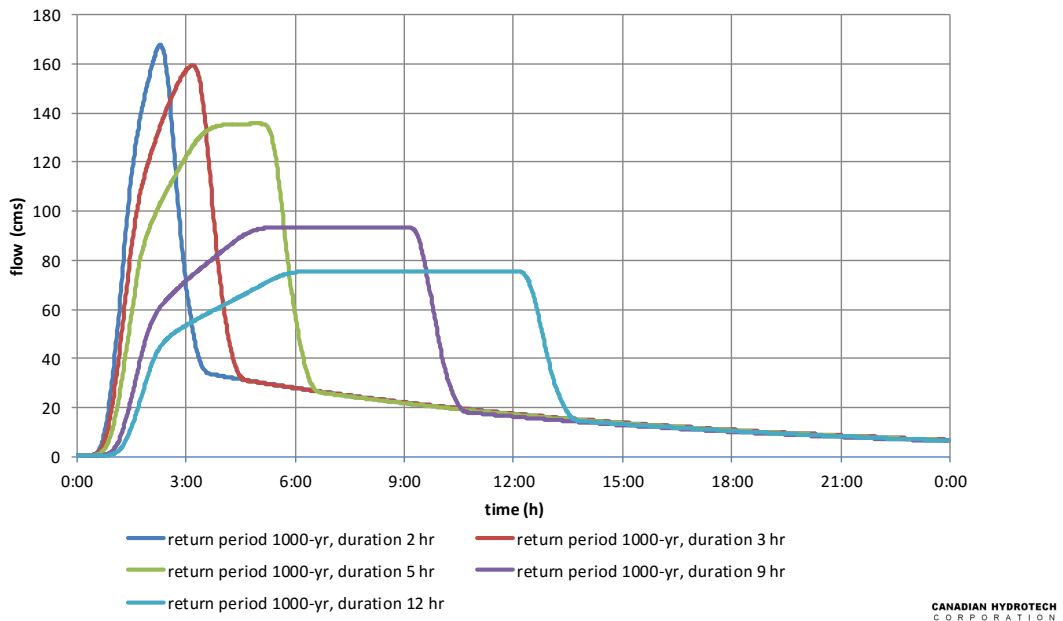


Figure 28: IDF-hydrographs for precipitation scenarios with a return period of 1,000 years

09.02 Storage Capacity and Throttle Setting

The capability of the structure to retain floods depends on the following factors:

- Topographic situation at the proposed retention area
- Structure height

- Cross sectional area of the throttle

Considering the above factors, besides accessibility, construction volume and costs, the optimal location was identified at the fan apex, directly upstream of a narrow creek section as outlined in Figure 8, Figure 9 and in the corresponding design drawings LTMM CC-GEN-010 and LTMM CC-DAM-501.

The storage curve for this location is shown in Figure 29. The topographic data used for the determination of the relationship between height of impoundment and storage volume is a LiDAR dataset with a ground sampling distance of 1m, created from a bare earth point cloud (see chapter 04.09).

Within previous hydrodynamic 2D analyses of bedload transport, erosion and remaining freeboard at culverts at the channel, a maximum allowable clear-water discharge of 45m³/s was determined. This value refers to the current state of channel and existing culverts. Considering a maximum value of 45m³/s for remaining peak discharge at normal operating conditions, the utilization characteristics, according to Table 31, Table 32 and Table 33, result from precipitation related flood scenarios. Table 34 lists the theoretical utilization characteristic for the back calculated June 2013 event. Table 35 lists the conditions for landslide dam outbreak floods (LDOF) based on the assumption that a 1,000 year return period flood or a 3,000 year return period flood are impacting and eroding a 30m high landslide dam at creek chainage KM 4+800, resulting from a maximum probable rockslide. Considering a structure with 29.85m of height, measured from the bottom of the throttle to the crest, floods resulting from storms with rainfall durations within a range of 2 and 12 hours and return periods of up to 100 years are retained. Three hundred year return period scenarios are covered for rainfall durations of up to 4 hours. One thousand year return period scenarios are covered for a rainfall duration of 2 hours. The back calculated June 2013 storm would have been retained as well as the worst case LDOF scenarios. Figure 31, Figure 32 and Figure 33 show inflow and outflow characteristics as well as impoundment heights for the most relevant scenarios in terms of structure utilization, under normal operating conditions.

Considering a rectangular 4% inclined bottom outlet with a throttle assuring a maximum peak discharge of 45m³/s at full impoundment (29.85m) results in a discharge curve as shown in Figure 30. The governing equation for calculating the water-level related outflow is:

$$Q = \mu \cdot a \cdot b \cdot \sqrt{(2gh_0)}$$

Equation 9 (Preissler, 2000)

where

- μ dimensionless discharge coefficient, herein set to 0.6
- a width of the throttle [m]
- b height of the throttle [m]
- g gravitational acceleration [m/s²]
- h_0 height of the relating water level [m]

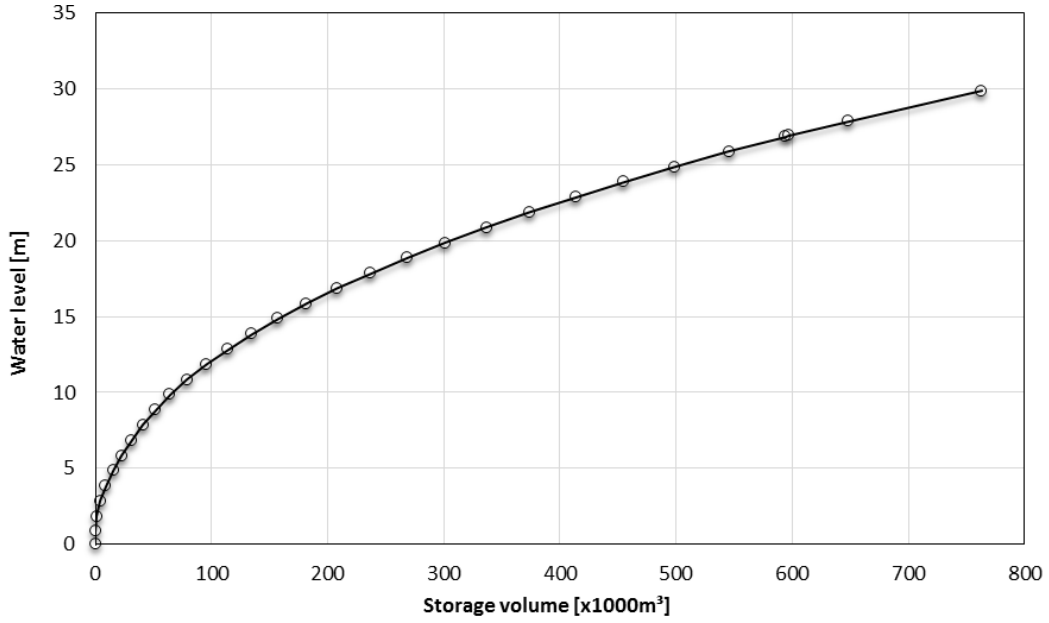


Figure 29: Storage curve at the selected location for retention structure

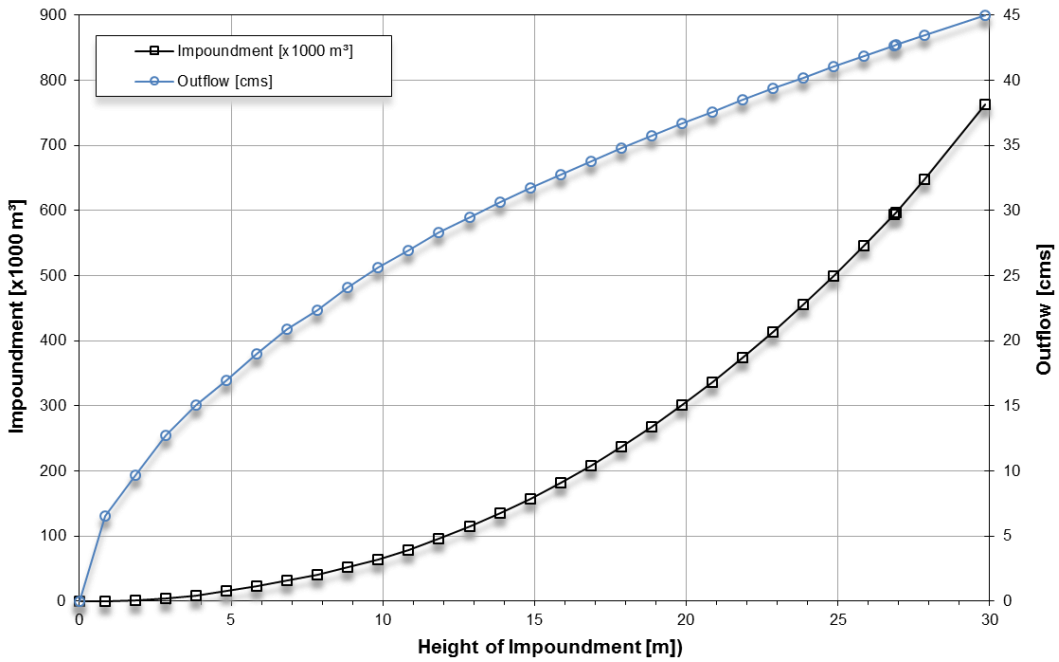


Figure 30: Discharge curve for the planned retention structure height

Table 30: Characteristic storage and discharge data of the retention structure

Water Level [MASL]	Height of Impoundment [m]	Water Surface [m²]	Integrated Volume of Impoundment [m³]	Discharge (m³/s)
1421.15	0.00	0	0	0.0
1422.00	0.85	305	86	6.6
1423.00	1.85	2,236	1,209	9.7
1424.00	2.85	3,916	4,246	12.7
1425.00	3.85	5,644	8,999	15.1
1426.00	4.85	6,885	15,254	16.9
1427.00	5.85	8,028	22,703	19.0
1428.00	6.85	9,129	31,275	20.9
1429.00	7.85	10,279	40,974	22.4
1430.00	8.85	11,334	51,776	24.1
1431.00	9.85	13,584	64,218	25.6
1432.00	10.85	15,631	78,814	26.9
1433.00	11.85	17,780	95,508	28.3
1434.00	12.85	19,698	114,238	29.5
1435.00	13.85	21,490	134,826	30.6
1436.00	14.85	23,450	157,289	31.7
1437.00	15.85	25,596	181,804	32.8
1438.00	16.85	27,572	208,382	33.8
1439.00	17.85	29,796	237,059	34.8
1440.00	18.85	32,056	267,978	35.7
1441.00	19.85	34,303	301,151	36.7
1442.00	20.85	36,503	336,548	37.6
1443.00	21.85	38,419	374,005	38.5
1444.00	22.85	40,568	413,494	39.4
1445.00	23.85	42,782	455,164	40.2
1446.00	24.85	45,136	499,118	41.0
1447.00	25.85	47,593	545,477	41.9
1448.00	26.85	50,134	594,335	42.7
1448.05	26.90	52,877	596,910	42.7
1449.00	27.85	55,835	648,541	43.4
1451.00	29.85	58,742	763,106	45.0

Table 31: Height and volume of impoundment, outflow and spillway utilization for 100-yr return period IDF's

Rainfall Duration	Peak Inflow [m ³ /s]	Impoundment [1,000m ³]	Elevation of Water Level [MASL]	Peak Outflow [m ³ /s]	Water Depth [m]	Spillway Discharge [m ³ /s]
2 hours	102.7	321	1441.50	37.2	20.35	-
3 hours	99.9	443	1444.70	40.0	23.55	-
5 hours	94.8	655	1449.10	43.5	27.95	-
9 hours	66.3	708	1450.00	44.2	28.85	-
12 hours	54.5	551	1447.10	42.0	25.95	-

Table 32: Height and volume of impoundment, outflow and spillway utilization for 300-yr return period IDF's

Rainfall Duration	Peak Inflow [m ³ /s]	Impoundment [1,000m ³]	Elevation of Water Level [MASL]	Peak Outflow [m ³ /s]	Water Depth [m]	Spillway Discharge [m ³ /s]
2 hours	135.7	484	1445.60	40.7	24.45	-
3 hours	131.1	656	1449.10	43.5	27.95	-
4 hours	120.4	760	1450.90	45.0	29.75	-
5 hours	114.8	849	1451.50	86.2	30.35	41.2
9 hours	79.8	827	1451.40	75.7	30.25	30.7
12 hours	64.8	791	1451.20	58.6	30.05	13.6

Table 33: Height and volume of impoundment, outflow and spillway utilization for 1,000-yr return period IDF's

Rainfall Duration	Peak Inflow [m ³ /s]	Impoundment [1,000m ³]	Elevation of Water Level [MASL]	Peak Outflow [m ³ /s]	Water Depth [m]	Spillway Discharge [m ³ /s]
2 hours	167.8	650	1449.00	43.4	27.85	-
3 hours	159.4	831	1451.40	77.8	30.25	32.8
5 hours	135.7	886	1451.80	135.6	30.65	90.6
9 hours	93.6	863	1451.60	93.1	30.45	48.1
12 hours	75.7	827	1451.40	75.5	30.25	30.5

Table 34: Height and volume of impoundment, outflow and spillway utilization for the back calculated June 2013 event

Rainfall Duration	Peak Inflow [m ³ /s]	Impoundment [1,000m ³]	Elevation of Water Level [MASL]	Peak Outflow [m ³ /s]	Water Depth [m]	Spillway Discharge [m ³ /s]
June 2013	108.3	700	1449.90	44.1	28.75	-

Table 35: Height and volume of impoundment, outflow and spillway utilization for worst case LDOF scenarios

Rainfall Duration	Peak Inflow [m ³ /s]	Impoundment [1,000m ³]	Elevation of Water Level [MASL]	Peak Outflow [m ³ /s]	Water Depth [m]	Spillway Discharge [m ³ /s]
1Mio m ³ LDOF +1000-yr flood	192.0	571	1447.50	42.3	26.35	-
1Mio m ³ LDOF +3000-yr flood	251.6	748	1450.70	44.8	29.55	-

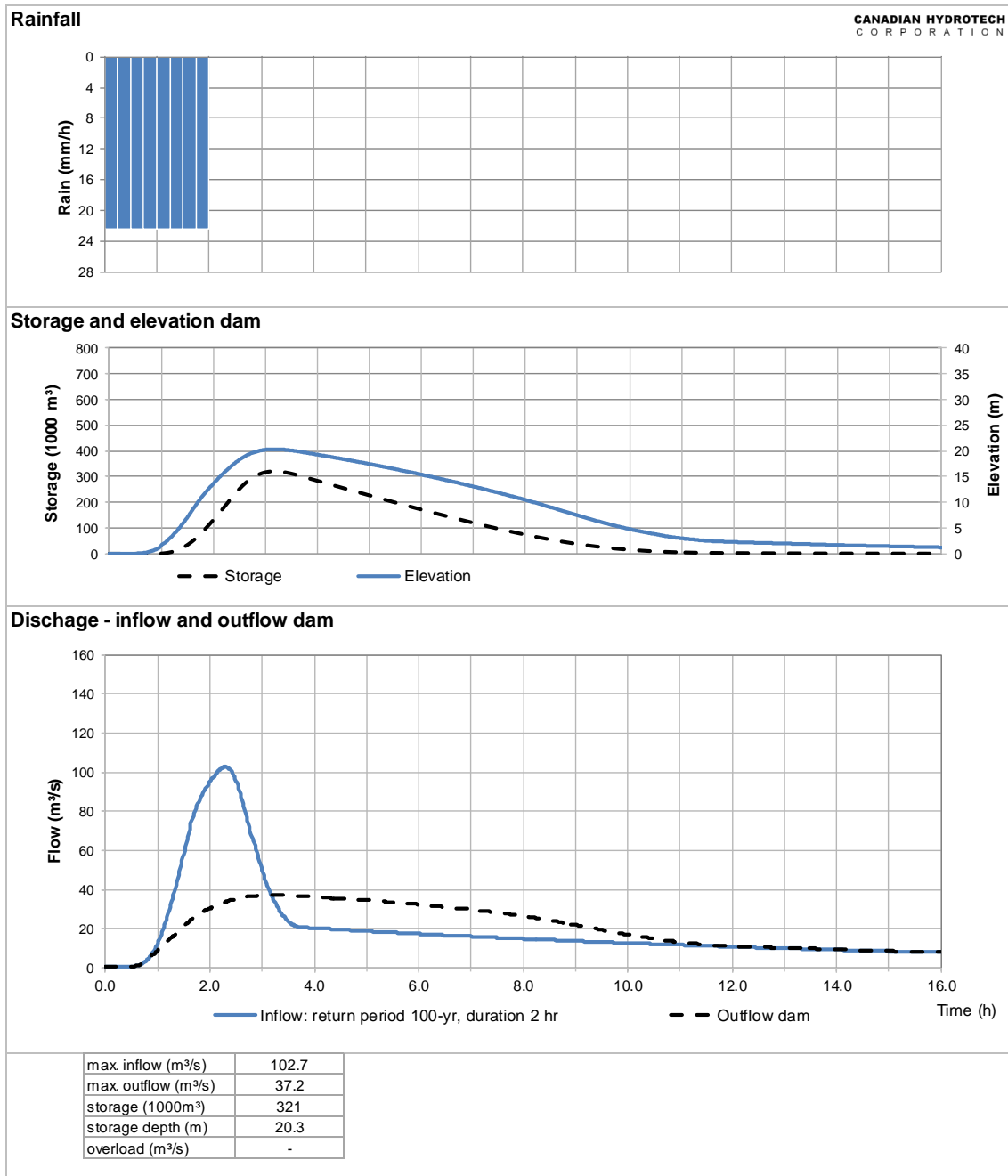


Figure 31: Inflow and outflow hydrographs for a 100 year return period related scenario with 2 hours of rainfall duration

Assuming a 100-year return period related storm event with a rainfall duration of two hours, the retention area is impounded up to a height of 20.35m with approximately 320,000m³ of floodwater. The reservoir is emptied within approximately 10 hours after initial impoundment and approximately 7 hours after reaching the maximum storage level (see Figure 31).

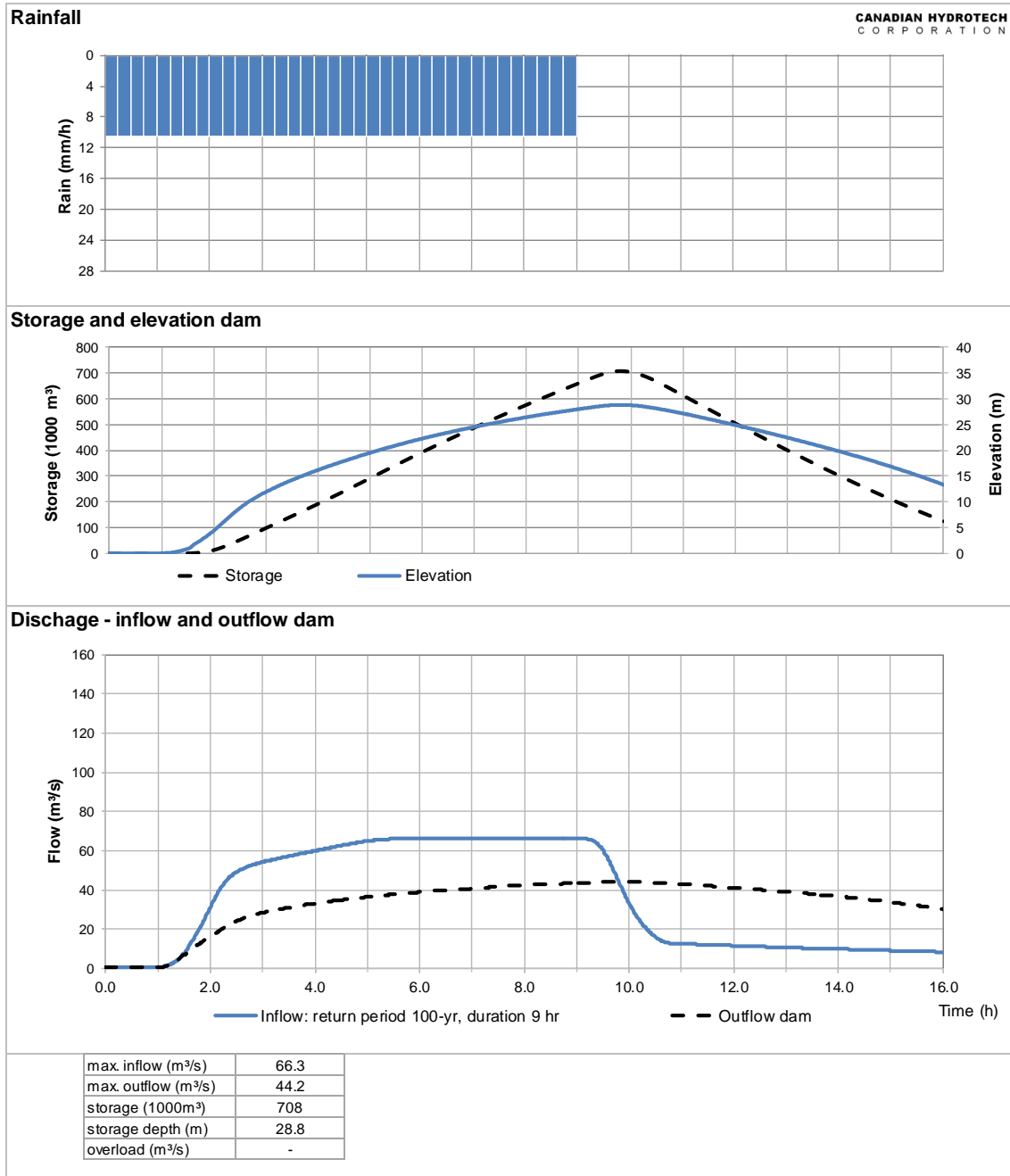


Figure 32: Inflow and outflow hydrographs for a 100 year return period related scenario with 9 hours of rainfall duration

Assuming a 100-year return period related storm event with a rainfall duration of nine hours, the retention area is impounded up to a height of 28.85m with approximately 710,000m³ of floodwater. The reservoir is emptied within approximately 16 hours after initial impoundment and approximately 8 hours after reaching the maximum impoundment level (see Figure 32).

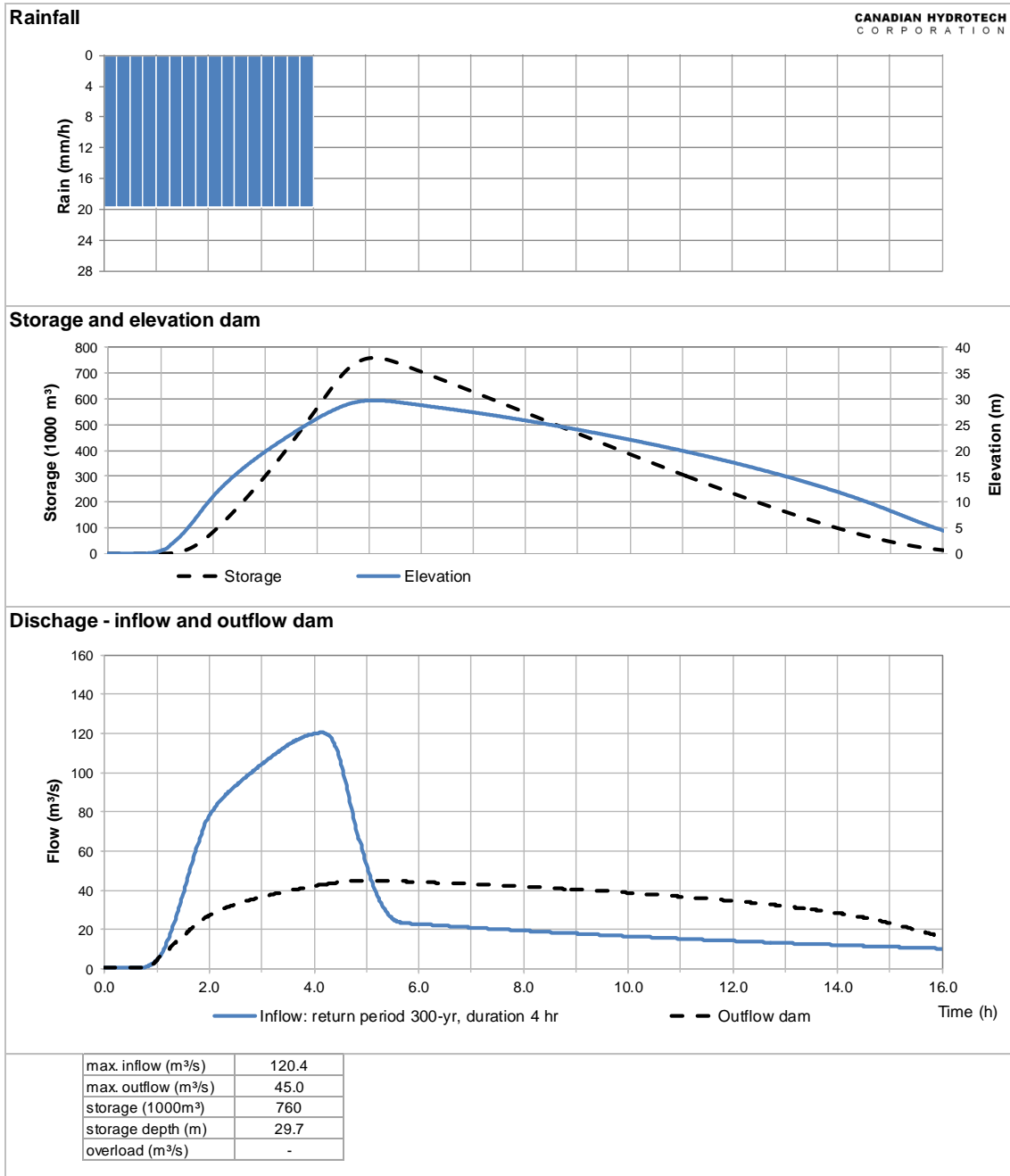


Figure 33: Inflow and outflow hydrographs for a 300 year return period related scenario with 4 hours of rainfall duration

Assuming a 300-year return period related storm event with a rainfall duration of four hours, the retention area is impounded up to a height of 29.75m with approximately 760,000m³ of floodwater. The reservoir is emptied within approximately 15 hours after initial impoundment and approximately 11 hours after reaching the maximum impoundment level (see Figure 33).

Looking at the back calculated June 2013 storm event, the behavior of the retention area is shown in Figure 34. The retention basin would have been impounded up to a height of 28.75m with approximately 700,000m³ of floodwater. Although the back calculated peak discharge of 95m³/s is comparably small, the structure’s capacity would have almost been completely utilized, because of the comparably long duration of the June

2013 event with multiple peaks. The June 2013 storm was classified as a 235-year return period event (BGC, 2014). This estimate corresponds to the flood discharge estimates within the hydrological assessment (Appendix J), where the June 2013 is within a range between a 100-year and a 300-year return period event.

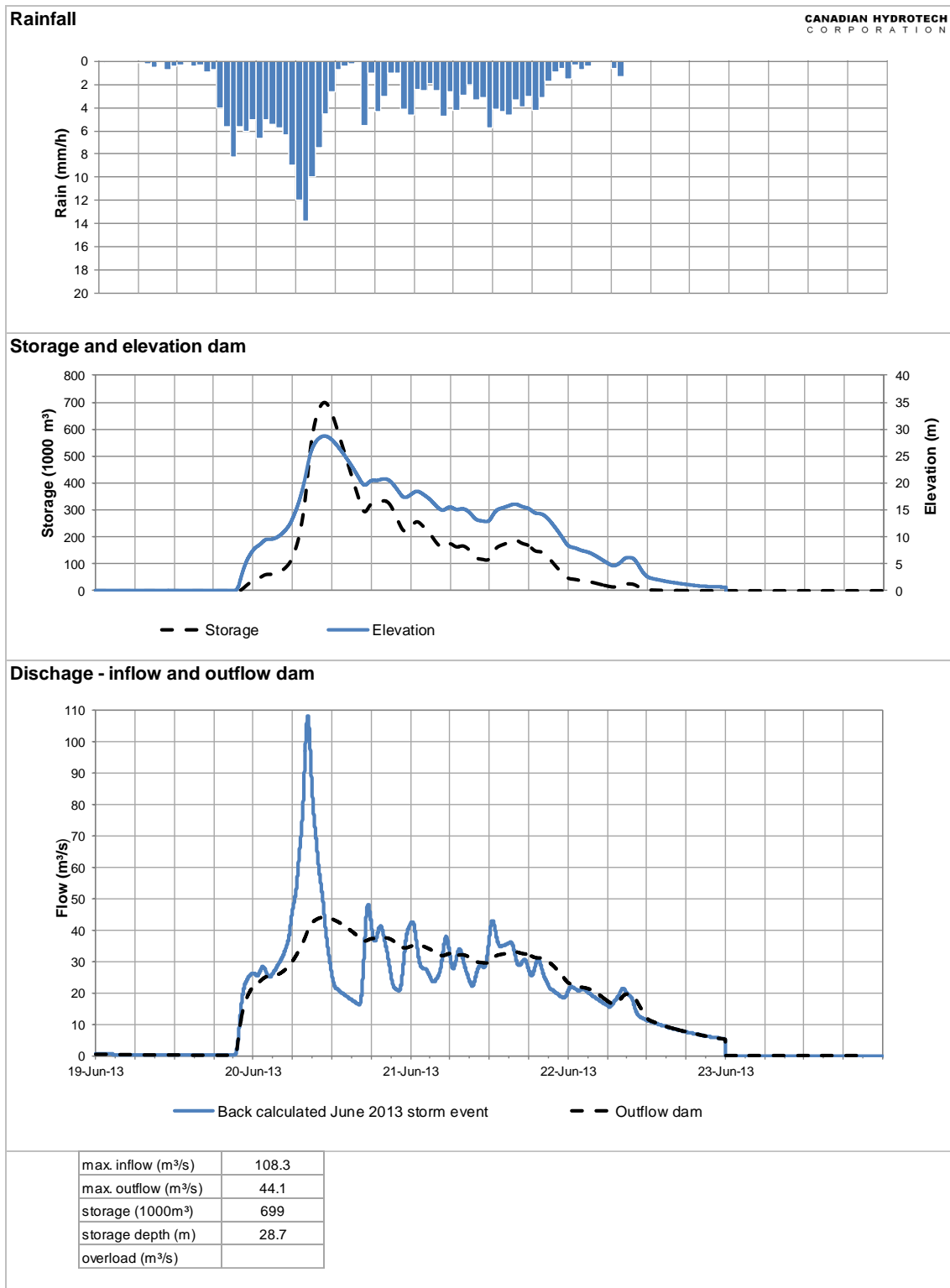


Figure 34: Inflow and outflow hydrographs for the back calculated June 2013 storm event

09.03 Bottom Outlet Structure, Throttle and Ventilation

The maximum discharge capacity of the box-shaped bottom outlet structure (see drawing LTMM CC-DAM-508 R00) is approximately 200m³/s, referring to Equation 9. Assuming a free flow velocity of 5m/s for the state of maximum discharge with 45m³/s, a cross-sectional area of 9m² is required and available. Ventilation of the throttle is required to avoid cavitation.

Considering a discharge of 45m³/s at the throttle with a cross-sectional area of 3.1m², the resulting flow velocity is 14.52m/s referring to Equation 10. The Froude number is 4.1, referring to Equation 11 for a free flow height at the semicircle shaped outlet channel with a radius of 1.275m. The minimum required airflow at the throttle is 16m³/s under full loading conditions. A set of two ventilation pipes (see design drawing LTMM CC-DAM-504 R00 and LTMM CC-DAM-508 R00), 1m in diameter each, requires an airflow velocity of 10.6m/s, referring to the relationship according to Equation 14.

$$Q_w = v_c \cdot A \quad \text{Equation 10}$$

$$Fr_c = \frac{v_c}{\sqrt{g \cdot h_c}} \quad \text{Equation 11 (Sharma, 1976)}$$

$$Q_{air} = \beta_{so} \cdot Q_w \quad \text{Equation 12 (Sharma, 1976)}$$

$$\beta_{so} = 0.09 \cdot Fr_c \quad \text{Equation 13 (Sharma, 1976)}$$

$$Q_{air} = v_{air} \cdot A \quad \text{Equation 14 (Sharma, 1976)}$$

where

- Q_w discharge [m³/s]
- v_c flow velocity of water discharged through the throttle [m/s]
- A cross-sectional area [m²]
- Fr_c Froude number
- g gravitational acceleration [m/s²]
- h_c flow height [m]
- Q_{air} air flux [m³/s]
- β_{so} air requirement coefficient

09.04 Overflow Section, Spillway

The overflowable section at the dam crest is approximately 100m wide and the complete downstream section forms the spillway, confining the flow by means of training walls at the abutments. Considering a spillway flood of 346m³/s, a flow height of 1.65m at the dam crest results according to Equation 15.

$$Q_{spillway} = \frac{2}{3} \mu w \sqrt{2 \cdot g} \cdot H^{\frac{2}{3}} \quad \text{Equation 15 (Poleni in Preissler, 2000)}$$

where

- μ discharge coefficient, set to 0.55
- w width of the overflow section (crest) [m]
- H resulting flow-height [m]
- g gravitational acceleration [m/s²]

The assessment of PMF's is covered within the hydrological assessment (Appendix J) and results are summarized in Table 36.

Table 36: Summary of estimated PMF peak flows according to Appendix J – Hydrological Assessment

Duration	Rainfall [mm]	Water from Snow Melt [mm]	Peak Discharge [m ³ /s]
PMP 4-hr	281	-	435
Spring PMP 6-hr	308	56	423
5000-yr floods 6-hr + 2-hr	223	-	247
100-yr flood 2hr + snow melt	44	11	143
PMP 24-hr	375	-	98
Spring PMP 24-hr	281	70	94

09.05 Stilling Basin

According to the Dam Safety Guidelines by the Canadian Dam Association (2013), the risk the planned structure poses to the Town of Canmore in case of a failure is “Very High”. The Inflow Design Flood for a “Very High” consequence dam should be two-thirds of the way between the flood with a return period of 1,000 years and the PMF. For Cougar Creek, the peak discharge for the 1,000 year flood is 168 m³/s, and 435 m³/s for the PMF. Therefore, the Inflow Design Flood for the hydraulic design of the spillway and the stilling basin to be selected is 346 m³/s. Referring to Equation 16, the required height of a counter-sill for a 20.64 m long stilling basin is 4.4m. Additional piers and baffles create a clear and well defined hydraulic jump and effective energy dissipation directly at the toe of the spillway as shown in the physical scaled model (IAN 2016).

$$h_2 = -\frac{h_1}{2} + \sqrt{\frac{h_1^2}{4} + \frac{2 \cdot v_1^2 \cdot h_1}{g}} \quad \text{Equation 16 (Vischer, 1993)}$$

where

- h_1 Depth of inflow water jet [m]
- h_2 Conjugated water depth [m]
- v_1 cross sectional flow velocity [m/s]
- g gravitational acceleration [m/s²]

General parameters and the results from the hydraulic spillway calculation are listed in Table 37.

Table 37: Results and Parameters from dimensioning of the stilling basin

Parameter	Abbreviation	Value	Unit
IDF	Q	346.00	[m ³ /s]
Width of Spillway	w	30.00	[m]
Specific Discharge PMF/b	Q	11,53	[m ³ /s*m]
Coefficient of roughness according to Strickler	k_{st}	20	[m ^{1/3} /s]
Inclination of the Spillway	l	0.57	[-]
Depth of Inflow Water Jet $f(q, k_{st}, l)$	h_1	0.85	[m] (Strickler)
Cross-Sectional Flow Velocity q/h_1	v_1	13.57	[m/s]
Energy Head	E	9.38	[m]
Froude-Number	Fr	4.70	[-]
Conjugated Water Depth	h_2	5.24	[m]

Parameter	Abbreviation	Value	Unit
Length of the Stilling Basin	L_T	21.94	[m]
Height of Counter Sill (selected)	h_s	4.40	[m]
Minimum depth of tail-water	h_{u-min}	0.84	[m]
Targeted degree of Impoundment	ε	1.05	
Targeted depth of tail-water	h_u	1.10	[m]

The calculations indicate the requirement of a counter sill with a height of 4.4m for a conjugate water depth of 4.94m. To reach a degree of impoundment of 1.05, the downstream section of the stilling basin is formed in a way to obtain a minimum flow depth of 0.84m, considering the design spillway flood accordingly. These calculations are not considering baffles and piers.

09.06 Scaled Physical Modelling of Inflow Structure and Gravel Rake

For optimizing the inflow structure, in terms of maximum possible discharge of aggraded sediments and reduction of clearance costs, physical modelling was performed by the Institute of Mountain Risk Engineering at the University of Natural Resources and Life Sciences in Vienna (BOKU), Austria. The rake design and the design of the inflow structure were refined within several model runs. Results are summarized in “Physical Modeling of the Cougar Creek Retention Structure” (IAN 2016). These tests also include the test of the stilling basin for functionality, and in particular for the design of piers and baffles placed at the toe of the spillway.

10 GEOTECHNICAL DESIGN

10.01 Detailed Construction Concept

The dam construction concept as outlined in the design drawing LTMM CC-DAM-503 (see Figure 35), consists of a zoned earth-rock fill embankment dam with an impervious monolithic reinforced concrete seal wall. The concrete seal wall is placed on a secant pile wall that cuts off seepage in the alluvium. The abutments of the concrete seal wall and the secant pile wall are tied into bedrock. Bedrock will be grouted to an acceptable remaining transmissivity of 10 Lugeon (water take of 10 l/m/min at 10 bar reference pressure). Structural grouting is for sealing all interfaces between improved bedrock and concrete structures as well as between the secant pile wall and the concrete seal wall. The preliminary design extent of the grout curtain is shown in the design drawing LTMM CC-DAM 505 (see Figure 36). The structure is designed to be overtoppable and the full width of the crest and the downstream slope form the spillway. Therefore, the downstream shell is armored with grouted heavy rock stone pitching placed in a reinforced concrete bed. To protect the abutments from erosion the design includes training walls. The stilling basin is equipped with piers and baffles to obtain a controlled hydraulic jump regardless of oblique inflow from the sides. This setup was investigated by means of a physical scaled model (IAN 2016).

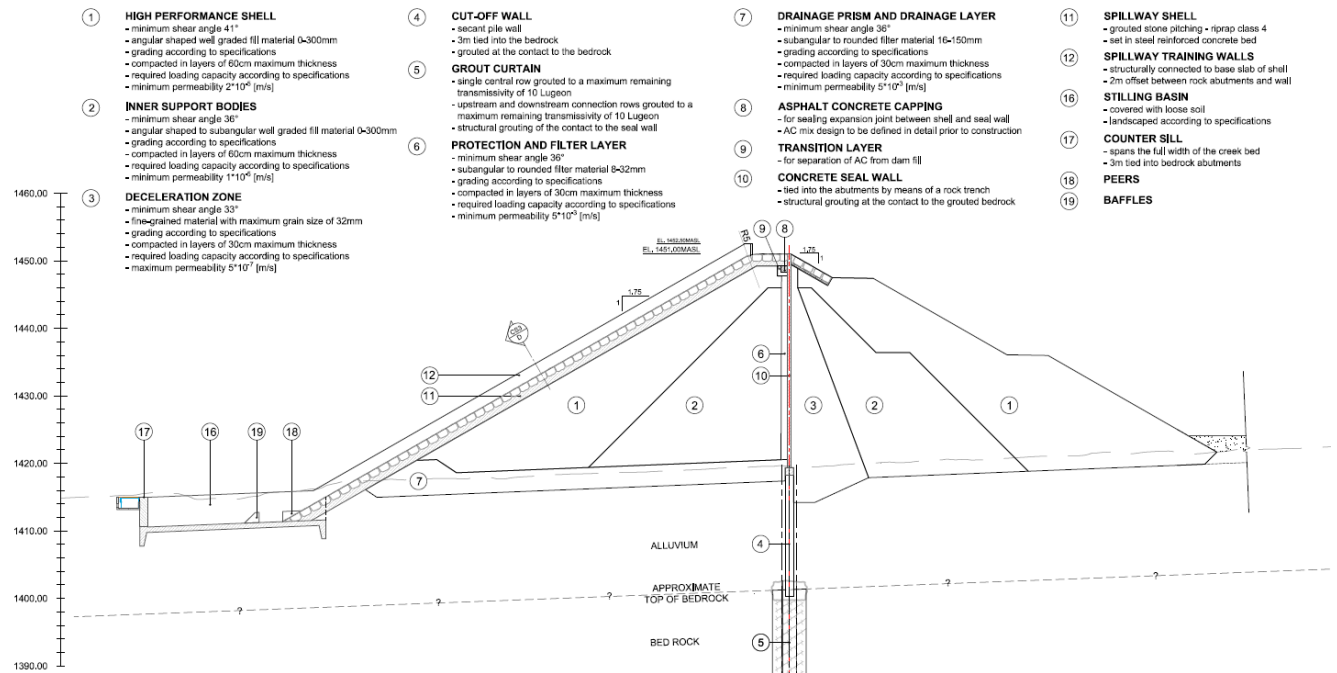


Figure 35: Dam construction concept according to drawing LTMM-CC-DAM-503

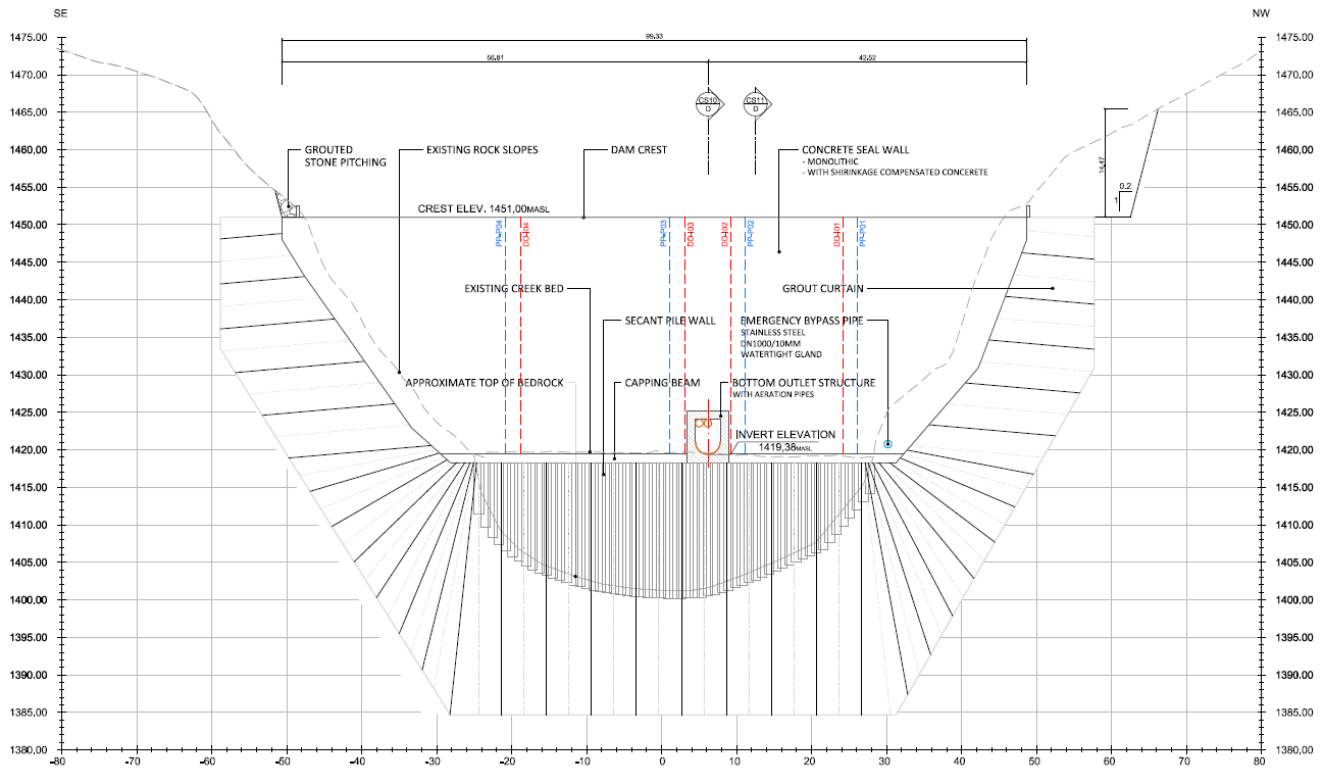


Figure 36: Cut-off measures and grout curtain according to drawing LTMM-CC-DAM-505

10.02 Seepage

10.02.01 Seepage Calculations

Seepage calculations are performed for all investigated loading cases and discussed ahead of dam stability calculations (see chapter 10.04 and subchapters).

Seepage volumes calculated for loading case A - ground water flow with already installed cut-off measures but neglecting drainage through the bottom outlet structure, yield approximately 20 to 25 liters per minute which need to be discharged by drainage pipes. FE-seepage calculation and the resulting phreatic line are shown in Figure 50.

For loading case E - full impoundment, approximately 150 to 160 liters per minute need to be taken into account for discharge through drainage pipes. FE-seepage calculation for loading case E and the resulting phreatic line are shown in Figure 92.

10.02.02 Seepage Control Measures

The design of seepage control measures are based on rock and soil characteristics, permeability data for the alluvial deposits and the results from water pressure tests, provided by the Geotechnical Investigation Report Phase 2B (Thurber Engineering Ltd., 2015b).

The design provides following seepage control measures:

- A secant pile wall for seepage cut-off in the alluvial deposits consisting of primary piles, 1.25m in diameter and reinforced secondary piles, 1.25m in diameter as well. Secondary piles cut a secant section of the primary piles. Nominal final pile spacing is 0.9m. Selection of intersection and pile

diameter account for deviations during piling that the required wall thickness is sufficient. The piles are bored through the alluvium and socketed into the bedrock with sufficient depth to assure sufficient embedment. The secant pile-wall layout is based on structural considerations as discussed in chapter 10.05.01.

- A grout curtain, to reduce seepage through the bedrock to an acceptable limit. The design and construction objective is to sufficiently treat the bedrock by means of cement based grouting such that the remaining transmissivity is below or equal to 10 Lugeon (10 l/m/min at 10 bar reference pressure). The spatial extent of the grout curtain is designed to obtain a phreatic line and seepage quantities suitable for a safe and stable dam structure.
- An impervious reinforced concrete seal wall, which is structurally connected to the secant pile wall and tied into the grouted bedrock by means of rock trenches. All seal wall interfaces are sealed by means of structural grouting conducted subsequently with construction height. Aside of structural grouting, the seal wall is constructed with shrinkage compensated concrete which is expanding during hydration so that no substantial voids are developing.
- A vertical layer of impervious fill material placed upstream of the concrete seal wall to provide primary sealing. This layer leads to self-sealing of the concrete seal wall in case minor cracks should occur.
- A vertical drainage layer downstream of the concrete seal wall, which is connected to the horizontal drainage layer and drainage prism at the downstream footprint of the structure. The drainage layer and the drainage prism are equipped with drainage pipes for collecting seepage water. Collected seepage water is monitored by means of Thompson weirs located downstream of the stilling basin directly at the abutments.

10.03 Grading Design of Filters

10.03.01 General

To provide a safe dam design regarding internal erosion, piping and in consequence for dam stability, grading of different fill materials must be matched up and grading needs to be designed accordingly.

According to the Canadian Foundation Engineering Manual (CGS, 2006) a graded granular filter shall satisfy the following performance requirements:

- The voids of the filter should be small enough to restrict particles of the base soil from penetrating or washing through it, fulfilling a criterion of "soil retention."
- The filter material should be more pervious than the base soil, fulfilling a "permeability criterion."
- The filter should be sufficiently thick to ensure a representative gradation.
- The filter should not segregate during processing, handling, placing, spreading or compaction.
- The filter material should be physically durable, and chemically inert.
- The filter should not be susceptible to internal instability, whereby seepage flow acts to induce migration of the finer fraction of the gradation.
- The filter gradation should be compatible with the size, location and distribution of openings in drainage pipes.

Interfaces between fill materials and/or alluvial deposits at the footprint as listed in Table 38 are subject of filter design criteria.

Table 38: Dam fill zones, alluvial deposits and their interfaces

Dam Zone and Onsite Material		Adjacent Zone
1-Outer Support Body	-	6-Protection Layer
1-Outer Support Body	-	7-Drainage Layer
2-Inner Support Body	-	1-Outer Support Body
2-Inner Support Body	-	6-Protection Layer
2-Inner Support Body	-	7-Drainage Layer
3-Deceleration Zone	-	1-Outer Support Body
3-Deceleration Zone	-	2-Inner Support Body
3-Deceleration Zone	-	Cougar Creek Alluvium
6-Protection Layer	-	7-Drainage Layer
Cougar Creek Alluvium	-	1-Outer Support Body
Cougar Creek Alluvium	-	2-Inner Support Body
Cougar Creek Alluvium	-	7-Drainage Layer

10.03.02 Design Criteria for Grading

Design criteria for grading are discussed in chapter 05.03.02.

10.03.03 Preliminary Grading Bands

Zone 1 – Outer Support Body, 300 mm and minus

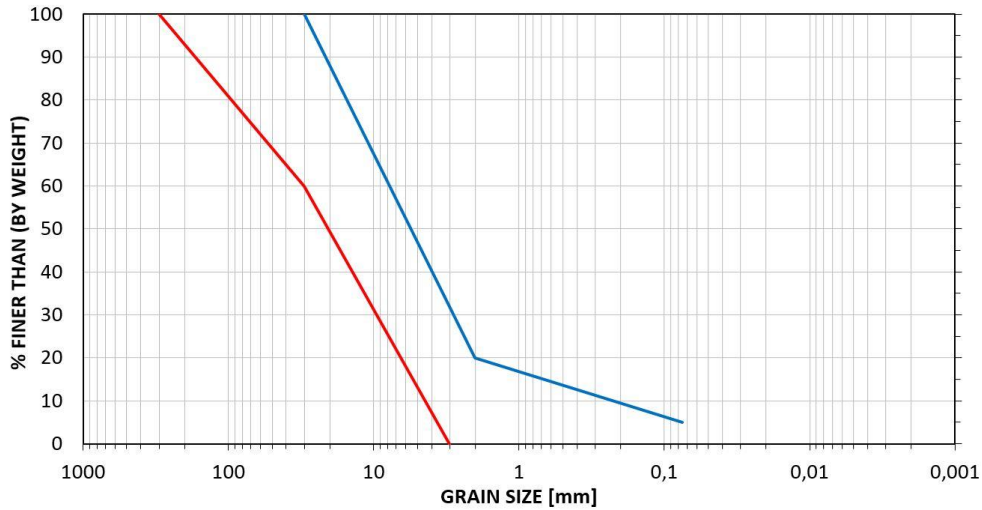


Figure 37: Design Grading Band, Dam Zone 1 – Outer Support Body; the red line indicates the upper limit, the blue one the lower limit.

Table 39: Preliminary Design Grading Band, Outer Support Body – Dam Zone 1

Design Grading Band – Outer Support Body – Zone 1		
Grain Size [mm]	% finer than (by Weight)	
0.075	5	-

Design Grading Band – Outer Support Body – Zone 1		
2	20	-
3		0
30	100	60
300	-	100

Zone 2 – Inner Support Body, 150 mm and minus

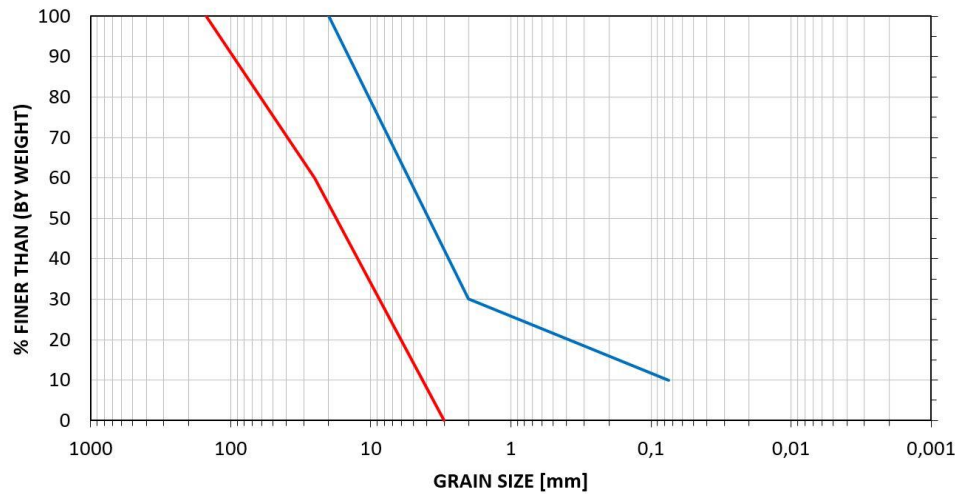


Figure 38: Design Grading Band, Dam Zone 2 – Inner Support Body; the red line indicates the upper limit, the blue one the lower limit.

Table 40: Preliminary Design Grading Band, Inner Support Body - Dam Zone 2

Design Grading Band – Inner Support Body - Zone 2		
Grain Size [mm]	% finer than (by Weight)	
0.075	10	-
2	30	-
3		0
20	100	
25	-	60
150	-	100

Zone 3 – Deceleration Zone, 10mm and minus

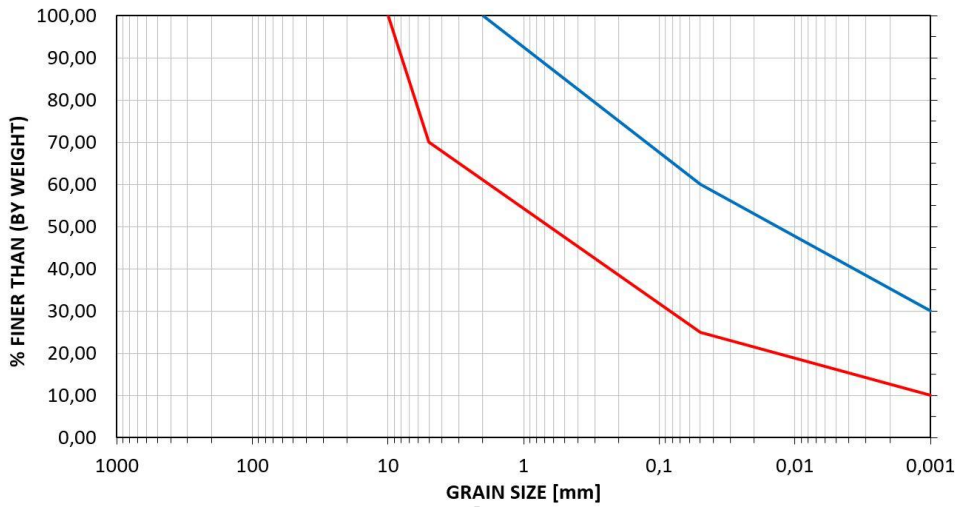


Figure 39: Design Grading Band, Dam Zone 3 – Deceleration Zone; the red line indicates the upper limit, the blue one the lower limit.

Table 41: Preliminary Design Grading Band, Deceleration Zone - Zone 3

Design Grading Band – Deceleration Zone – Zone 3		
Grain Size [mm]	% finer than (by Weight)	
0.001	30	10
0.05	60	25
2	100	
5	-	70
10	-	100

Zone 6 – Protection Layer

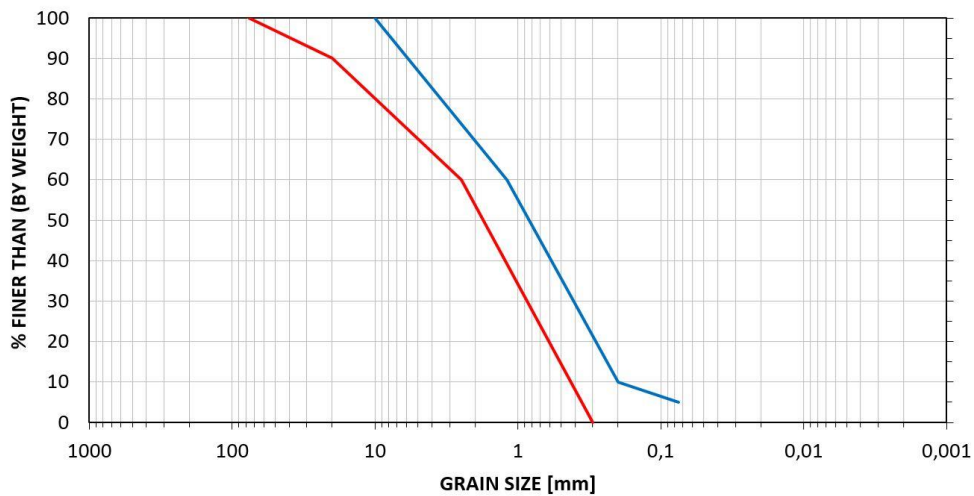


Figure 40: Design Grading Band, Dam Zone 6; the red line indicates the upper limit, the blue one the lower limit.

Table 42: Preliminary Design Grading Band, Protection Layer, Zone 6

Design Grading Band – Protection Layer – Zone 6		
Grain Size [mm]	% finer than (by Weight)	
0.075	5	-
0.2	10	-
0.3		0
1.2	60	
2.5		60
10	100	
20	-	90
75	-	100

Zone 7 – Drainage Layer

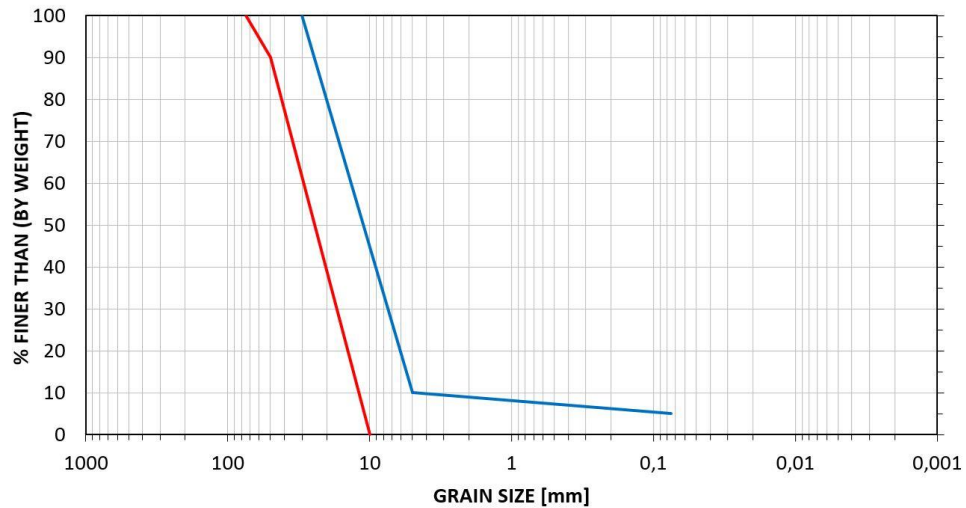


Figure 41: Design Grading Band, Dam Zone 7 – Drainage Prism and Drainage Layer; the red line indicates the upper limit, the blue one the lower limit.

Table 43: Preliminary Design Grading Band, Drainage Layer, Zone 7

Design Grading Band – Protection Layer – Zone 6		
Grain Size [mm]	% finer than (by Weight)	
0.075	5	-
5	10	-
8		-
10		0
30	100	
50	-	90
75	-	100

Cougar Creek Alluvium

The filter design for material adjacent to the modern Cougar Creek alluvium is based on samples from test pits TP14-10 and TP14-12, collected at approximate depths of 0.5m and 2.0m. These samples are very similar to those of the Stoneworks Creek alluvium, which is the preferred source material for dam zone 2, the inner support body.

Design Grading Bands for Transition Layers

To fulfill filter stability criteria, transition layers as listed in Table 44 are required.

Table 44: Summary of fulfilled filter criteria and required transition layers

Dam Zone/On Site Material	Transition Layer	Dam Zone/On Site Material
1-Outer Support Body	→	6-Protection Layer
1-Outer Support Body	→ A →	7-Drainage Layer
1-Outer Support Body	→	Cougar Creek Alluvium
2-Inner Support Body	→	1-Outer Support Body
2-Inner Support Body	→	6-Protection Layer
2-Inner Support Body	→ A →	7-Drainage Layer
2-Inner Support Body		Cougar Creek Alluvium
3-Deceleration Zone	→ B →	1-Outer Support Body
3-Deceleration Zone	→ B →	2-Inner Support Body
3-Deceleration Zone	→ B →	Cougar Creek Alluvium
6-Protection Layer	→	7-Drainage Layer
Cougar Creek Alluvium	→ A →	7-Drainage Layer

Transition Layer A

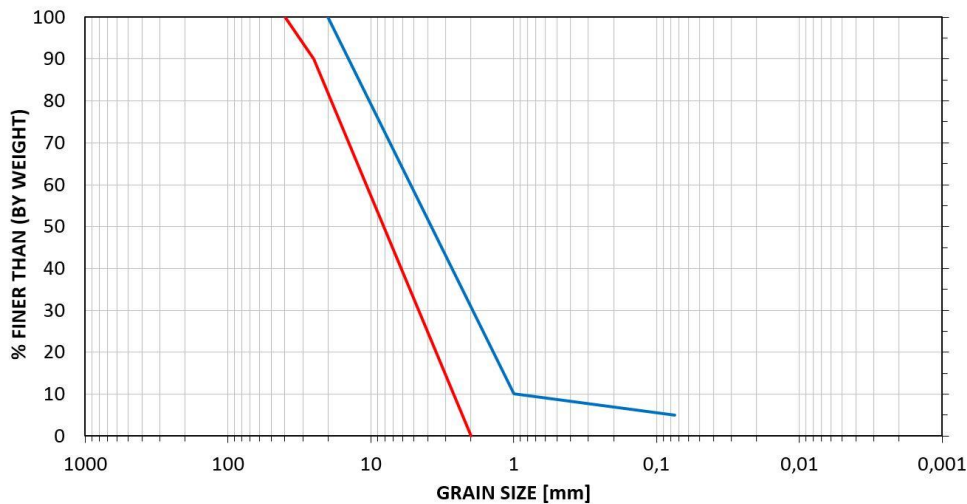


Figure 42: Preliminary Design Grading Band, Transition Layer A; the red line indicates the upper limit, the blue one the lower limit.

Table 45: Preliminary Design Grading Band, Transition Layer A

Design Grading Band – Transition Layer A

Design Grading Band – Transition Layer A		
Grain Size [mm]	% finer than (by Weight)	
0.075	5	-
0.2	10	-
0.3		0
1.2	60	
2.5		60
10	100	
20	-	90
75	-	100

Transition Layer B

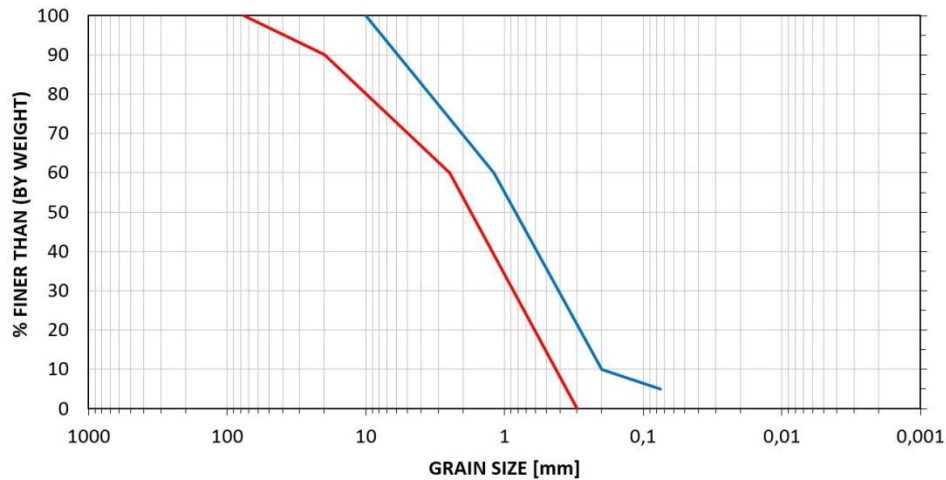


Figure 43: Preliminary Design Grading Band, Transition Layer B; the red line indicates the upper limit, the blue one the lower limit.

Table 46: Preliminary Design Grading Band, Transition Layer B

Design Grading Band – Transition Layer B – Zone 3-2		
Grain Size [mm]	% finer than (by Weight)	
0.075	5	-
0.2	10	-
0.3		0
1.2	60	
2.5		60
10	100	
20	-	90
75	-	100

10.03.04 Permeability Estimates

The permeability of soil material is directly related to grading and grain shape. Several empirical approaches are available as presented in the following formulation:

$$k = \frac{g}{\nu} \cdot C \cdot f(n) \cdot d_e^2$$

Equation 17 (Vukovic & Soro, 1992)

with $\nu = \frac{\mu}{\rho}$

where

- k hydraulic conductivity
- g acceleration due to gravity
- ν kinematic viscosity
- μ dynamic viscosity
- ρ fluid (water) density
- C sorting coefficient
- f(n) porosity function
- d_e effective grain diameter

The values of C, f(n) and d_e are related to different methods used in the grain size analysis. The available methods differ in acceptance and reliability and usually apply on specific soil types.

Table 47: Methods to estimate hydraulic conductivity

Equation	Domain of applicability	Method
$k = \frac{g}{\nu} \cdot 6 \cdot 10^{-4} [1 + 10(n - 0.26)] d_{10}^2$	$U = d_{60}/d_{10} < 5$, $0.1 < d_e < 3.0 \text{ mm}$	Hazen (Hazen, 1892)
$k = \frac{g}{\nu} \cdot 6 \cdot 10^{-4} \log \frac{500}{U} d_{10}^2$	$1 < U < 20$ $0.06 < d_e < 0.6$	Beyer (Beyer, 1964)
$k = \frac{g}{\nu} \cdot 8.3 \cdot 10^{-3} \left[\frac{n^3}{(1-n)^2} \right] d_{10}^2$	$d_e < 3 \text{ mm}$ not appropriate for clayey soils	Kozeny – Carman (Kozeny, 1927), (Carman, 1937)
$k = \frac{g}{\nu} \cdot C_t \left(\frac{n - 0.13}{\sqrt[3]{1-n}} \right)^2 \cdot d_{10}^2$	coarse sand with $6.1 \cdot 10^{-3} < C_t < 10.7 \cdot 10^{-3}$	Terzaghi (Terzaghi & Peck, 1964)
$k = \frac{g}{\nu} \cdot 4.8 \cdot 10^{-4} \cdot d_{20}^{0.3} \cdot d_{20}^2$	$U < 5$ medium to coarse sand	USBR (Vukovic & Soro, 1992)

Table 48: Estimated permeability for the different dam zones

Dam Zone	Base Soil	estimated permeability [m/s]
1 - Outer Support Body	Lafarge	$4.4 \cdot 10^{-5} < k < 3.3 \cdot 10^{-2}$
2 - Inner Support Body	Stoneworks Creek	$1.2 \cdot 10^{-5} < k < 1.0 \cdot 10^{-1}$
3 – Deceleration Zone	Stewart Creek	$1.9 \cdot 10^{-11} < k < 4.3 \cdot 10^{-9}$
6 – Protection Layer	-	$6.3 \cdot 10^{-3} < k < 6.7 \cdot 10^{-2}$
7 – Drainage Layer	-	$1.5 \cdot 10^{-2} < k < 7.7 \cdot 10^{-1}$
Transition Layer-A	-	$6.3 \cdot 10^{-3} < k < 6.7 \cdot 10^{-2}$
Transition Layer-B	-	$2.2 \cdot 10^{-4} < k < 1.5 \cdot 10^{-3}$
On Site Material	Cougar Creek Alluvium	$1.2 \cdot 10^{-5} < k < 1.0 \cdot 10^{-1}$

The permeability estimates as shown in Table 48 are potentially varying by a factor of 0.3 to 3 but normally not by an order of magnitude.

10.04 Dam Stability

According to the Dam Safety Guidelines by the Canadian Dam Association (CDA, 2007), dam structures need to be investigated in terms of stability and deformation. Dam deformation is discussed in Chapter 10.04.05.10.

10.04.01 Software Description

10.04.01.01 Slide 7.0

For limit state equilibrium slope stability and seepage analysis, the Software Slide (version 7.0) was used. Slide is a 2D slope stability software developed by Rocscience Inc. It evaluates the global factor of safety using circular and non-circular slip surfaces in soil or rock slopes.

Slide analyses the stability of slip surfaces using vertical or non-vertical slice limit equilibrium methods such as Bishop, Sharma, Spencer and Morgenstern-Price. The software provides methods for the analysis of individual slip surfaces, for the determination of critical slip surfaces at given slope geometries and allows for the definition of additional boundary conditions like minimal allowable depth or weight of generated slip surfaces.

Slide also has the capability to carry out a finite element groundwater seepage calculations and to perform pseudo static seismic stability analysis.

10.04.01.02 Fides-Wintube-2D

Fides-Wintube is a geotechnical finite elements software package based on the FE software kernel of Sofistik. It allows the analysis of deformations and stability in geotechnical and structural engineering.

The software has commonly used soil models implemented like the Mohr-Coulomb or hyperbolic stress strain models. It allows the derivation of forces and moments acting on concrete structures and the stress strain behaviour of structures. The software has the functionality of the analysis of different load and construction stages and of superimposing forces and moments from prior load stages.

Fides-Wintube further has the capability to carry out a steady state and transient finite element groundwater seepage and thermal analysis.

10.04.02 Theory and Numerical Approaches for Seepage Calculations

10.04.02.01 Slide 7.0

The finite element method for seepage calculation implemented in the software Slide is for both, steady state and transient groundwater flow analysis. There are a number of applicable formulations for steady state flow analysis for saturated and unsaturated soils, depending on whether isotropic or anisotropic conditions are assumed, or if heterogeneous or homogenous soils are being examined. The flow equations used in Slide 7.0 are comprehensively discussed in Fredlund & Radhardjo (1993).

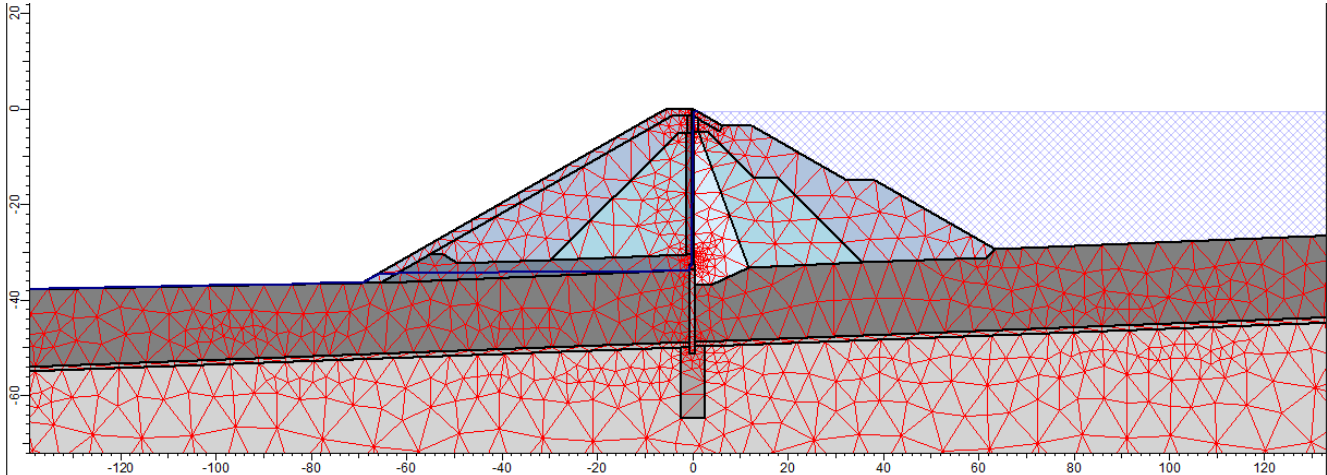


Figure 44: Slide 7.0 steady state FEA seepage calculation, triangular elements, LC-E

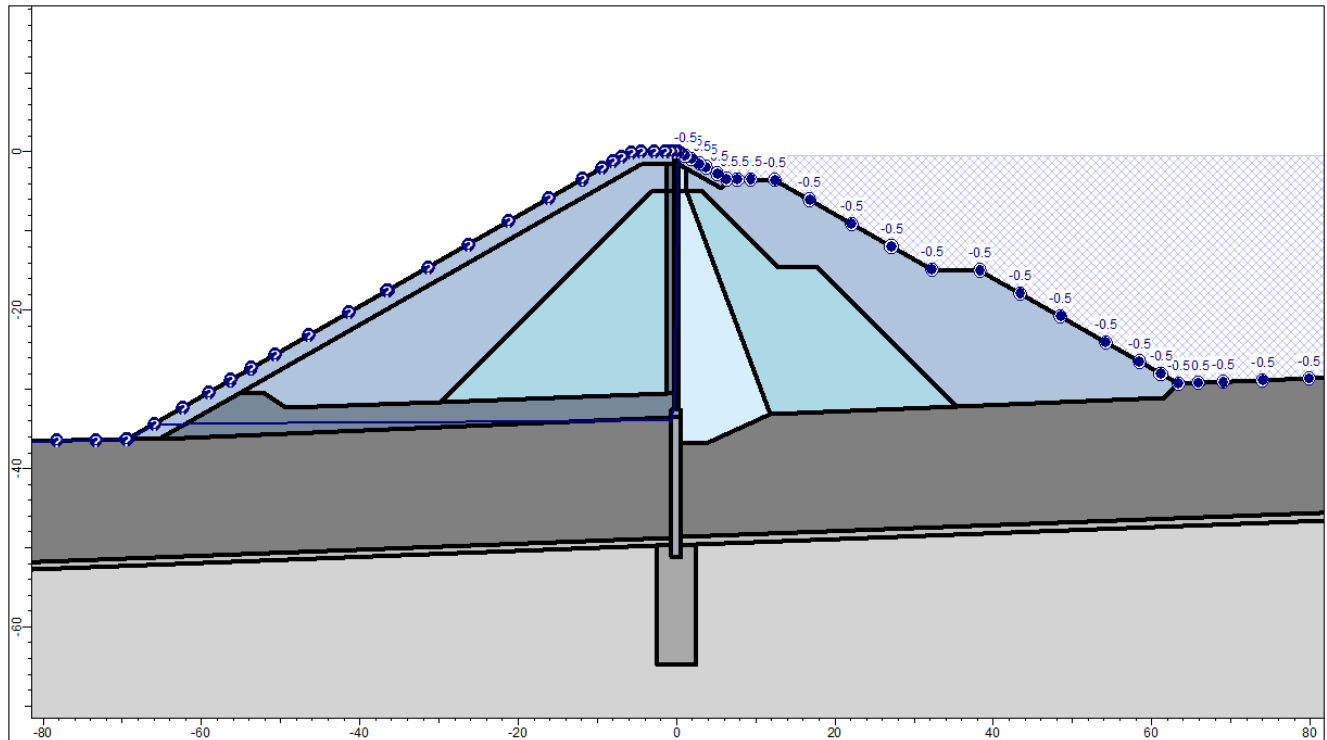


Figure 45: Slide 7.0 steady state boundary conditions, LC-E

10.04.02.02 B-Bar Method for Rapid drawdown

One of the simplest approaches to determine slope stability during a rapid drawdown is to remove the weight of the reservoir water and assume that the post-drawdown table is at the ground surface (groundwater level) while keeping the water table inside the earth structure at the long-term steady-state condition of the full impoundment. This procedure is driven by the assumption that the change in pore pressure is equal to the vertical change in water level. It is also assumed that the total stress change is equal to the pore pressure change so that the effective stress remains unchanged.

Another way to describe this simple approach is that it is equivalent to a B-Bar of 1.0. Equation 18 is a common way of looking at changes in pore pressure with changes in total stress.

$$\Delta u = \bar{B} \Delta \sigma_v$$

Equation 18

In Equation 18, \bar{B} (B-Bar) is the overall pore pressure coefficient for a certain material. In Slide this assumption is used to simulate the pore pressure change due to rapid drawdown of ponded water in earth and rock-fill embankment dams.

Within Slide, the rapid drawdown analysis using the B-Bar method consists of following steps:

- An initial water table is defined. This defines the initial pore pressure distribution and the initial weight of ponded water.
- For a complete drawdown scenario, it is assumed that all ponded water is removed from the model. The change in pore pressure for undrained materials is calculated by removal (unloading) of ponded water according to Equation 18. The final pore pressure at any point is the sum of the initial pore pressure and the (negative) excess pore pressure.
- For a partial drawdown scenario, a drawdown water table is defined. In this case, the unloading is due to removal of ponded water to the drawdown level. This determines the change in pore pressure for undrained materials. The pore pressure in drained materials is calculated from the drawdown water table.

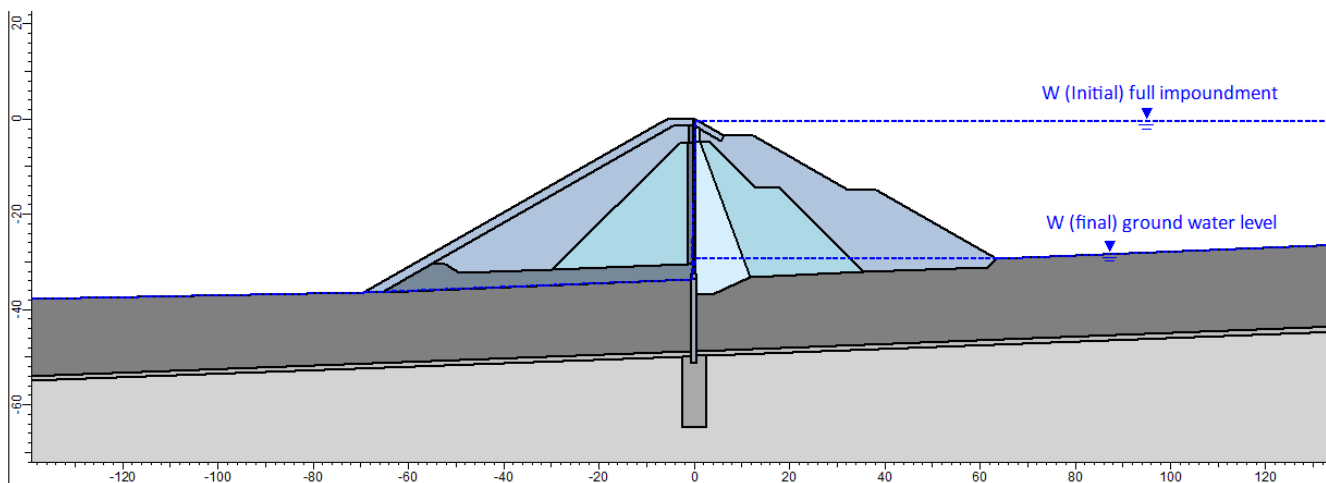


Figure 46: Slide 7.0, Rapid drawdown boundary conditions, B-Bar method

10.04.02.03 Fides-Wintube-2D

Fides-WinTube supports a much wider variety of seepage and thermal analysis tools using the finite elements method. Within this project, the linear method by Darcy was used to calculate the seepage and for analysing groundwater flow. The methods and equations are described in Sofistik (2014).

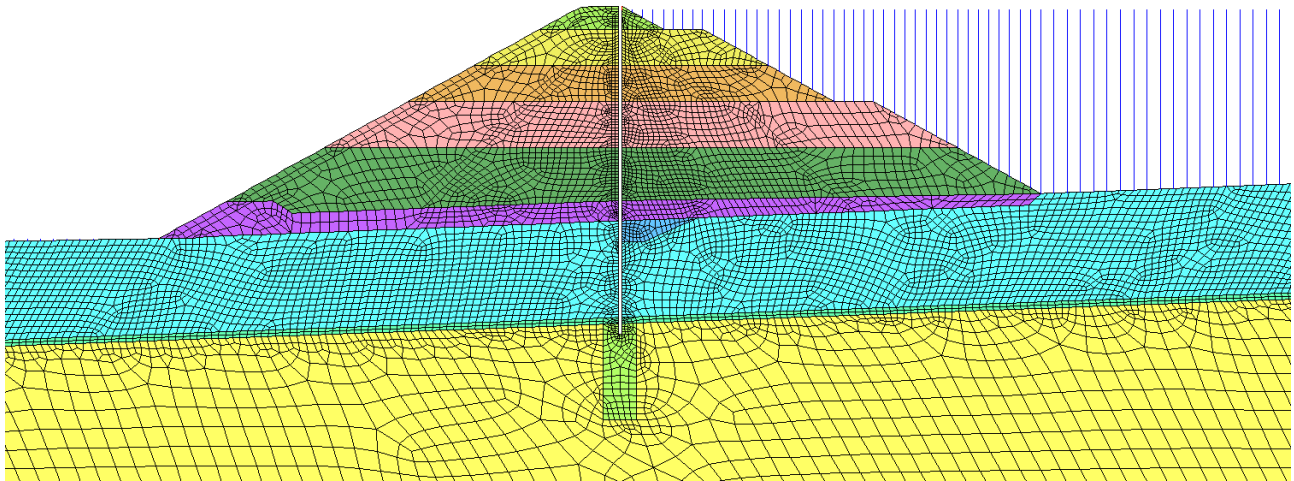


Figure 47: WinTube steady state FEA seepage calculation, quadrilateral elements, piezometric head boundary conditions

10.04.03 Applied Failure Models

10.04.03.01 Morgenstern-Price for Slope Stability Assessment

Morgenstern-Price is a slope stability analysis method developed on the basis of limit state equilibrium considerations. It requires satisfying equilibrium of forces and moments acting on individual blocks of slices. The blocks are created by dividing the body (2D face) above the slip surface by dividing it into single individual planes. The Morgenstern-Price limit equilibrium method (Morgenstern & Price, 1965) is based on the Spencer limit equilibrium method (Spencer, 1967) and forces acting on these individual blocks are abstracted in Figure 48.

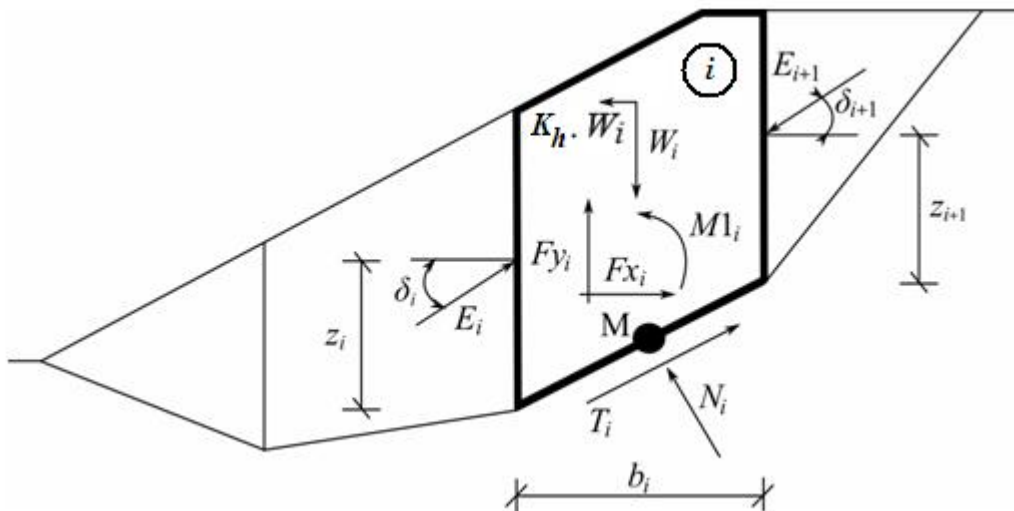


Figure 48: Static scheme - Spencer Method

The Morgenstern-Price method is based on the assumption that each block contributes due to following forces:

- W_i block weight, including the influence of the coefficient of vertical earthquake K_v
- $K_h * W_i$ horizontal inertia forces representing the effect of earthquake, K_h is the factor of horizontal acceleration during earthquake
- N_i normal forces on the slip surface
- T_i shear forces on the slip surface
- E_i, E_{i+1} forces exerted by neighboring blocks, they are inclined from a horizontal plane by angle δ
- F_{x_i}, F_{y_i} other horizontal and vertical forces acting on block
- M_1 moment of forces F_{x_i}, F_{y_i} , rotation about point M, which is the center of the i^{th} segment of the slip surface
- U_i pore pressure resultant on the i^{th} segment of slip surface

The following assumptions are introduced in the Spencer method to calculate the limit equilibrium of forces and moment on individual blocks:

- dividing planes between blocks are always vertical
- the line of action of weight of block W_i passes through the center of the i^{th} segment of slip surface represented by point M
- the normal force N_i is acting in the center of the i^{th} segment of slip surface, at point M
- inclination of forces E_i acting between blocks is constant for all blocks and equals to δ , only at slip surface end points $\delta = 0$

The only difference in the assumptions between Spencer and Morgenstern-Price method is the consideration of different inclination angles δ_i of forces E_i between each block.

The Morgenstern-Price method adapts following equations of the Spencer Method:

$$N_i = N'_i + U_i \quad \text{Equation 19 (Spencer, 1967)}$$

Equation 19 represents the relationship between effective and total value of the normal force acting on a slip surface.

$$T_i = (N_i - U_i) \tan \varphi_i + c_i \frac{b_i}{\cos \alpha_i} = N'_i \tan \varphi_i + c_i \frac{b_i}{\cos \alpha_i} \quad \text{Equation 20 (Spencer, 1967)}$$

Equation 20 corresponds to the Mohr-Coulomb condition representing the relation between the normal and shear forces on a given segment of the slip surface.

$$N'_i + U_i - W_i \cos \alpha_i + K_h W_i \sin \alpha_i + F_{y_i} \cos \alpha_i - F_{x_i} \sin \alpha_i + E_{i+1} \sin(\alpha_i - \delta_{i+1}) - E_i \sin(\alpha_i - \delta_i) = 0 \quad \text{Equation 21 (Spencer, 1967)}$$

Equation 21 represents the force equation of equilibrium in the direction normal to the i^{th} segment of the slip surface.

$$N'_i \frac{\tan \varphi_i}{FS} + \frac{c_i}{FS \cos \alpha_i} - W_i \sin \alpha_i - K_h W_i \cos \alpha_i + F_{y_i} \sin \alpha_i + F_{x_i} \cos \alpha_i - E_{i+1} \cos(\alpha_i - \delta_{i+1}) + E_i \sin(\alpha_i - \delta_i) = 0 \quad \text{Equation 22 (Spencer, 1967)}$$

Equation 22 represents force equation of equilibrium along the i^{th} segment of the slip surface. FS is the factor of safety, which is used to reduce the soil parameters.

$$E_{i+1} \cos \delta_{i+1} \left(z_i - \frac{b_i}{2} \tan \alpha_i \right) - E_{i+1} \sin \delta_{i+1} \frac{b_i}{2} - E_i \cos \delta_i \left(z_i - \frac{b_i}{2} \tan \alpha_i \right) - E_i \sin \delta_i \frac{b_i}{2} + M1_i - K_h W_i (y_M - y_{gi}) = 0 \quad \text{Equation 23 (Spencer, 1967)}$$

Equation 23 corresponds to the moment equation of equilibrium about point M, where y_{gi} is the vertical coordinate of the point of application of the weight of block and y_M is the vertical coordinate of point M.

Modifying the force Equation 21 and Equation 22 allows to calculate all forces E_i acting between blocks for given values of δ_i and factor of safety FS. This solution assumes that at the slip surface origin the value of E is known an equal to $E_1=0$.

$$E_{i+1} = \frac{[(W_i - Fy_i) \cos \alpha_i - (K_h W_i - Fx_i) \sin \alpha_i - U_i + E_i \sin(\alpha_i - \delta_i)] \frac{\tan \phi_i}{FS} + \frac{c_i - b_i}{FS \cos \alpha_i} (W_i - Fy_i) \sin \alpha_i - (K_h W_i - Fx_i) \cos \alpha_i + E_i \cos(\alpha_i - \delta_i)}{\sin(\alpha_i - \delta_{i+1}) \frac{\tan \phi_i}{FS} + \cos(\alpha_i - \delta_{i+1})} \quad \text{Equation 24}$$

$$z_{i+1} = \frac{\frac{b_i}{2} [E_{i+1} (\sin \delta_{i+1} - \cos \delta_{i+1} \tan \alpha_i) + E_i (\sin \delta_i - \cos \delta_i \tan \alpha_i)]}{E_{i+1} \cos \delta_{i+1}} + \frac{E_i z_i \cos \delta_i - M1_i + K_h W_i (y_M + y_{gi})}{E_{i+1} \cos \delta_{i+1}} \quad \text{Equation 25}$$

Equation 25 allows calculating all arms z_i of forces acting between blocks for a given value of δ_i .

The calculation of the factor of safety of the Morgenstern-Price method follows following iteration process:

1. The initial value of angels δ_i is set according to a half-sine function ($\delta_i = \lambda * f(x_i)$)
2. Calculating the factor of safety for a given value of δ_i while assuming the value of $E_{i+1} = 0$ at the end of the slip surface.
3. Recalculating δ_i using the values of E_i determined in the previous step with the requirement of having the moment of the last block equal to zero. Functional values $f(x_i)$ are always the same during the iteration, only the parameter λ is iterated. For the value z_{i+1} the moment equation of equilibrium about point M has to be satisfied.
4. The steps 2 and 3 are then repeated until the values of δ_i (respectable parameter λ) does not change.

It is necessary to avoid unstable solutions for the iteration process (division by zero). Therefore, the value of δ_i must be found in the interval $(-\pi/2; \pi/2)$.

10.04.03.02 Phi-c reduction method for FE Stability Assessment

The phi-c reduction method in Fides-WinTube is based on the Fellenius rule. The Fellenius rule defines safety as the ratio between actual shear strength and mobilized shear strength for the system limit state.

$$\eta_\phi = \frac{\tan(\phi_{inp})}{\tan(\phi_{mob})} \quad \text{and} \quad \eta_c = \frac{\tan(c_{inp})}{\tan(c_{mob})} \quad \text{Equation 26 (Sofistik, 2014)}$$

Therefore, the algorithmic framework of the load stepping scheme (Equation 26), initially aiming at the gradual increase of the effective system load, has been adjusted and is now used to gradually decrease the system's resistance (Equation 28).

$$g(u) \equiv [F_i(u) - F_i(\sigma_{plc})] - \lambda * \frac{[P - F_i(\sigma_{plc})]}{F_{ef}} \stackrel{!}{=} 0 \quad \text{Equation 27 (Sofistik, 2014)}$$

where

- $F_i(u)$ internal reaction forces as functions of the displacement u
- $F_i(\sigma_{plc})$ internal reaction forces resulting from the primary stress state σ_{plc}
- P external load vector
- F_{ef} effective external load vector

$$g(u) \equiv [F_i(u, \eta) - F_i(\sigma_{plc})] \leq 0$$

Equation 28 (Sofistik, 2014)

In this notation, the material safety factor η is introduced. Furthermore, it is assumed that the procedure is launched from a balanced system state, which means that for the effective system load $F_{ef} = 0$ is fulfilled. Starting with $\eta = 1.0$, the algorithm decreases the system's resistance by iteratively increasing the material safety. Adopting a synchronized increase of the safety factors $\eta_\phi = \eta_c = \eta$, the effective shear strength for step n is determined according to Equation 29.

$$\eta_\phi = \frac{\tan(\phi_{inp})}{\eta_n} \quad \text{and} \quad c_n = \frac{c_{inp}}{\eta_n}$$

Equation 29 (Sofistik, 2014)

If local strength violations are induced by the given loading state, stress redistribution takes place and the iterative procedure tries to establish a new system deformation state " u " that both conforms with the strength conditions and represents a state of equilibrium. This way, the system resistance is gradually reduced until no further stress redistribution is possible and a (numerical) failure mechanism forms.

Similar to the load stepping the procedure terminates either in case of the maximum specified safety level η_{max} being reached, or in case of undershooting the specified minimum safety increment $\Delta\eta_{min}$.

After successful calculation, a sequence of system states is established, each associated with a certain safety level η . Assessing these system states helps to analyze the system's sensitivity with respect to strength induced failure and also provides some insight into the formation of possible failure mechanisms. Having identified the ultimate permissible system state, the associated safety factor η directly represents the corresponding computational Fellenius safety according to Equation 26.

The phi-c reduction in Fides-WinTube applies to all nonlinear soil material models. However, the particular hardening capabilities of advanced soil models like the hardening soil and double hardening soil model are irrelevant for the stability analysis. In the context of the phi-c reduction, the formulation is therefore automatically reduced to standard elastoplastic behaviour with a Mohr-Coulomb failure criterion (Sofistik, TALPA Manual, 2D Finite Elements in Geotechnical Engineering, 2014).

10.04.04 Geotechnical Design Parameters

Geotechnical design parameters are outlined and discussed comprehensively in the Geotechnical Design Basis Memorandum (LTMM CC - M - GTDB-01 - CHT 2016).

Most relevant parameters and nonlinear shear functions are summarized in chapter 06.02.01 of this report as well.

10.04.05 Results of Dam Stability Analysis

10.04.05.01 Summary

Dam stability analysis was performed by means of slip circle calculations and non-circular slip surface analysis. Considering the design values for material properties, the smallest determined Factors of Safety (FoS) are above the requirements as listed in the guidelines of the CDA, outlined in chapter 05.03.01. Determined and required FoS resulting from stability calculations under consideration of the design values for material properties and for all relevant load cases are summarized in Table 49. In addition, and independently from formal requirements for stability checks, the seismic yield acceleration for the empty and the fully impounded structure have been analyzed.

The phreatic line in the downstream embankment is in all load cases lower than the top of the horizontal drainage layer and therefore not listed separately.

Table 49: Summary of minimum Factors of Safety of the slope stability analysis

Load Combination		Method	Factor of Safety		
ID	Description		Downstream Embankment	Upstream Embankment	Required FoS acc. to CDA
LC A	Empty Structure	Slip Surface	1.64	1.88	1.3
		Phi-c Reduction	1.62		1.3
LC A 1	Empty Structure plus Ground Movement	Slip Surface / pseudo static	1.35	1.61	1.0
LC B	Impoundment 1/3 of structure height	Slip Surface	1.63	1.88	1.3
LC C	Impoundment 1/2 of structure height	Slip Surface	1.62	1.88	1.3
LC D	Impoundment 2/3 of structure height	Slip Surface	1.61	1.87	1.3
LC E	full impoundment	Slip Surface	1.60	1.88	1.5 (steady state impoundment)
		Phi-c Reduction	1.61		1.5
LC F	Overtopping	Slip Surface	1.58	1.79	not specified
LC G	Rapid draw down	Slip Surface	-	1.34	1.2 (1.3 if frequent)
		Phi-c Reduction	1.57		

For the loading condition steady state full impoundment (LC-E), the smallest Factor of Safety determined is 1.60, which is above the required FoS of 1.5.

For comparison and for plausibility check, FE-calculations with phi-c reduction method were conducted. Results are corresponding to those of limit state stability calculations. The lowest FoS determined with FE calculations under consideration of full impoundment is 1.60, considering design parameters. The FoS for overtopping is 1.58.

The investigation of the critical seismic coefficient for loading case A, the dry structure, results in values as listed in Table 53. For loading case E, full impoundment, results are listed in Table 51. Applying 0.5xPGA for seismic design coefficients, calculations indicate that the structure is safe for earthquakes with return periods greater than 10,000 years for both, the dry and the fully impounded structure. Referring seismic hazard values are listed in Table 52.

Table 50: critical seismic coefficient k_h for LC-A and its estimated return period

Failure Surface	seismic coefficient k_h	Return Period for $k_h=1.0*PGA$	Return Period for $k_h=0.5*PGA$
circular	0.286	>10,000	>10,000
non-circular	0.275	>10,000	>10,000
circular	$\geq 0.312, 0.402$	>10,000	>10,000
non-circular	$\geq 0.312, 0.372$	>10,000	>10,000

Failure Surface	seismic coefficient k_h	Return Period for $k_h=1.0*PGA$	Return Period for $k_h=0.5*PGA$
-----------------	---------------------------	---------------------------------	---------------------------------

Table 51: critical seismic coefficient k_h for LC-E and its estimated return period

Failure Surface	seismic coefficient k_h	Return Period for $k_h=1.0*PGA$	Return Period for $k_h=0.5*PGA$
circular	0.266	>5,000	>10,000
non-circular	0.257	>5,000	>10,000
circular	$\geq 0.188, 0.280$	>5,000	>10,000
non-circular	$\geq 0.203, 0.283$	>5,000	>10,000

Table 52: Seismic hazard values according to the NBCC Site Class B and C

PGA in [g] for NBCC Site Class C			PGA in [g] for NBCC Site Class B		
Return Period [years]	median	mean	Return Period [years]	median	mean
100	0.020	0.025	100	0.016	0.020
475	0.054	0.074	475	0.043	0.059
975	0.080	0.109	975	0.064	0.087
2,475	0.120	0.167	2475	0.096	0.134
5,000	0.168	0.235	5000	0.134	0.188
10,000	0.235	0.335	10000	0.188	0.268

10.04.05.02 Load Case A

Table 53: LC-A, Factor of Safety, Method: GLE/Morgenstern - Price

LC-A, Factor of Safety			
downstream slope		upstream slope	
circular	non-circular	circular	non-circular
1.68	1.64	$\geq 1.88, 2.12$	$\geq 1.88, 2.00$

Seepage

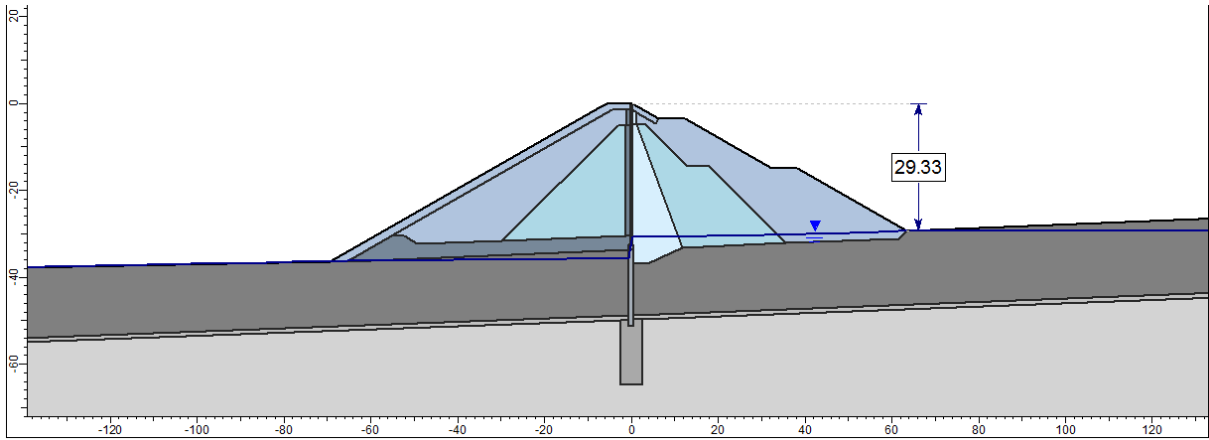


Figure 49: Groundwater, STL-A

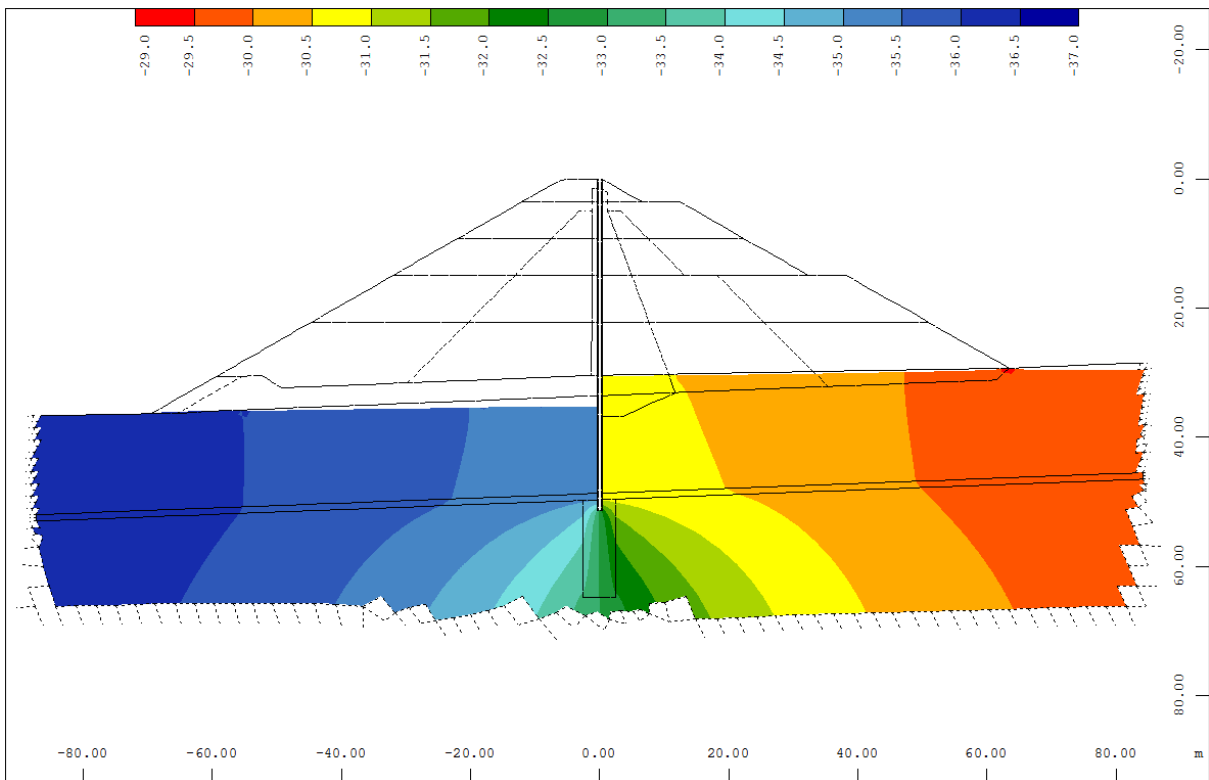


Figure 50: Seepage calculation for ground water flow only, potentials [m] and free surface, WinTube, STL-A

Stability Analysis assuming a Circular Slip Surface

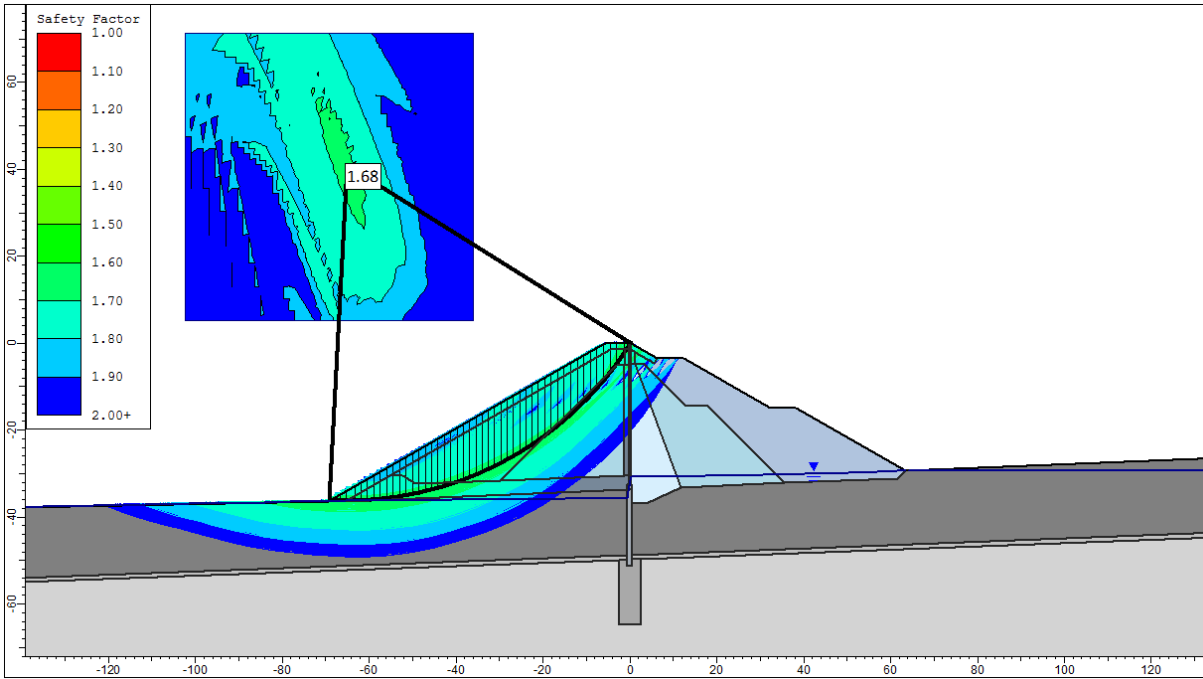


Figure 51: LC-A, circular surface, GLE, FoS = 1.68

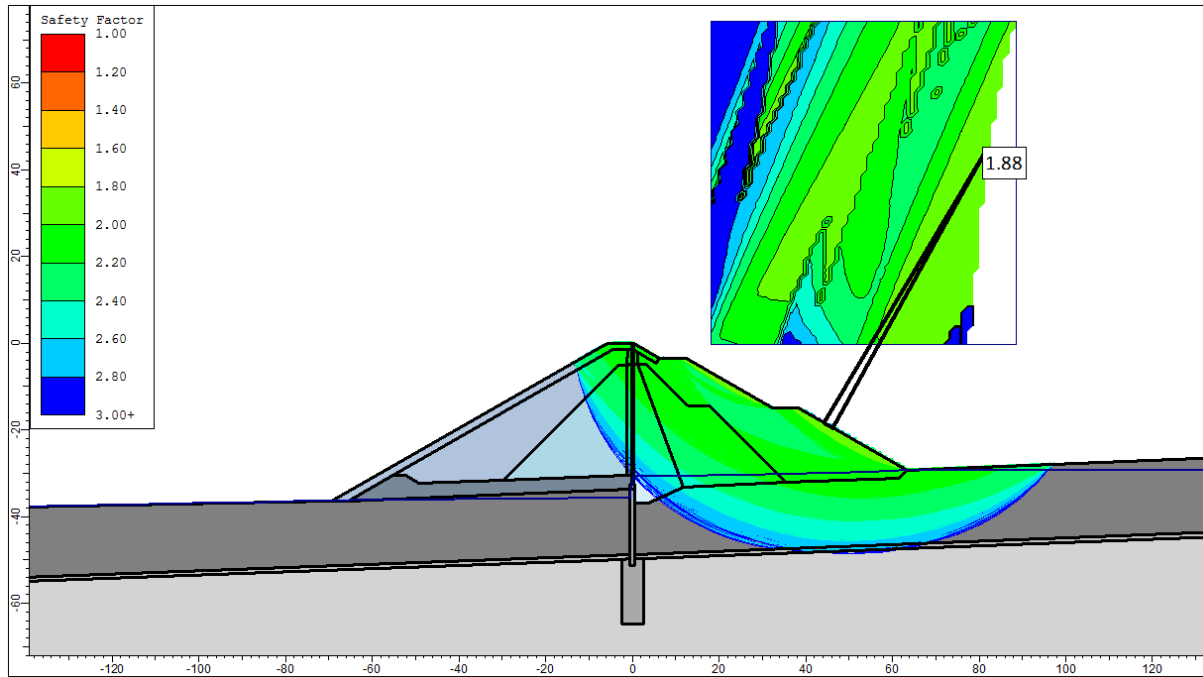


Figure 52: LC-A, circular surface, GLE, FoS ≥ 1.88

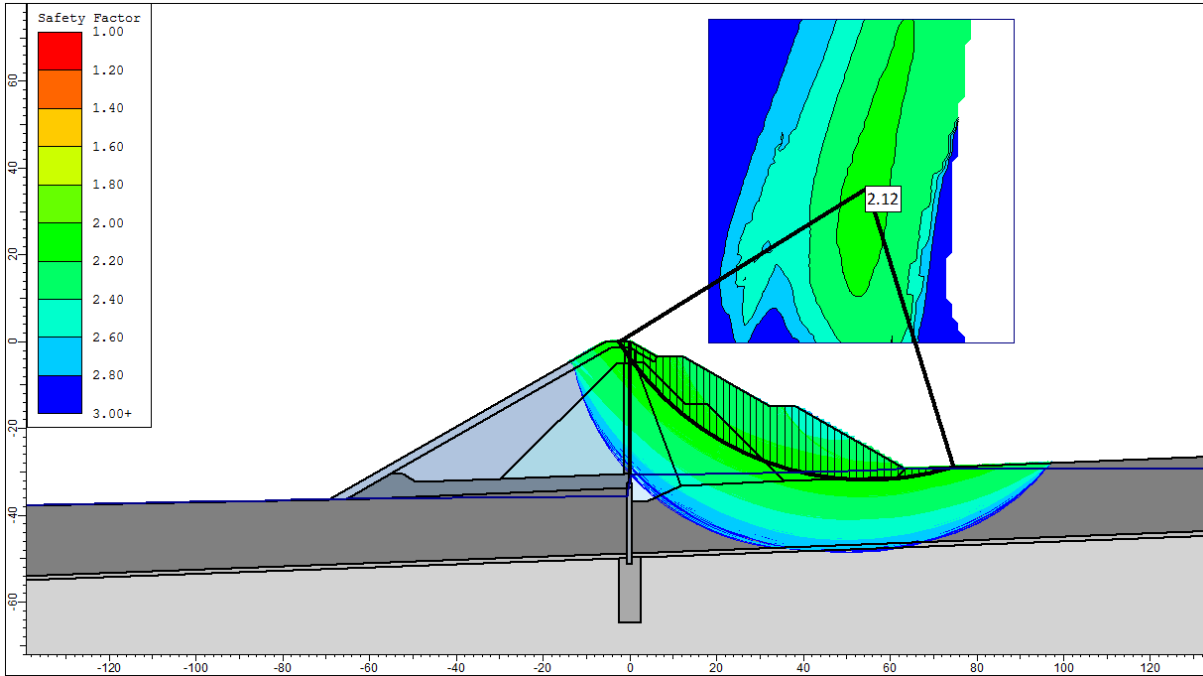


Figure 53: LC-A circular surface with at least 6 m depth, GLE, FoS = 2.12

Stability Analysis assuming a Non-Circular Slip Surface

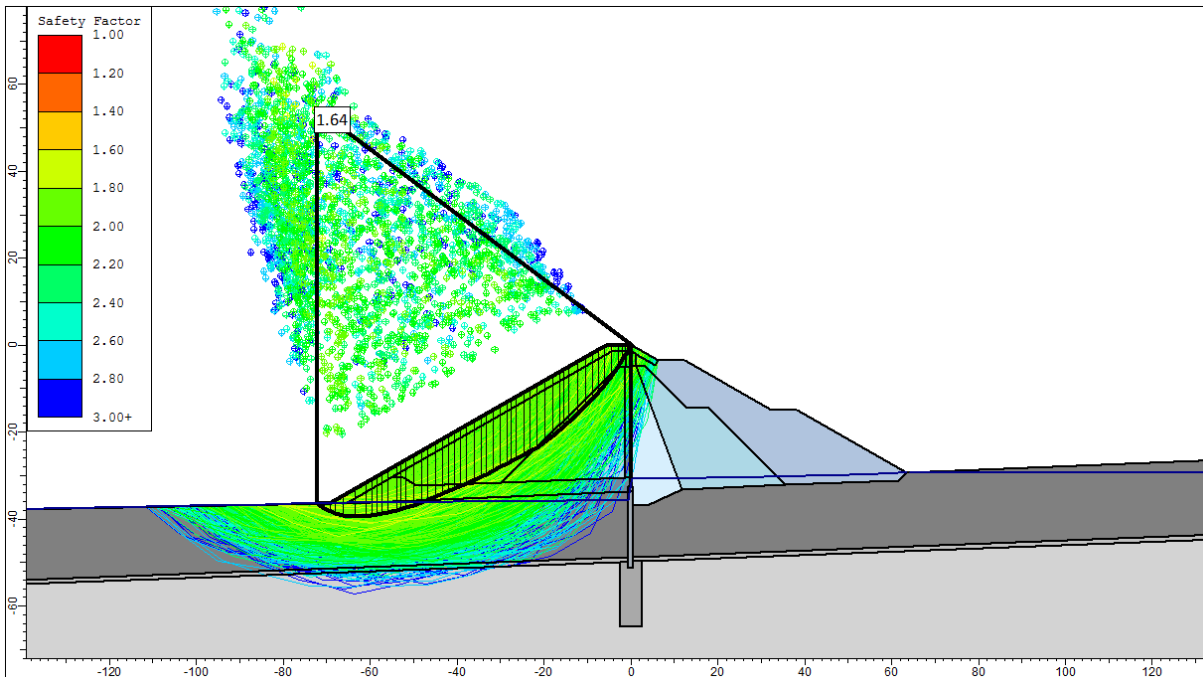


Figure 54: LC-A, non-circular surface, GLE, FoS = 1.64

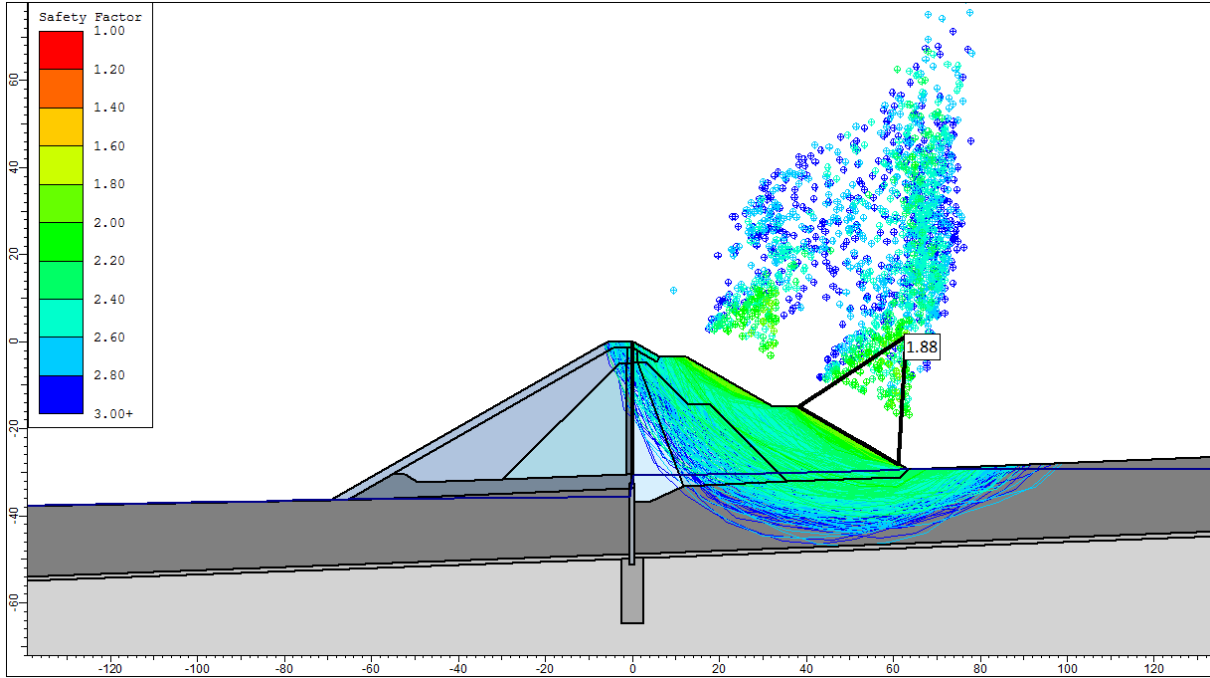


Figure 55: LC-A, non-circular surface, GLE, FoS ≥ 1.88

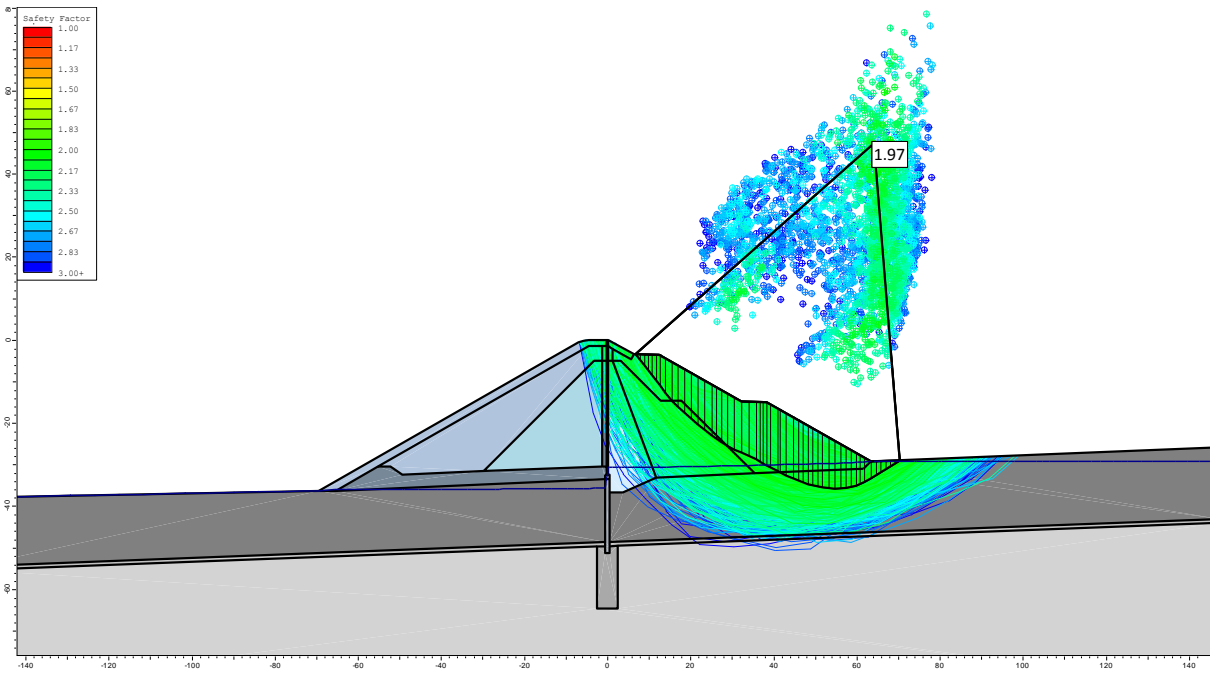


Figure 56: LC-A, non-circular surface with at least 5 m depth, GLE, FoS = 2.00

FE Stability Assessment with Phi-c Reduction

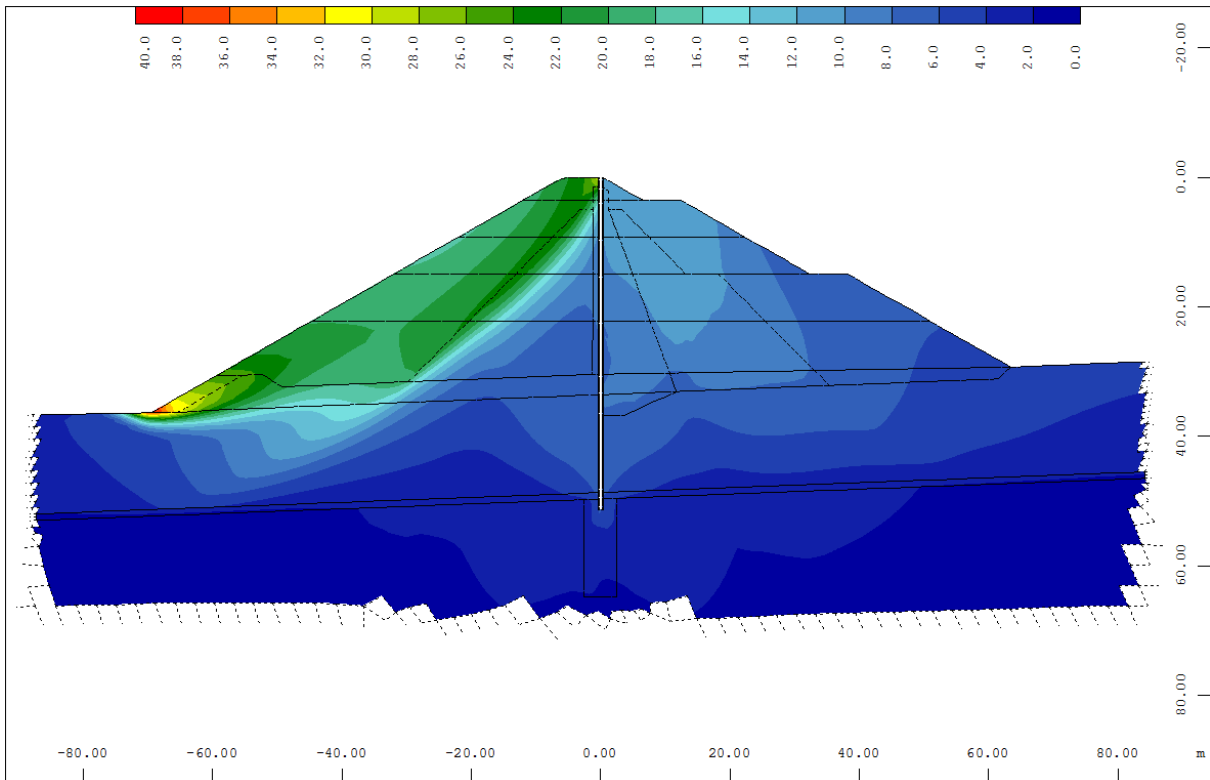


Figure 57: LC-A, phi-c reduction, nodal displacement vector [mm], FoS = 1.62

10.04.05.03 Load Case A-1

Table 54: LC-A-1, $e_v = + 2/3 e_h$, Factor of Safety, Method: GLE/Morgenstern - Price

LC-A-1, $e_v = + 2/3 e_h$, Factor of Safety			
downstream slope		upstream slope	
circular	non-circular	circular	non-circular
1.38	1.36	≥1.55, 1.72	≥1.58, 1.62

Table 55: LC-A-1, $e_v = - 2/3 e_h$, Factor of Safety, Method: GLE/Morgenstern - Price

LC-A-1, $e_v = - 2/3 e_h$, Factor of Safety			
downstream slope		upstream slope	
circular	non-circular	circular	non-circular
1.38	1.35	≥ 1.51, 1.70	≥ 1.54 , 1.61

Seepage

The Seepage is identical to LC-A as shown in Figure 49.

Seismic Load

For the empty retention structure in LC-A-1 the seismic load is based on the 5,000 year return period with $0.5 \cdot \text{PGA}$ considered. The horizontal seismic load coefficient e_h is always considered to act in the direction of failure. The vertical seismic load coefficient can act upwards (-) and downwards (+).

Stability Analysis assuming a Circular Slip Surface

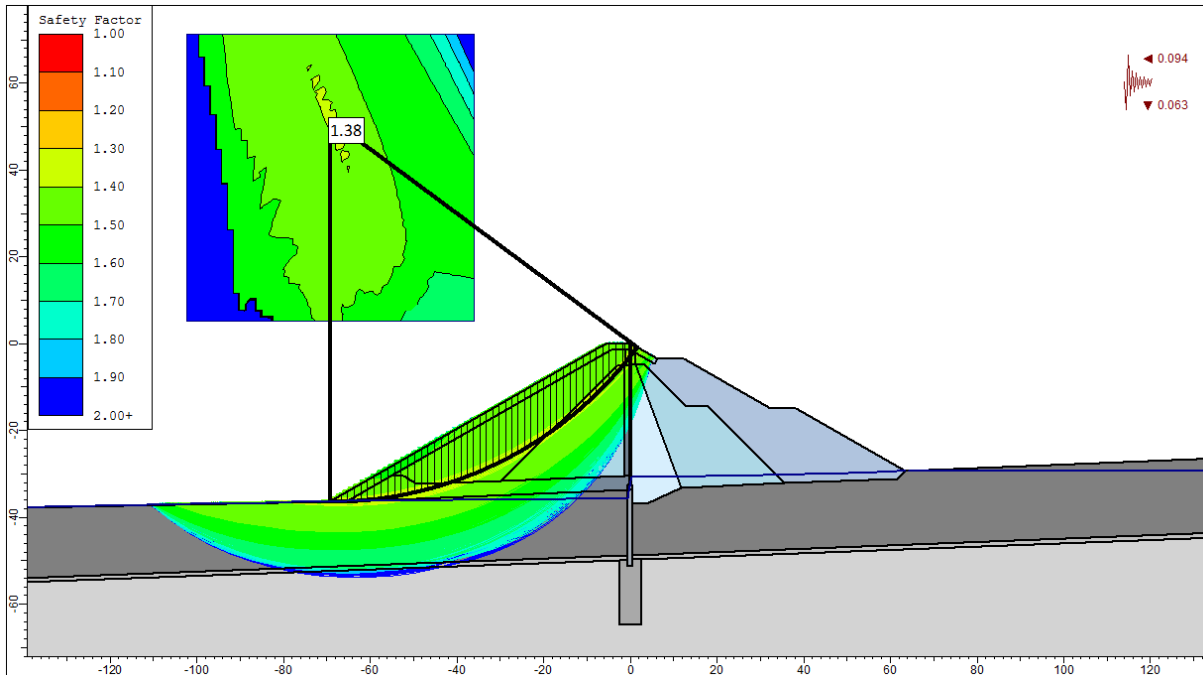


Figure 58: LC-A-1, $0.5 \cdot \text{PGA}$, 5,000yr return period, $e_v = + 2/3 e_h$, circular surface, GLE, FoS = 1.38

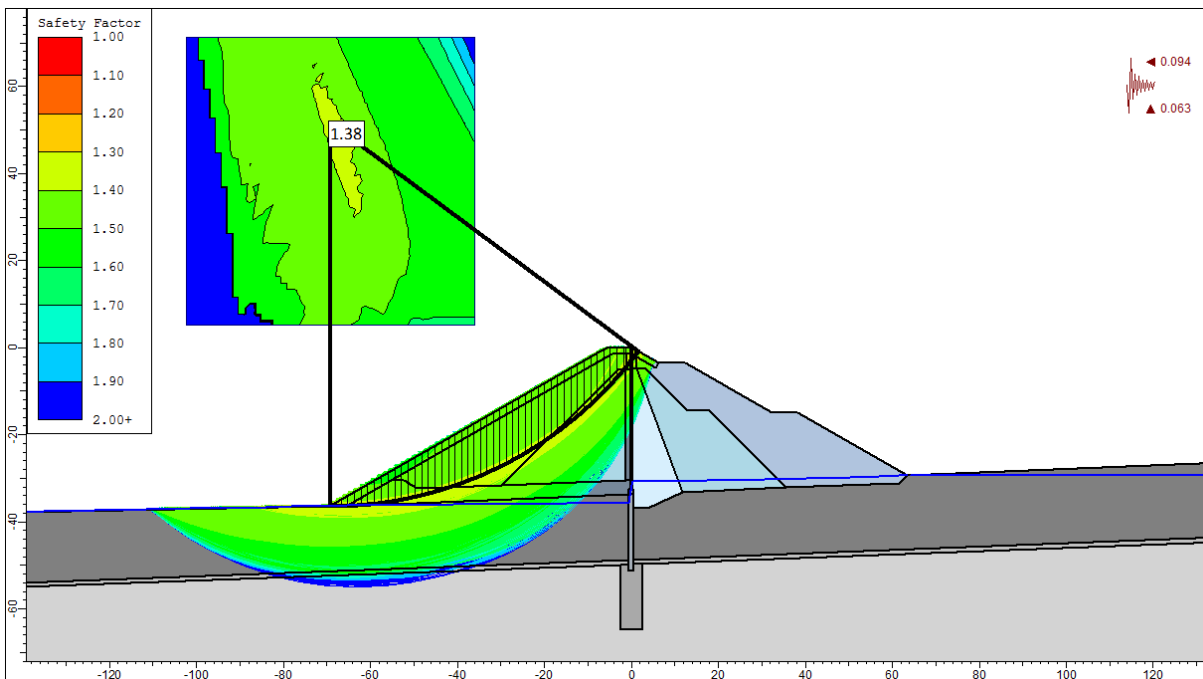


Figure 59: LC-A-1, 0.5*PGA, 5,000yr return period, $e_v = -2/3 e_n$, circular surface, GLE, FoS = 1.38

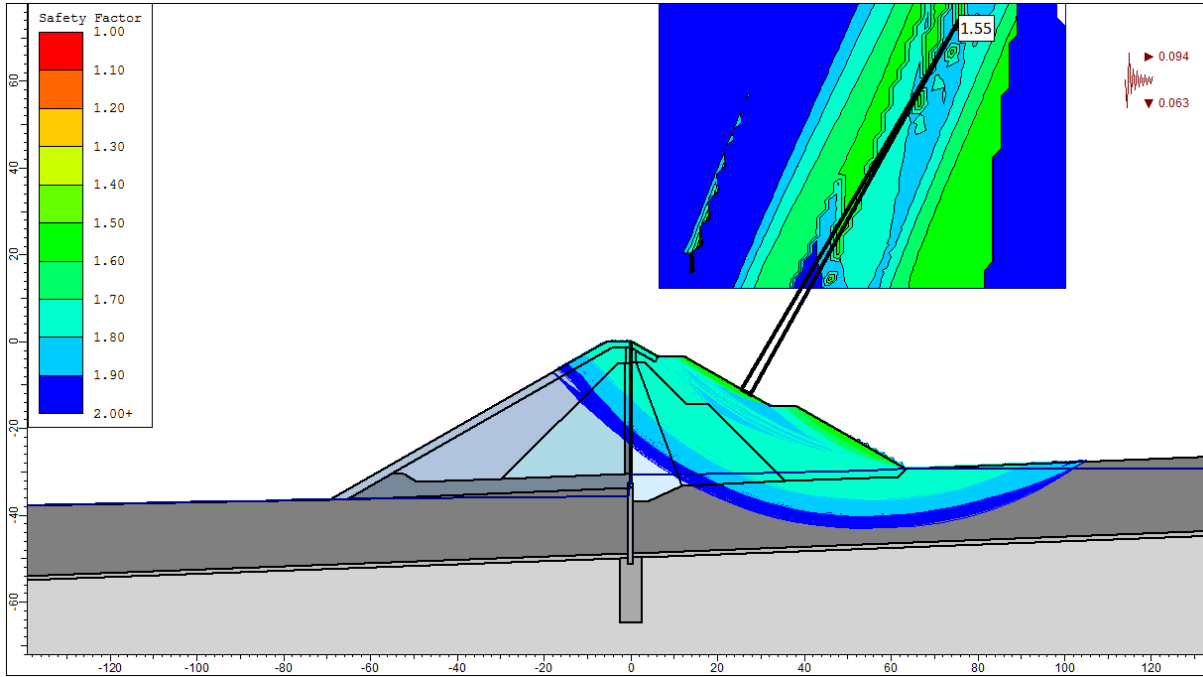


Figure 60: LC-A-1, 0.5*PGA, 5,000yr return period, $e_v = +2/3 e_n$, circular surface, GLE, FoS ≥ 1.55

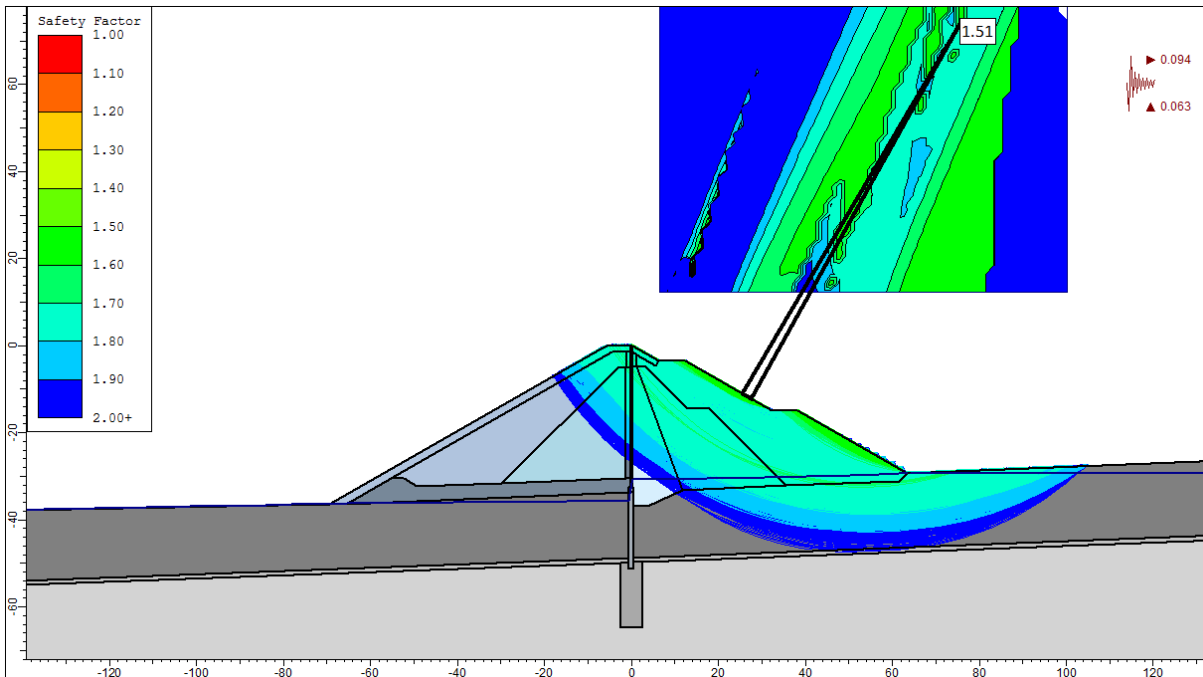


Figure 61: LC-A-1, 0.5*PGA, 5,000 yr return period, $e_v = -2/3 e_n$, circular surface, GLE, FoS ≥ 1.51

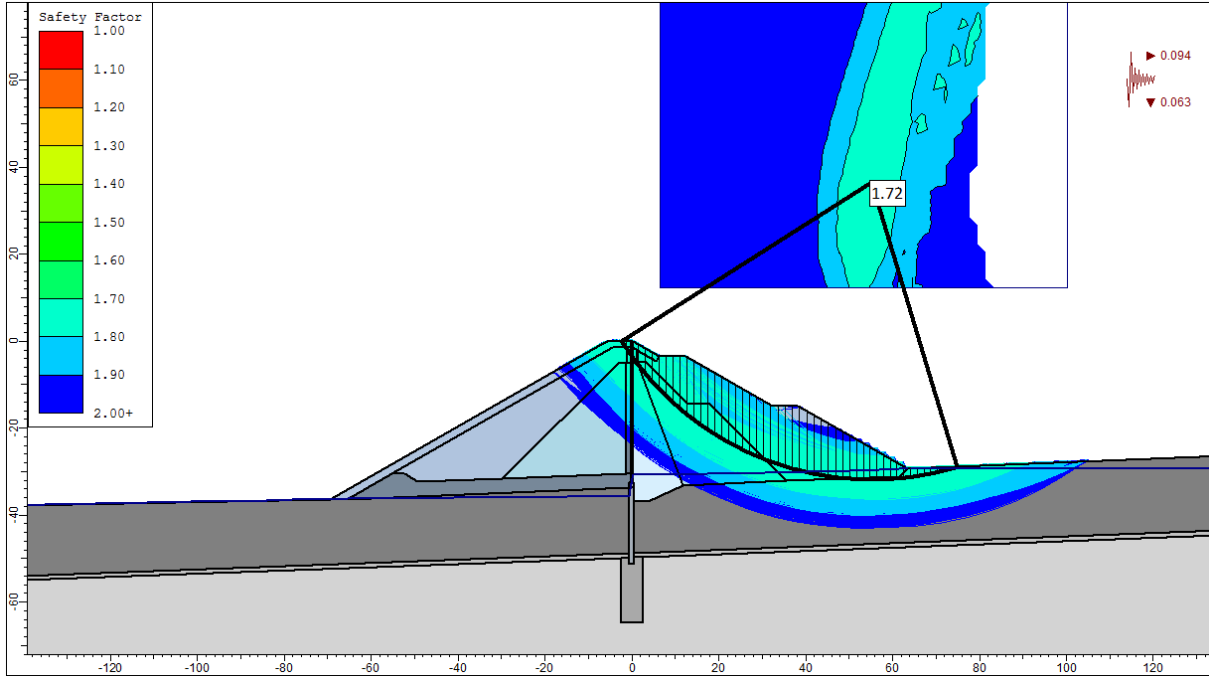


Figure 62: LC-A-1, 0.5*PGA, 5,000 yr return period, $e_v = + 2/3 e_h$, circular surface with at least 5 m depth, GLE, FoS ≥ 1.72

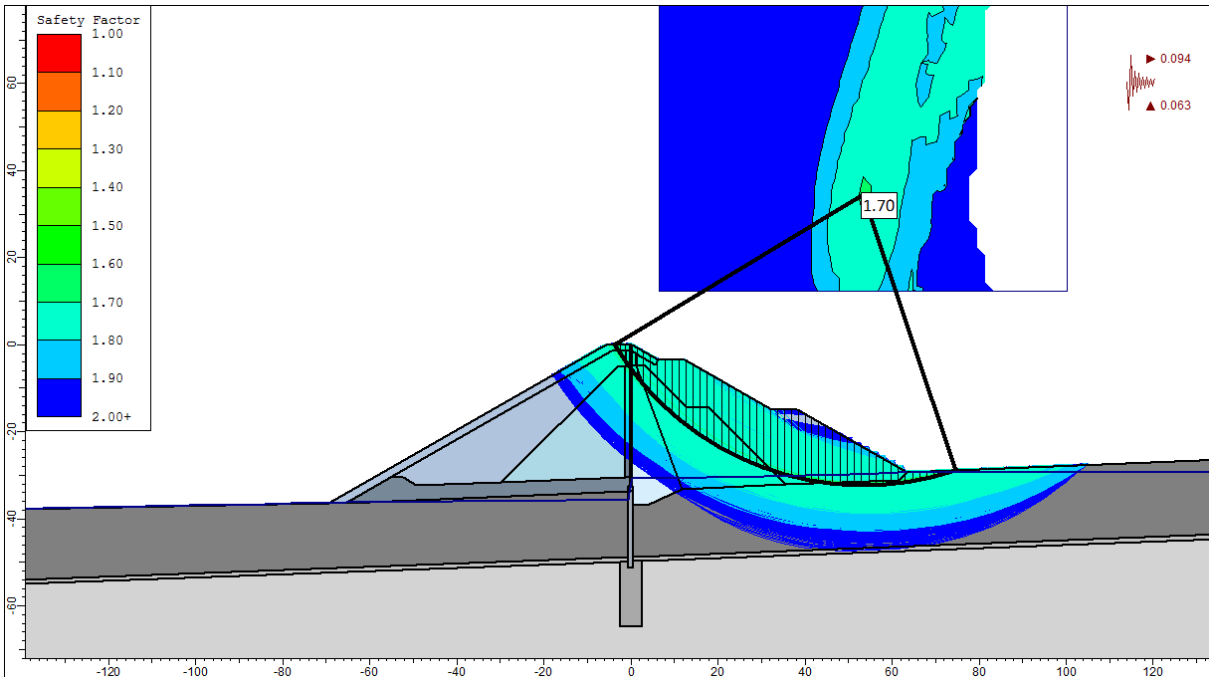


Figure 63: LC-A-1, 0.5*PGA, 5,000 yr return period, $e_v = - 2/3 e_h$, circular surface with at least 5 m depth, GLE, FoS ≥ 1.70

Stability Analysis assuming a Non-Circular Slip Surface

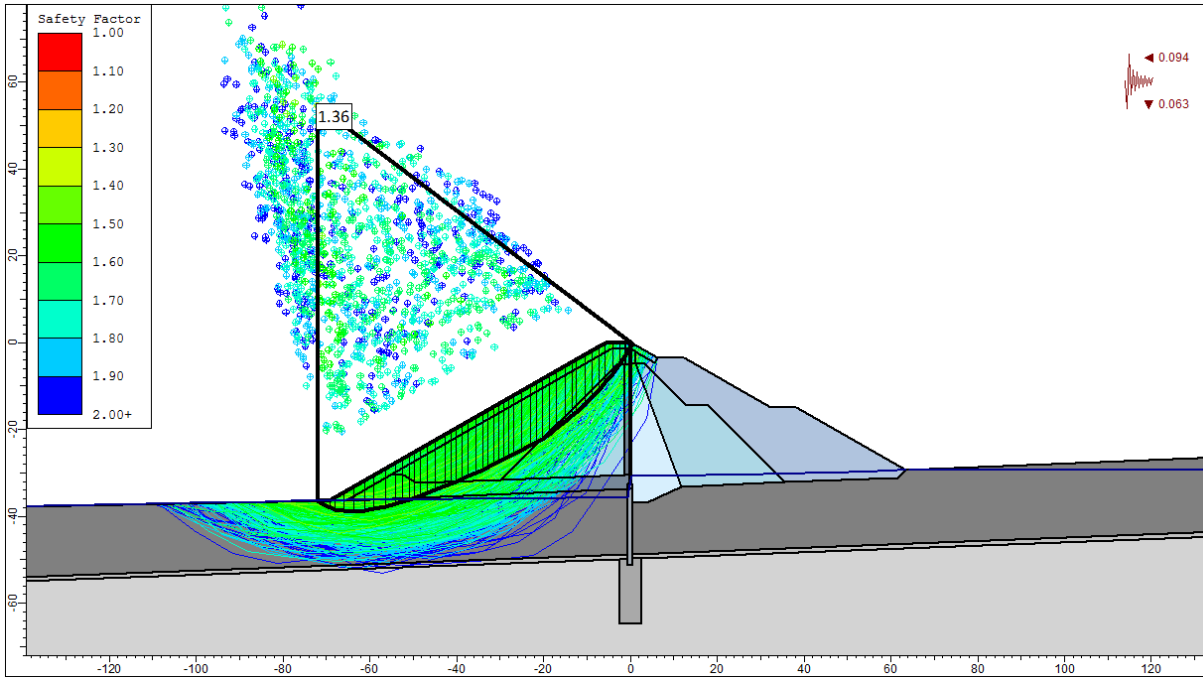


Figure 64: LC-A-1, 0.5*PGA, 5,000 yr return period, $e_v = + 2/3 e_h$, non-circular surface, GLE, FoS = 1.36

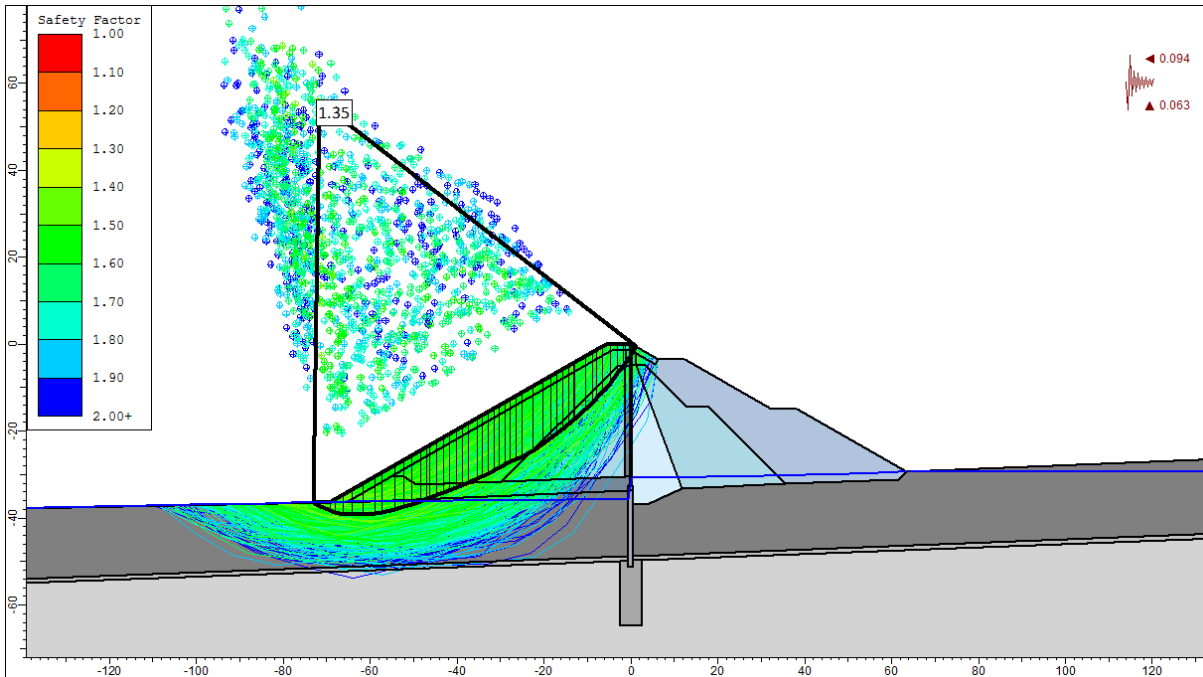


Figure 65: LC-A-1, 0.5*PGA, 5,000 yr return period, $e_v = - 2/3 e_h$, non-circular surface, GLE, FoS = 1.35

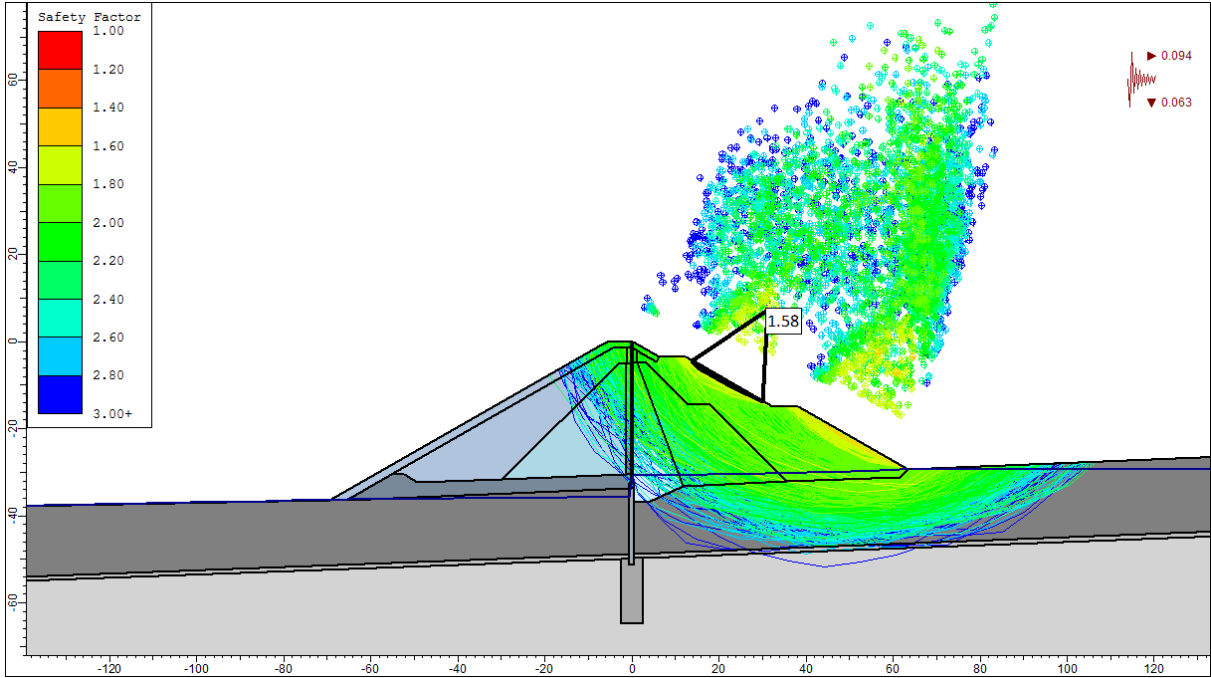


Figure 66: LC-A-1, 0.5*PGA, 5,000 yr return period, $e_v = + 2/3 e_h$, non-circular surface, GLE, FoS ≥ 1.58

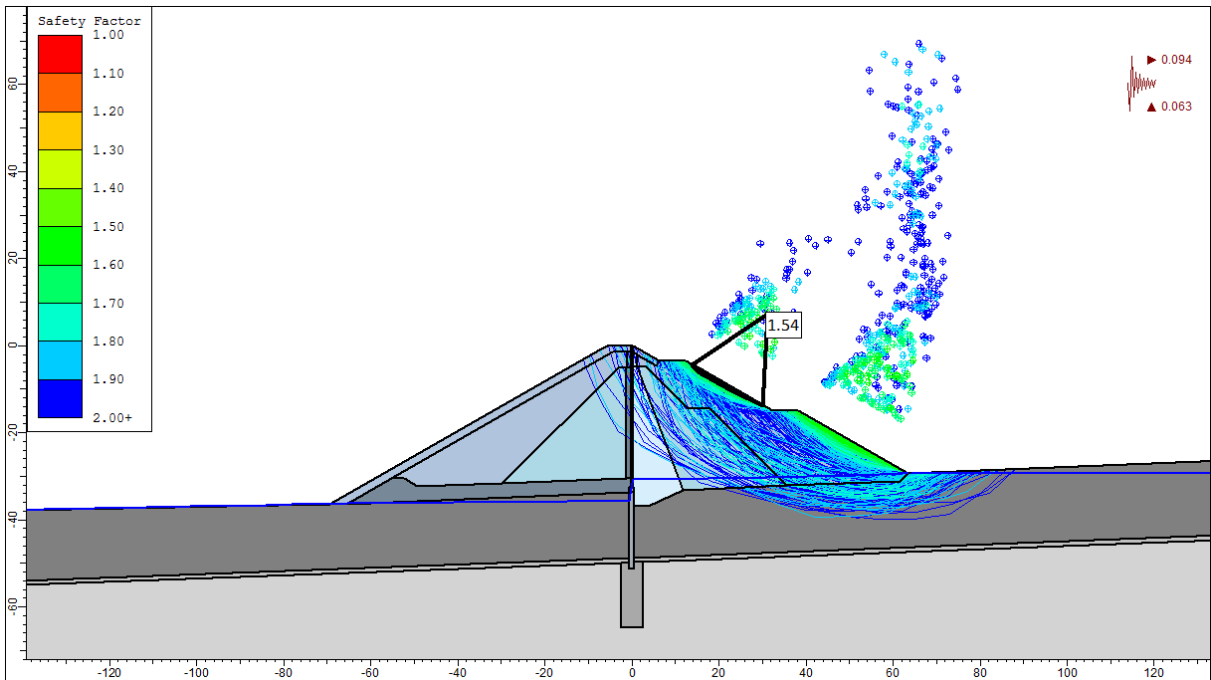


Figure 67: LC-A-1, 0.5*PGA, 5,000 yr return period, $e_v = - 2/3 e_h$, non-circular surface, GLE, FoS ≥ 1.54

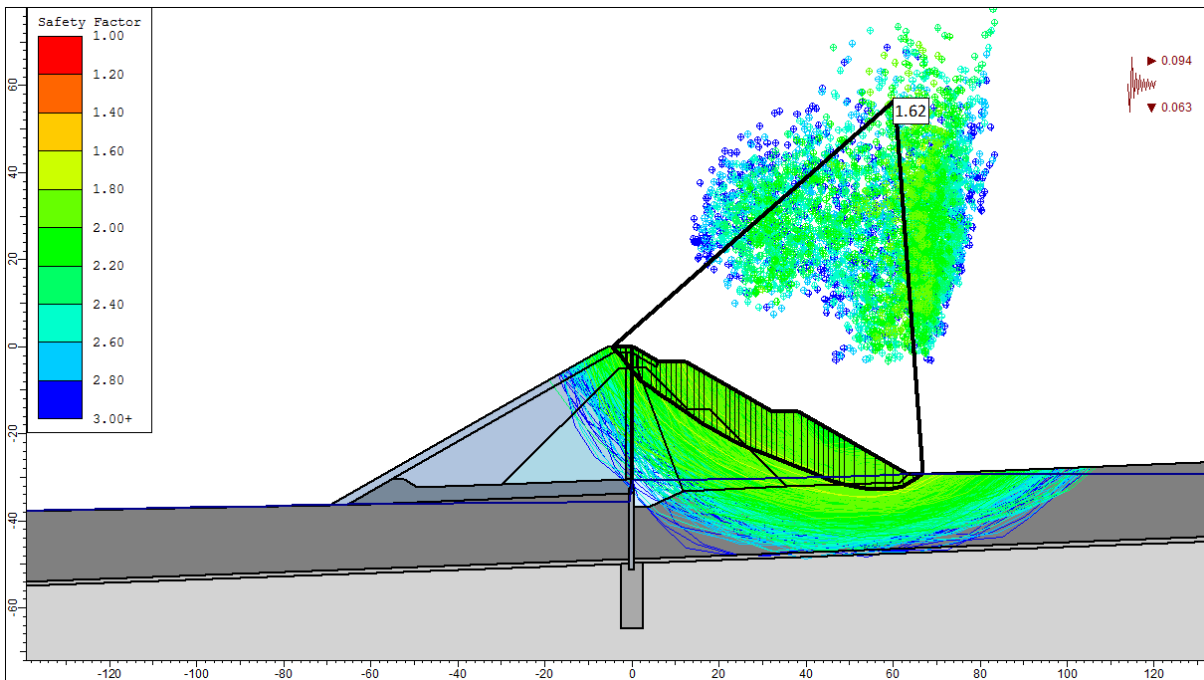


Figure 68: LC-A-1, 0.5*PGA, 5,000 yr return period, $e_v = + 2/3 e_h$, non-circular surface with at least 5 m depth, GLE, FoS = 1.62

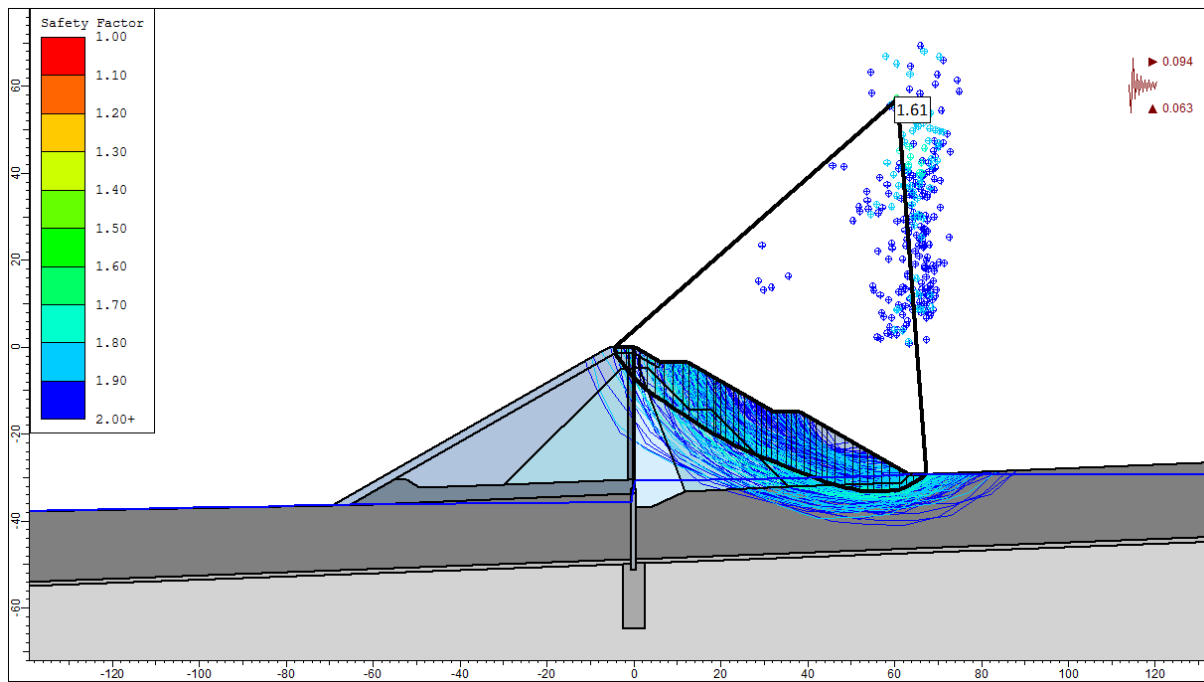


Figure 69: LC-A-1, 0.5*PGA, 5,000 yr return period, $e_v = - 2/3 e_h$, non-circular surface with at least 5 m depth, GLE, FoS = 1.61

10.04.05.04 Load Case B

Table 56: LC-B, Factor of Safety, Method: GLE/Morgenstern - Price

LC-B, Factor of Safety			
downstream slope		upstream slope	
circular	non-circular	circular	non-circular
1.67	1.63	≥ 1.88, 2.05	≥ 1.88, 2.01

Seepage

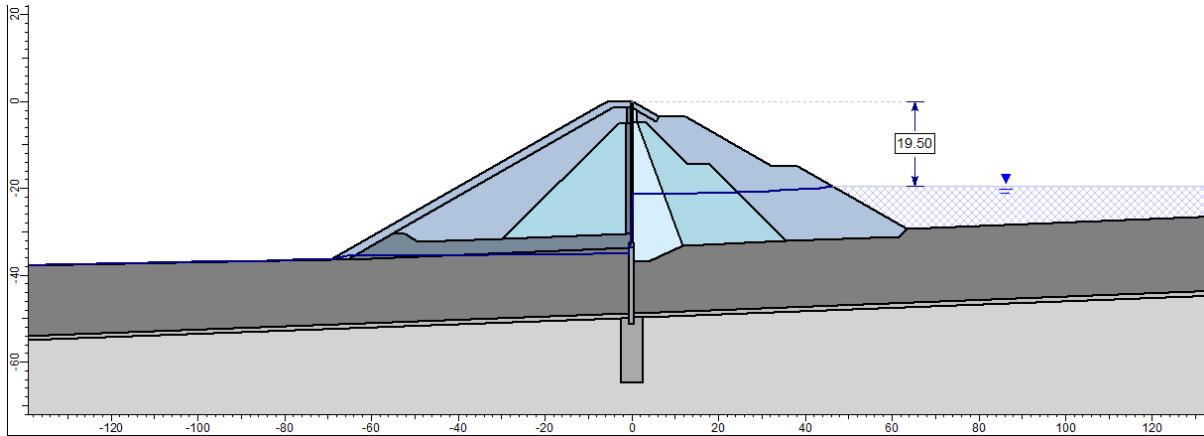


Figure 70: Impoundment level at approximately 1/3 dam height STL-B,

Stability Analysis assuming a Circular Slip Surface

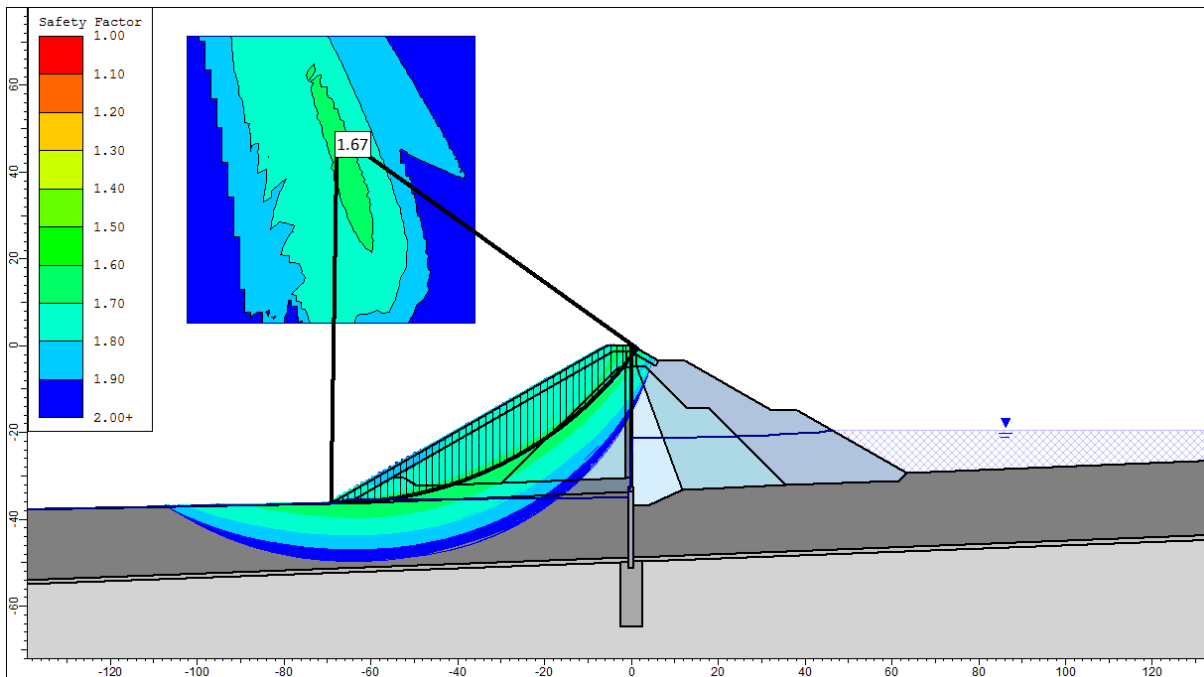


Figure 71: LC-B, circular surface, GLE, FoS = 1.67

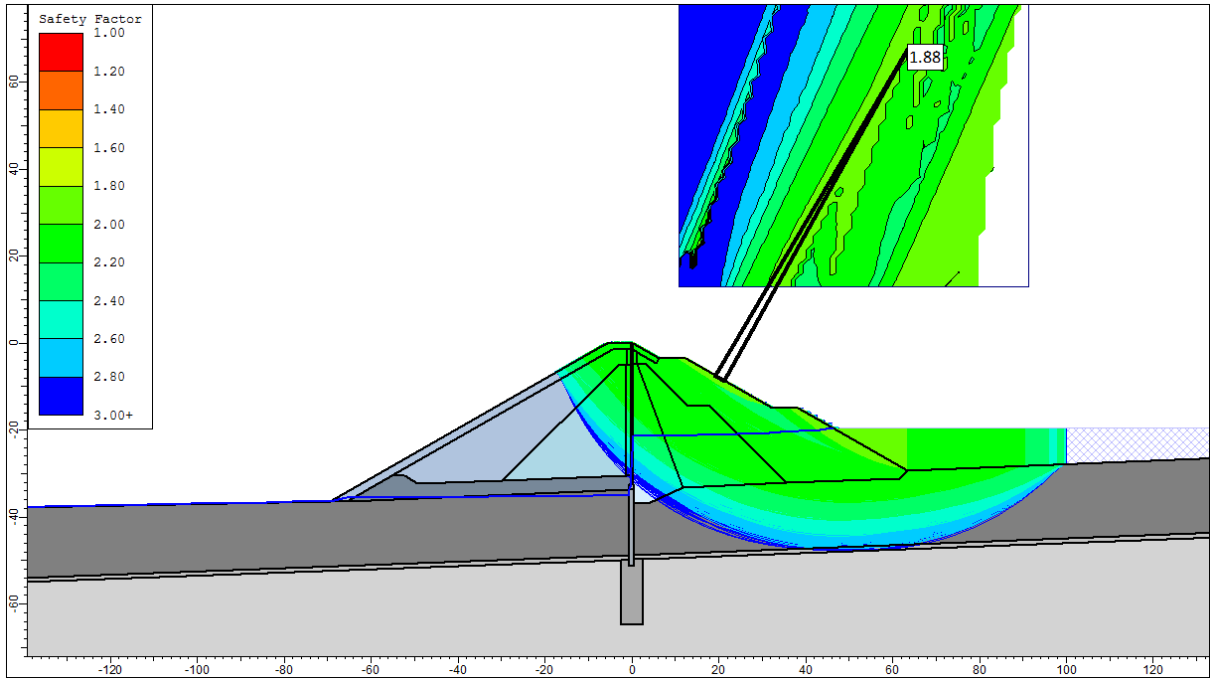


Figure 72: LC-B, circular surface, GLE, FoS ≥ 1.88

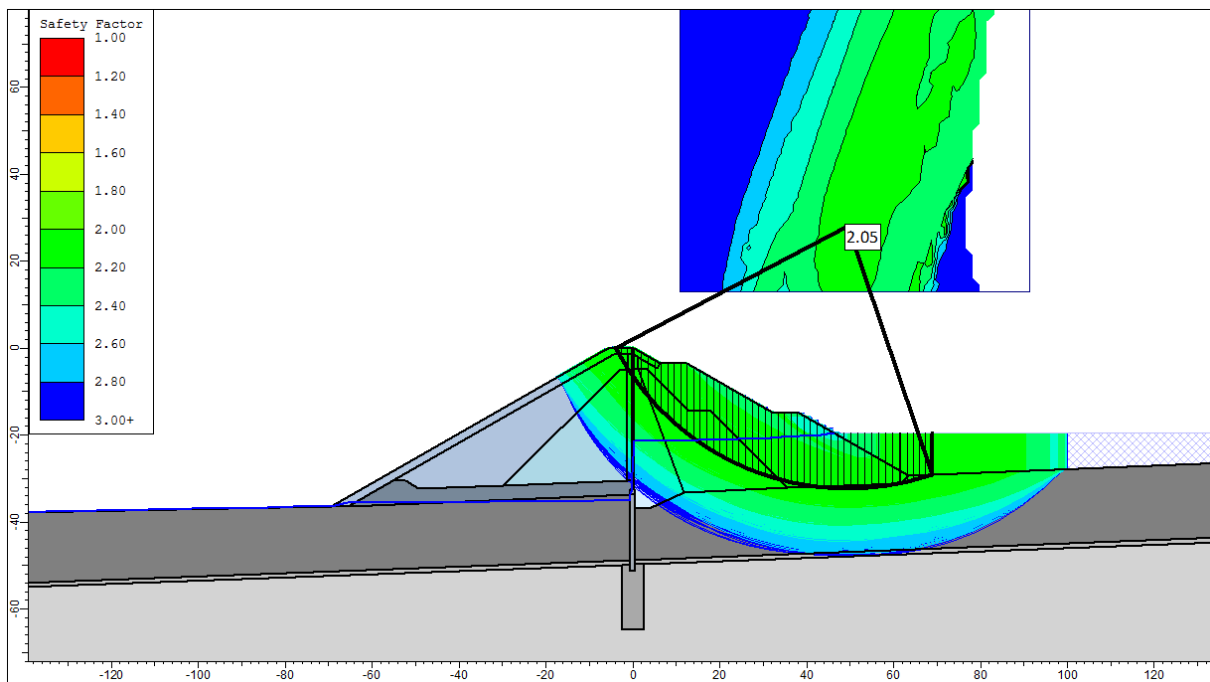


Figure 73: LC-B, circular surface with at least 4 m depth, GLE, FoS = 2.05

Stability Analysis assuming a Non-Circular Slip Surface

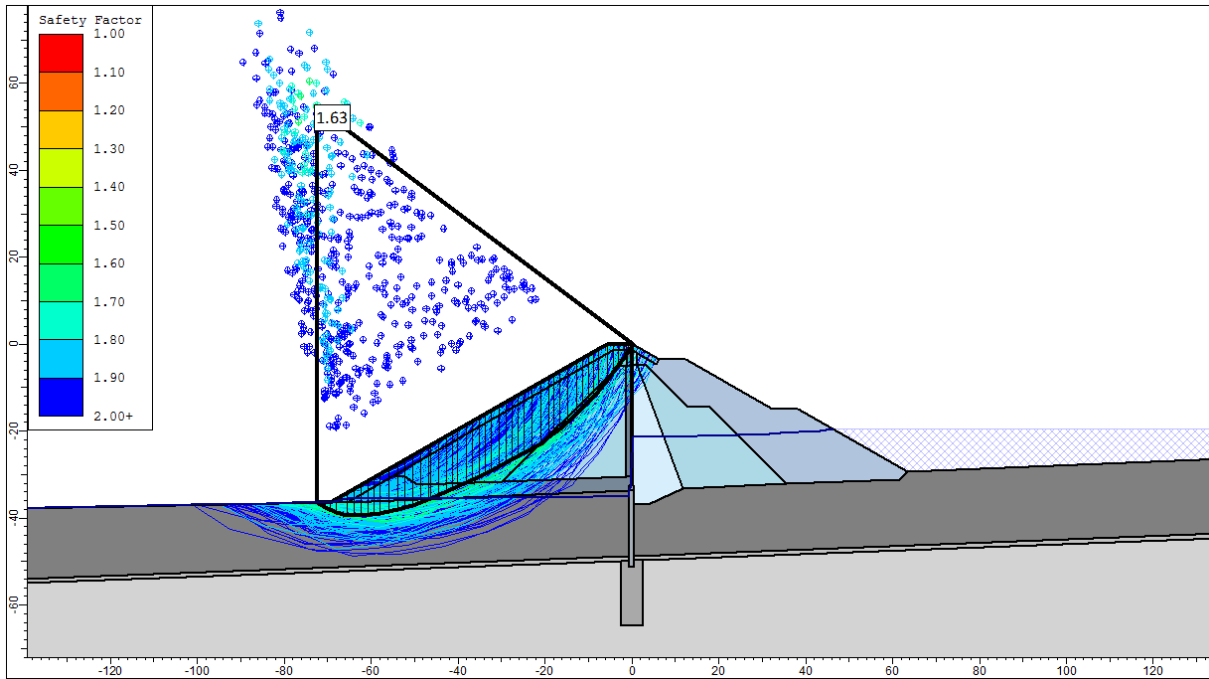


Figure 74: LC-B, non-circular surface, GLE, FoS = 1.63

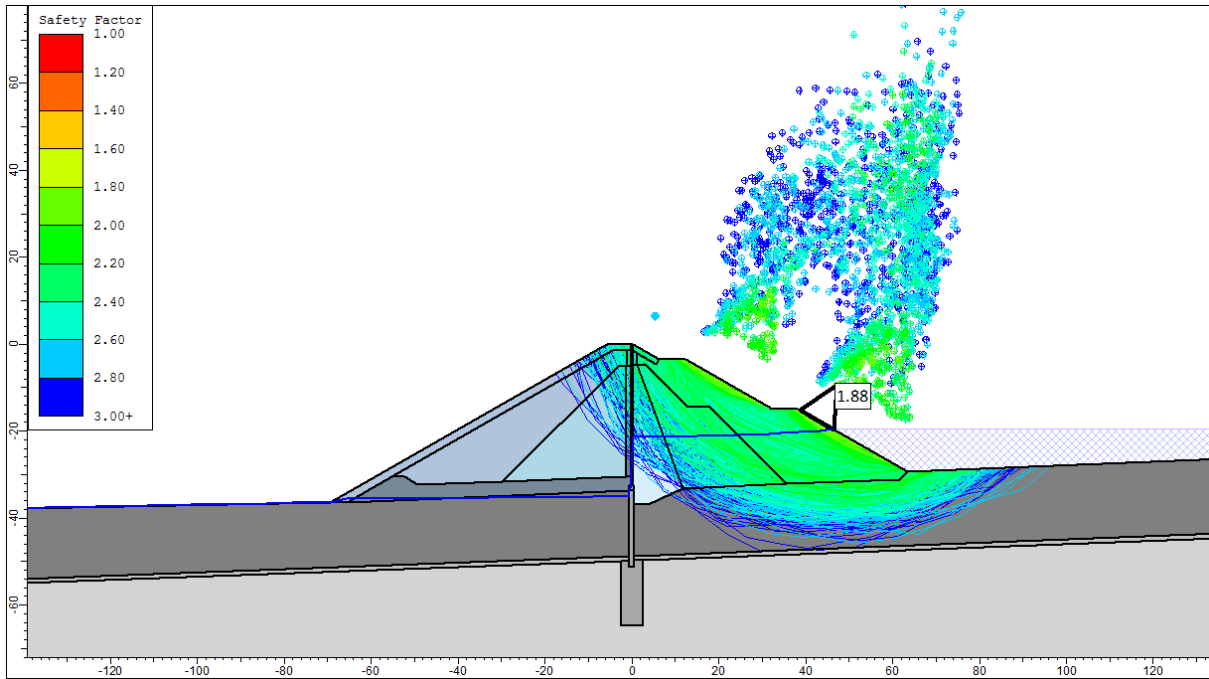


Figure 75: LC-B, non-circular surface, GLE, FoS ≥ 1.88

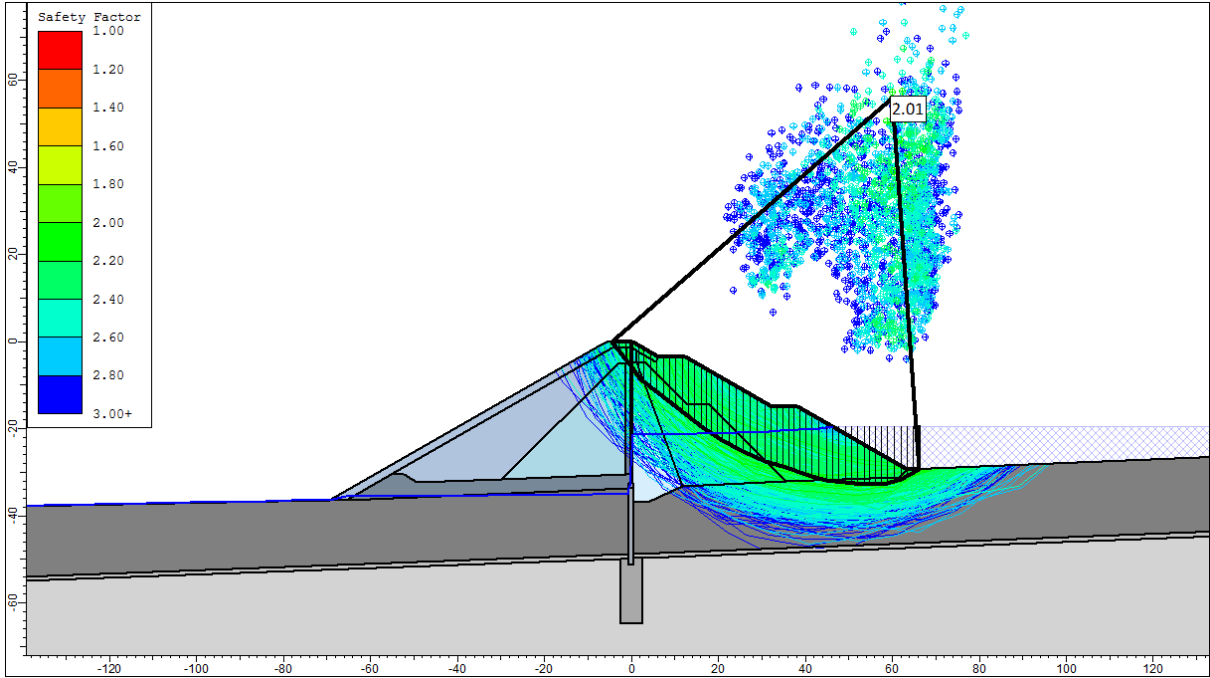


Figure 76: LC-B, non-circular surface with at least 4 m depth, GLE, FoS = 2.01

10.04.05.05 Load Case C

Table 57: LC-C, Factor of Safety, Method: GLE/Morgenstern - Price

LC-C, Factor of Safety			
downstream slope		upstream slope	
circular	non-circular	circular	non-circular
1.67	1.62	≥ 1.88, 2.10	≥ 1.88, 2.06

Seepage

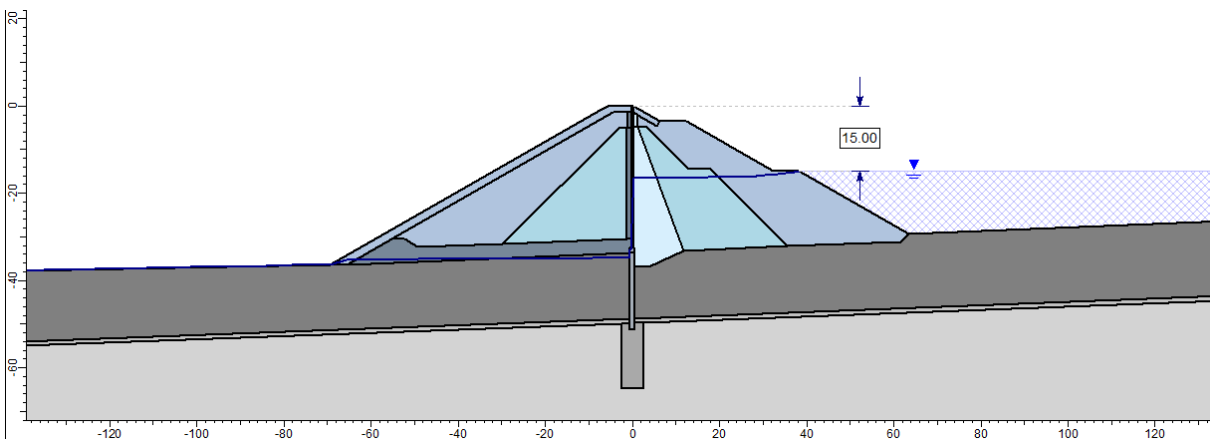


Figure 77: impoundment level at approximately 1/2 dam height, STL-C

Stability Analysis assuming a Circular Slip Surface

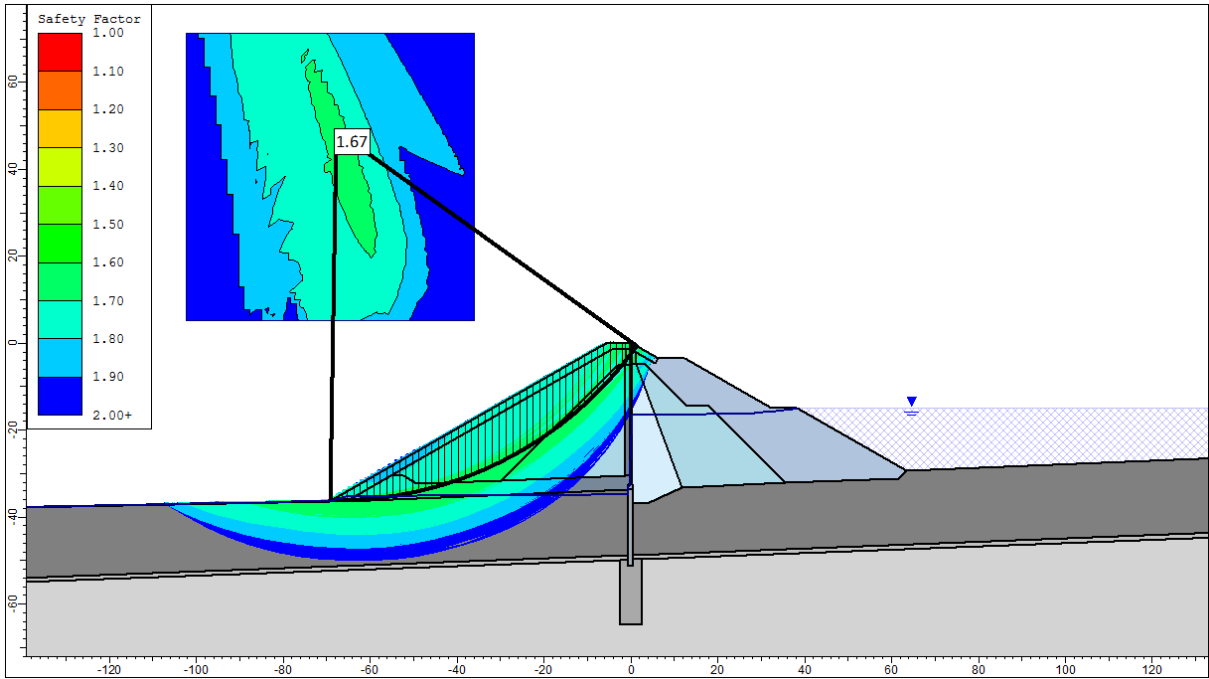


Figure 78: LC-C, circular surface, GLE, FoS = 1.67

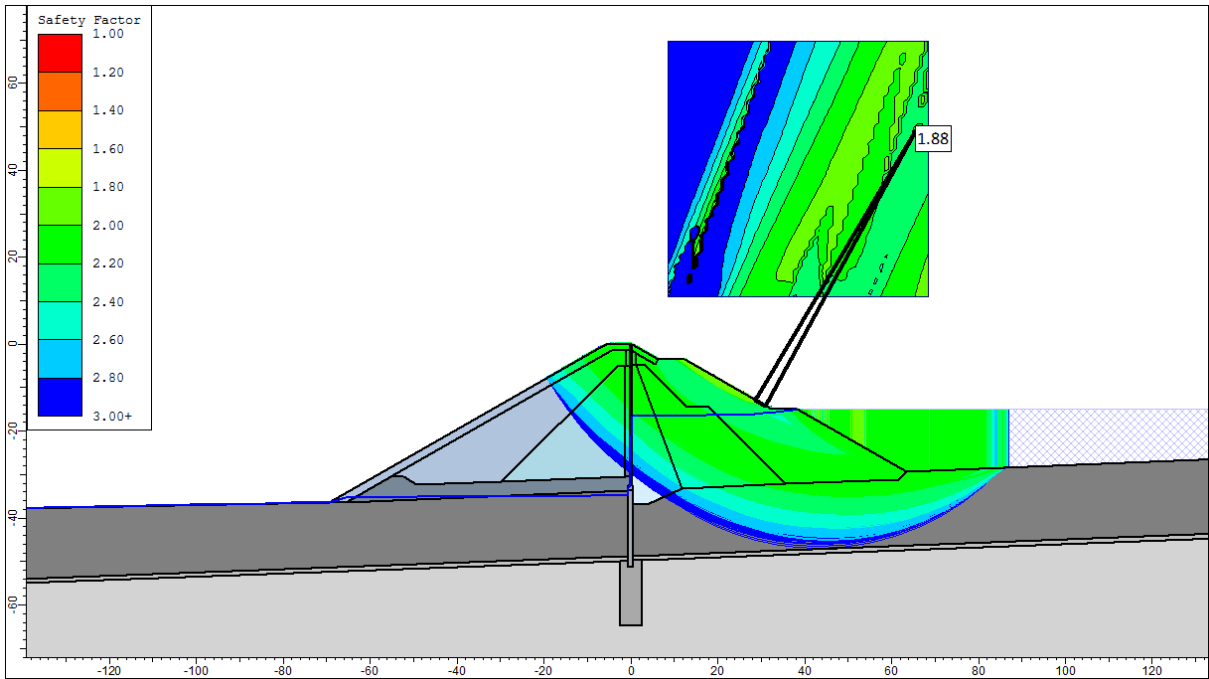


Figure 79: LC-C, circular surface, GLE, FoS \geq 1.88

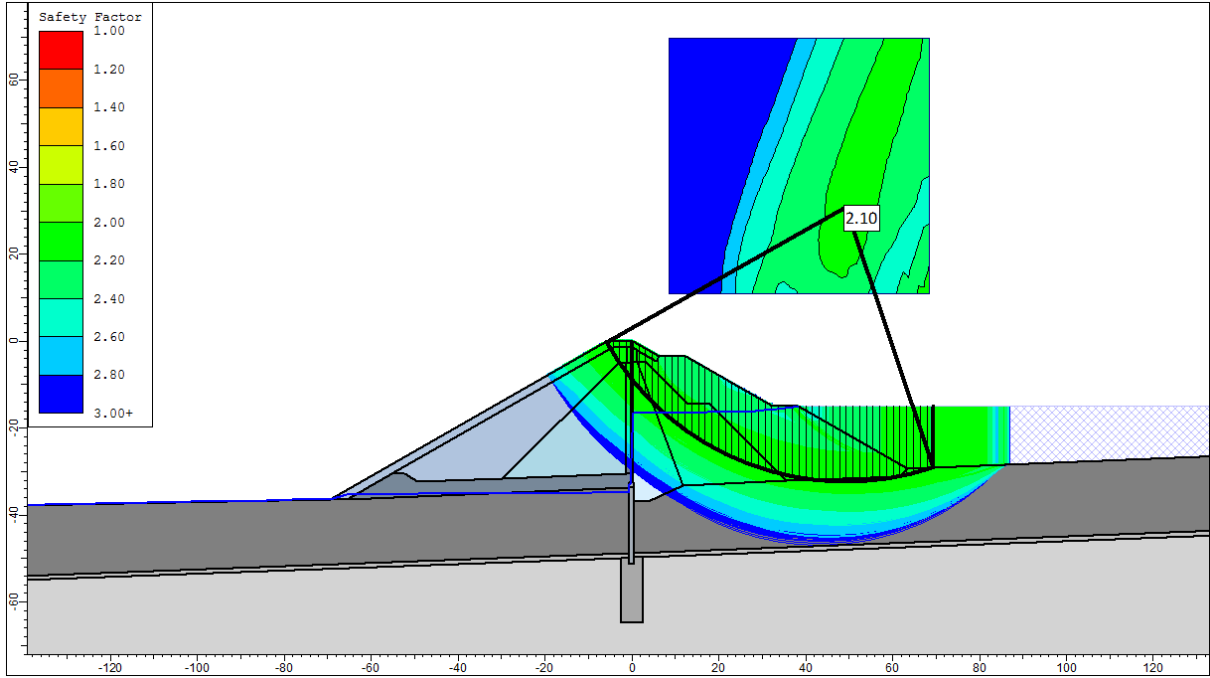


Figure 80: LC-C circular surface with at least 3 m depth, GLE, FoS = 2.10

Stability Analysis assuming a Non-Circular Slip Surface

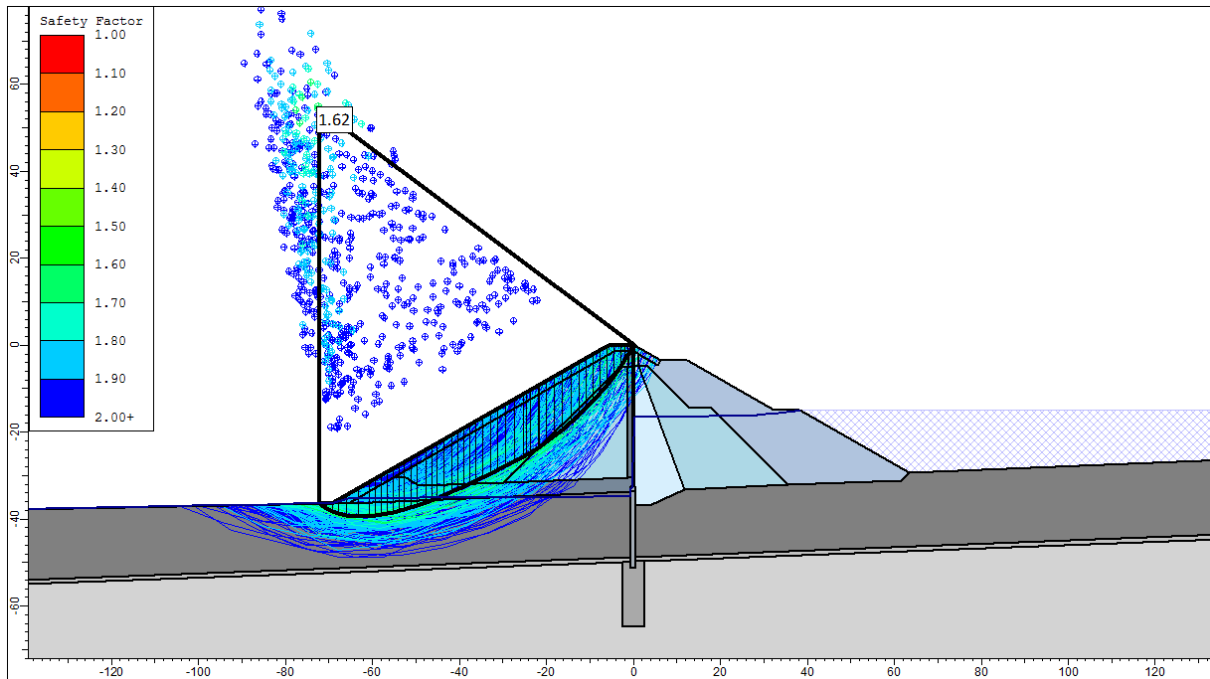


Figure 81: LC-C, non-circular surface, GLE, FoS = 1.62

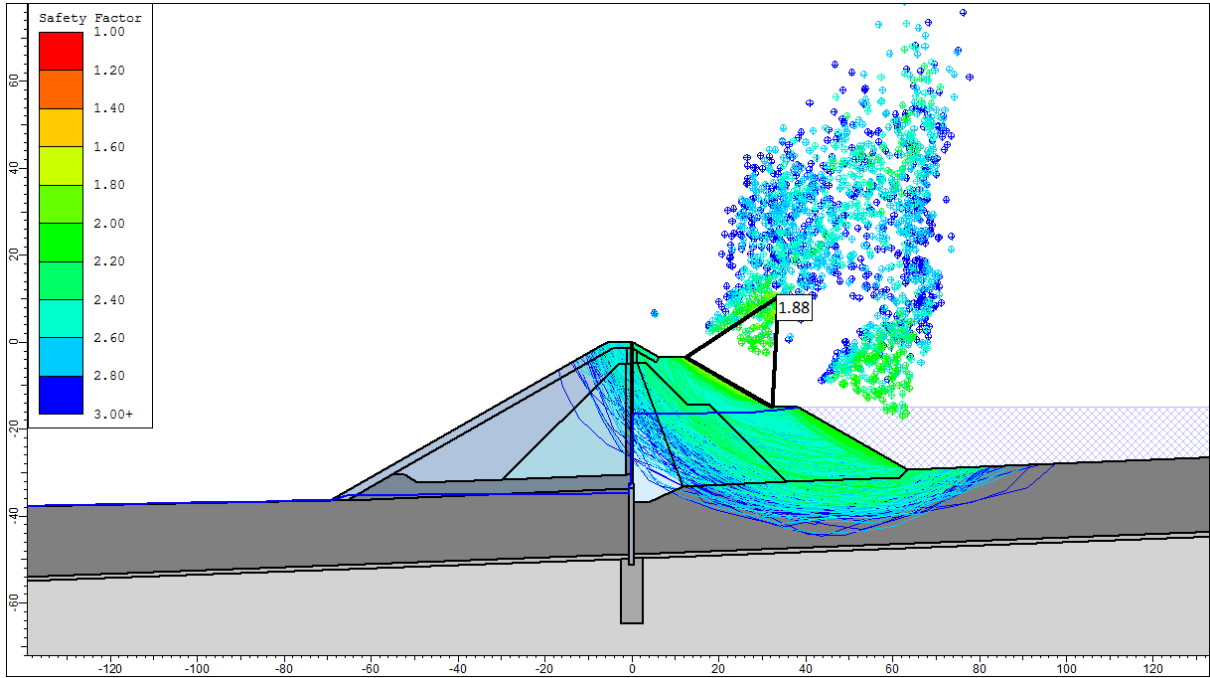


Figure 82: LC-C, non-circular surface, GLE, FoS ≥ 1.88

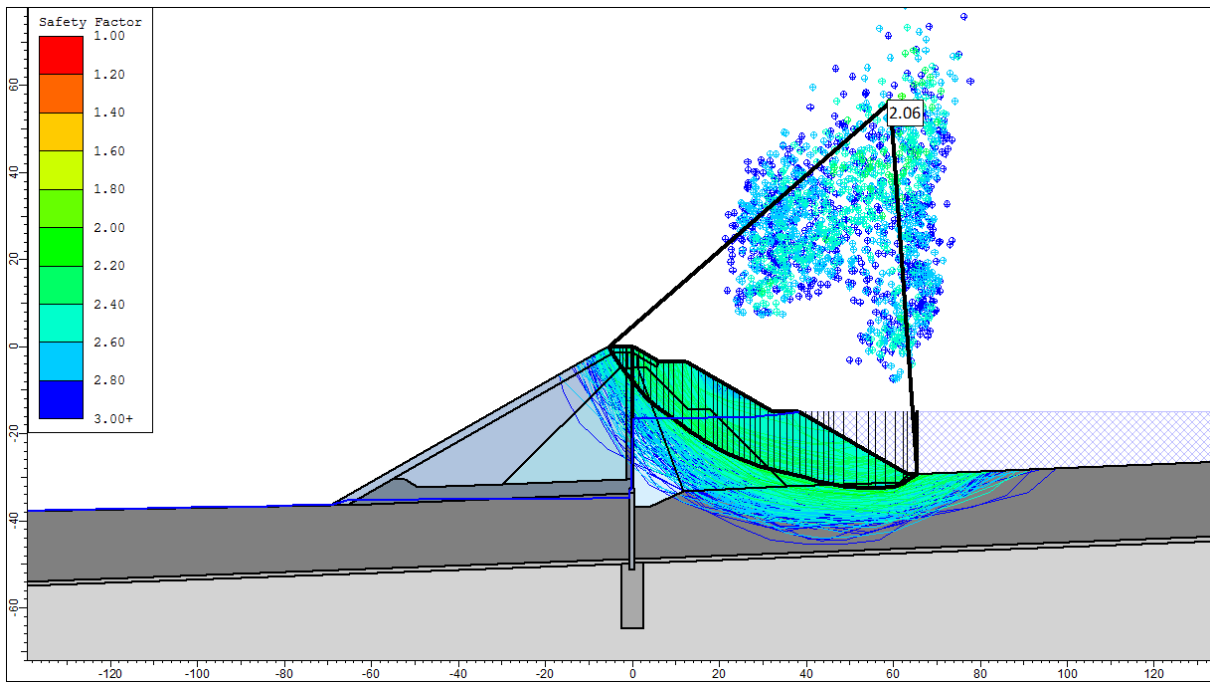


Figure 83: LC-C, non-circular surface with at least 4 m depth, GLE, FoS = 2.06

10.04.05.06 Load Case D

Table 58: LC-D, Factor of Safety, Method: GLE/Morgenstern - Price

LC-C, Factor of Safety			
downstream slope		upstream slope	
circular	non-circular	circular	non-circular
1.66	1.61	≥ 1.88, 2.21	≥ 1.87, 2.14

Seepage

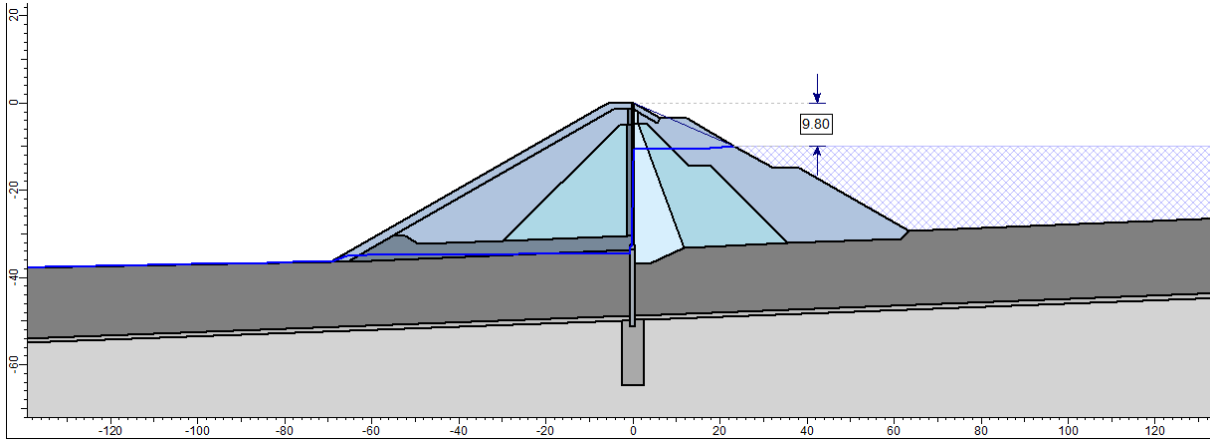


Figure 84: impoundment level at approximately 2/3 dam height, STL-D

Stability Analysis assuming a Circular Slip Surface

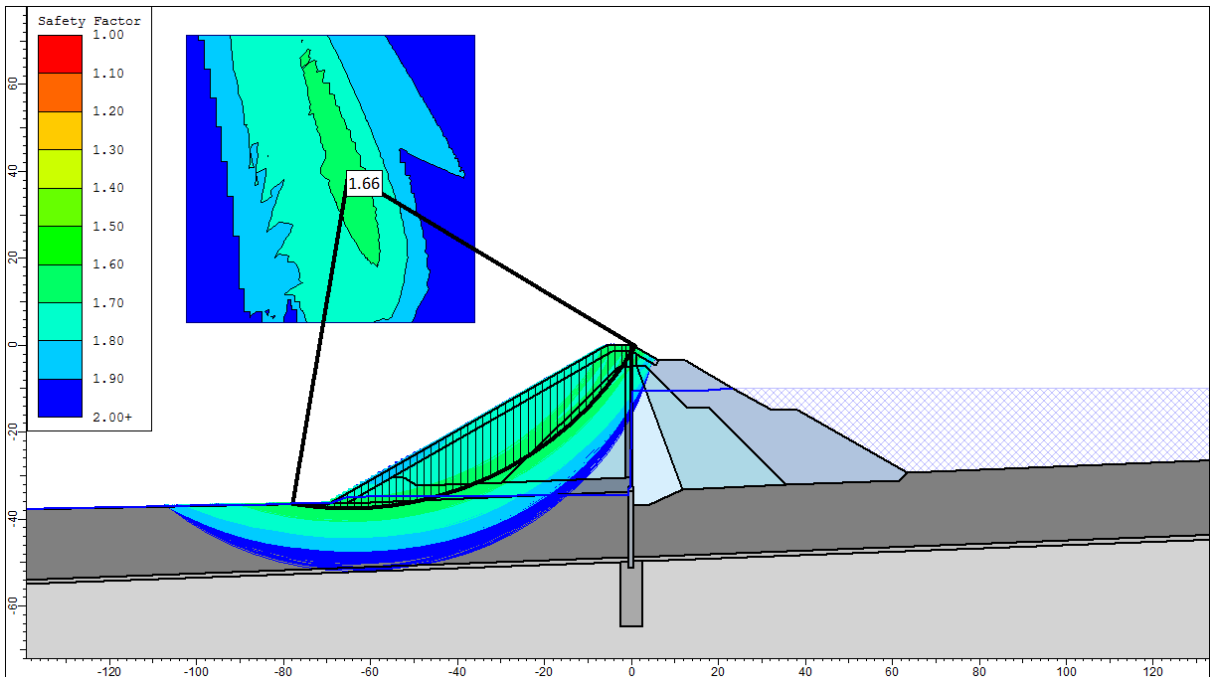


Figure 85: LC-D, circular surface, GLE, FoS = 1.66

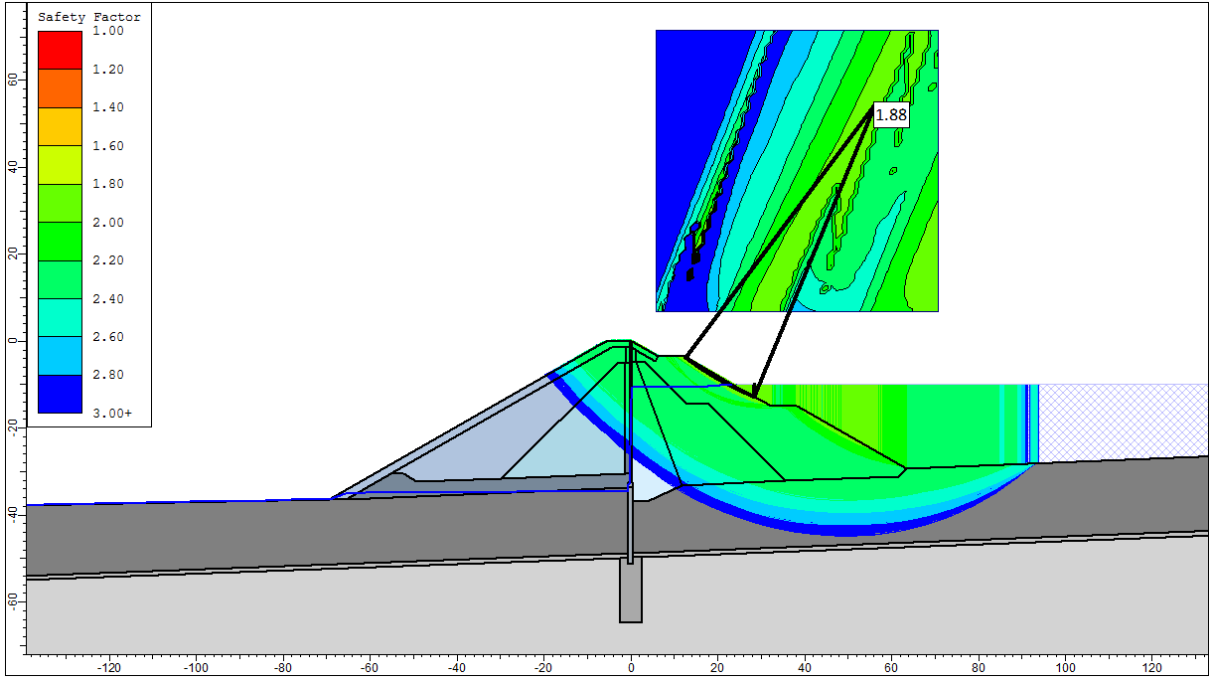


Figure 86: LC-D, circular surface, GLE, FoS \geq 1.88

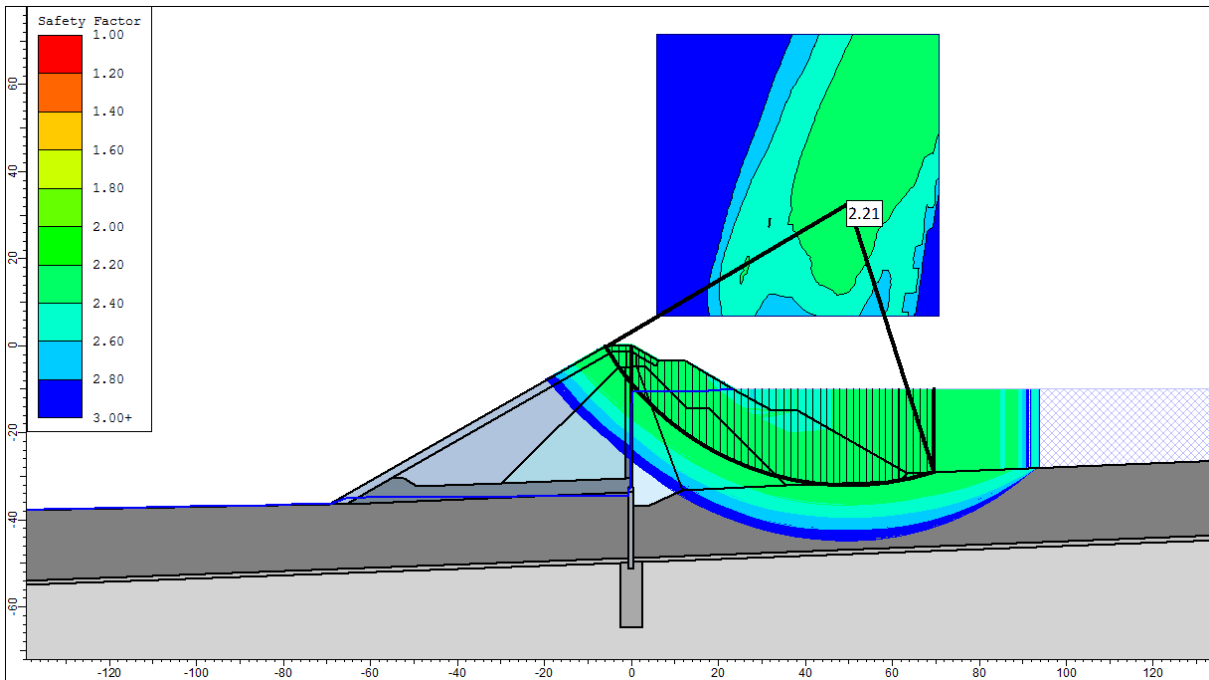


Figure 87: LC-D circular surface with at least 6 m depth, GLE, FoS = 2.21

Stability Analysis assuming a Non-Circular Slip Surface

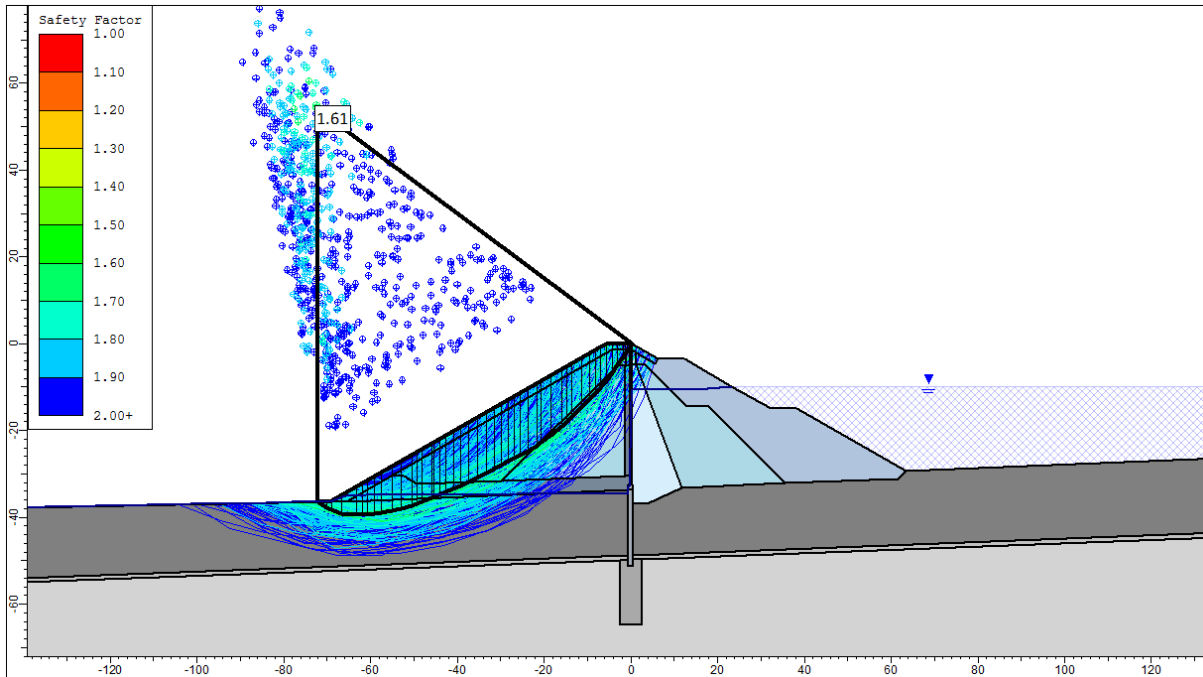


Figure 88: LC-D, non-circular surface, GLE, FoS = 1.61

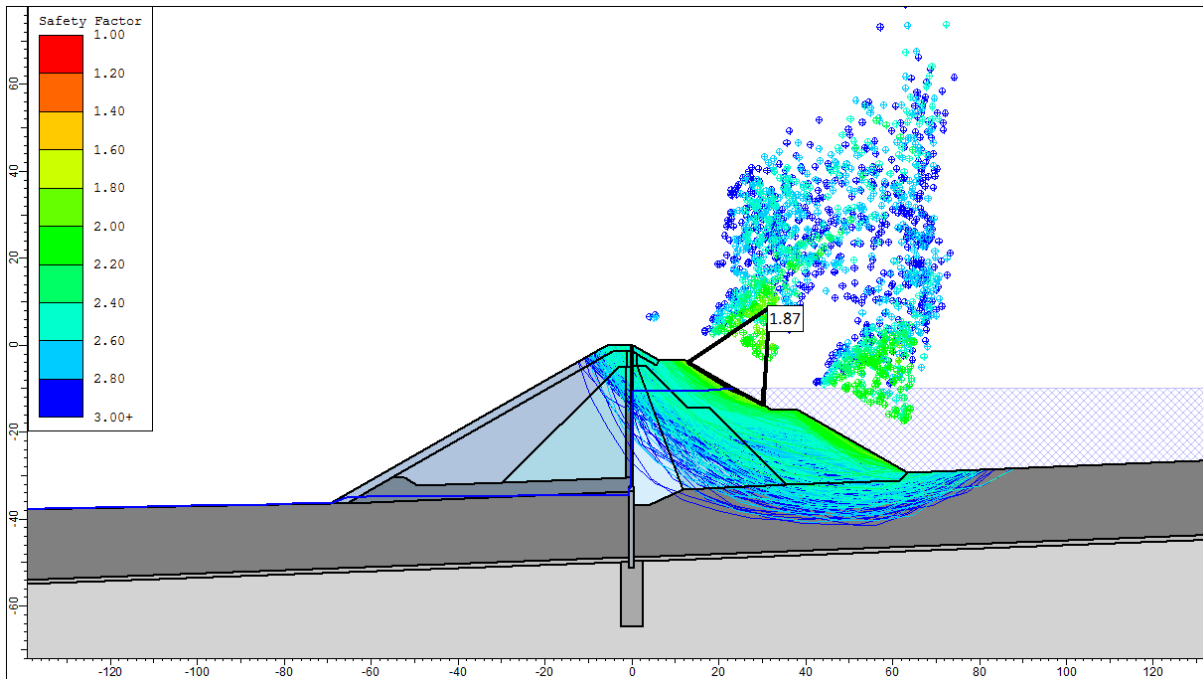


Figure 89: LC-D, non-circular surface, GLE, FoS \geq 1.87

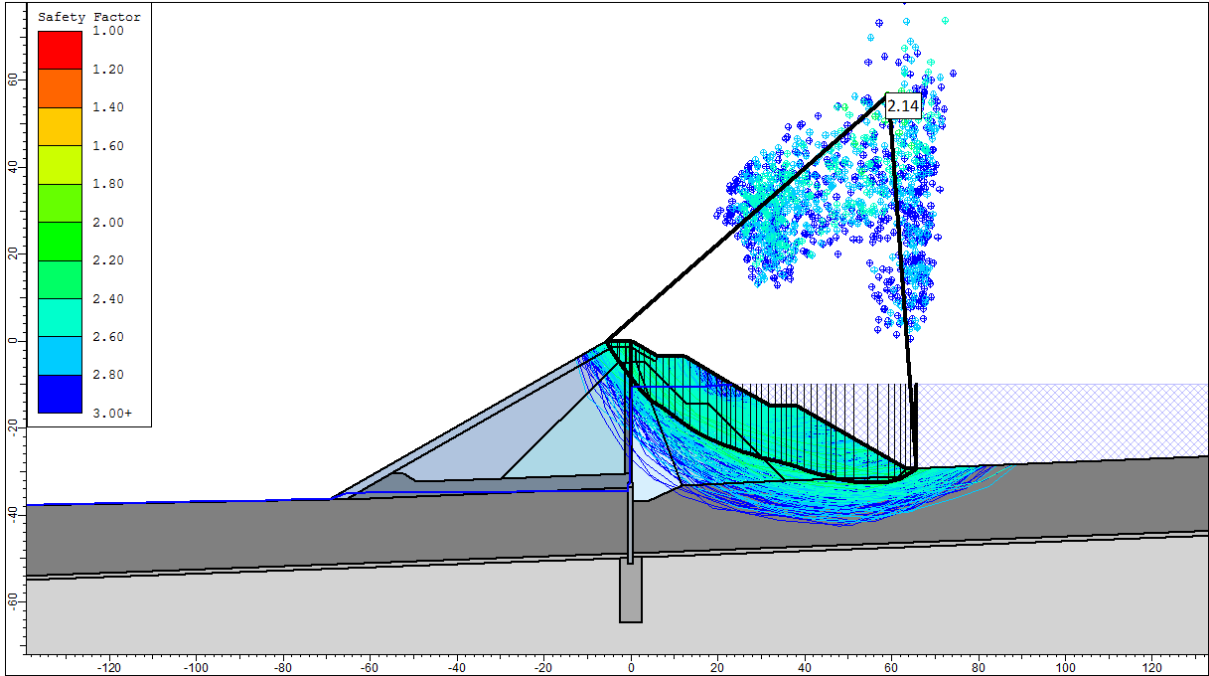


Figure 90: LC-D non-circular surface with at least 6 m depth, GLE, FoS = 2.14

10.04.05.07 Load Case E

Table 59: LC-E, Factor of Safety, Method: GLE/Morgenstern - Price

LC-E, Factor of Safety			
downstream slope		upstream slope	
circular	non-circular	circular	non-circular
1.65	1.60	≥ 1.88, 2.44	≥ 1.96, 2.41

Seepage

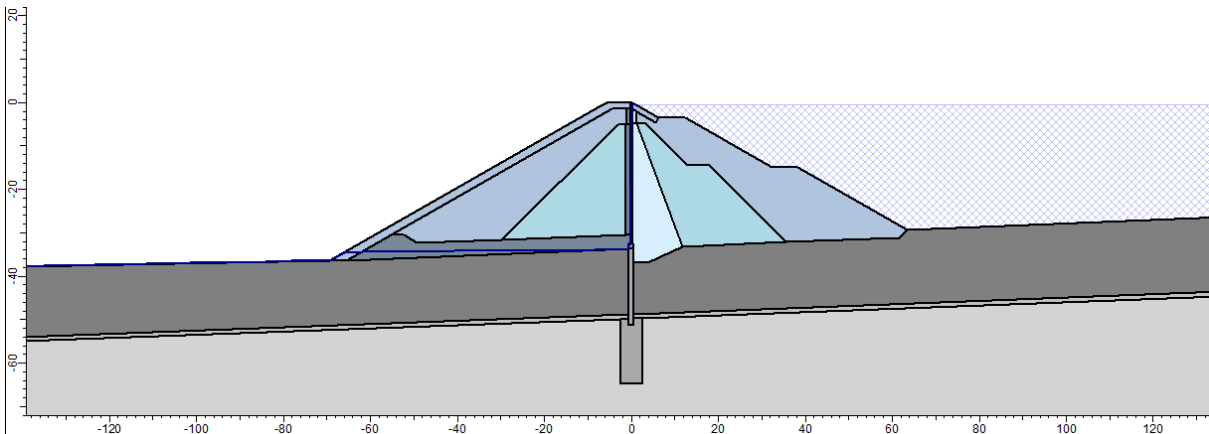


Figure 91: full impoundment, Slide 7.0, STL-E

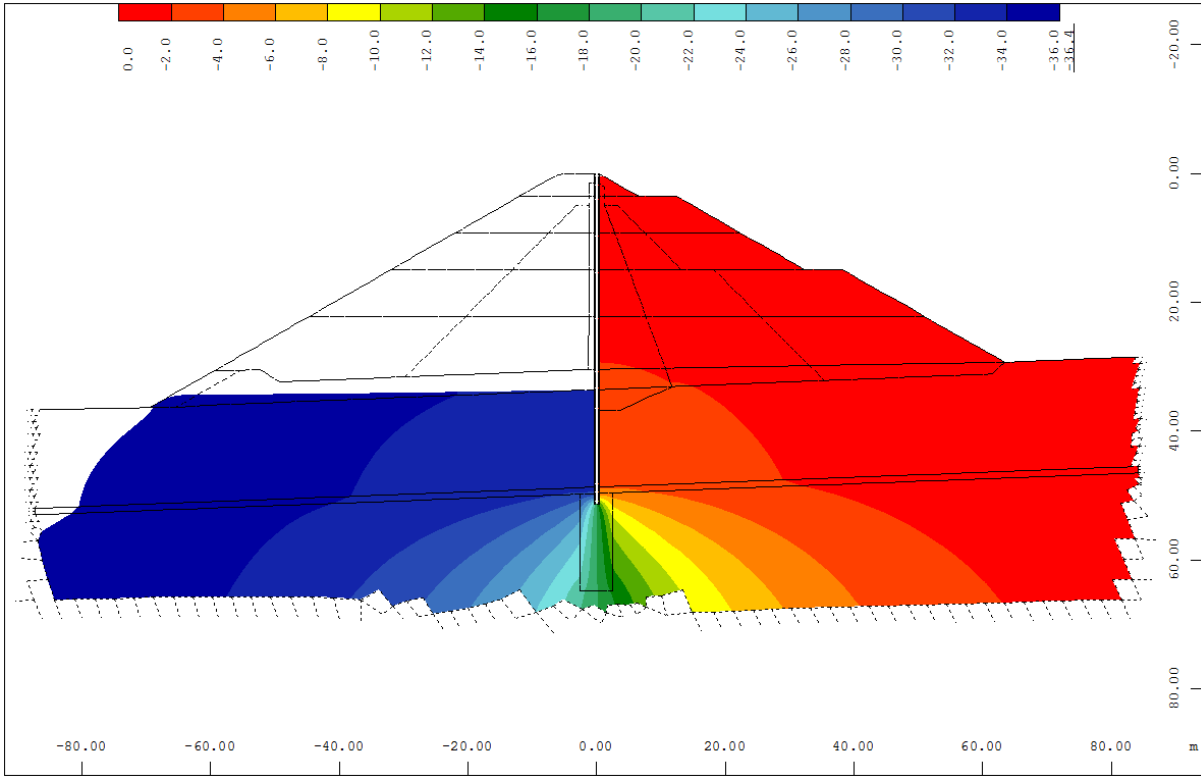


Figure 92: Seepage calculation for full impoundment, potentials [m] and free surface, WinTube, LC-E

Stability Analysis assuming a Circular Slip Surface

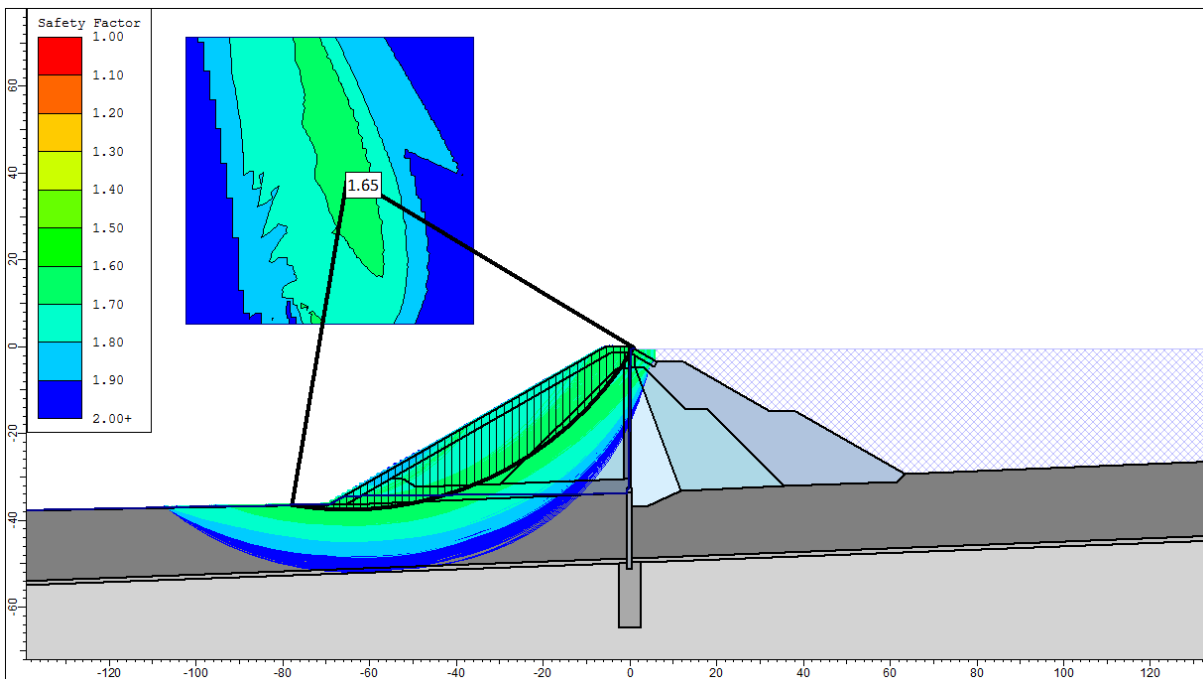


Figure 93: LC-E, circular surface, GLE, FoS = 1.65

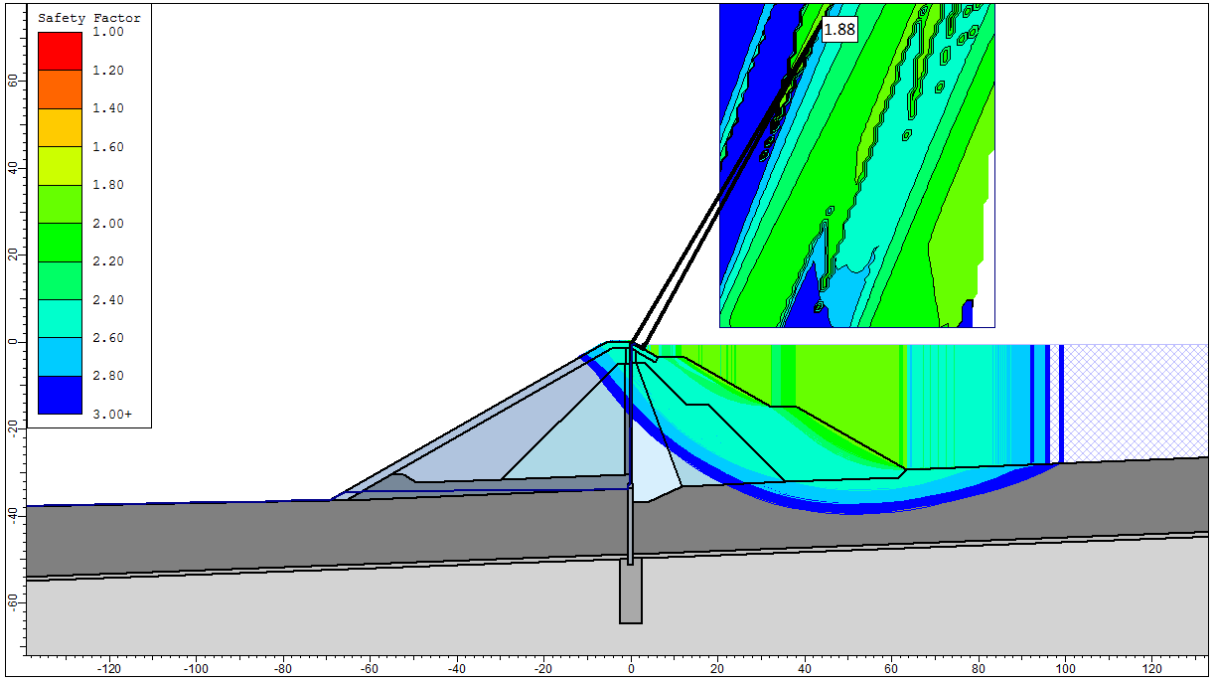


Figure 94: LC-E, circular surface, GLE, FoS ≥ 1.88

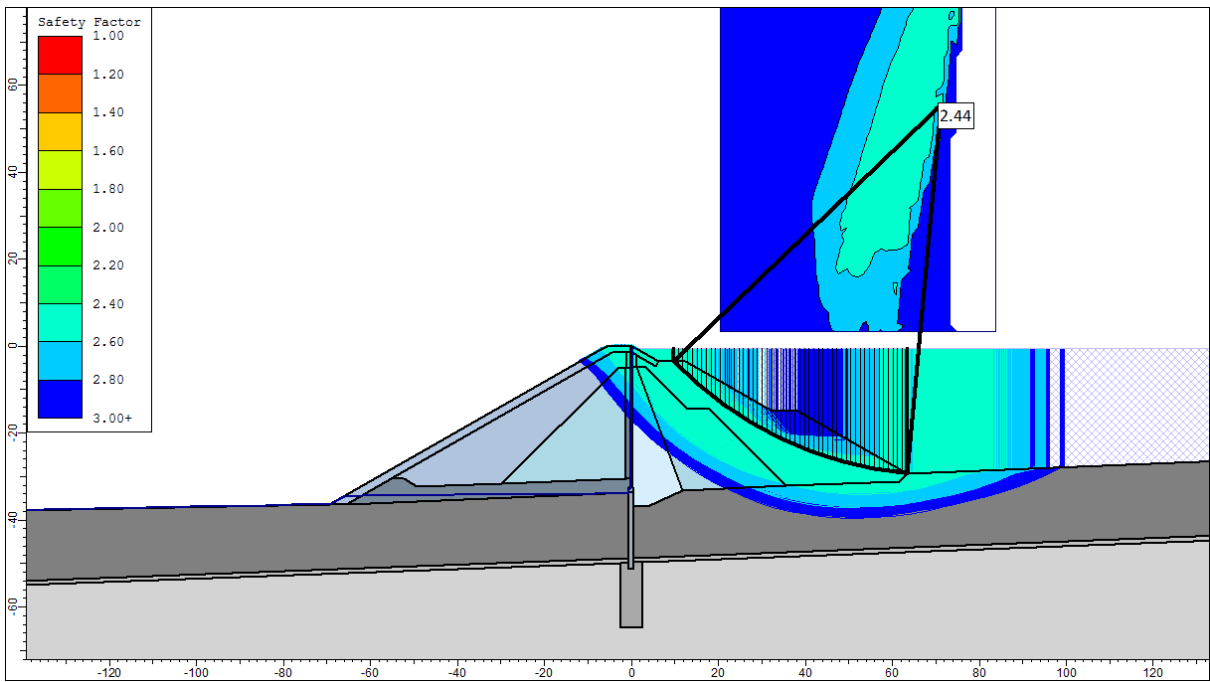


Figure 95: LC-E, circular surface with at least 8 m depth, GLE, FoS = 2.44

Stability Analysis assuming a Non-Circular Slip Surface

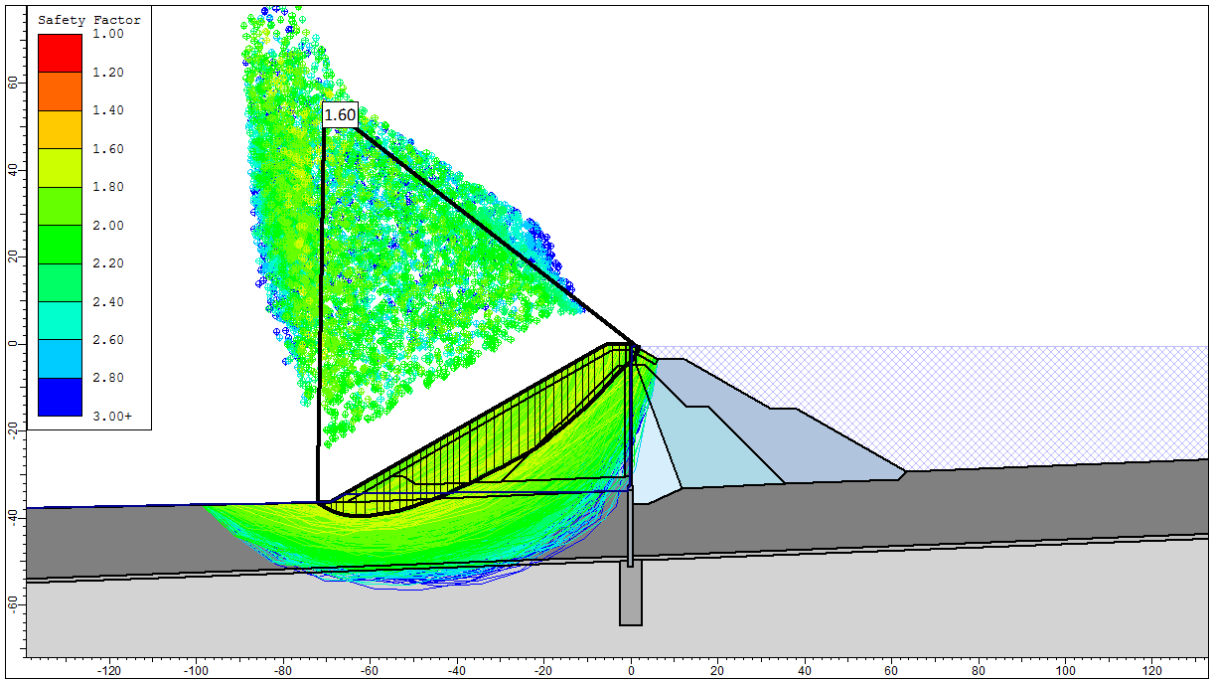


Figure 96: LC-E, non-circular surface, GLE, FoS = 1.60

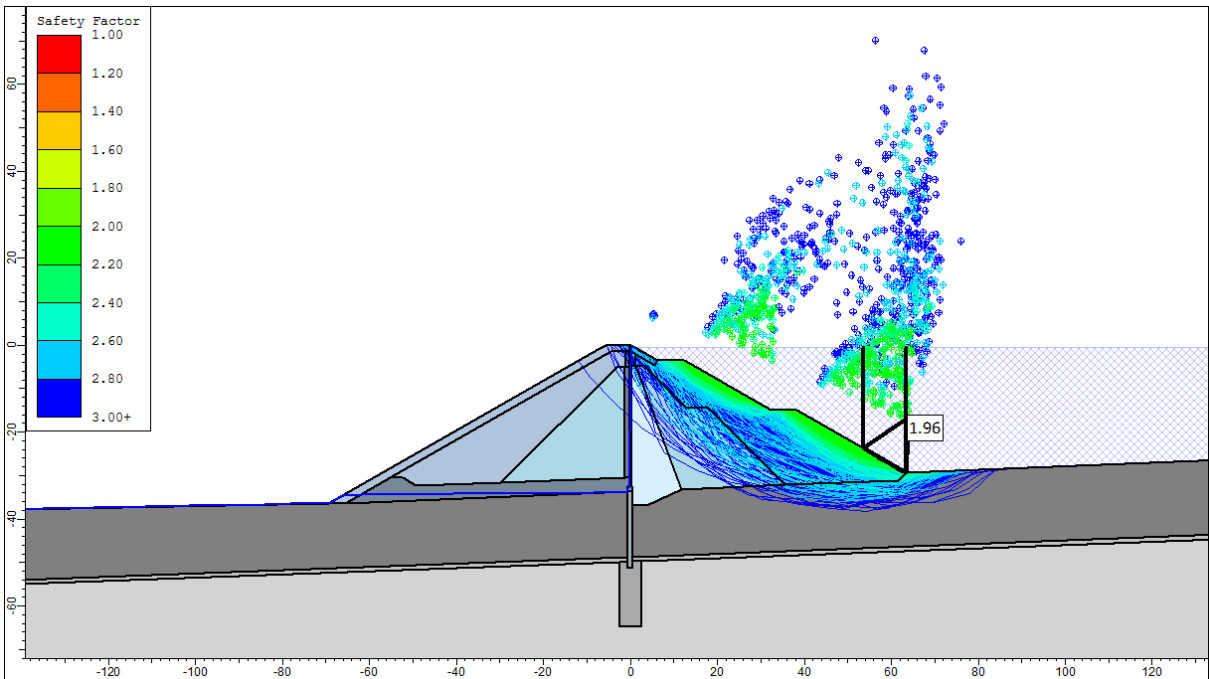


Figure 97: LC-E, non-circular surface, GLE, FoS ≥ 1.96

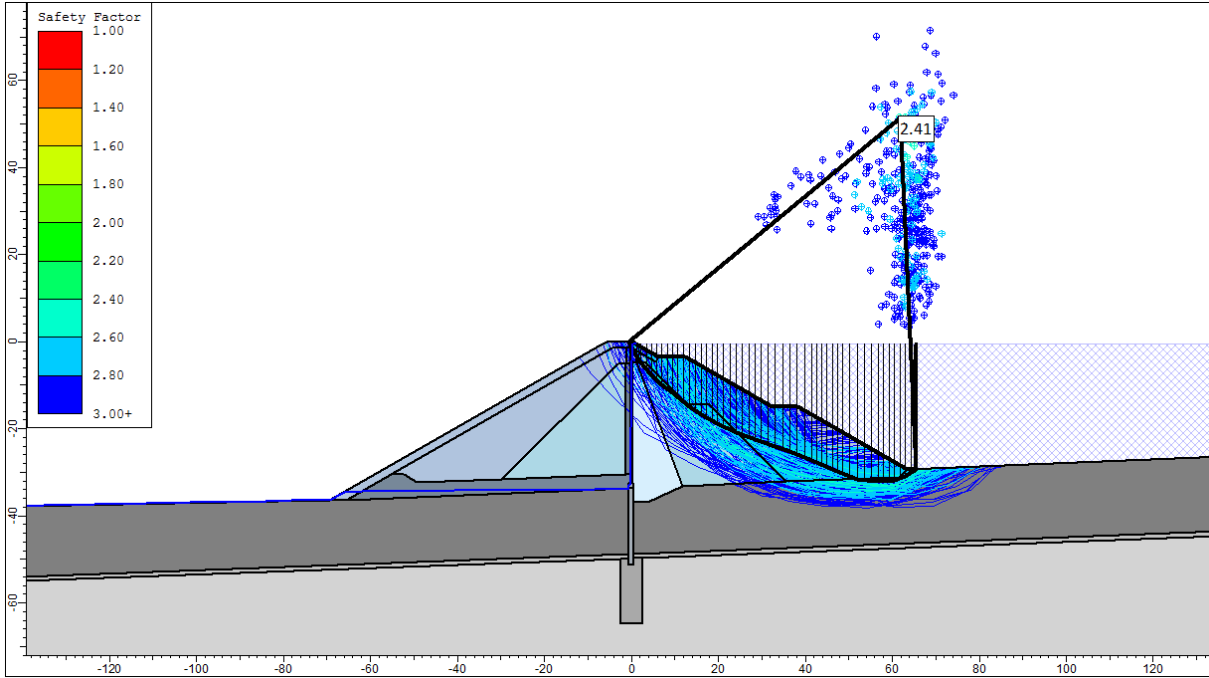


Figure 98: LC-E, non-circular surface with at least 8 m depth, GLE, FoS = 2.41

FE Stability Assessment with Phi-c Reduction

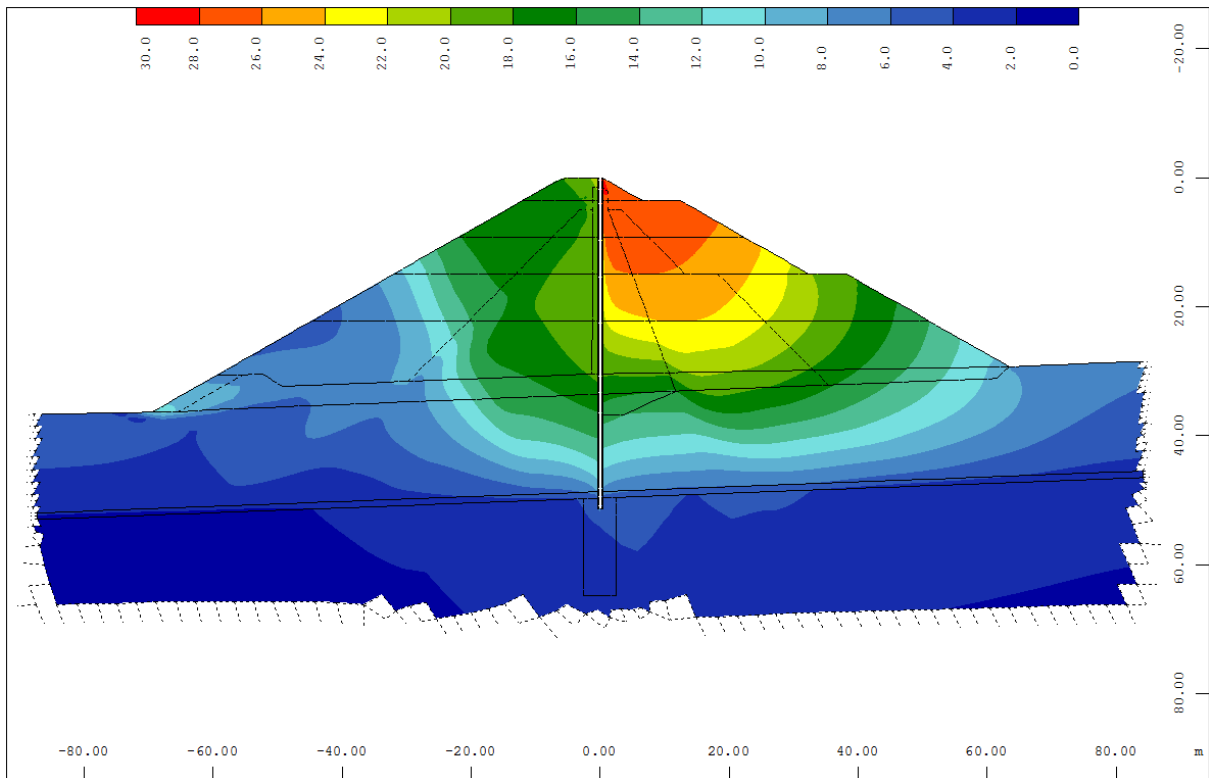


Figure 99: LC-E, phi-c reduction, nodal displacement vector [mm], FoS = 1.61

10.04.05.08 Load Case F

Table 60: LC-F, Factor of Safety, Method: GLE/Morgenstern - Price

LC-E, Factor of Safety			
downstream slope		upstream slope	
circular	non-circular	circular	non-circular
1.63	1.58	≥ 1.89, 2.53	≥ 1.93, 2.39

Seepage

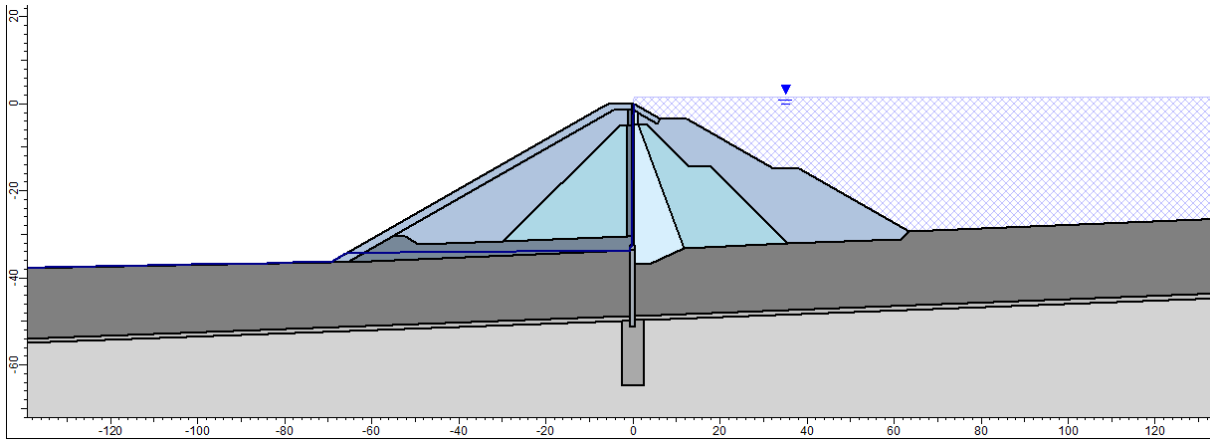


Figure 100: Overtopping, STL-F

Stability Analysis assuming a Circular Slip Surface

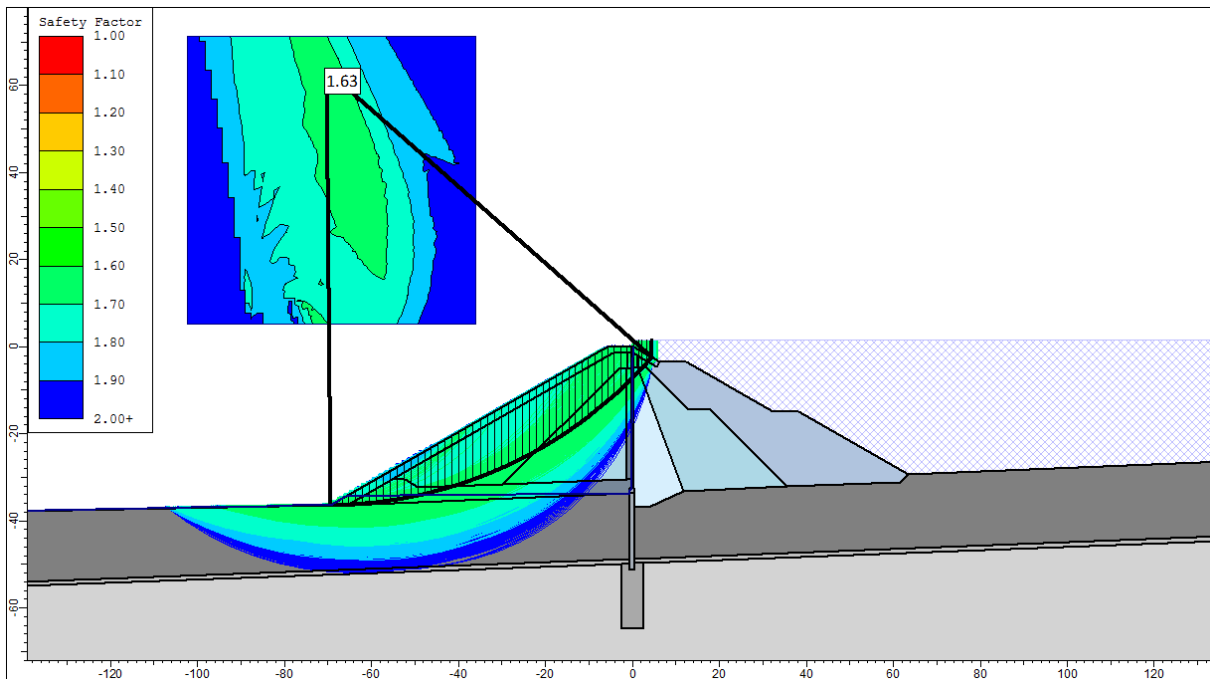


Figure 101: LC-F, circular surface, GLE, FoS = 1.63

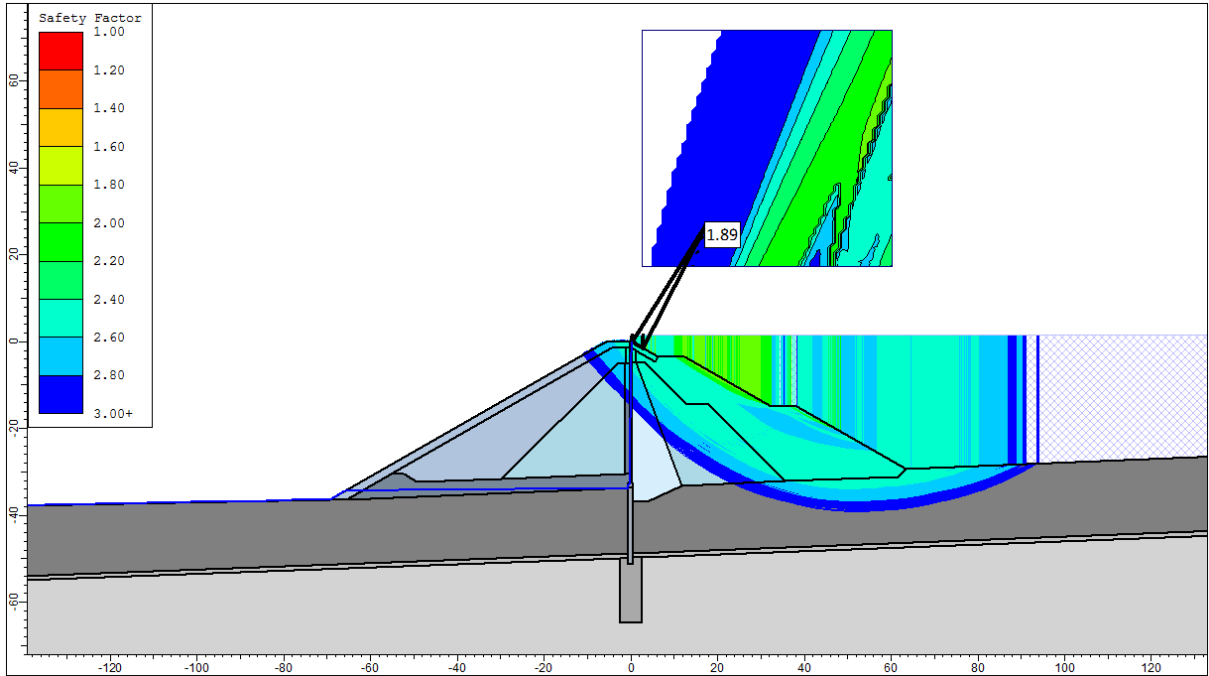


Figure 102: LC-F, circular surface, GLE, FoS \geq 1.89

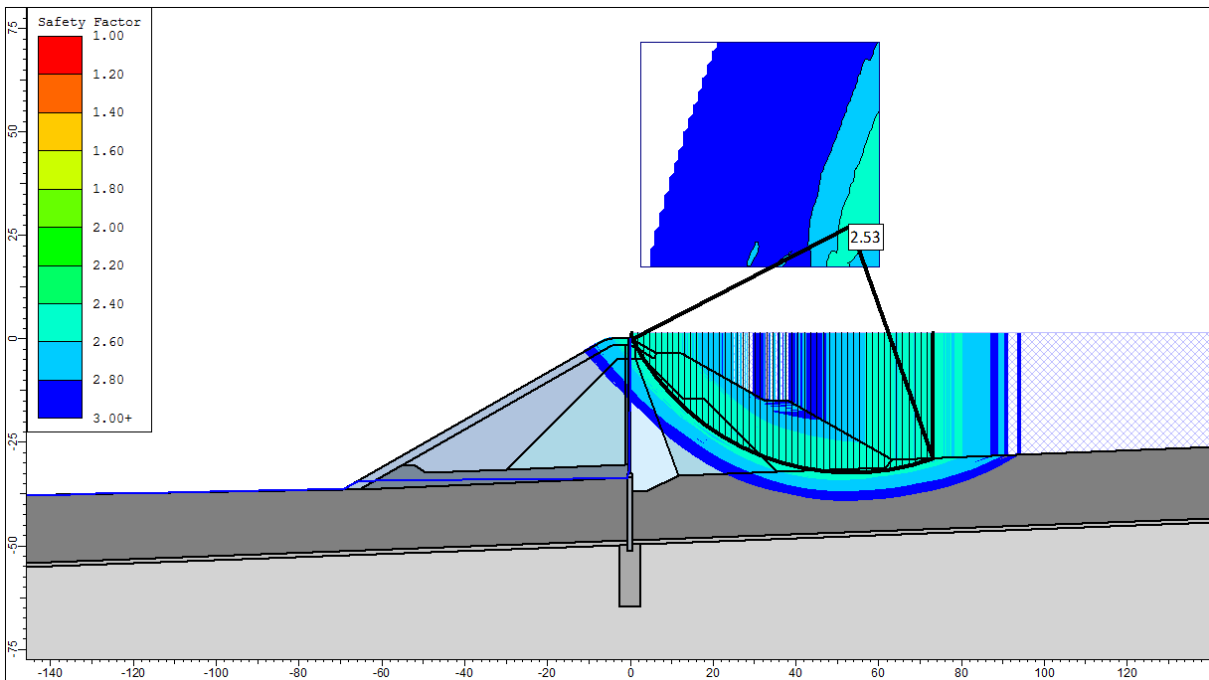


Figure 103: LC-F, circular surface with at least 5 m depth, GLE, FoS = 2.53

Stability Analysis assuming a Non-Circular Slip Surface

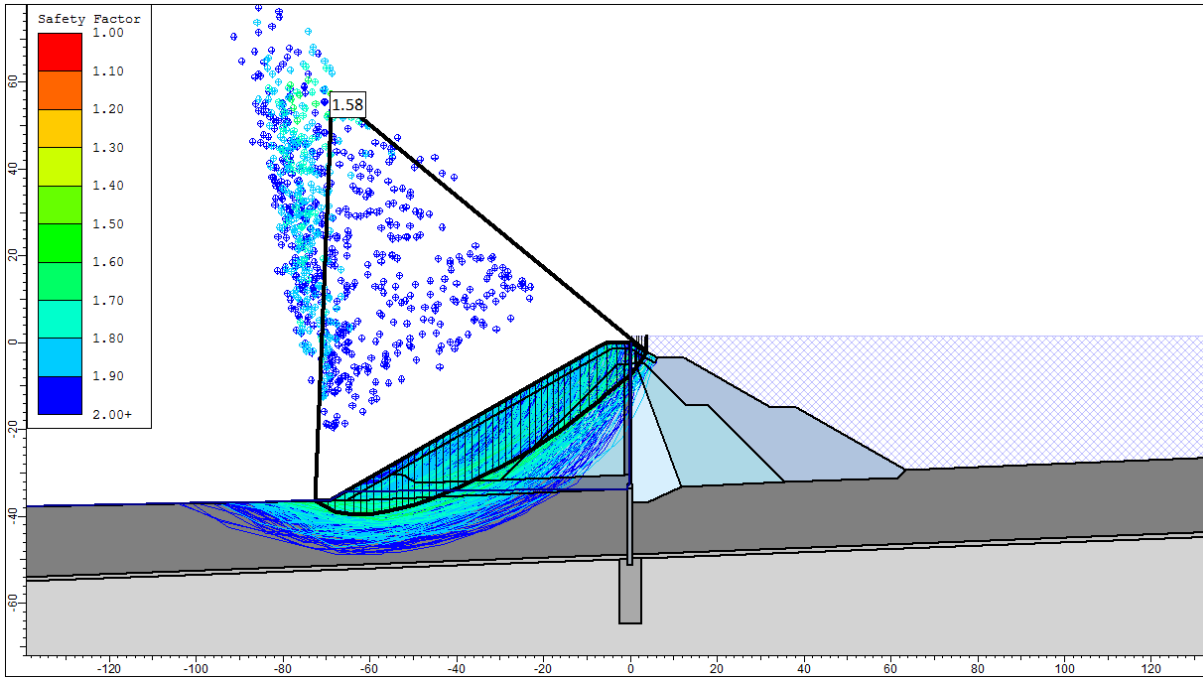


Figure 104: LC-F, non-circular surface, GLE, FoS = 1.58

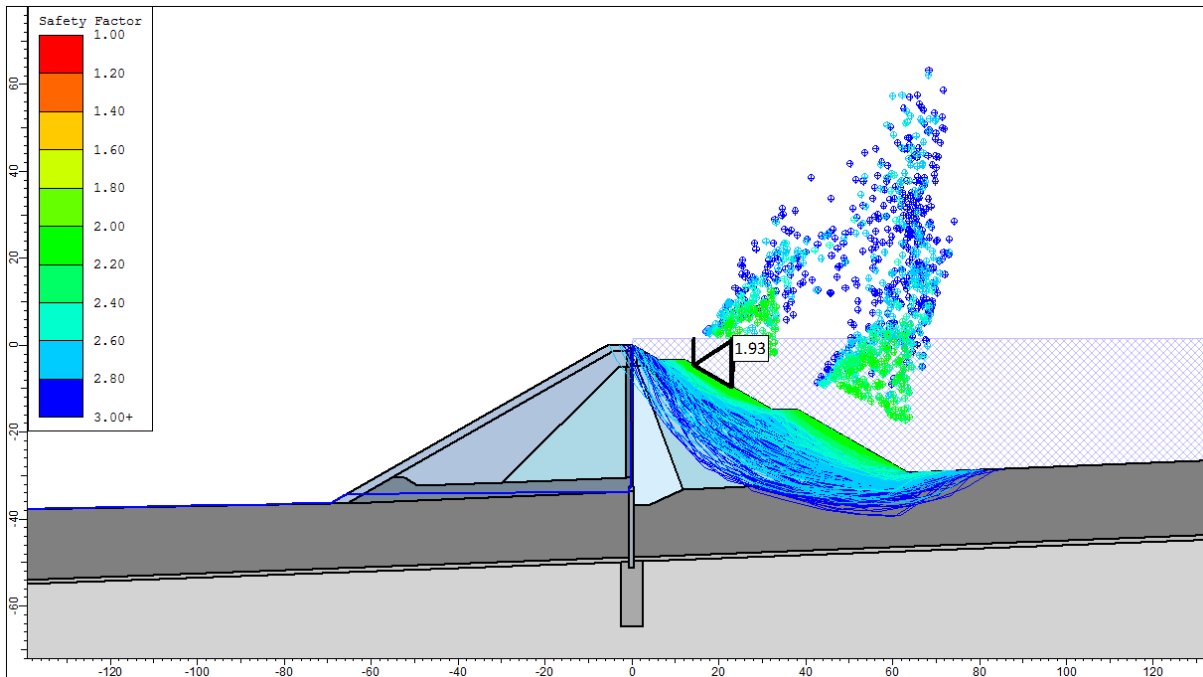


Figure 105: LC-F, non-circular surface, GLE, FoS ≥ 1.93

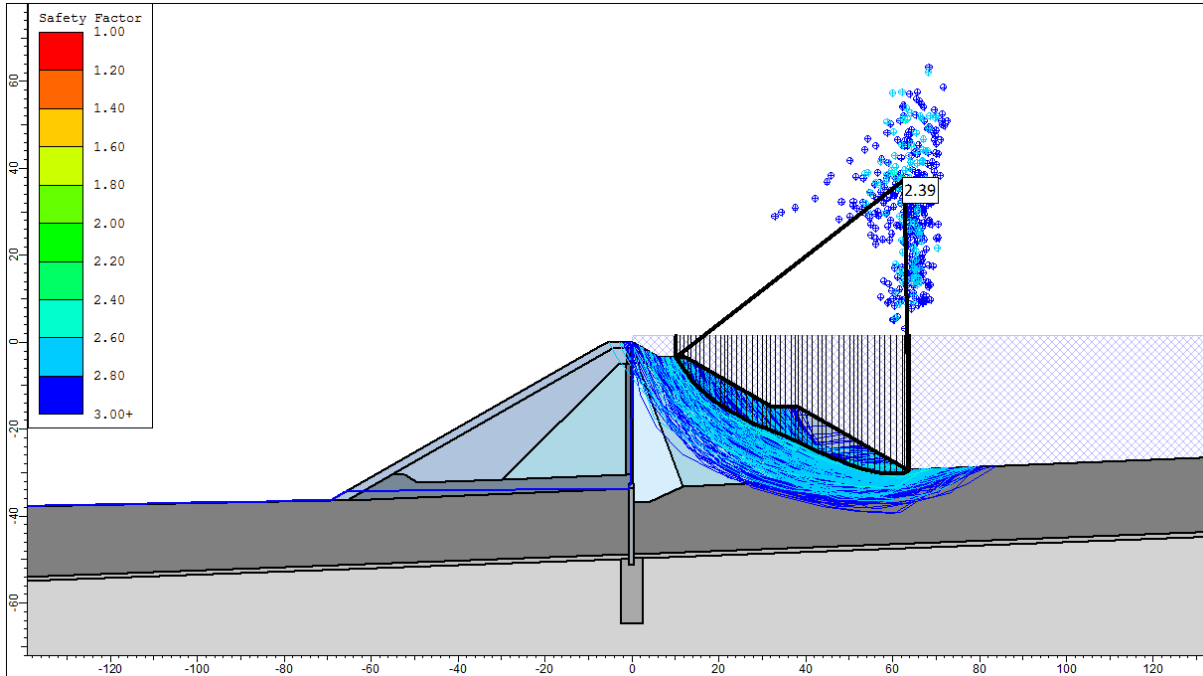


Figure 106: LC-F, non-circular surface with at least 8 m depth, GLE, FoS = 2.39

10.04.05.09 Load Case G – Rapid Drawdown

Applying the B-Bar rapid drawdown approach, it is assumed that Zone 3 is undrained with a defined B-Bar of 1.0. The granular fill materials of Zone 1 and 2 are considered to be free draining and therefore no undrained behavior is defined.

Table 61: LC-G, Factor of Safety, Method: GLE/Morgenstern – Price and B-Bar

LC-G, Factor of Safety, upstream slope, B-Bar =1.0					
Zone 3		Zone 2 and 3		Zone 2, 3 and Cougar Creek Alluvium	
circular	non-circular	circular	non-circular	circular	non-circular
2.08	1.95	1.60	1.55	1.37	1.34

Applying the Darcy law, which is implemented in the FE Software Wintube, for analyzing rapid drawdown, a different and more realistic result is obtained. As shown in Figure 108, after 10 days of full impoundment the deceleration zone is not water saturated and seepage cannot reach the core wall and thus rapid draw down is less relevant as assumed by applying the B-Bar method.

Seepage

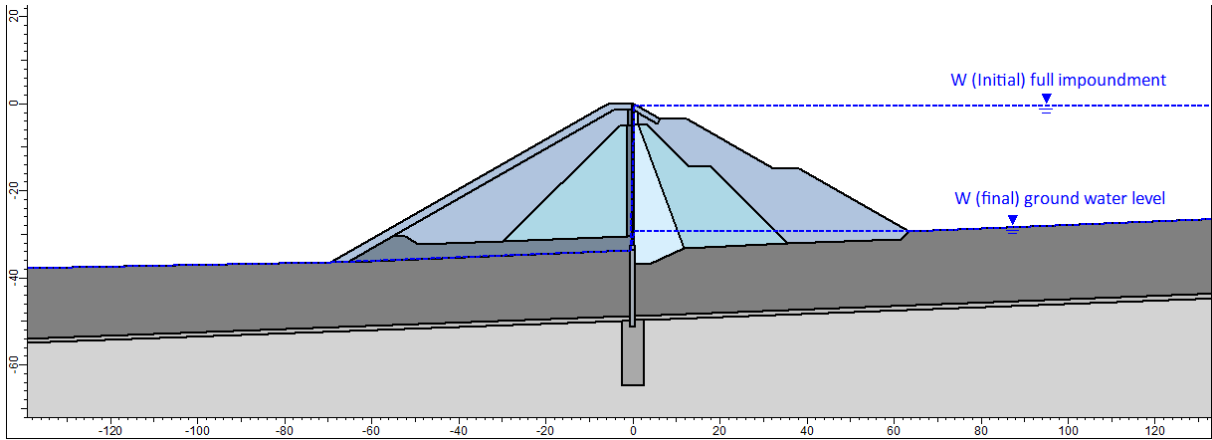


Figure 107: Seepage, Slide 7.0, STL-G

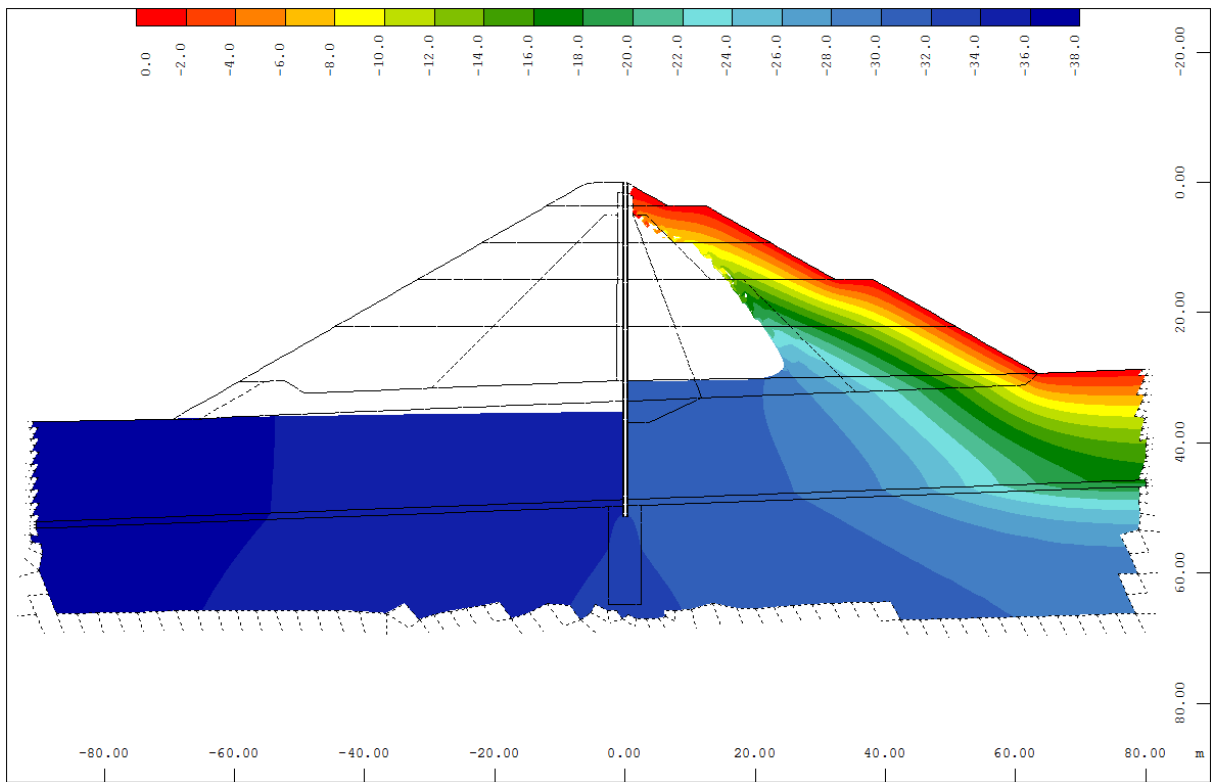


Figure 108: seepage, rapid drawdown after 10 days full impoundment, WinTube, LC-G

Stability Analysis assuming a Circular Slip Surface

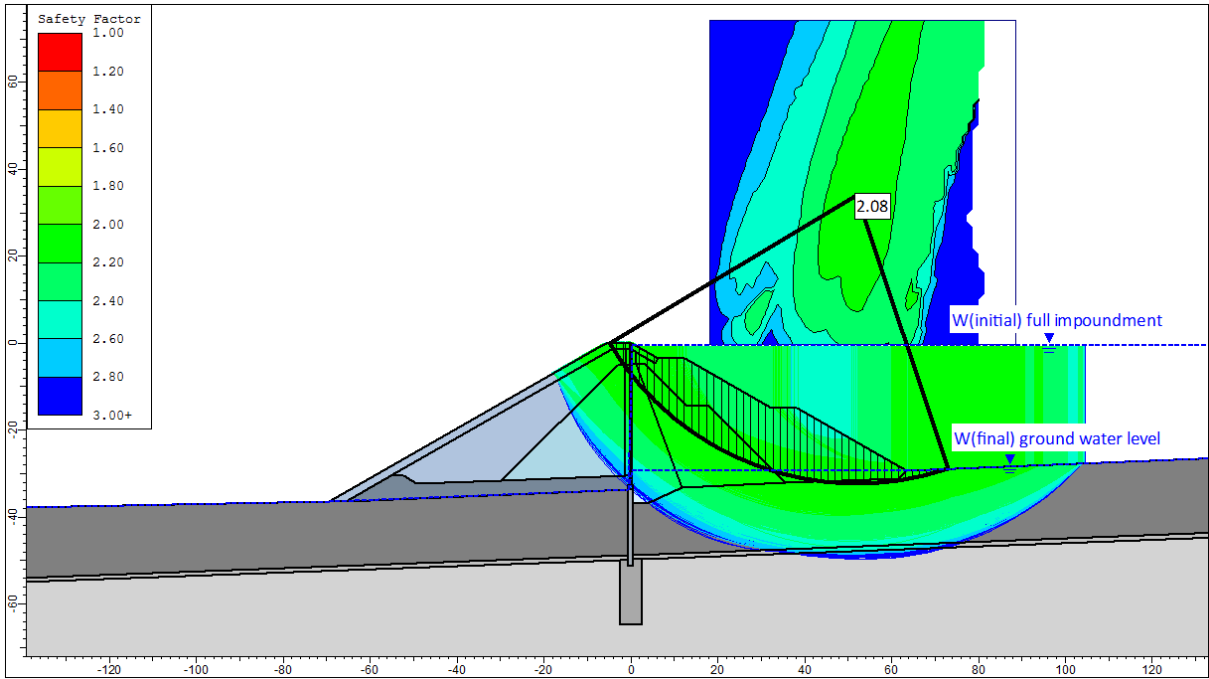


Figure 109: LC-G, B-Bar = 1.0 for Zone 3, circular surface with at least 5 m depth, GLE, FoS = 2.08

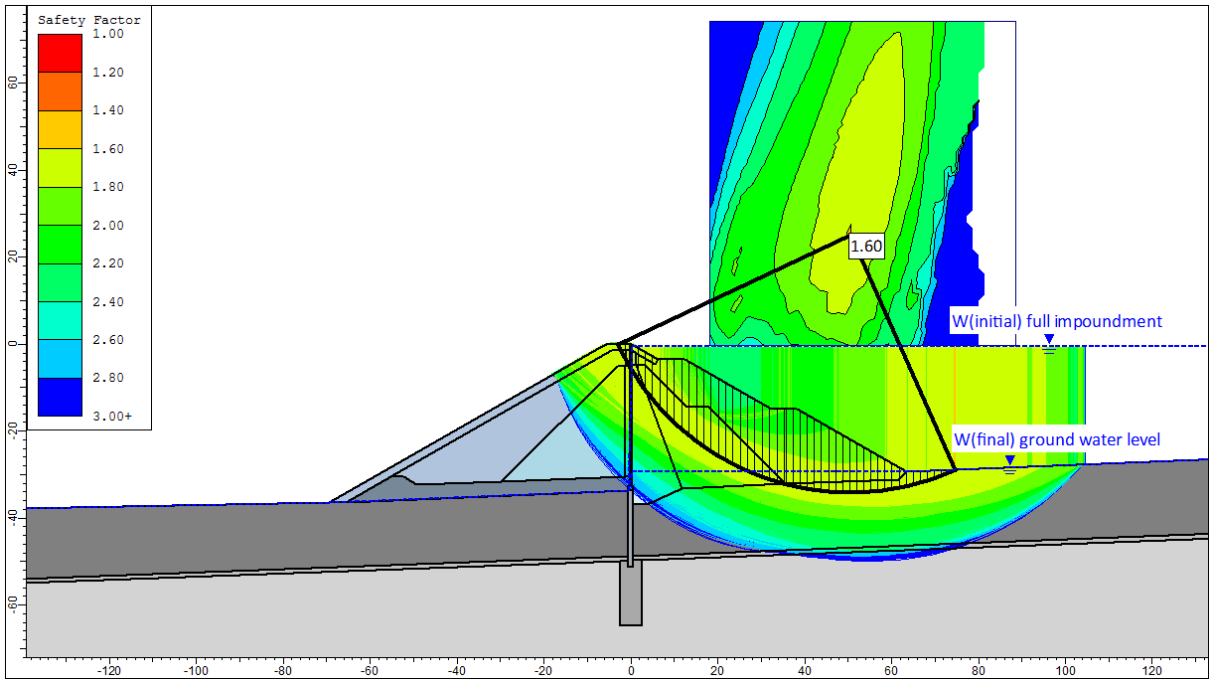


Figure 110: LC-G, B-Bar = 1.0 for Zone 2 and 3, circular surface with at least 5 m depth, GLE, FoS = 1.60

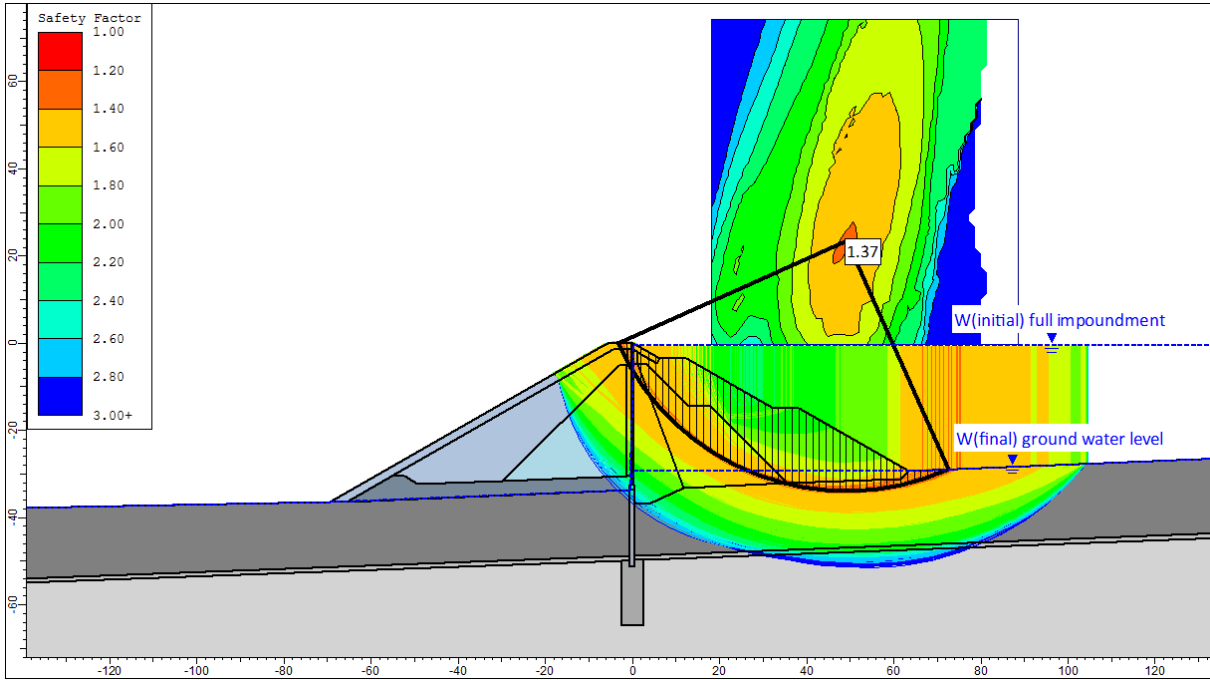


Figure 111: LC-G, B-Bar = 1.0 for Zone 2, 3 and the Cougar Creek Alluvium, circular surface with at least 5 m depth, GLE, FoS = 1.37

Stability Analysis assuming a Non-Circular Slip Surface

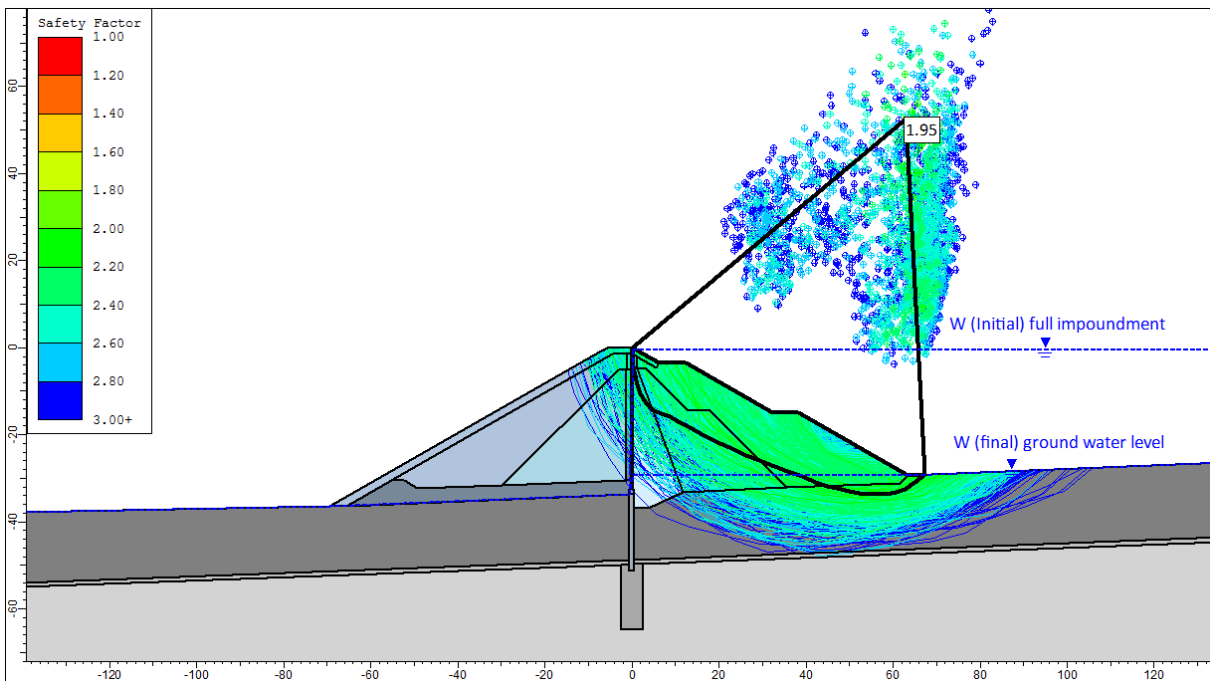


Figure 112: LC-G, B-Bar = 1.0 for Zone 3, non-circular surface with at least 5 m depth, GLE, FoS = 1.95

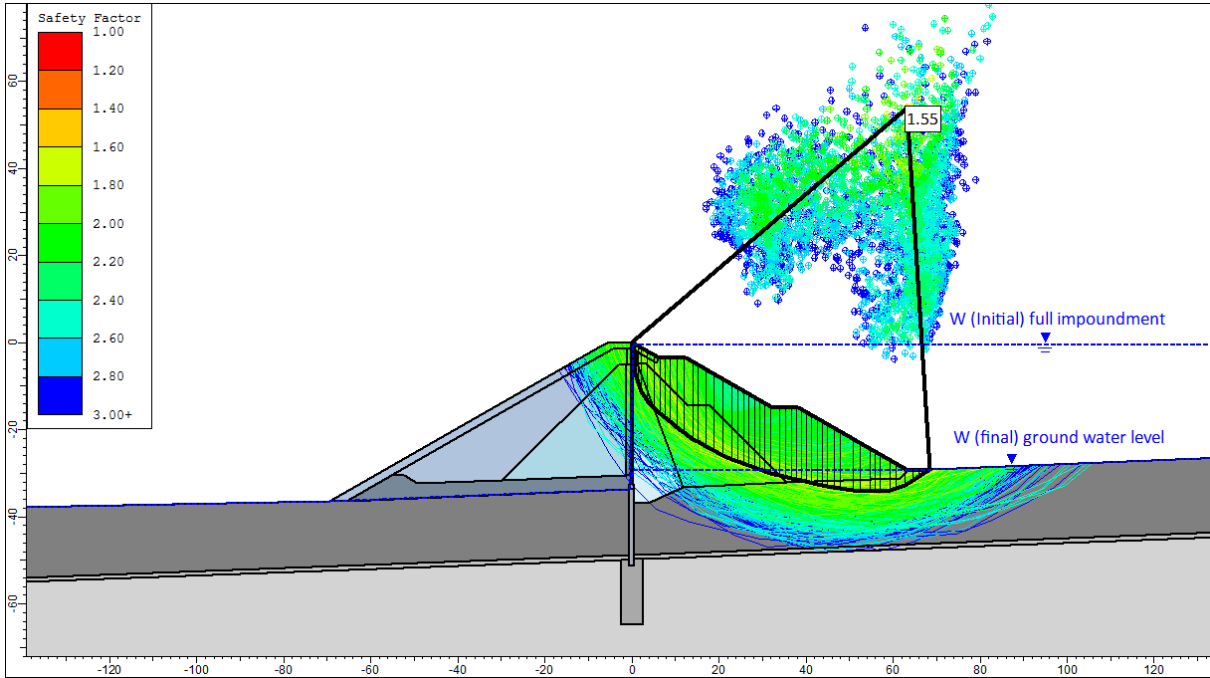


Figure 113: LC-G, B-Bar = 1.0 for Zone 2 and 3, non-circular surface with at least 5 m depth, GLE, FoS = 1.55

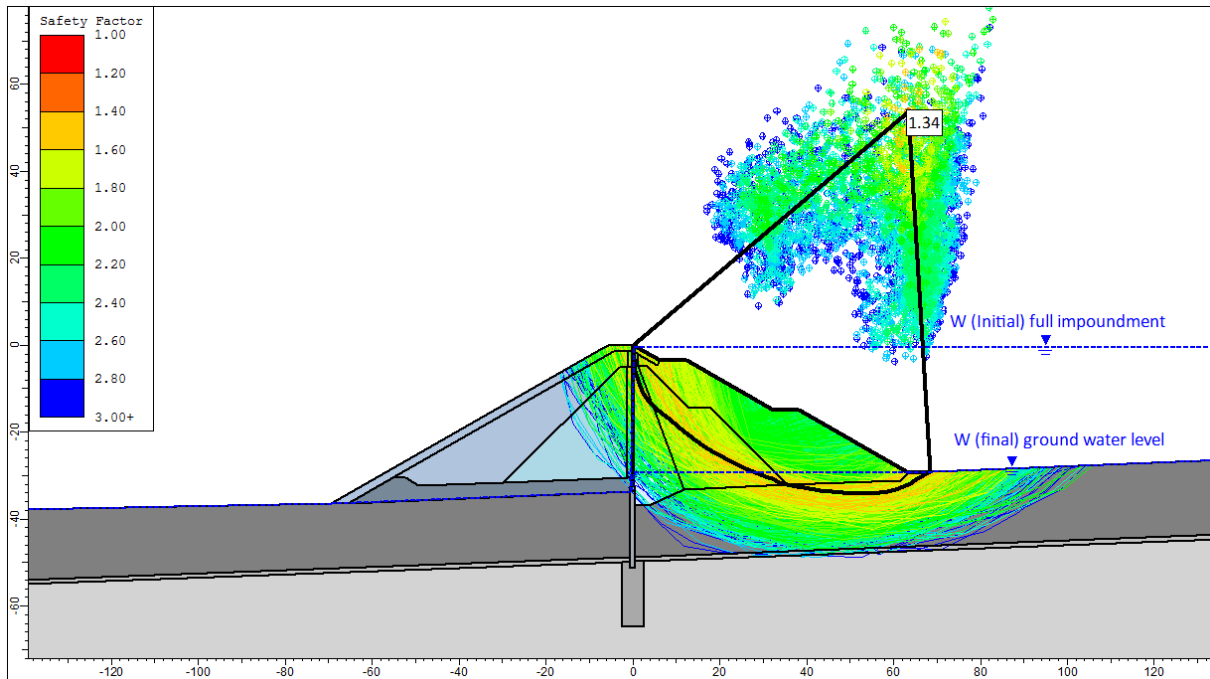


Figure 114: LC-G, B-Bar = 1.0 for Zone 2, 3 and the Cougar Creek Alluvium, non-circular surface with at least 5 m depth, GLE, FoS = 1.34

FE Stability Assessment with Phi-c Reduction

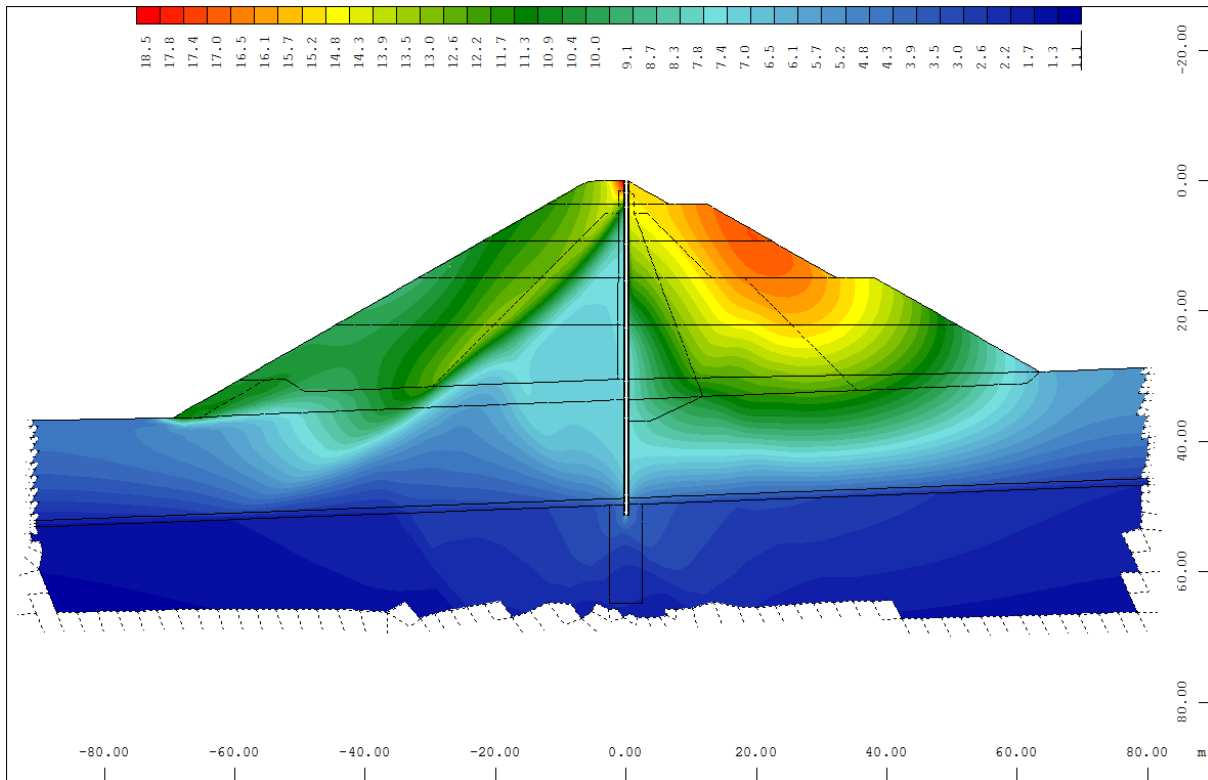


Figure 115: LC-G, phi-c reduction, rapid drawdown after 10 days full impoundment, nodal displacement vector [mm], FoS = 1.57

10.04.05.10 Investigation of the critical Seismic Coefficient – Seismic Yield Acceleration

The structure was checked for the critical seismic coefficient (k_h) indicating the ground acceleration that leads to the stability limit of the embankment slopes (factor of safety is 1.0). Slide 7 provides a tool for this analysis. The seismic coefficient is dimensionless and represents the earthquake acceleration as a fraction of the gravitational acceleration.

LC-A, Critical Seismic coefficient k_h for FoS = 1.0

Table 62: critical seismic coefficient, empty retention structure

LC-A, seismic coefficient k_h for critical FoS = 1.0			
downstream slope		upstream slope	
circular	non-circular	circular	non-circular
0.286	0.275	$\geq 0.312, 0.402$	$\geq 0.312, 0.372$

The critical seismic coefficients as listed in Table 62 are resulting without applying a vertical seismic acceleration ($k_v = 0$). Usually k_v is considered to be $2/3 * k_h$. Applying k_v as $\pm 2/3 * k_h$ results in slightly different factors of safety but not substantially. For the circular slip surface of the downstream embankment the factor of safety varies between 0.91 for $k_v = -2/3 e_h$, 1.00 for $k_v = 0$ and 1.05 for $k_v = +2/3 k_h$.

Stability Analysis assuming a Circular Slip Surface

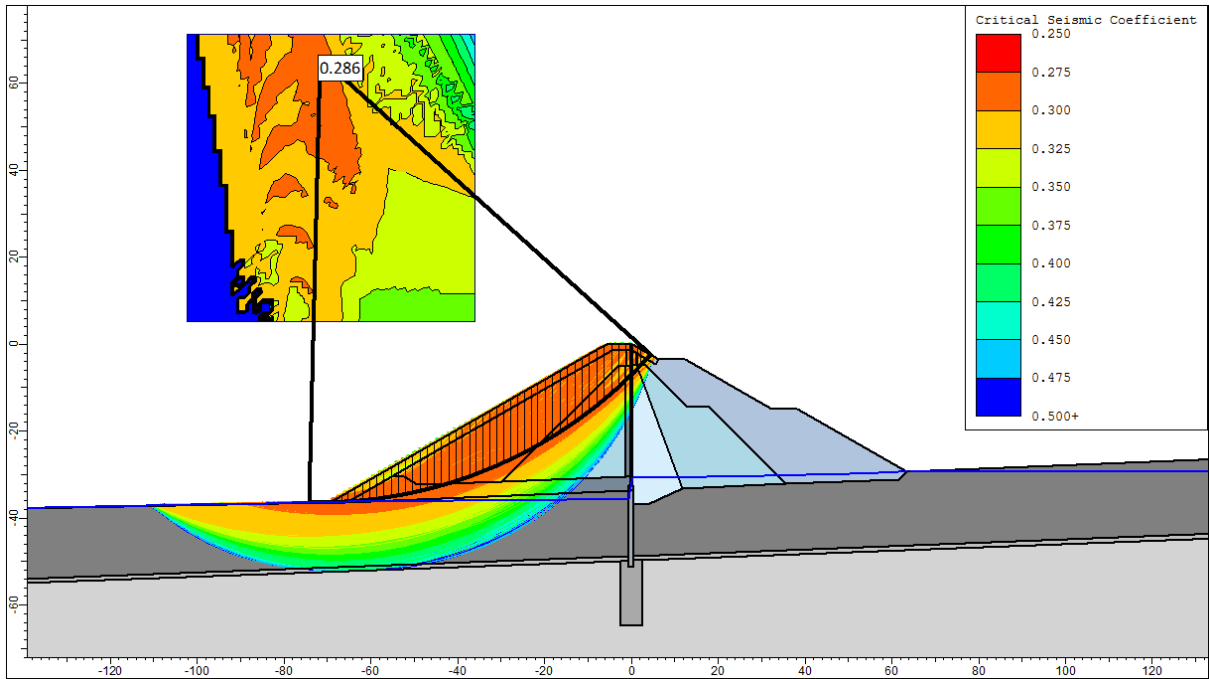


Figure 116: critical seismic coefficient, empty retention structure, circular surface, GLE, $k_h = 0.286$

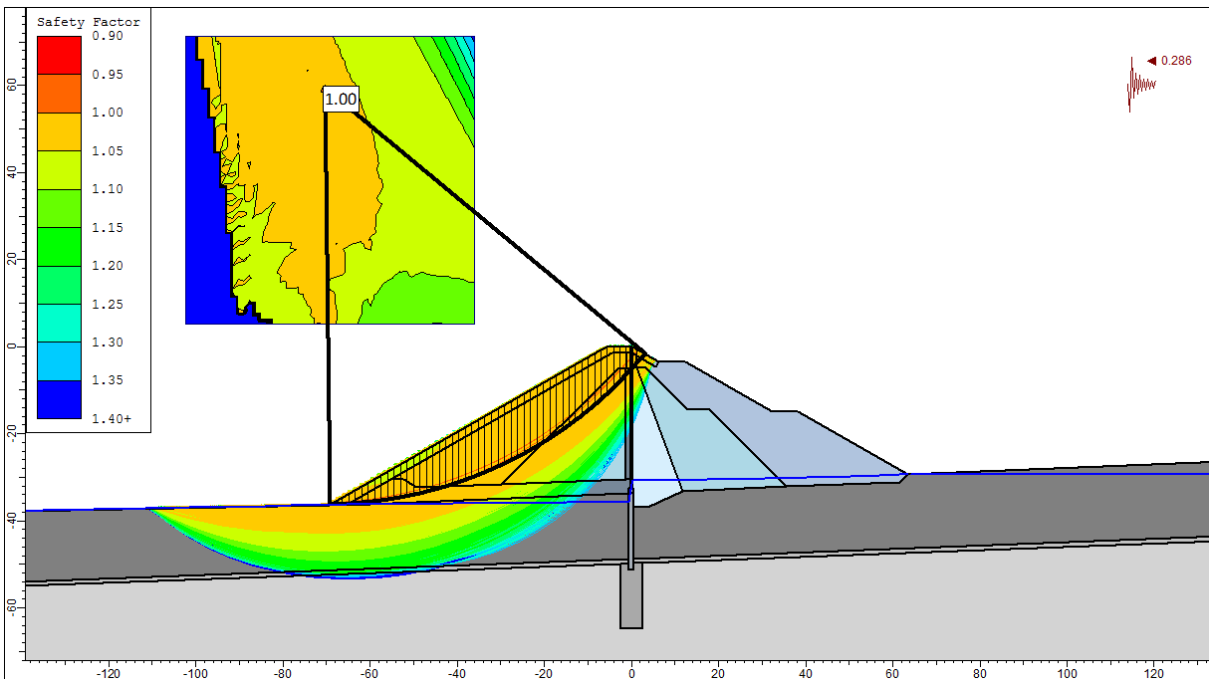


Figure 117: critical seismic coefficient, empty retention structure, circular surface, GLE, FoS = 1.00

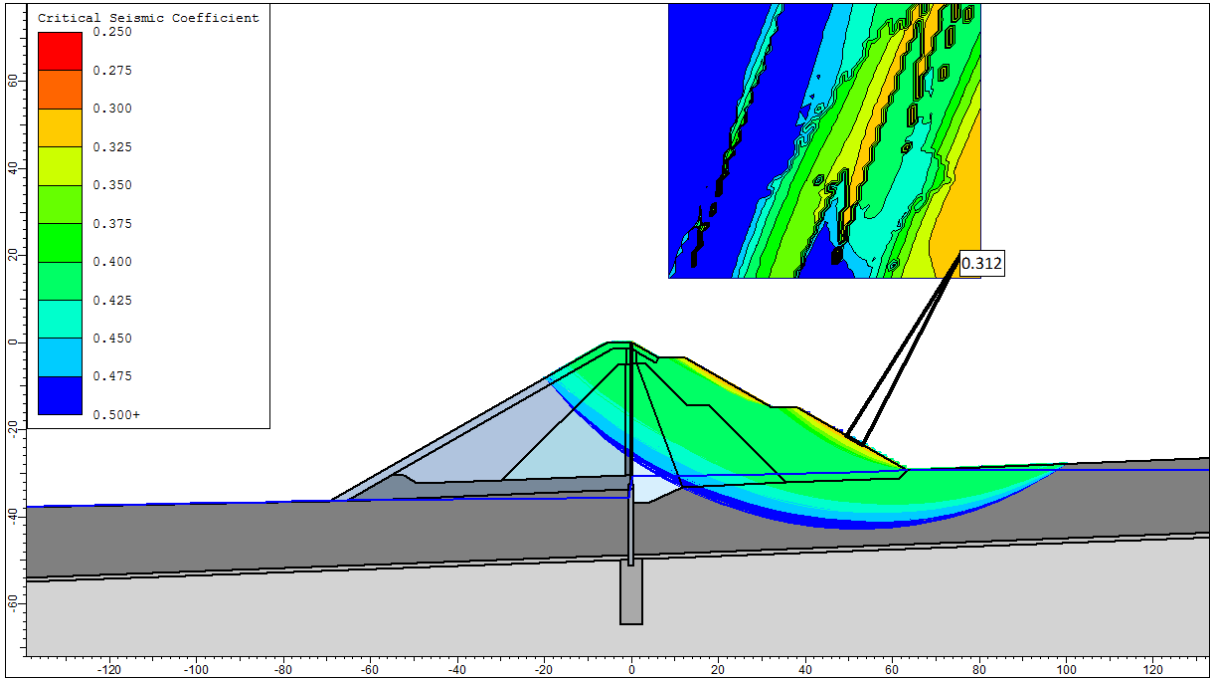


Figure 118: critical seismic coefficient, empty retention structure, circular surface, GLE, $k_h = 0.312$

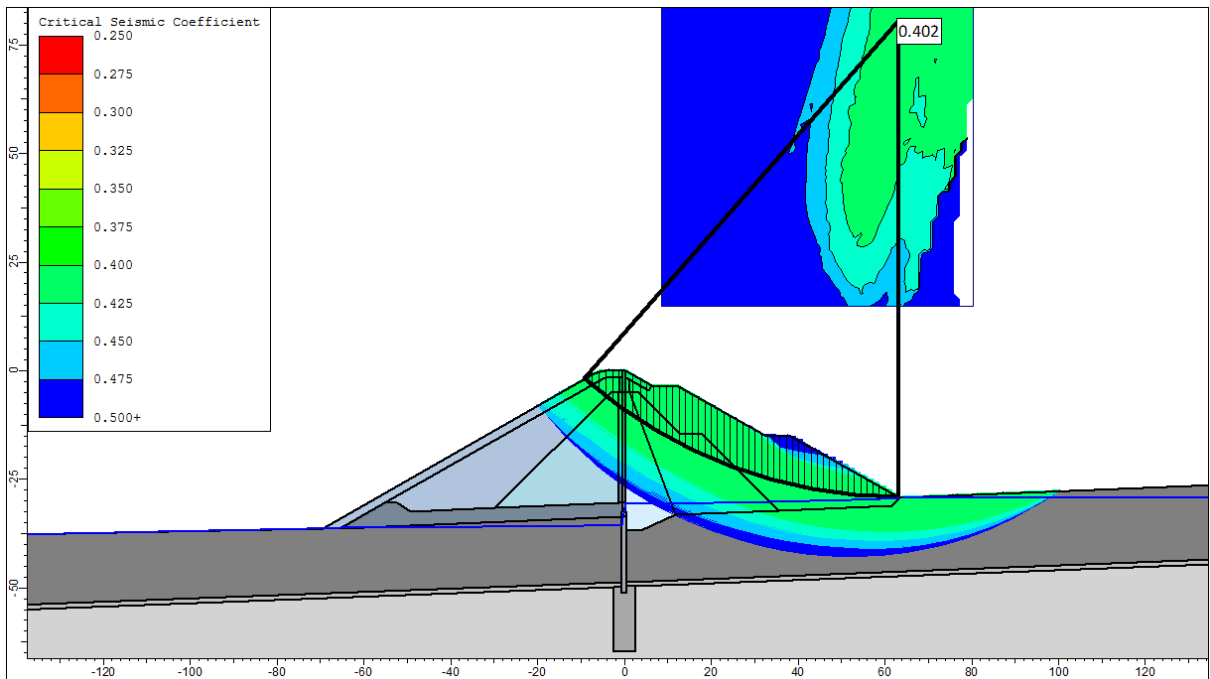


Figure 119: critical seismic coefficient, empty retention structure, circular surface with at least 5.0 m depth, GLE, $k_h = 0.402$

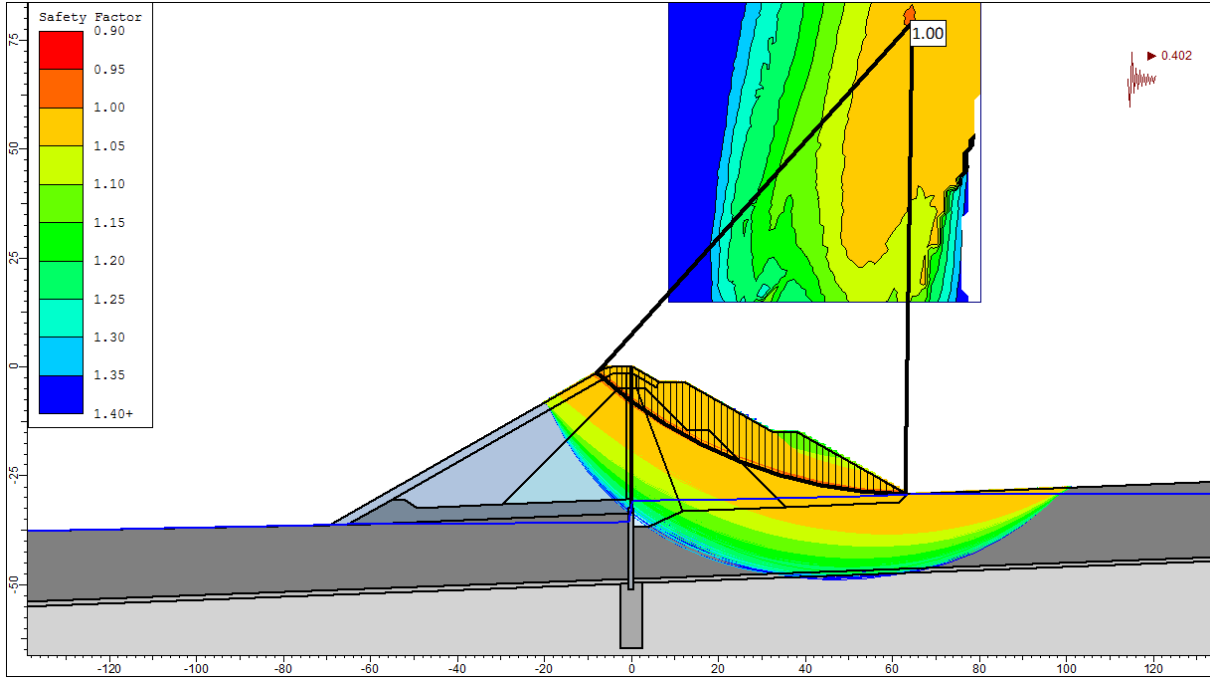


Figure 120: critical seismic coefficient, empty retention structure, circular surface with at least 5.0 m depth, GLE, FoS = 1.00

Stability Analysis assuming a Non-Circular Slip Surface

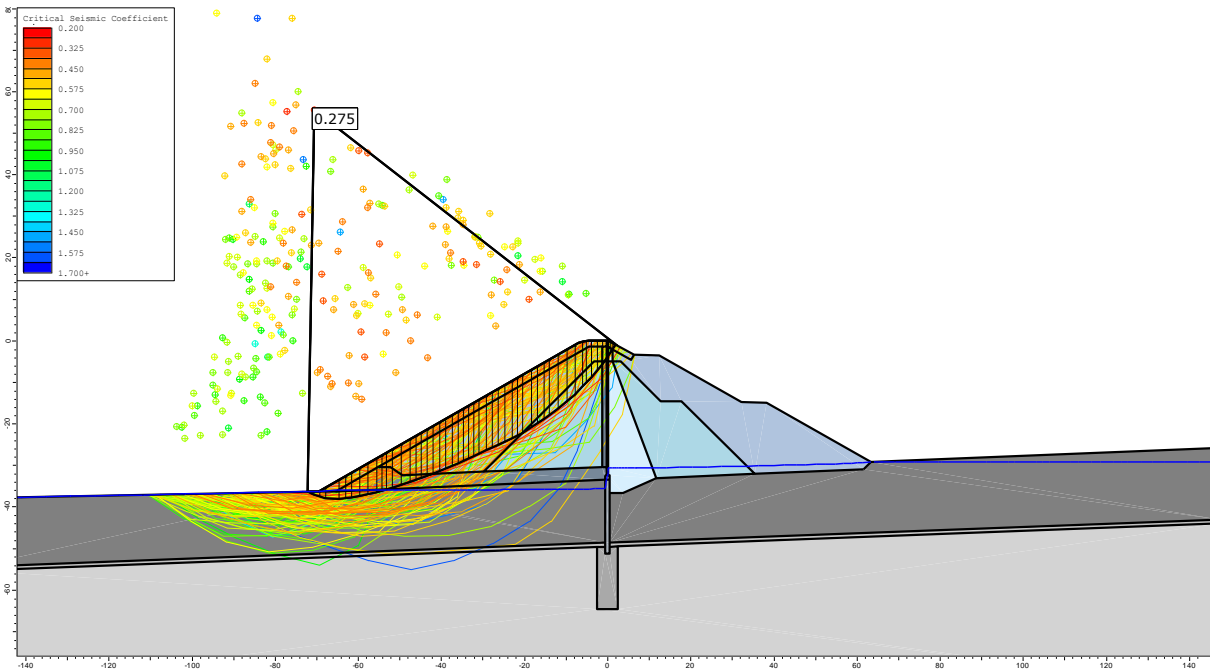


Figure 121: critical seismic coefficient, empty retention structure, non-circular surface, GLE, $k_h = 0.275$

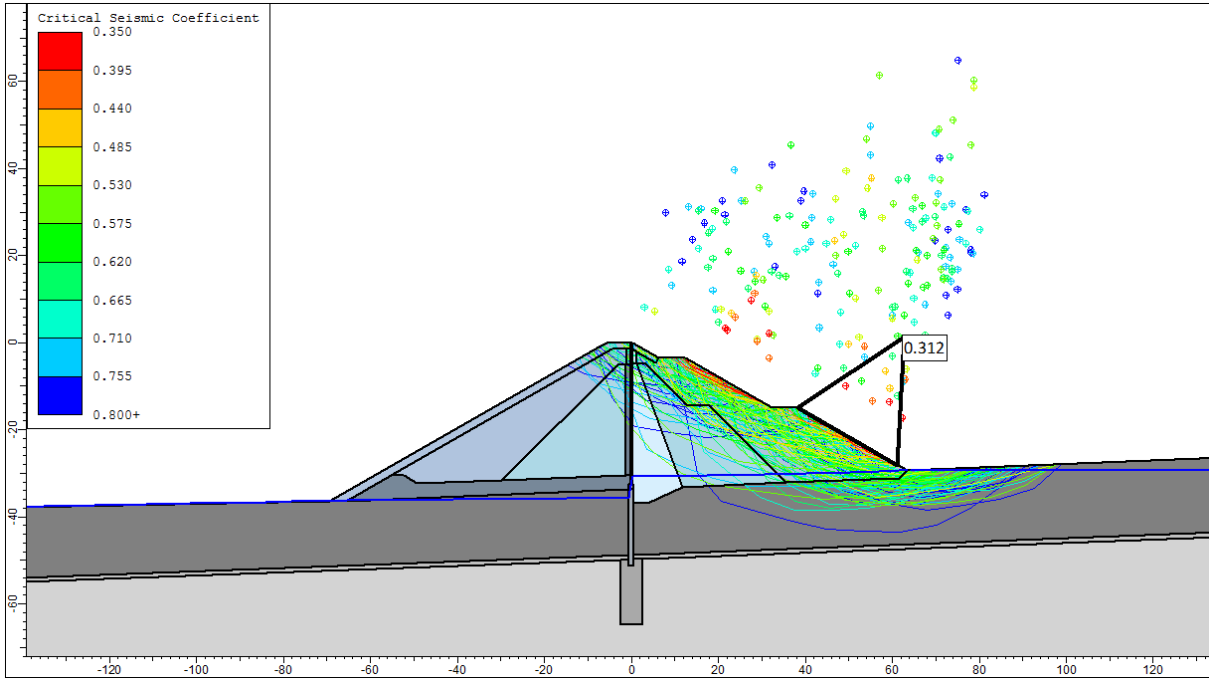


Figure 122: critical seismic coefficient, empty retention structure, non-circular surface, GLE, $k_h = 0.312$

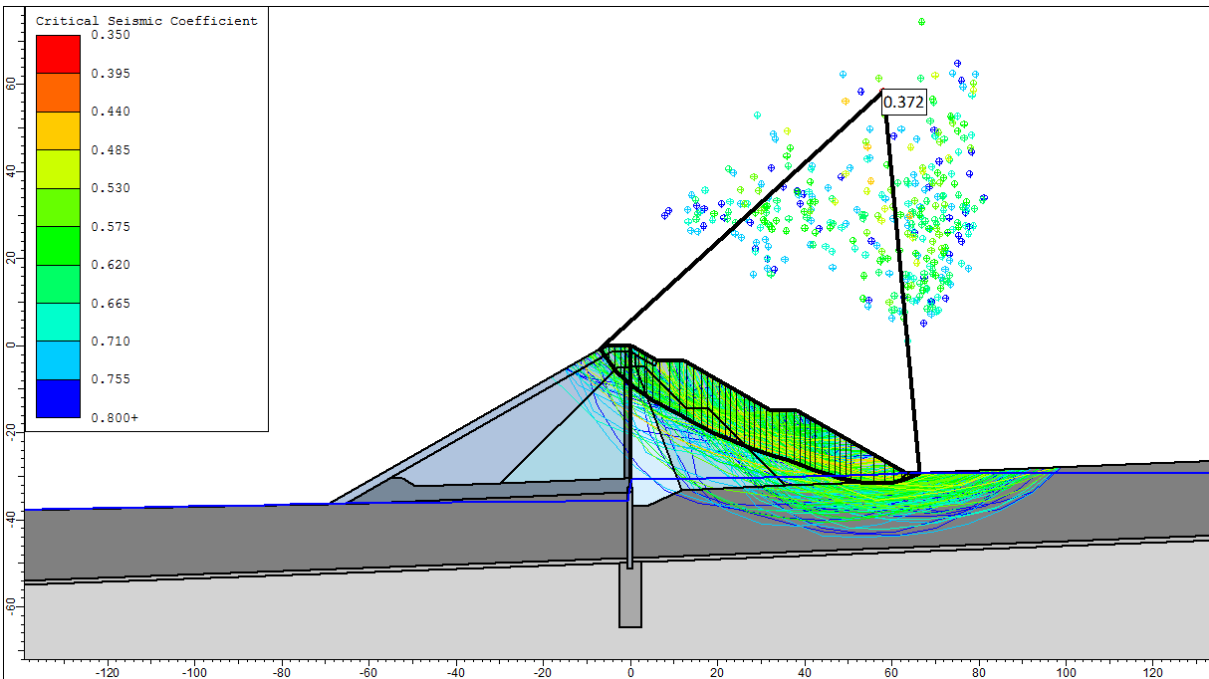


Figure 123: critical seismic coefficient, empty retention structure, non-circular surface with at least 6.0 m depth, GLE, $k_h = 0.372$

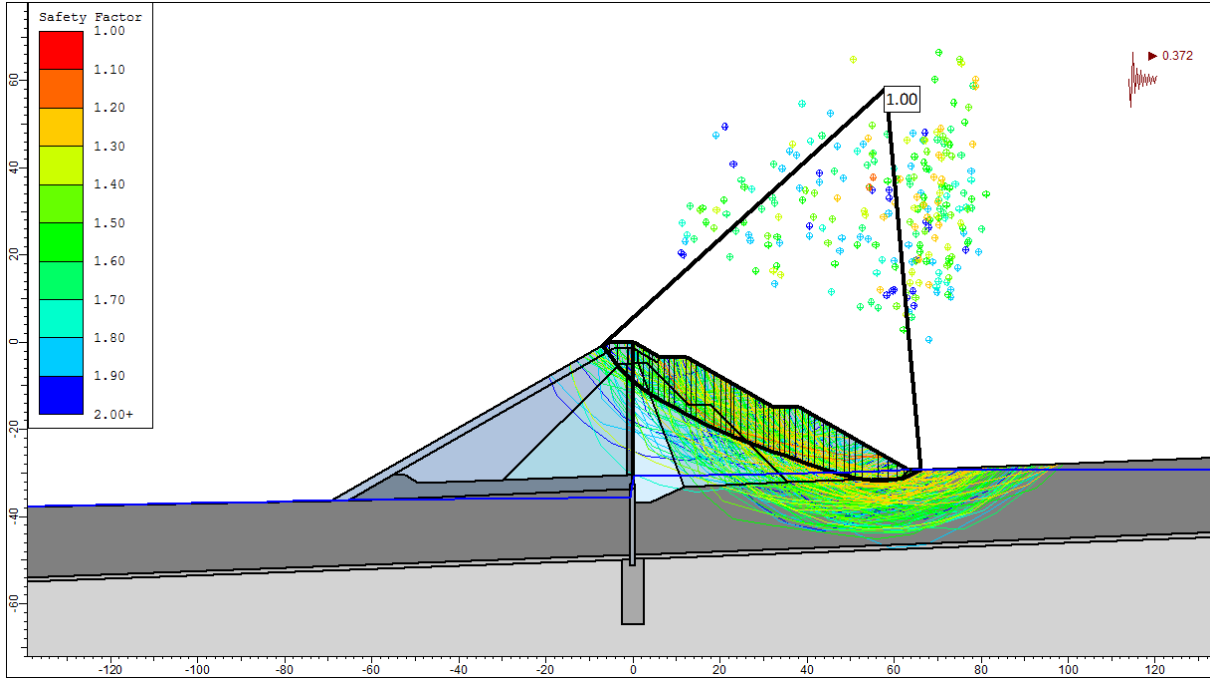


Figure 124; critical seismic coefficient, empty retention structure, non-circular surface with at least 6.0 m depth, GLE, FoS = 1.00

LC-E, Critical Seismic coefficient k_h (FoS = 1.0)

Table 63: critical seismic coefficient, full impoundment

LC-E, seismic coefficient k_h for critical FoS = 1.0			
downstream slope		upstream slope	
circular	non-circular	circular	non-circular
0.266	0.257	$\geq 0.188, 0.280$	$\geq 0.203, 0.283$

The critical seismic coefficients as listed in Table 63 are resulting without applying a vertical seismic acceleration ($k_v = 0$). Usually k_v is considered to be $2/3 * k_h$. Applying k_v as $\pm 2/3 * k_h$ results in slightly different factors of safety. For the slip surfaces of the downstream embankment the factor of safety varies between 0.91 for $k_v = -2/3 e_h$, 1.00 for $k_v = 0$ and 1.05 for $k_v = +2/3 k_h$.

Stability Analysis assuming a Circular Slip Surface

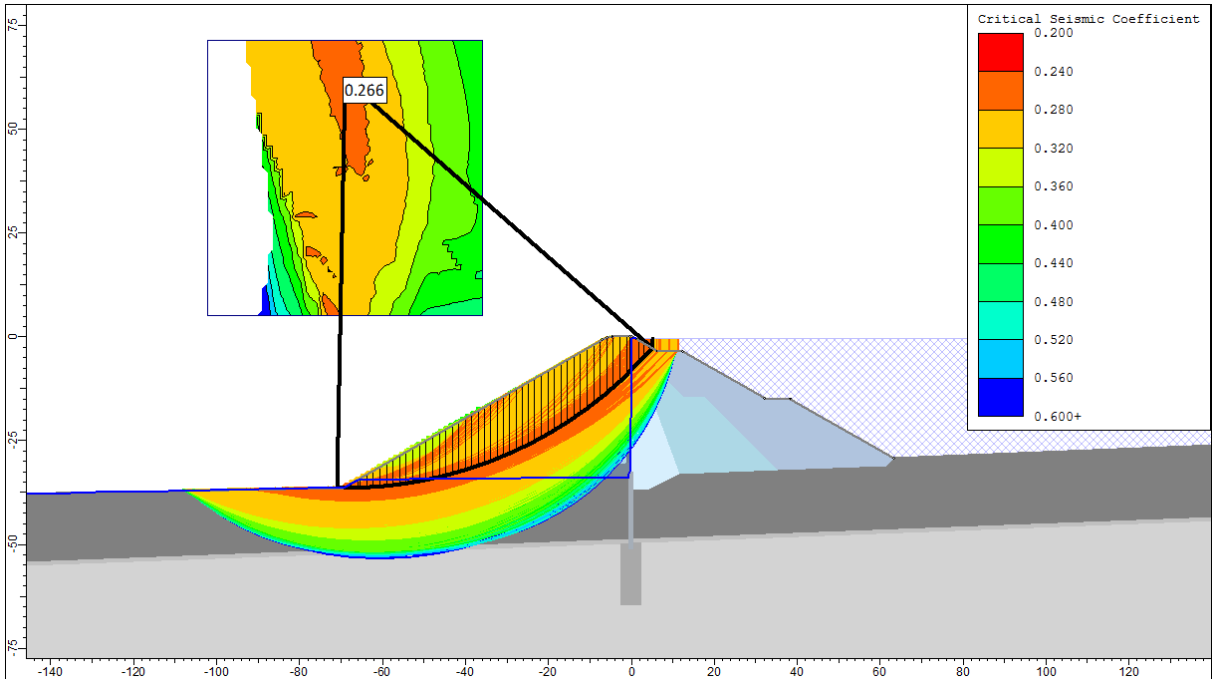


Figure 125: critical seismic coefficient, empty retention structure, circular surface, GLE, $k_h = 0.266$

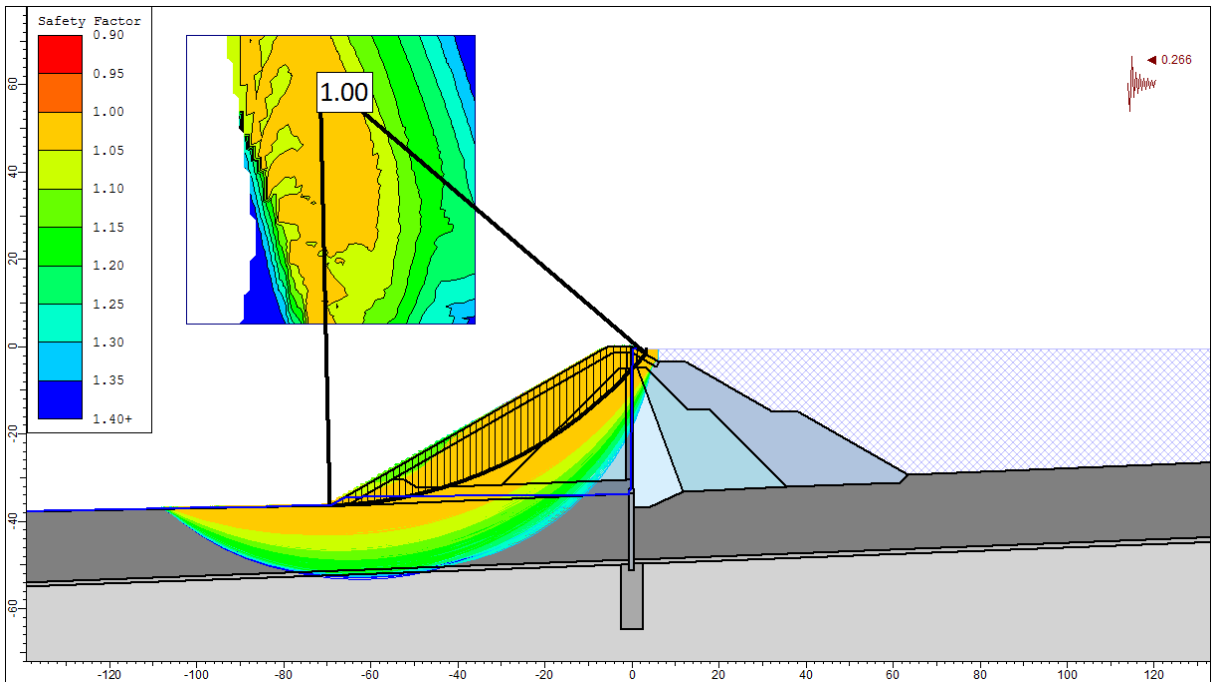


Figure 126: critical seismic coefficient, empty retention structure, circular surface, GLE, FoS = 1.00

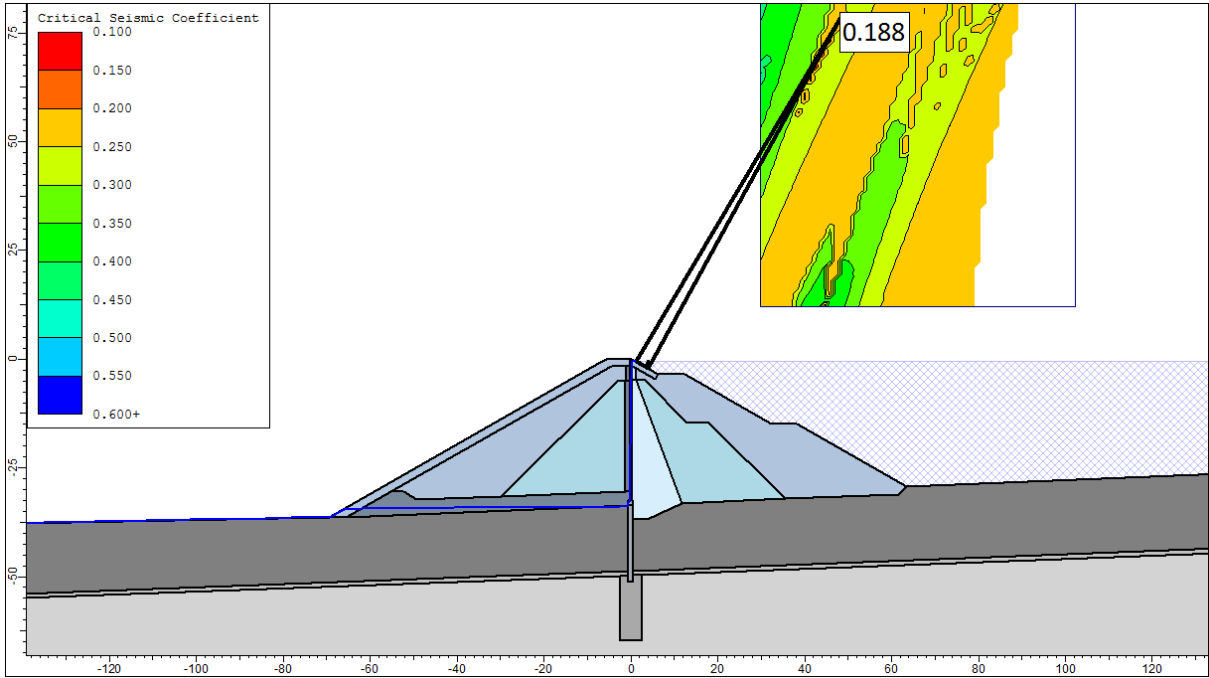


Figure 127: critical seismic coefficient, empty retention structure, circular surface, GLE, $k_h = 0.188$

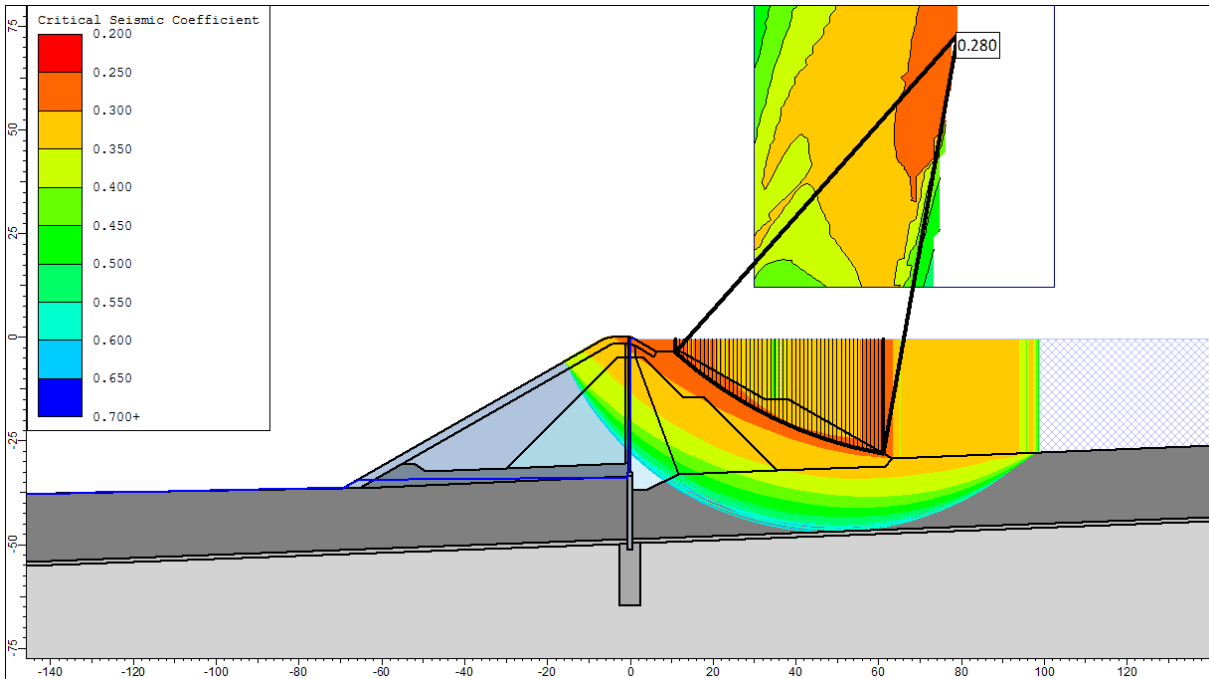


Figure 128: critical seismic coefficient, empty retention structure, circular surface with at least 6.0 m depth, GLE, $k_h = 0.280$

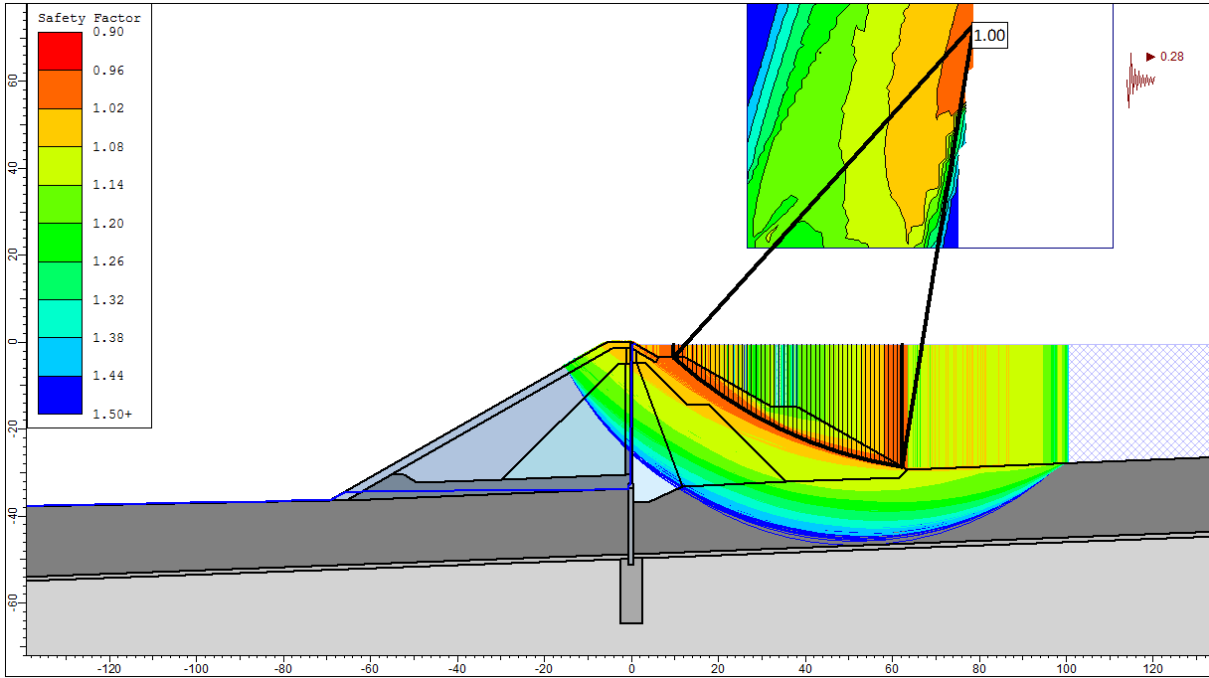


Figure 129: critical seismic coefficient, empty retention structure, circular surface with at least 6.0 m depth, GLE, FoS = 1.00

Stability Analysis assuming a Non-Circular Slip Surface

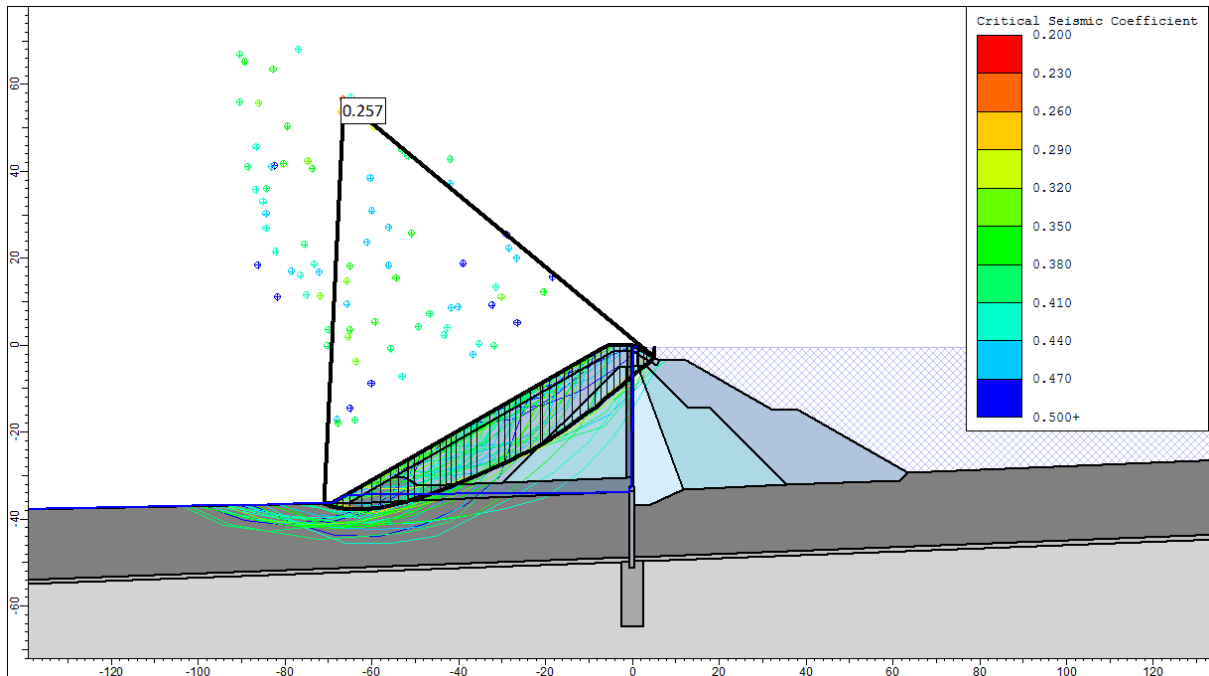


Figure 130: critical seismic coefficient, empty retention structure, non-circular surface, GLE, $k_h = 0.257$

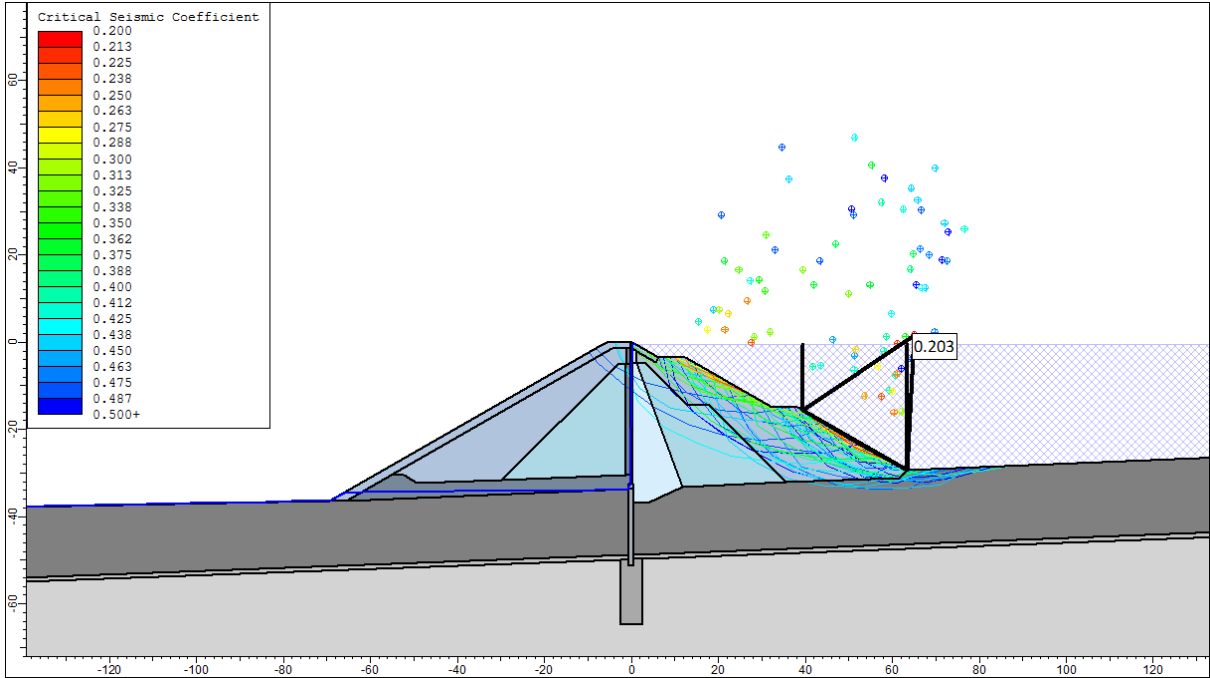


Figure 131: critical seismic coefficient, empty retention structure, non-circular surface, GLE, $k_h = 0.203$

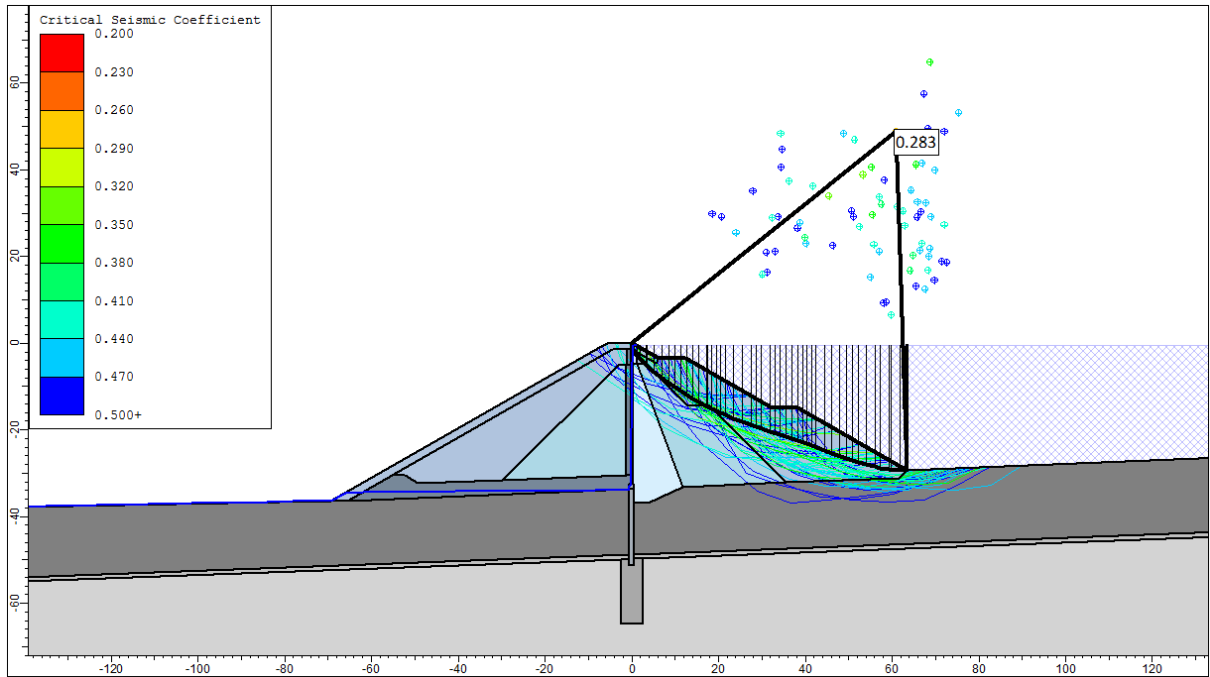


Figure 132: critical seismic coefficient, empty retention structure, non-circular surface with at least 6.0 m depth, GLE, $k_h = 0.283$

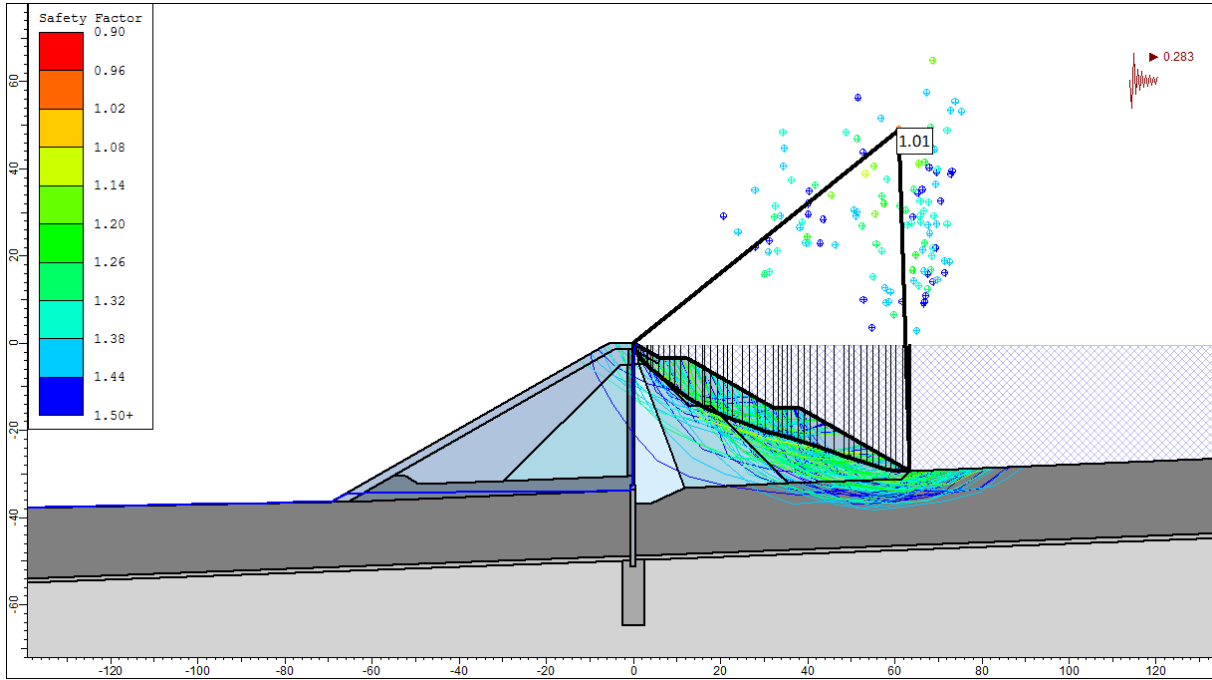


Figure 133; critical seismic coefficient, empty retention structure, non-circular surface with at least 6.0 m depth, GLE, FoS = 1.01

10.05 Dam Deformation, Forces and Moments acting on the Cut-Off Wall

10.05.01 Abstraction of the Structure for FEA

The model layout of the structure, according to the design drawings for FE analysis of dam deformation and the calculation of forces and moments acting on the seal wall, is shown in Figure 134. The different zones of the system are represented. Figure 135 shows construction and loading stages during construction.

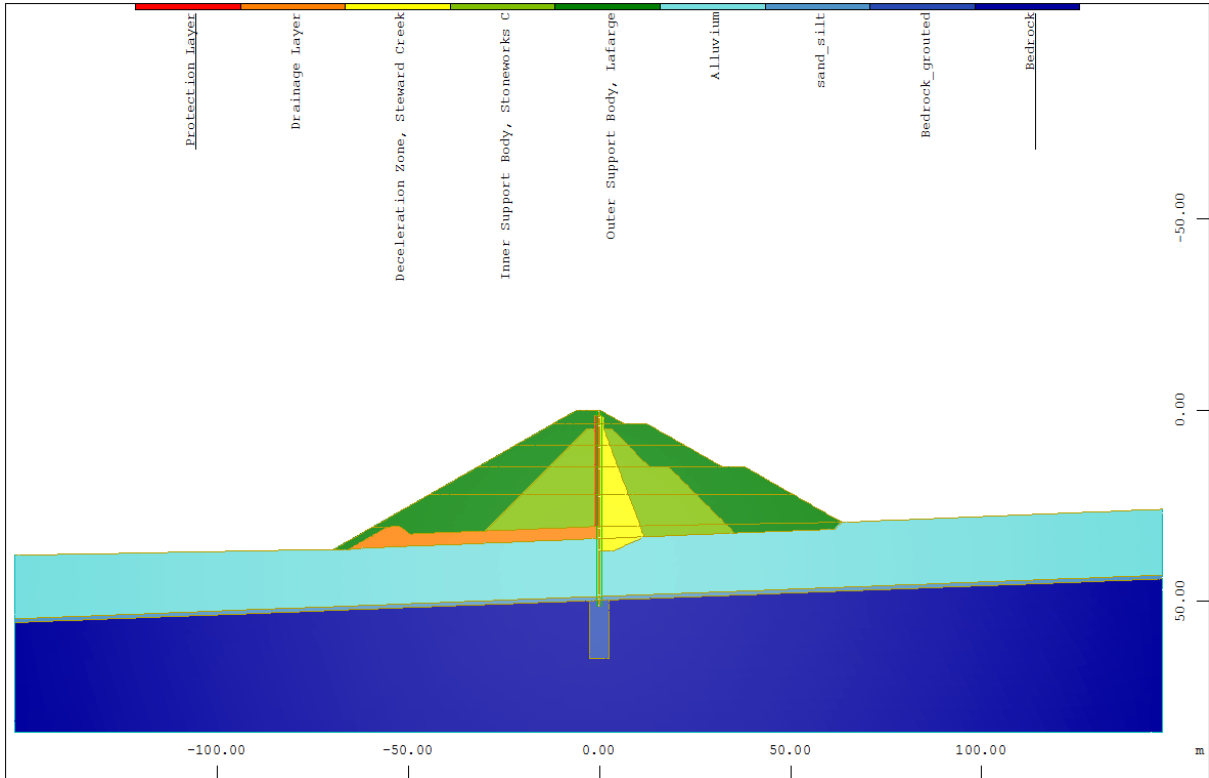


Figure 134: Dam Zones and Material

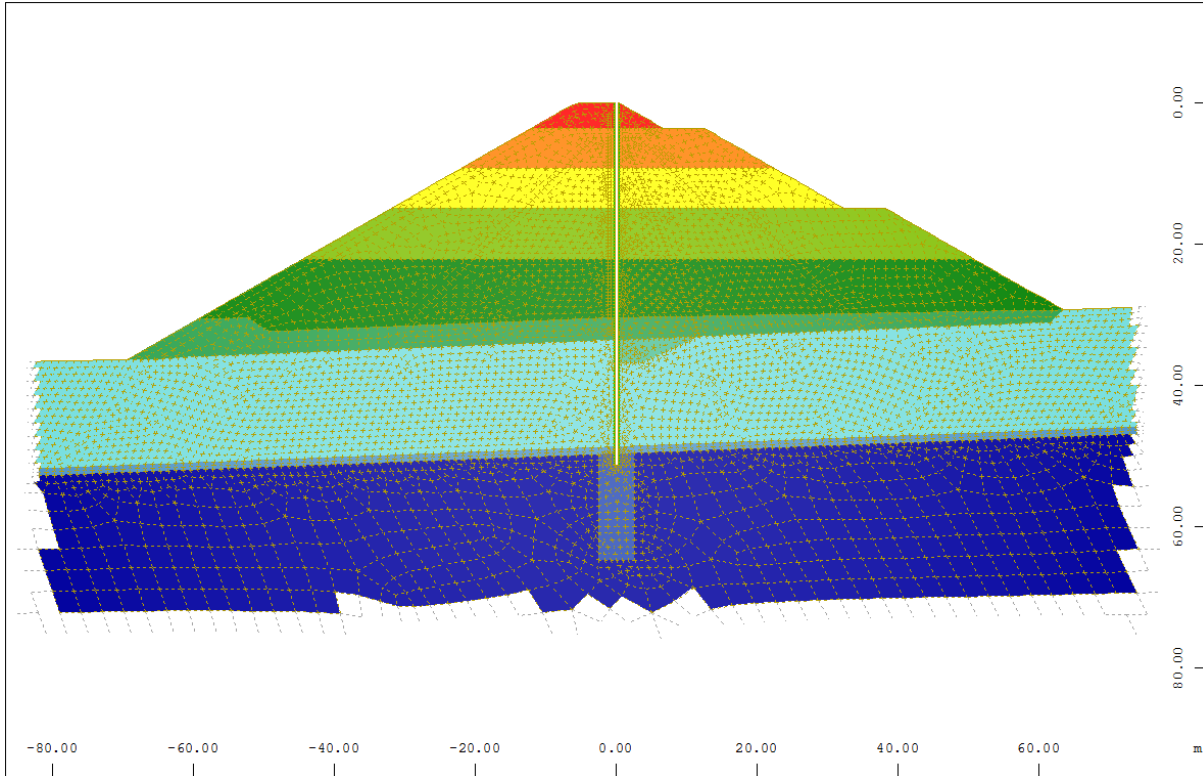


Figure 135: considered construction stages in WinTube

10.05.02 Deformation Analysis

10.05.02.01 Embankment Dam Structure

Dam deformation, acting forces and moments were calculated by considering the cut-off wall (secant pile wall and seal wall) and a soil-structure interaction defined by $1/3$ as well as $2/3$ of friction angle (ϕ) for adjacent soil.

Displacements during construction were subsequently calculated for six fill sequences.

Results for maximum node displacements are summarized in Table 64 for the scenario of $1/3$ of ϕ for the wall-soil friction and in Table 65 for $2/3$ of ϕ . Figure 136 to Figure 144 show dam deformation patterns for selected loading cases.

Table 64: nodal displacement, $\delta = 1/3 * \phi$

	LC-A		LC-E		LC-H	
	ux [mm]	uy [mm]	ux [mm]	uy [mm]	ux [mm]	uy [mm]
Seal Wall, bottom	-11.73	7.82	-42.15	4.89	-27.37	7.14
Seal Wall, middle	-12.67	8.11	-54.72	4.71	-35.31	7.51
Seal Wall, top	5.07	0.54	-41.60	-2.90	-21.99	-0.06
Dam Crest, downstream	5.49	22.69	-41.29	19.68	-21.65	24.59
Top Berm, upstream	-14.49	49.45	-55.62	61.63	-37.40	79.84

Table 65: nodal displacement, $\delta = 2/3 * \phi$

	LC-A		LC-E		LC-H	
	ux [mm]	uy [mm]	ux [mm]	uy [mm]	ux [mm]	uy [mm]
Seal Wall, bottom	-11.87	12.58	-43.70	9.18	-28.64	11.65
Seal Wall, middle	-13.77	12.67	-59.45	8.51	-39.10	11.88
Seal Wall, top	4.58	0.93	-47.95	-3.32	-26.84	0.13
Dam Crest, downstream	4.85	21.07	-47.76	17.25	-26.61	22.44
Top Berm, upstream	-13.09	47.03	-58.27	62.24	-38.16	79.20

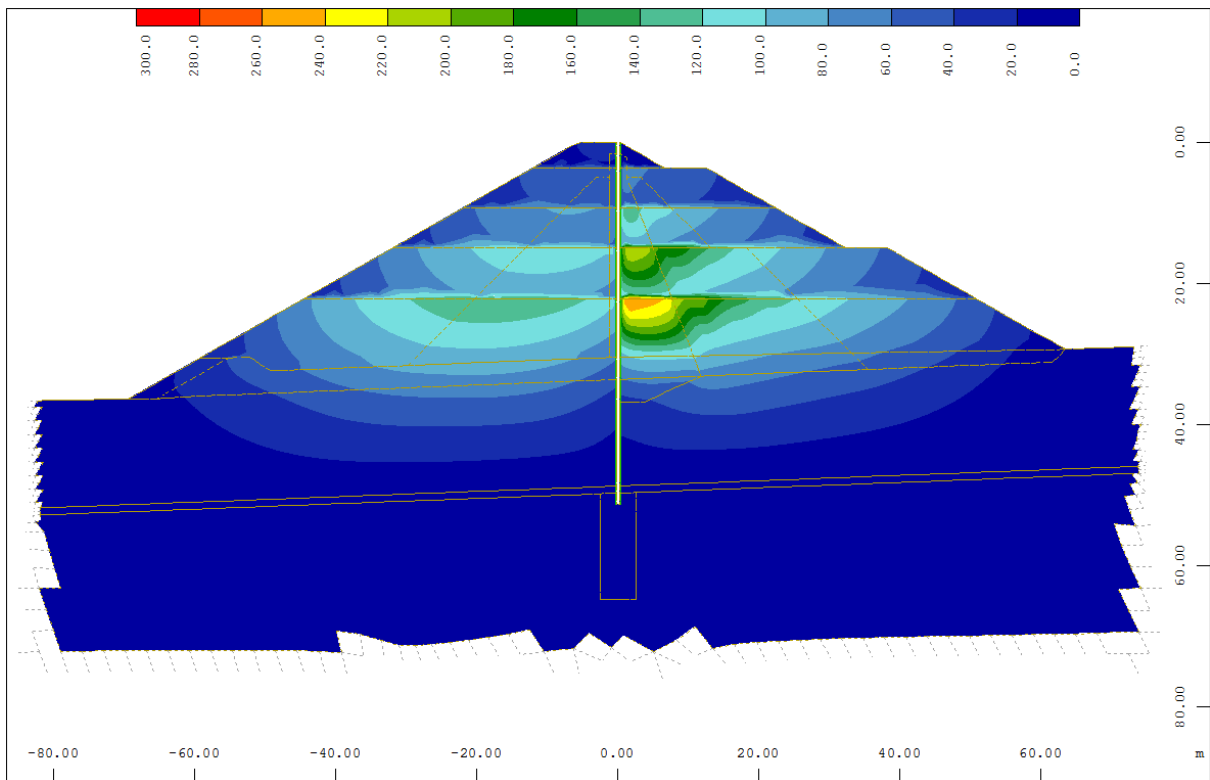


Figure 136: LC-A, dam deformation, nodal displacement u [mm] for 1/3 of ϕ for wall-soil interaction

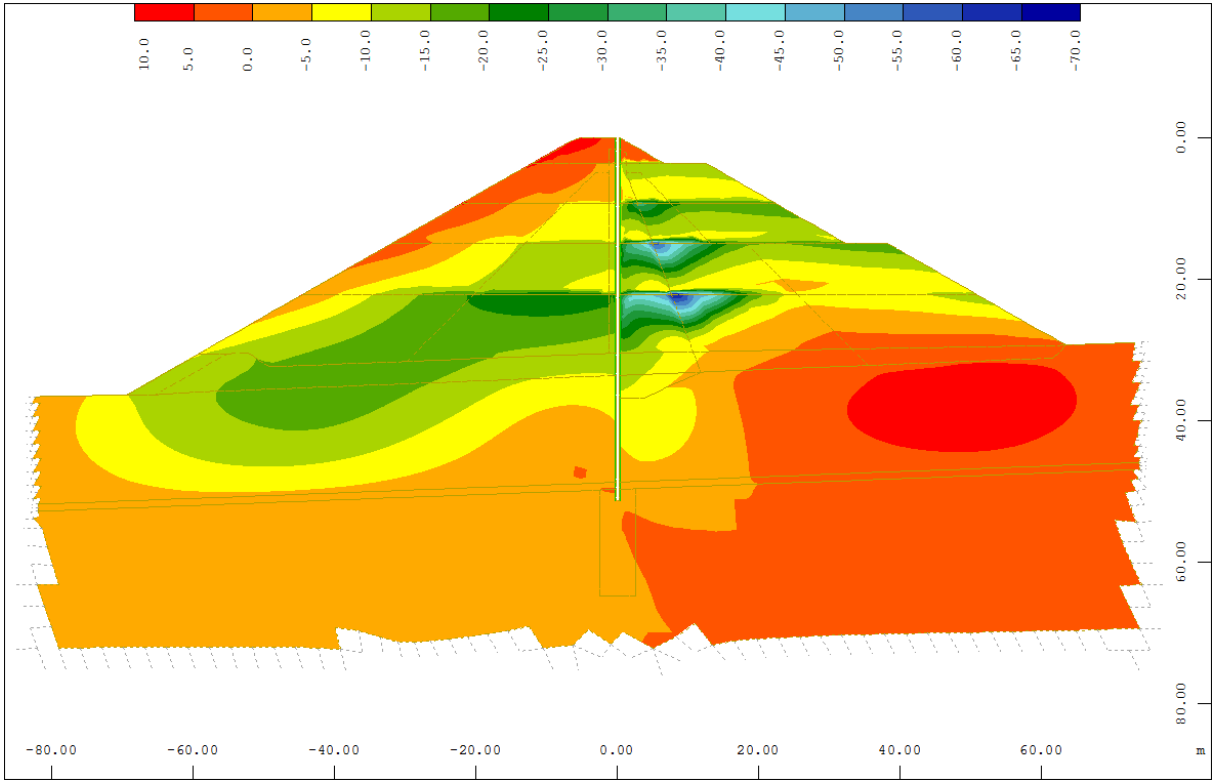


Figure 137: LC-A, horizontal nodal displacement u_x [mm] for $1/3$ of ϕ for wall-soil interaction

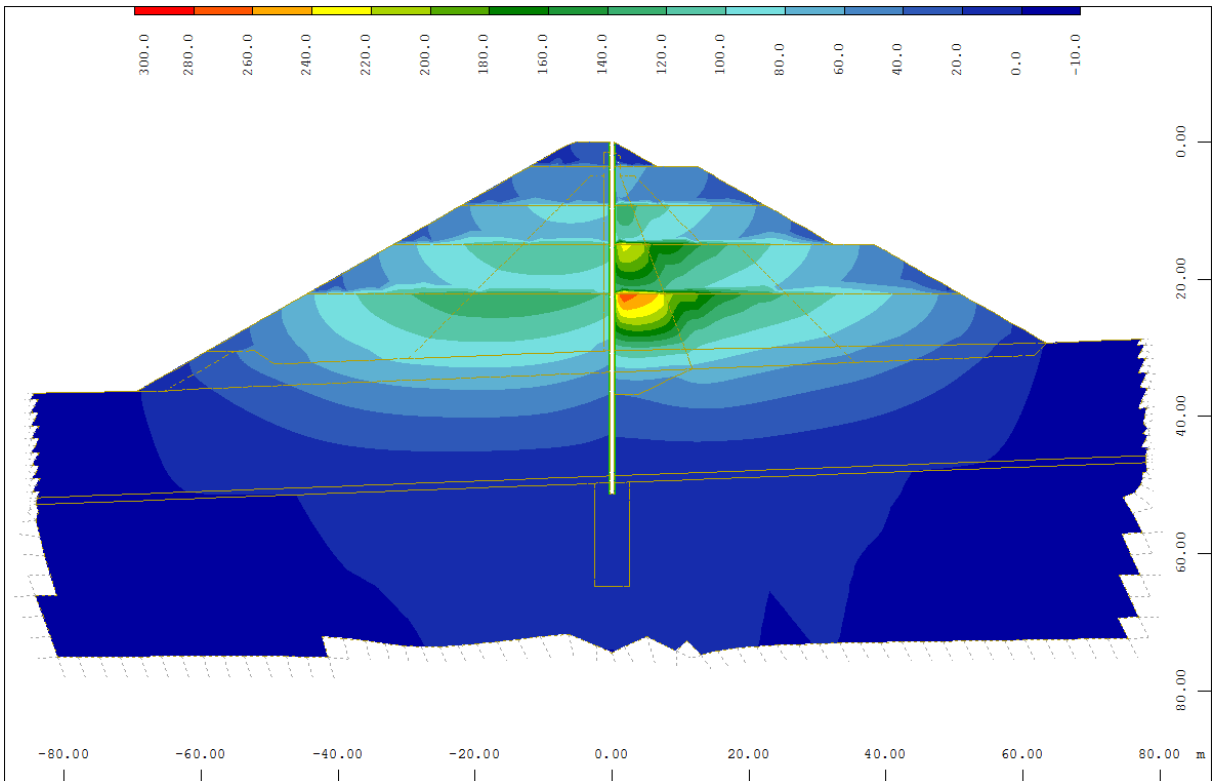


Figure 138: LC-A, vertical nodal displacement u_y [mm] for $1/3$ of ϕ for wall-soil interaction

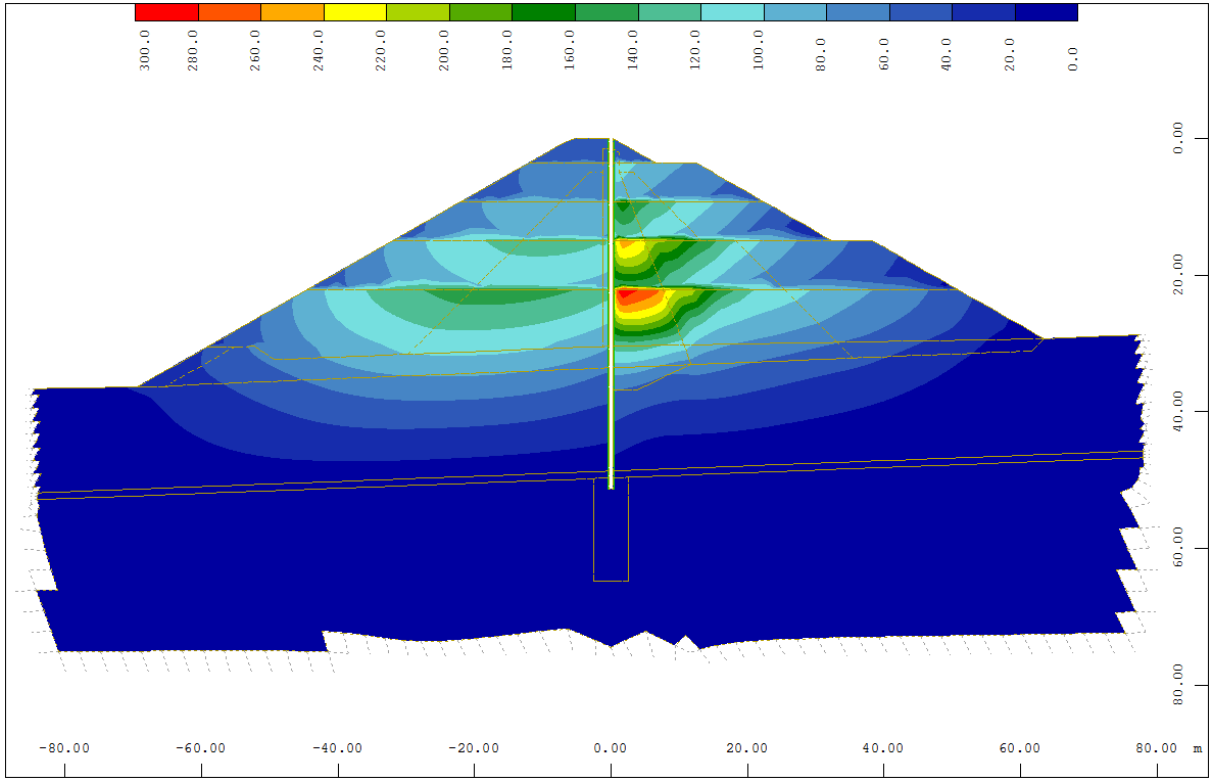


Figure 139: LC-E, dam deformation, nodal displacement u [mm] for 1/3 of ϕ for wall-soil interaction

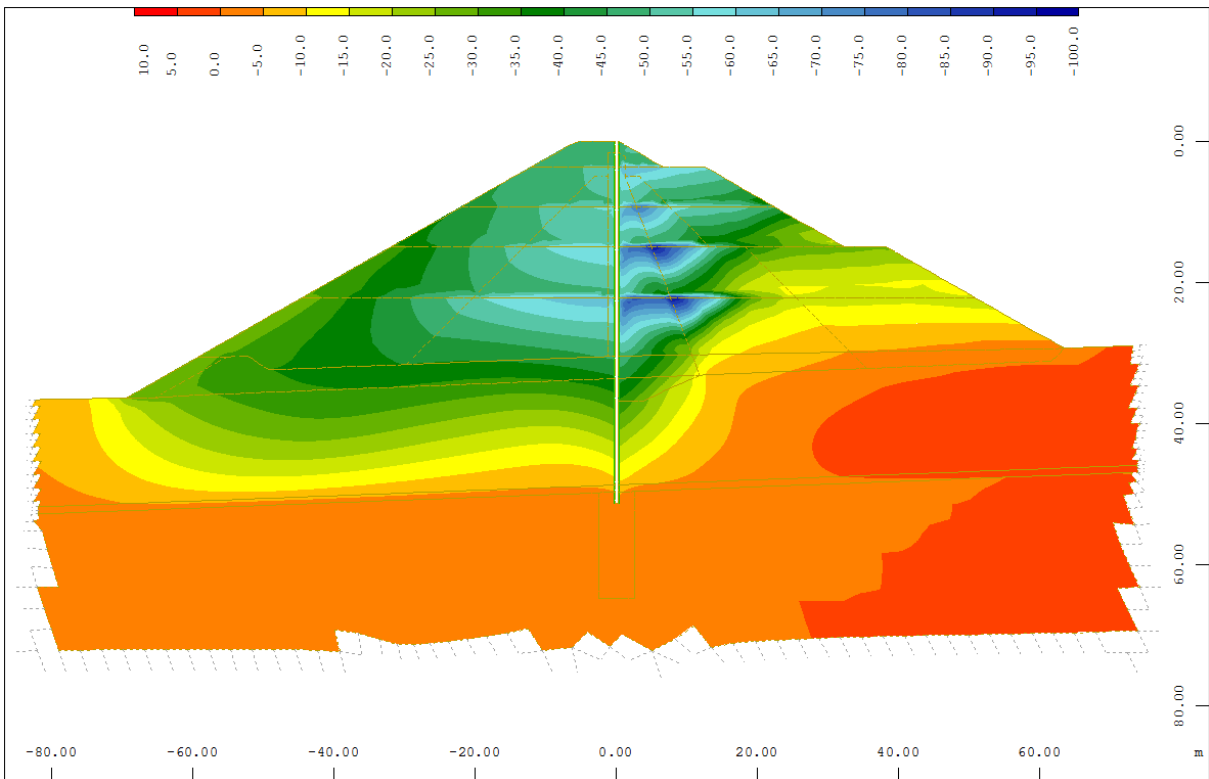


Figure 140: LC-E, horizontal nodal displacement ux [mm] for 1/3 of ϕ for wall-soil interaction

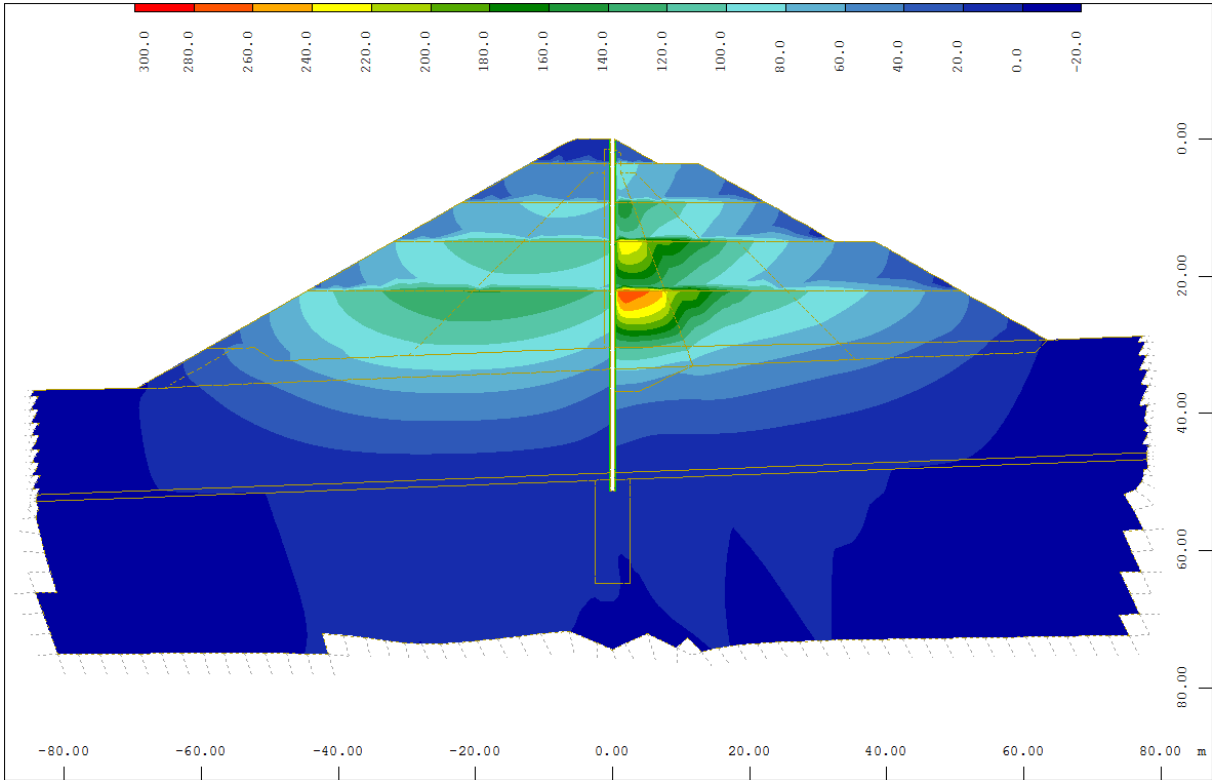


Figure 141: LC-E, vertical nodal displacement u_y [mm] for $1/3$ of ϕ for wall-soil interaction

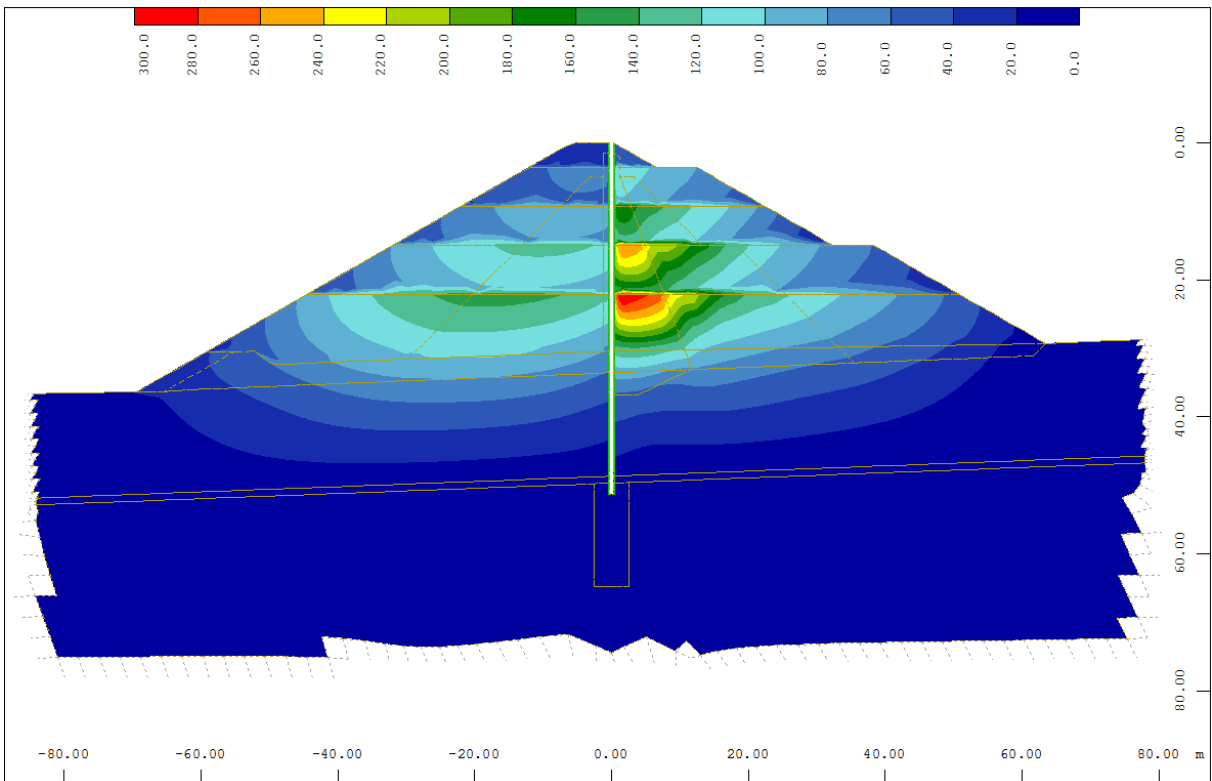


Figure 142: LC-H, dam deformation, nodal displacement u [mm] for $1/3$ of ϕ for wall-soil interaction

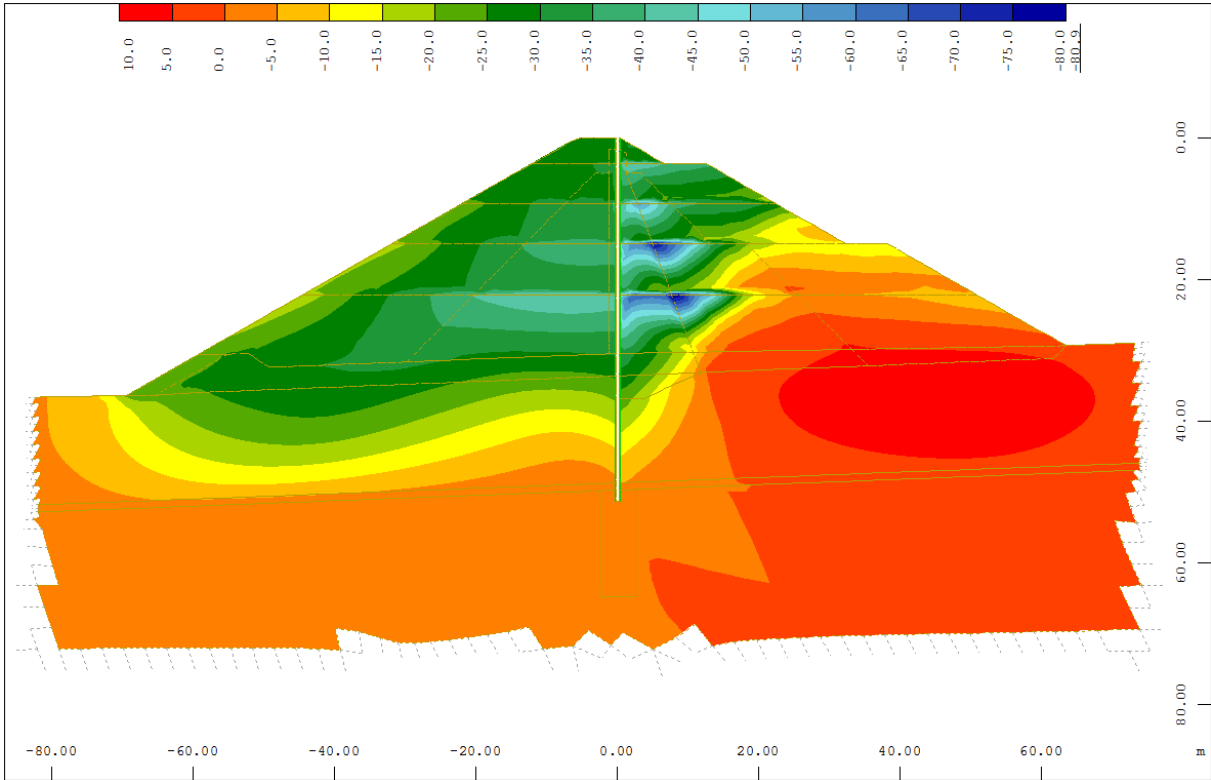


Figure 143: LC-H horizontal nodal displacement u_x [mm] for 1/3 of ϕ for wall-soil interaction

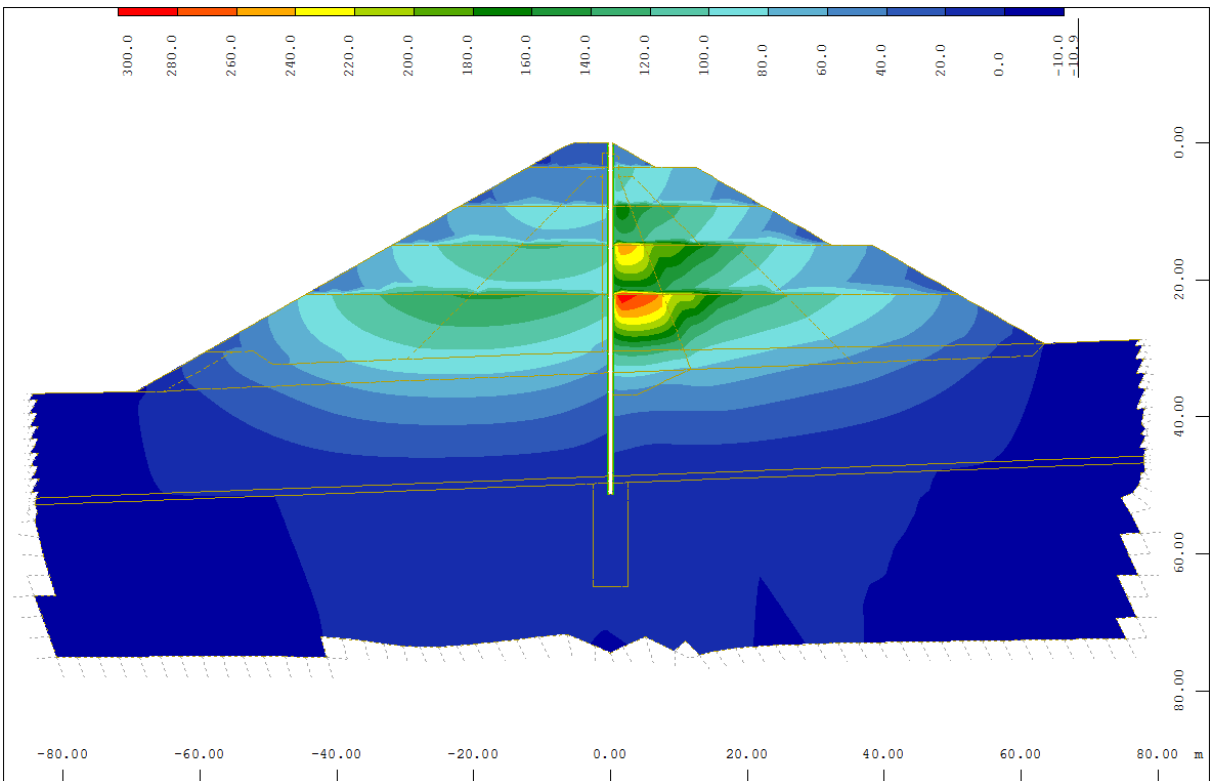


Figure 144: LC-H, vertical nodal displacement u_y [mm] for 1/3 of ϕ for wall-soil interaction

10.05.02.02 Seal Wall and Pile Wall

Horizontal displacements for wall-soil interaction of $2/3 \times \phi$ and $1/3 \times \phi$ are shown in Table 66, Table 67 and Table 68.

Table 66: horizontal nodal displacement u_x [mm], groundwater, LC-A

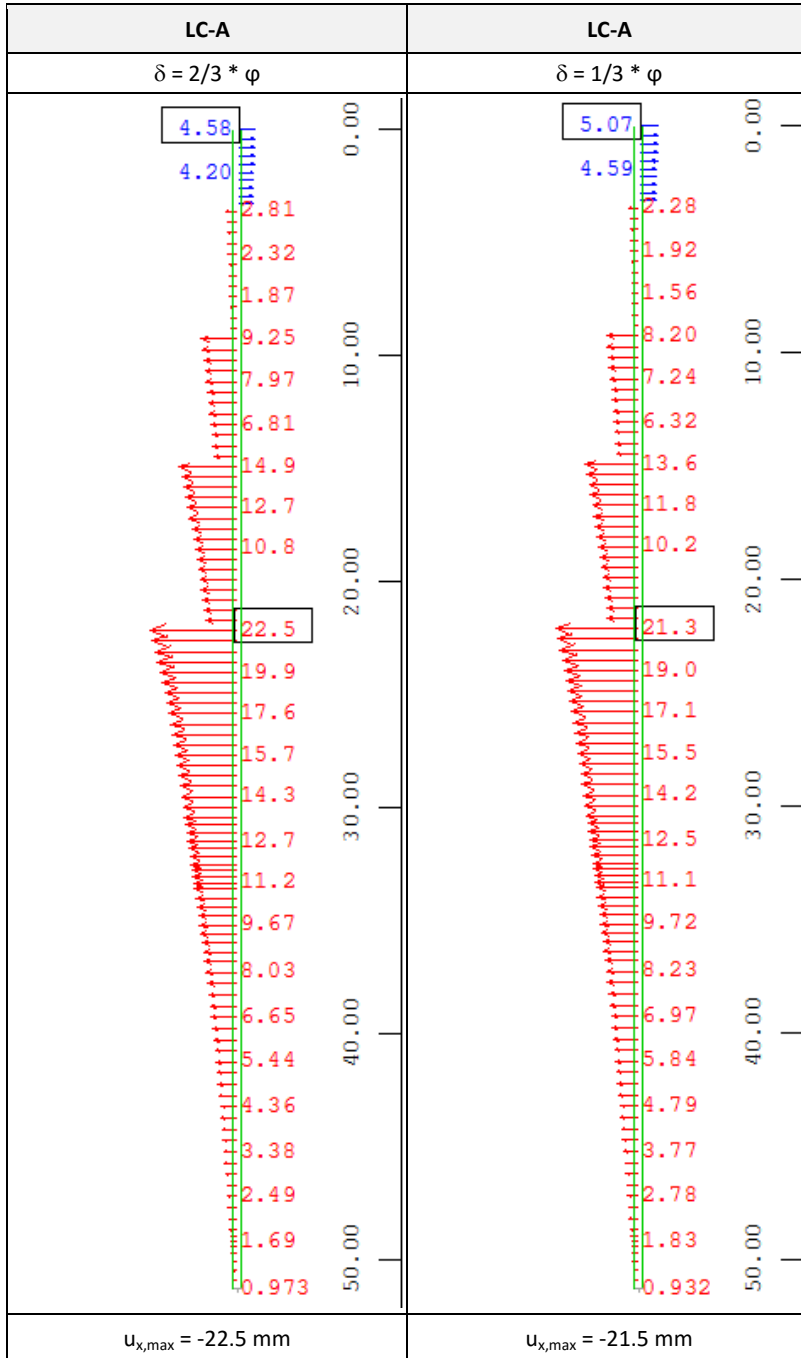


Table 67: horizontal nodal displacement u_x [mm], full impoundment, LC-E

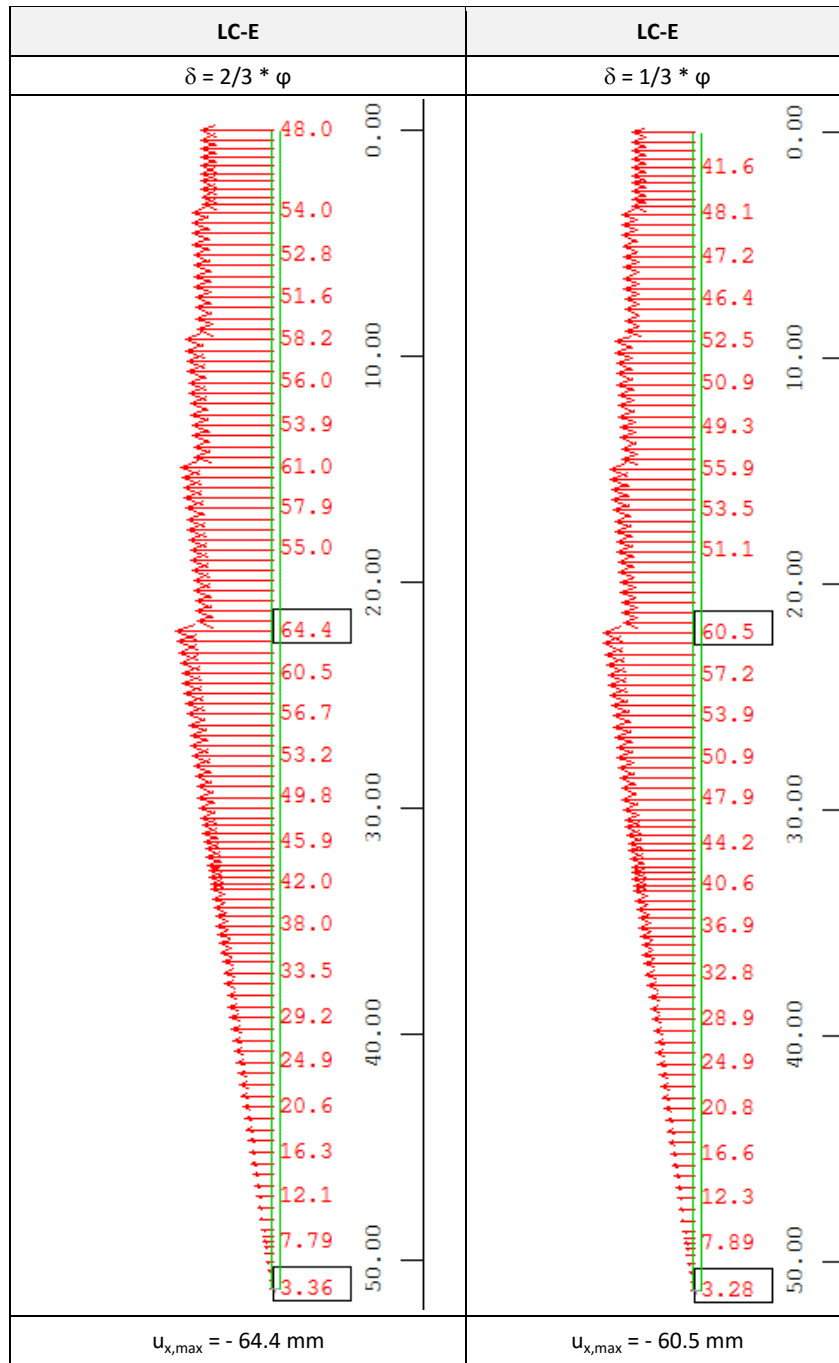
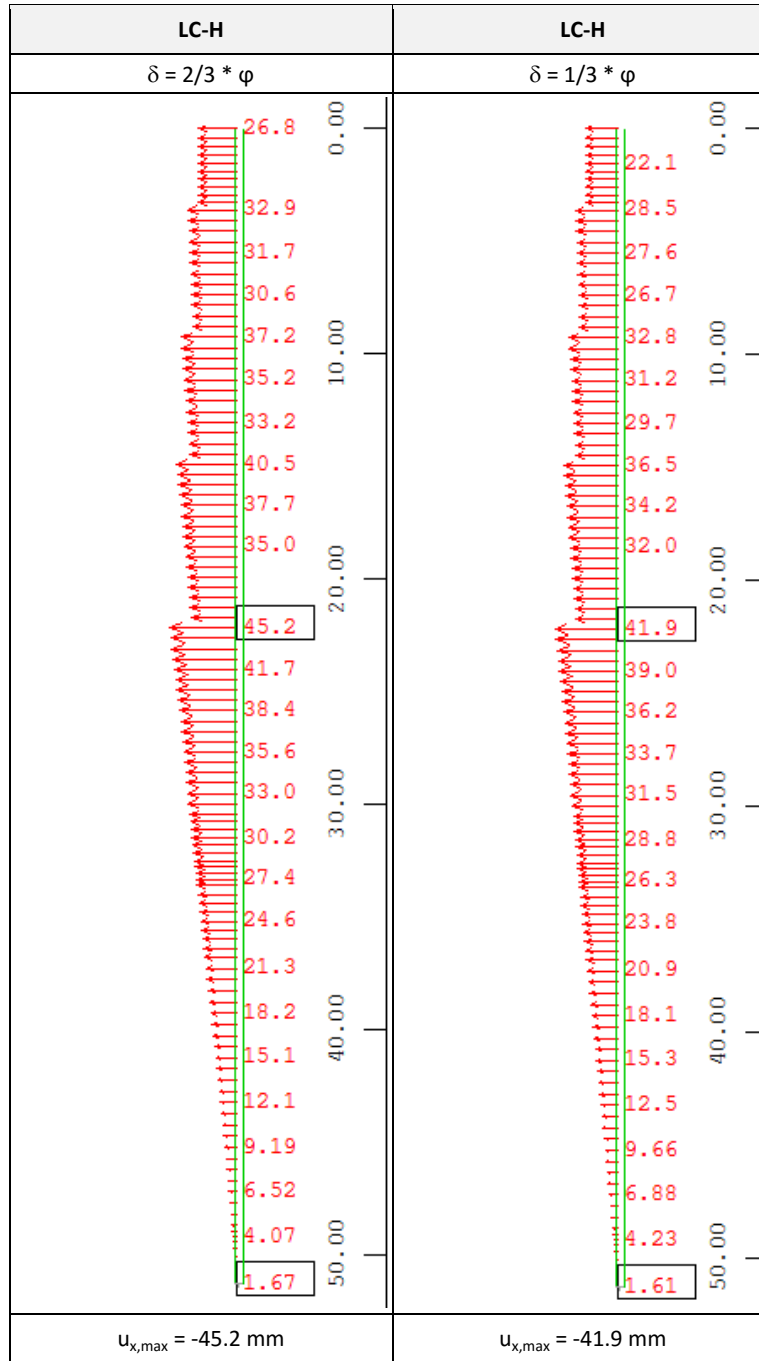


Table 68: horizontal nodal displacement u_x [mm], drawdown following full impoundment, LC-H



10.05.02.03 Foundation of the Bottom Outlet Structure (BOS)

Since the secant pile wall for seepage cut-off is keyed into bedrock, it will experience minimal vertical deformations. The reinforced secondary piles in conjunction with the non-reinforced primary piles are capable of carrying substantial vertical loads and are considerably stiff compared to the alluvium. This also applies to the seal wall, which is structurally connected with the secant pile wall.

On the other hand, without ground improvement, the adjacent segments of the bottom outlet structure would experience significant vertical displacement under the load of the embankment. In addition, the axis of the opening for the bottom outlet structure in the seal wall rotates under loading conditions, for a few millimeters in the case of full impoundment, while the adjacent upstream culvert segment will follow the horizontal displacement of the embankment and tends to rotate less.

To reduce differential displacements to an acceptable limit, ground improvement below the bottom outlet structure is required. Drawing LTMM-CC-DFG-401 shows a layout in plan of jet grouting columns arranged along the bottom outlet structure, 4m in diameter each. Jet grouted columns are placed underneath each joint and at the middle of each BOS segment. Reinforced bored piles are provided adjacent to the seal wall for minimizing differential displacements at the interface between the BOS and the seal wall. Dependent on the Young's modulus of jet-grouted columns, displacements according to Table 69 are resulting, considering bored reinforced pile support of the BOS next to the seal wall. A range of reachable Young's moduli for jet-grouted sand was demonstrated by Axtel & Stark at the DFI Conference in 2008. Covil & Skinner (1994) are reporting an elastic modulus of 6,000 MPa for the Soil Crete technology applied in sand. The highest potential strength and stiffness can be reached in gravel sand aggregates such as the existing alluvium at Cougar Creek, which is forming strength similar to concrete, dependent on the type of cement used.

Table 69: Vertical displacements at the BOS and the seal wall versus quality of ground improvement at full impoundment

Assessment of displacements at the BOS		Young's Modulus of Jet-Grouted Columns		
		1GPa	2 GPa	4 GPa
Maximum vertical displacement calculated	Seal wall	3.88	3.80	3.75
	BOS	11.3	8.18	7.29
Differential Displacement at interface BOS/SW		4.79-3.55 = 1.24mm	4.08-3.51 = 0.57mm	4.12-3.39 = 0.73

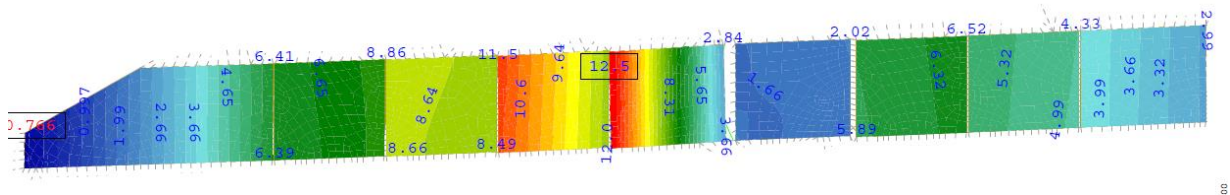


Figure 145: Vertical displacements [mm] of the BOS with jet-grouted columns with an E-Modulus of 1GPa, arranged as in the base design.

Spraying four columns in total, one underneath each of the first two upstream BOS segments and one at the first two downstream BOS segments, results in maximum differential displacements between BOS segments of approximately 4mm, which is within acceptable limits. Four additional piles support the joint between the seal wall and adjacent BOS segments.

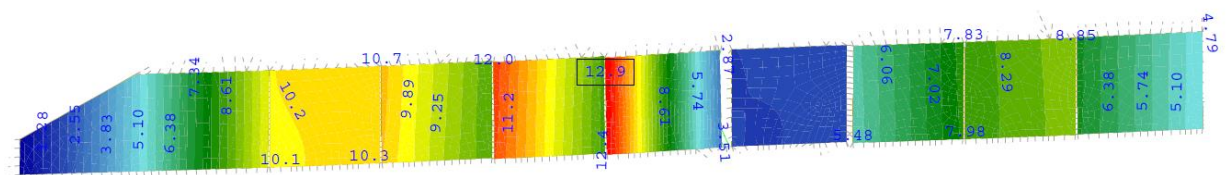


Figure 146: Vertical displacements [mm] of the BOS with jet-grouted columns with E=1GPa, sparing 4 columns at the intake and outlet.

10.05.03 Acting Forces and Moments on the Cut-Off Wall

Acting forces and moments on the secant pile wall and cut-off wall element for wall-soil interaction of $2/3 \times \phi$ and $1/3 \times \phi$ are shown in Table 70 to Table 78.

Table 70: Normal forces at the seal wall and pile wall, N_x [kN], groundwater, LC-A

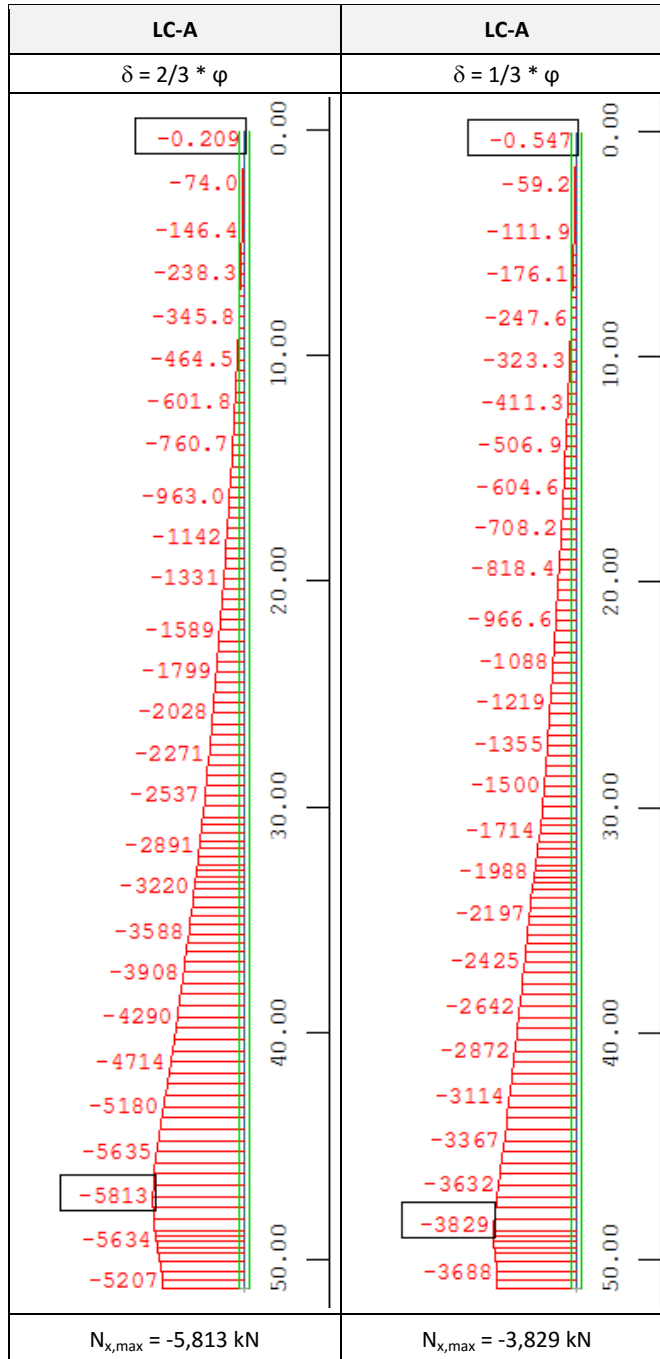


Table 71: Normal forces at the seal wall and pile wall, N_x [kN], full impoundment, LC-E

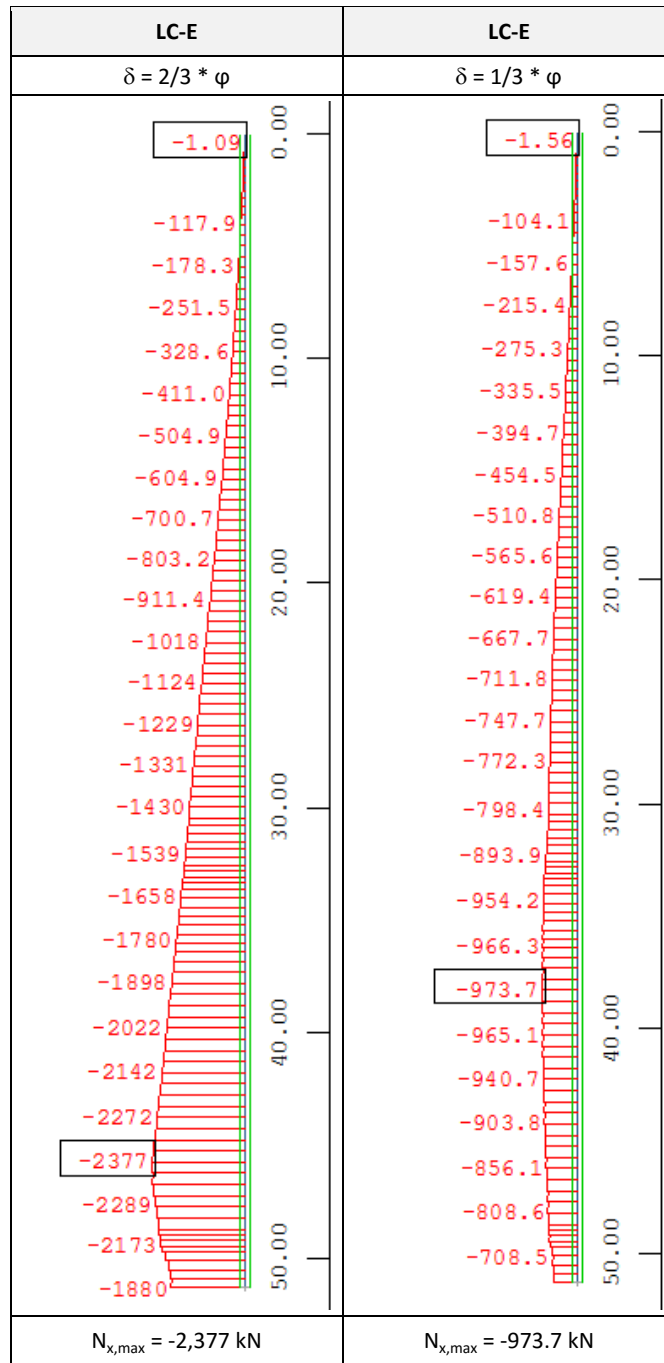


Table 72: Normal forces at the seal wall and pile wall, N_x [kN],], drawdown following full impoundment, LC-H

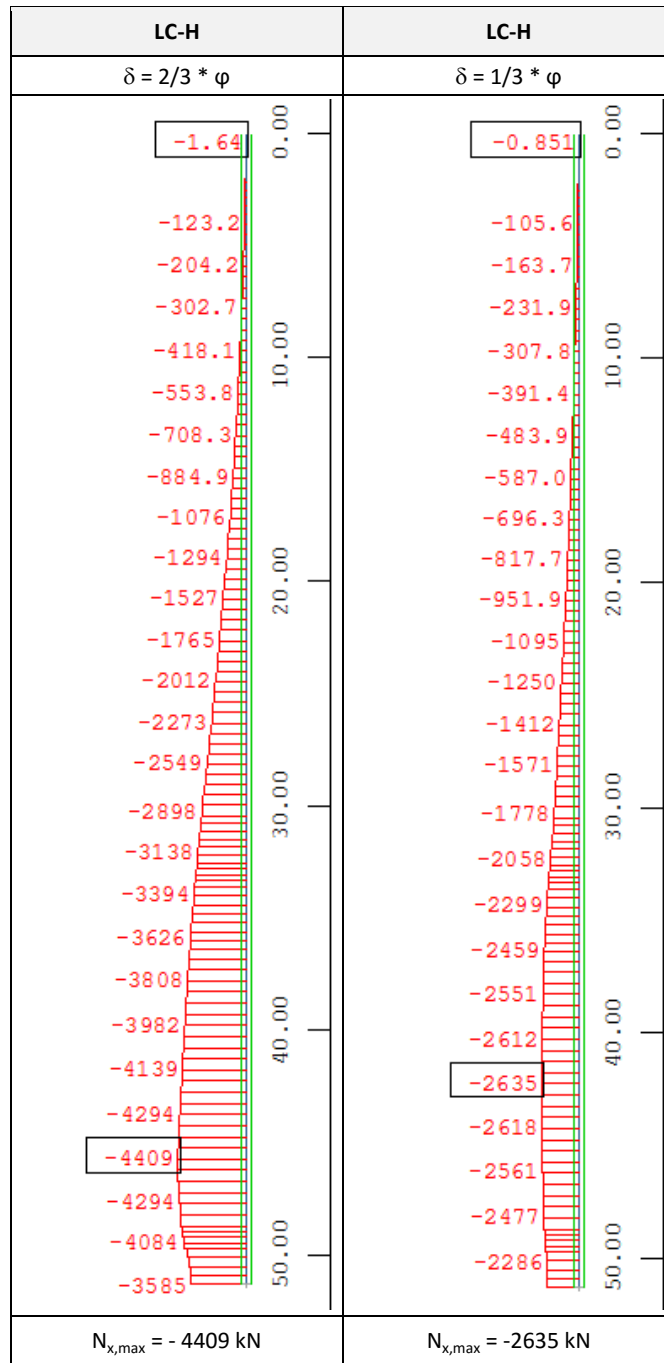


Table 73: Shear forces at the seal wall and pile wall, Vz [kN], groundwater, LC-A

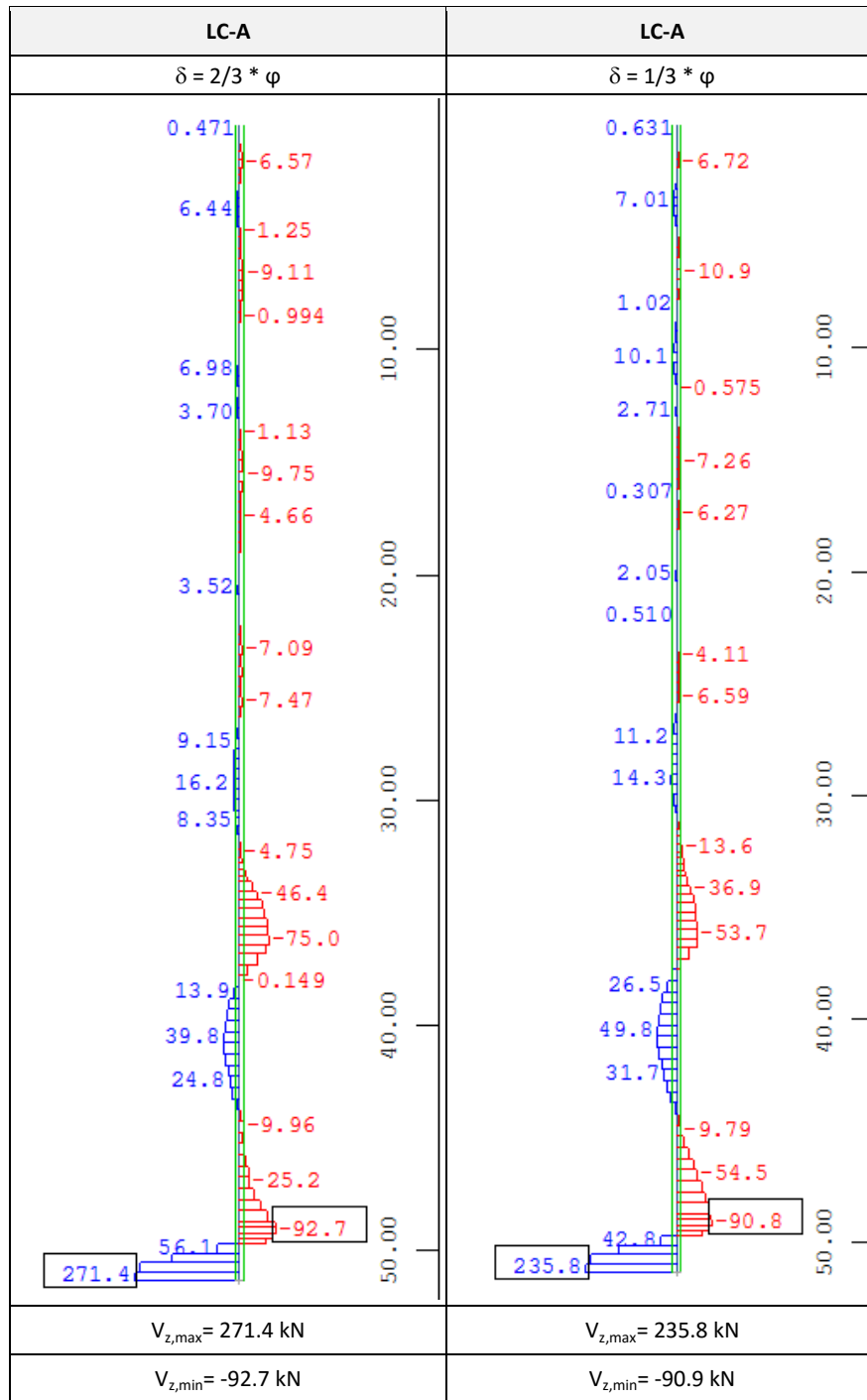


Table 74: Shear forces at the seal wall and pile wall, Vz [kN], full impoundment, LC-E

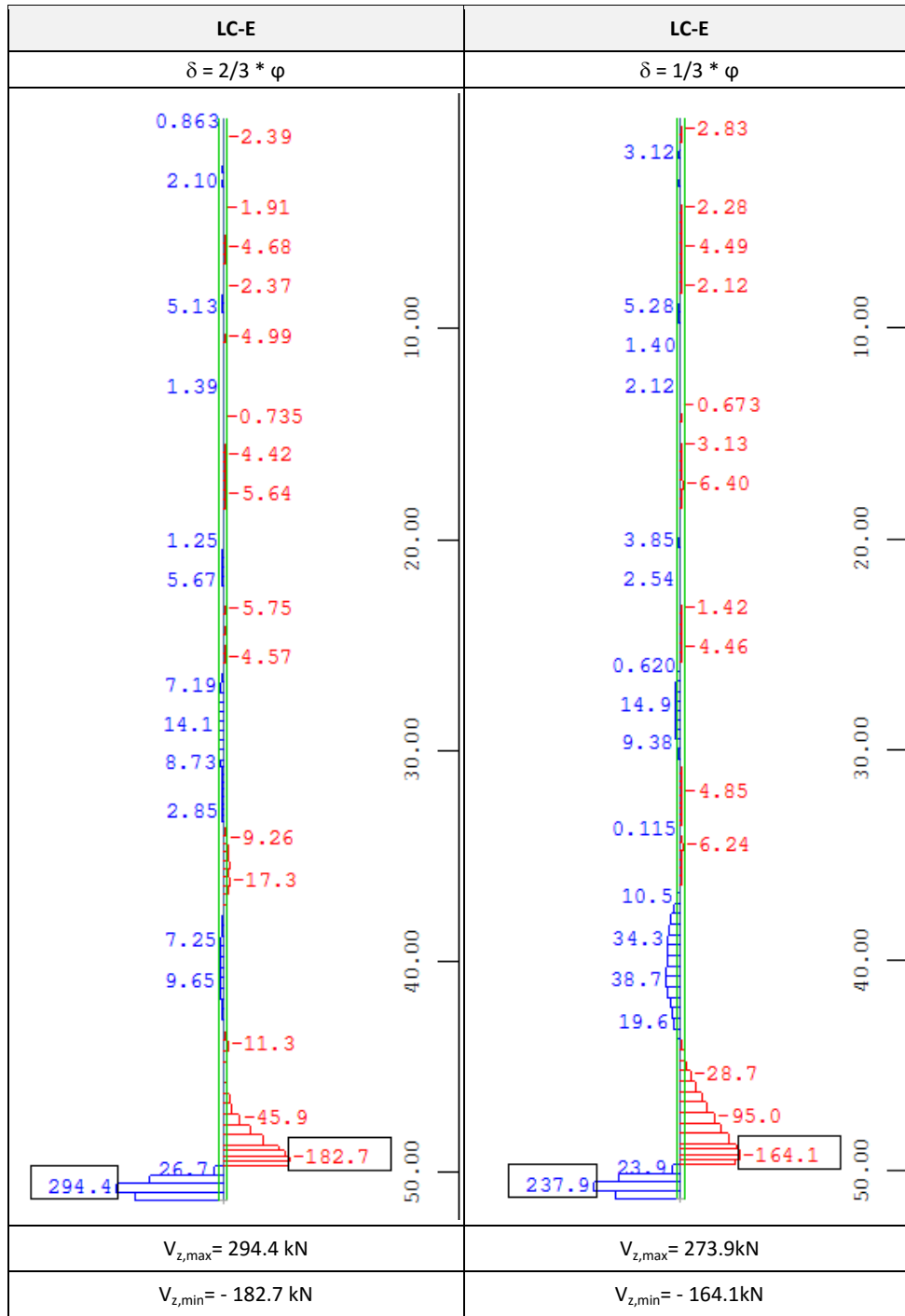


Table 75: Shear forces at the seal wall and the pile wall, V_z [kN], drawdown following full impoundment, LC-H

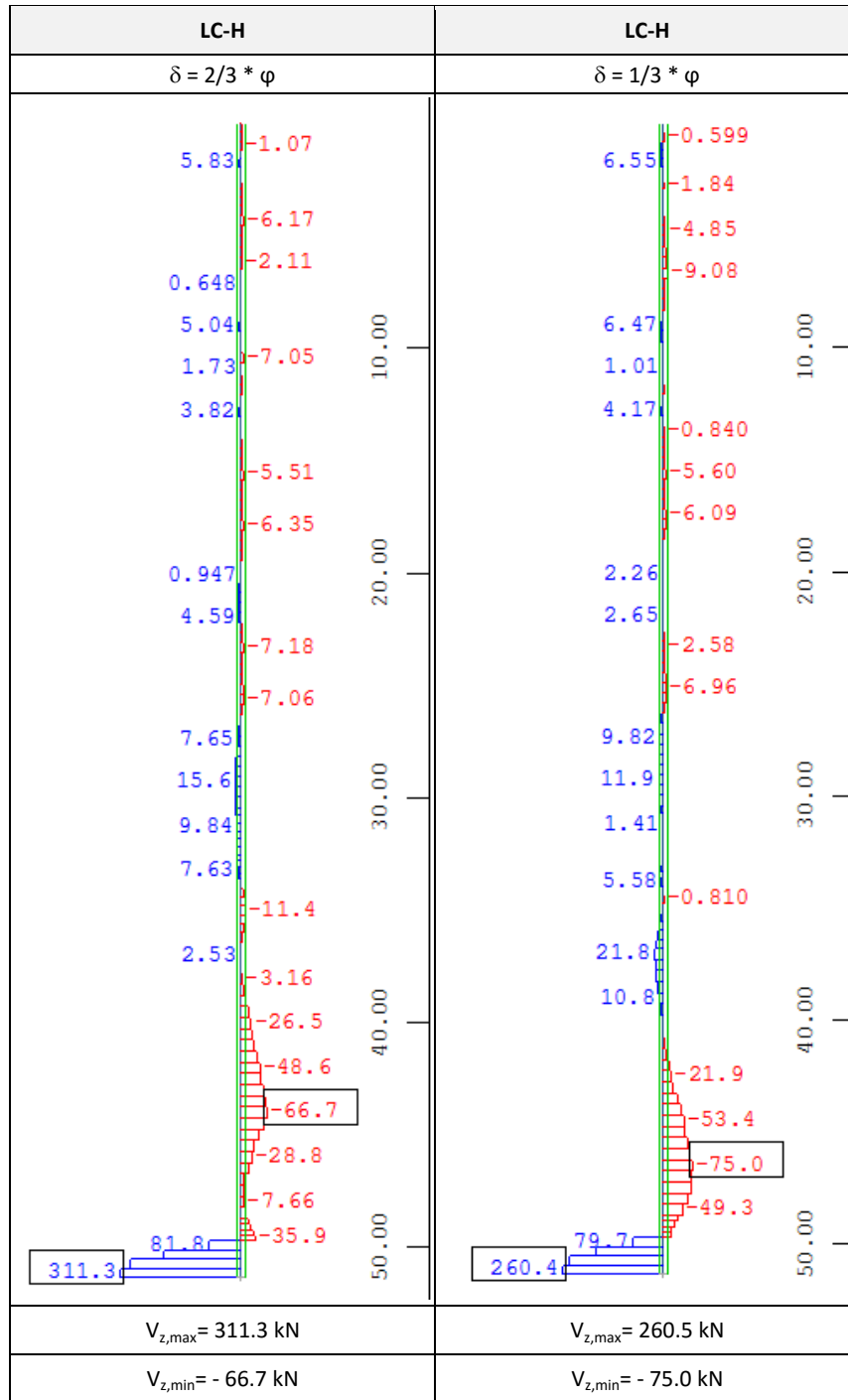


Table 76: Bending moments at the seal wall and pile wall, My [kNm], groundwater, LC-A

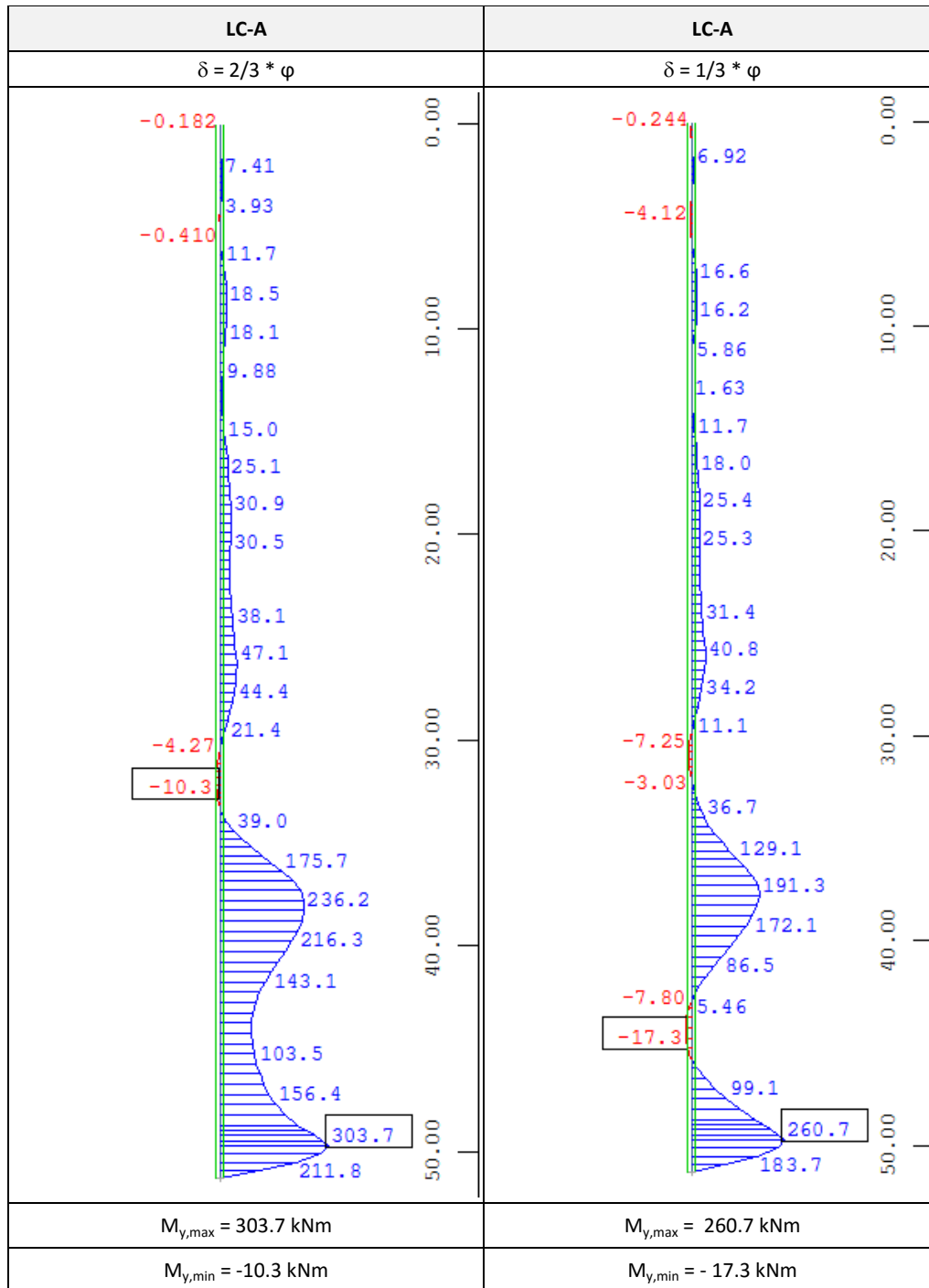


Table 77: Bending moments at the seal wall and pile wall, M_y [kNm], full impoundment, LC-E

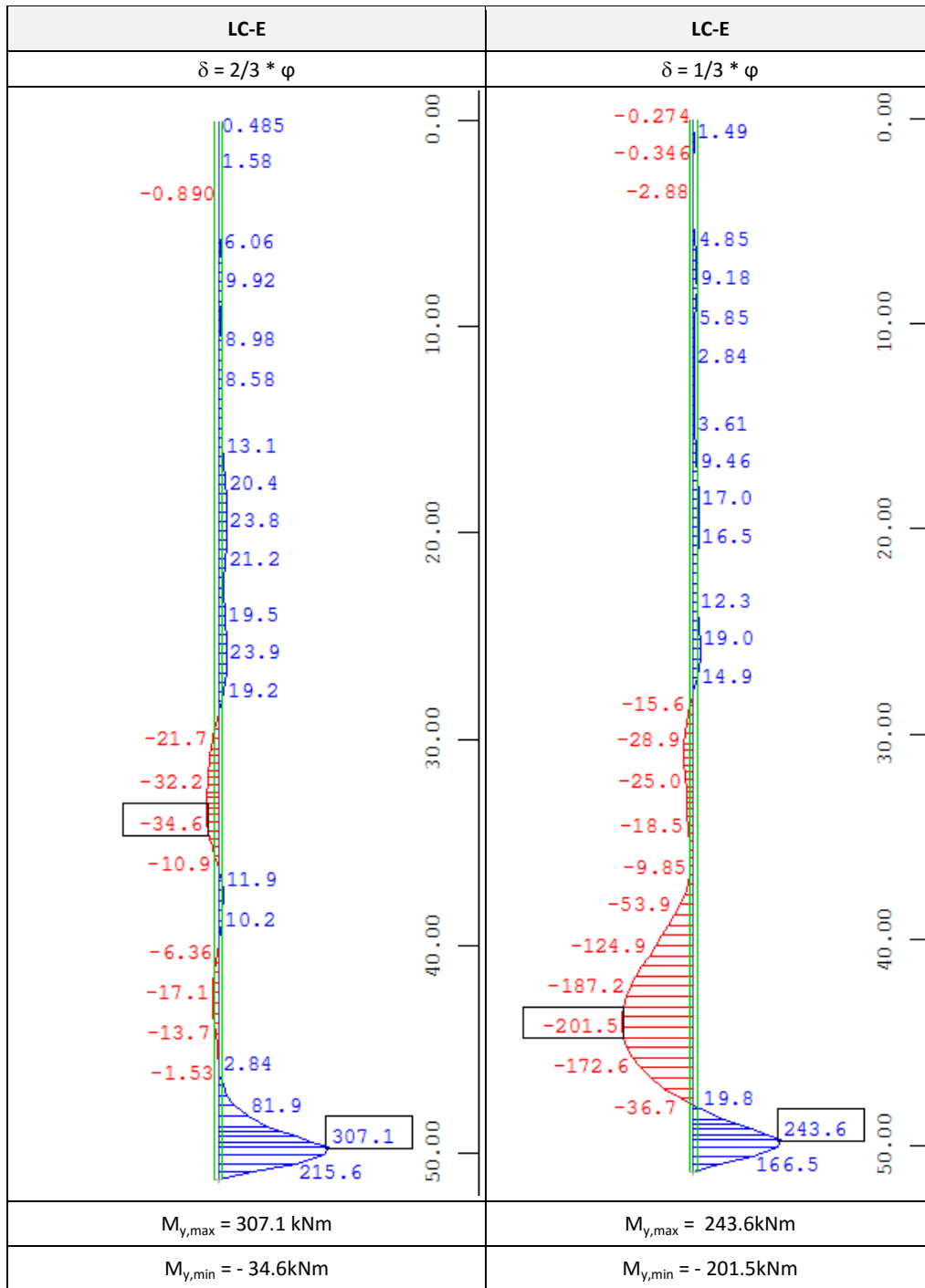
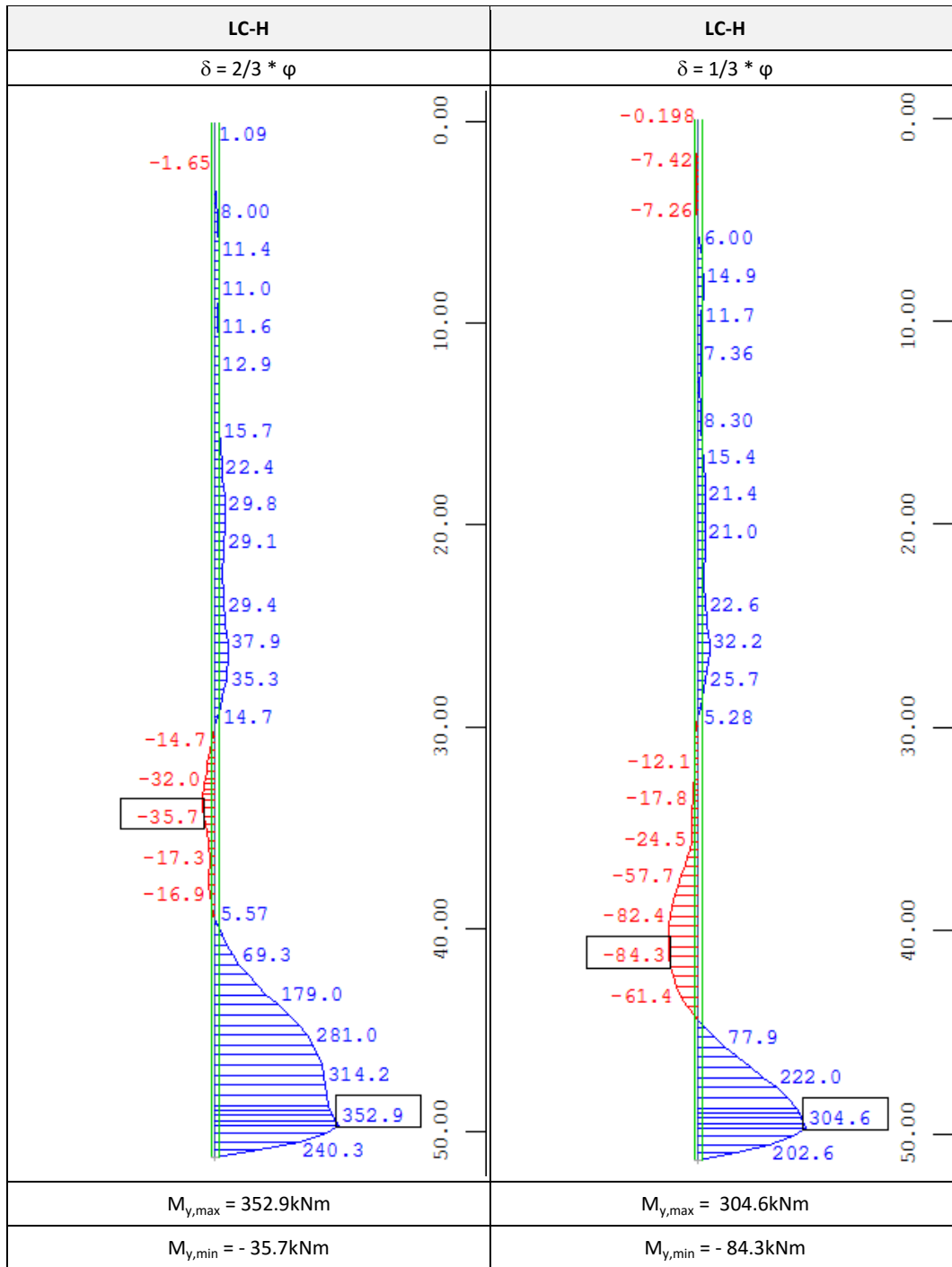


Table 78: Bending moments at the seal wall and the pile wall, M_y [kNm], drawdown following full impoundment, LC-H



11 STRUCTURAL DESIGN

The flood retention structure will comprise the following reinforced concrete elements for flow control and for seepage cut-off:

- Bottom outlet structure
- Concrete secant pile wall (caisson wall)
- Concrete seal wall
- Lining of downstream embankment slope and spillway training walls
- Intake box carrying the debris rake
- Stilling basin including piers and baffles

The following sections discuss structural design aspects.

11.01 Bottom Outlet Structure

The bottom outlet will be constructed with cast in-place concrete with 5.50 m × 6.85 m outside dimensions. The net discharge section has 3.3 m clear width and 4.65 m maximum height. The invert is shaped as a half circle for water flow requirements and will be armored by a steel plate for abrasion protection. Figure 147 shows the cross section of the outlet structure cross section used in structural analysis, which is slightly simplified compared to the design drawings.

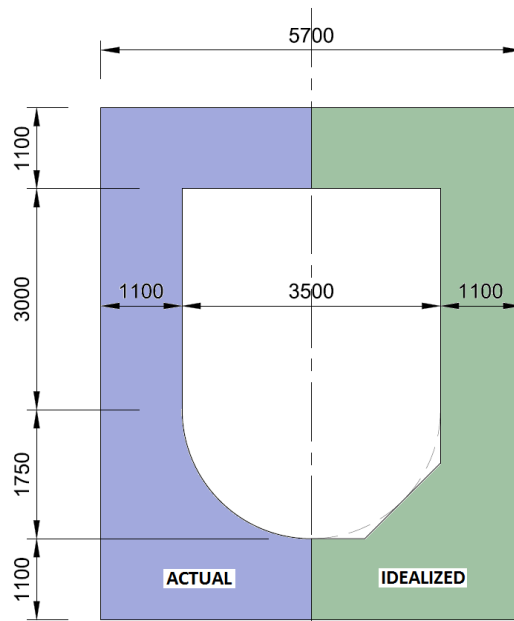


Figure 147: Simplification of the cross section of the bottom outlet structure for structural analyses

In longitudinal direction, the outlet runs for approximately 100m from the throttle through the upstream embankment, feeding through the concrete seal wall and through the downstream embankment to the outflow. The structural design of the outlet structure involves the analysis of both, the cross sectional direction and the longitudinal direction.

11.01.01 External loading for Load Case G – Spillway Flood

The bottom outlet cross section has to carry external earth and water pressure and its self-weight. The hydraulic design does not envisage a case of internal water pressure since the water flow inside the bottom outlet will be under open channel conditions (water level not reaching the deck slab).

Due to the sloping geometry of the rock abutments on either side of the creek, the embankment, which is filled and compacted in layers, will cause elevated lateral earth pressure on the bottom outlet wall. Subsequent settlement under the weight of subsequently built layers and initial consolidation need to be considered as well. To study these effects, a 2D plane strain model using Phase2 is used to calculate earth pressure on the side walls in dry conditions.

Figure 148 shows the finite element model of half the system utilizing symmetry. Since the bottom outlet will be divided into segments of 10–12m length in longitudinal direction, only plane stress analysis was performed.

The model assumes an average idealized rock slope and the bottom outlet is represented by a rigid solid block to reduce displacements, which is a conservative assumption. A “joint”, or interface element with small shear resistance, is arranged along the slope face of the rock abutment to allow for relative sliding of the embankment fill along the slope. This represents conditions during filling and subsequent compacting.

Figure 149 and Figure 150 show the stress trajectories plotted on the contour lines of the horizontal and vertical normal stress components (S_{xx} & S_{yy}). The stress contours are drawn on the deformed shape. From the drop in the embankment surface at the dam crest elevation, it is evident that relative slippage has taken place along the sloping face of the rock abutment.

From comparison of both stress components (S_{xx} & S_{yy}) acting on the face of the side walls of the bottom outlet, the contour lines indicated elevated lateral earth pressure above the at-rest value (K_o) obtained from the Jaky formula. The actual lateral pressure is variable from point to point, but the average ratio S_{xx}/S_{yy} is close to 0.95. For the structural design of the bottom outlet, the lateral earth pressure coefficient has therefore been assumed to be 1.0.

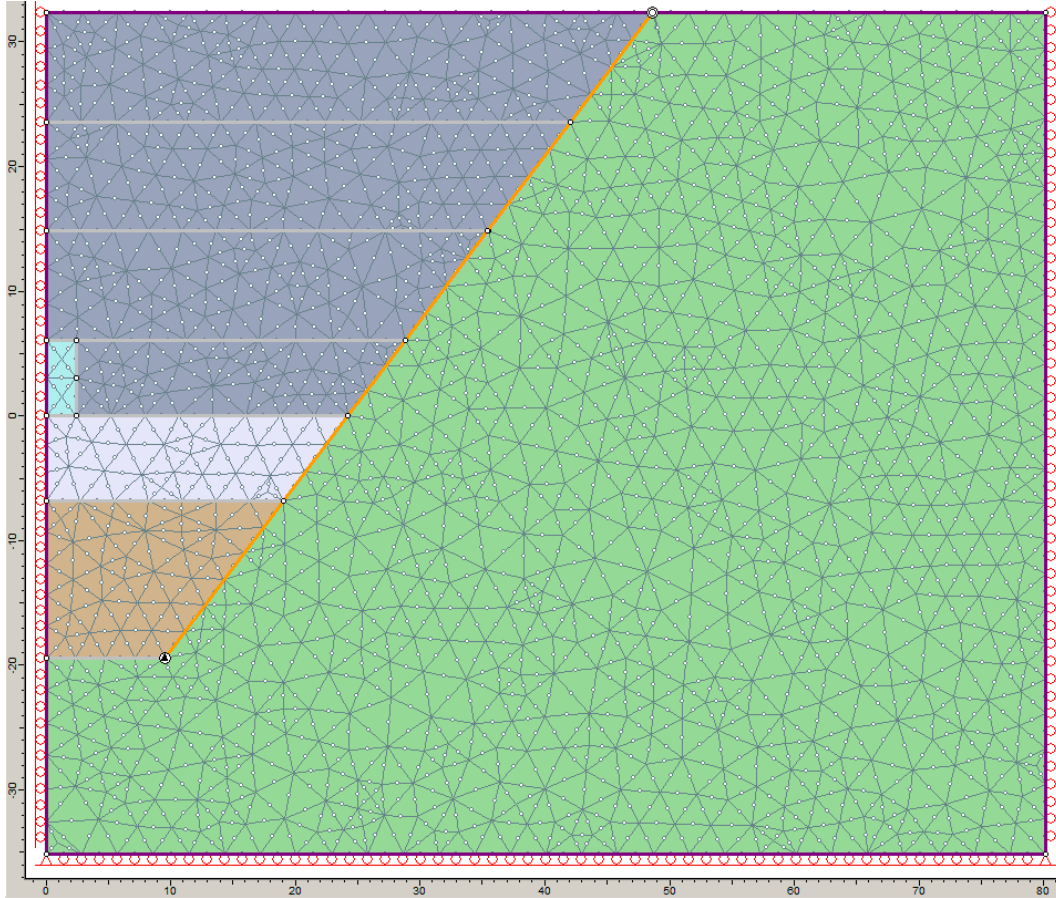


Figure 148: Phase2 model to calculate lateral earth pressure on walls

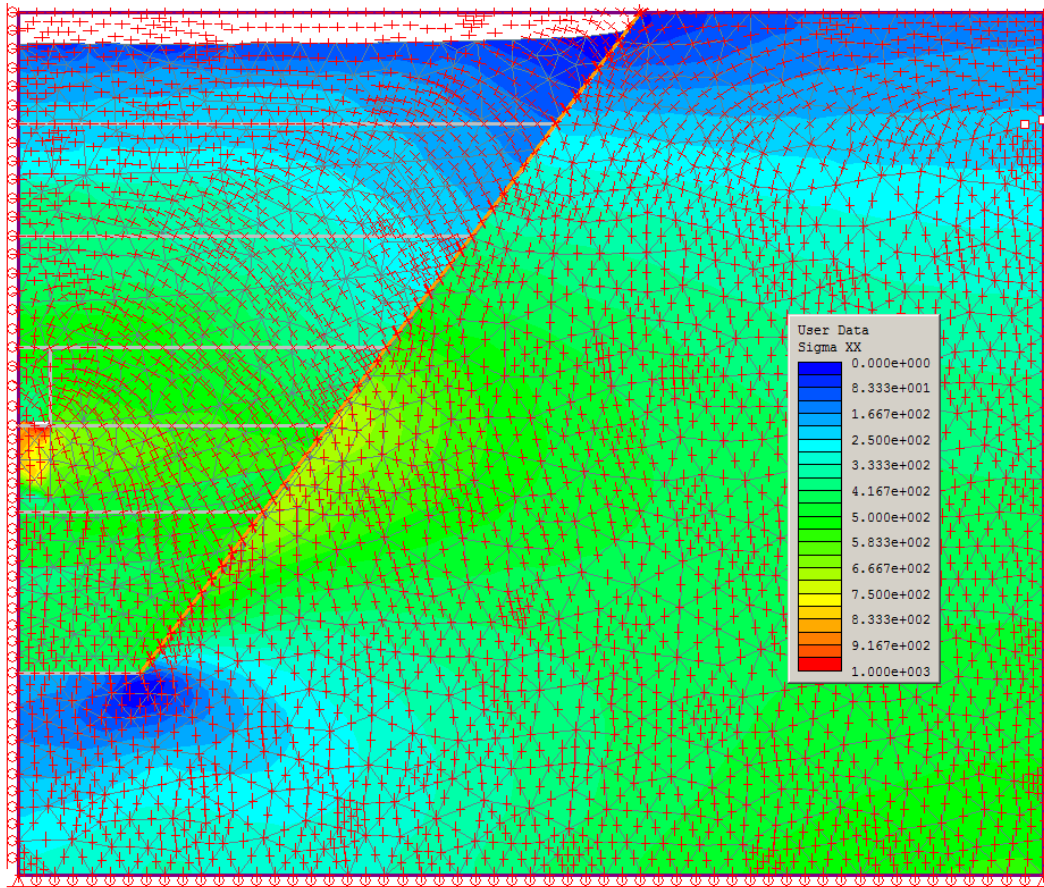


Figure 149: Horizontal stress S_{xx} [kPa] and stress trajectories showing arching in the embankment around the bottom outlet

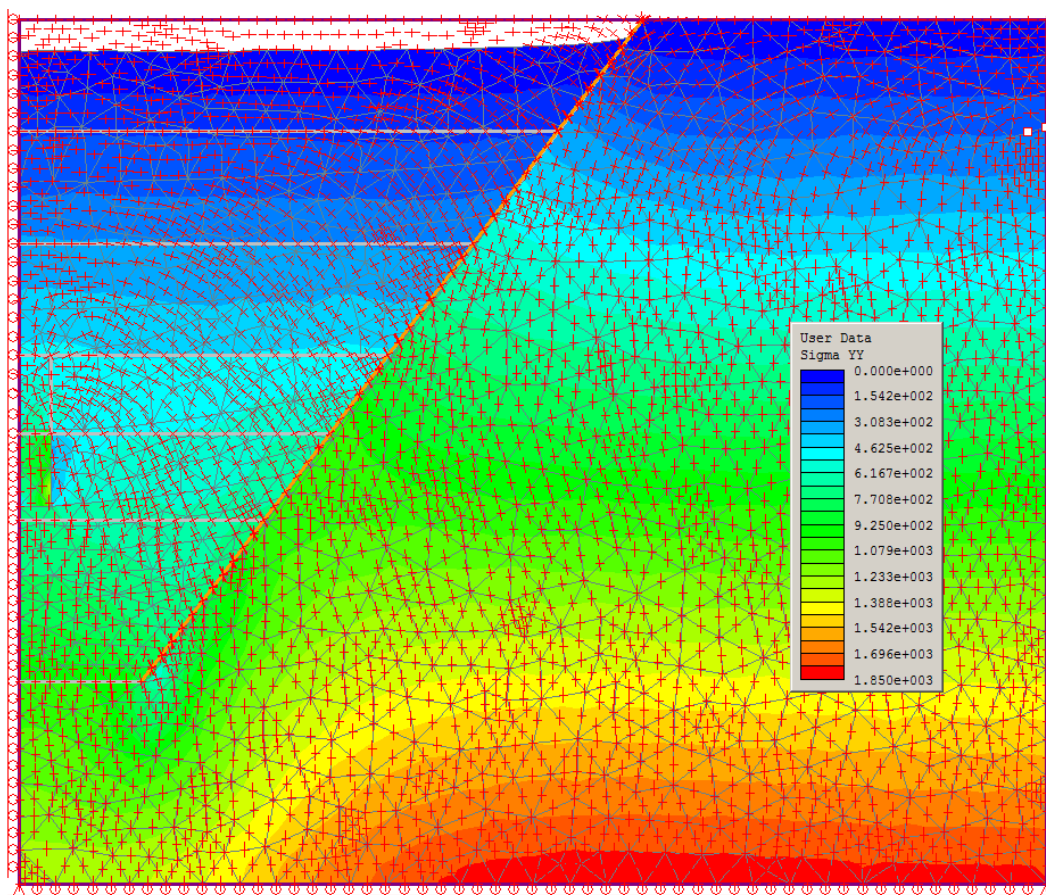


Figure 150: Vertical stress S_{yy} [kPa] and stress trajectories showing arching in the embankment around the bottom outlet

11.01.02 Internal Forces from structural 2D Analysis

The walls and slabs of the bottom outlet structure are considerably thick compared to the clear spans, in which case the stress distribution would not be identical to that in the beam theory. Particularly the corners and the lower chamfer are zones with 2D stress state.

In order to calculate internal forces and moments realistically, a 2D finite element model by Abaqus was used to calculate the internal forces in the bottom outlet cross section under external earth and water pressure. This model has the advantage that the actual wall thickness and the shape of the haunch in the lower corner are properly represented. The results obtained from this model is subsequently used to calibrate an equivalent frame model, which is more convenient for section design.

This section shows complete structural calculation for the bottom outlet segment under maximum external pressure, i.e. under the dam crest with maximum overburden depth. Internal water pressure is conservatively neglected.

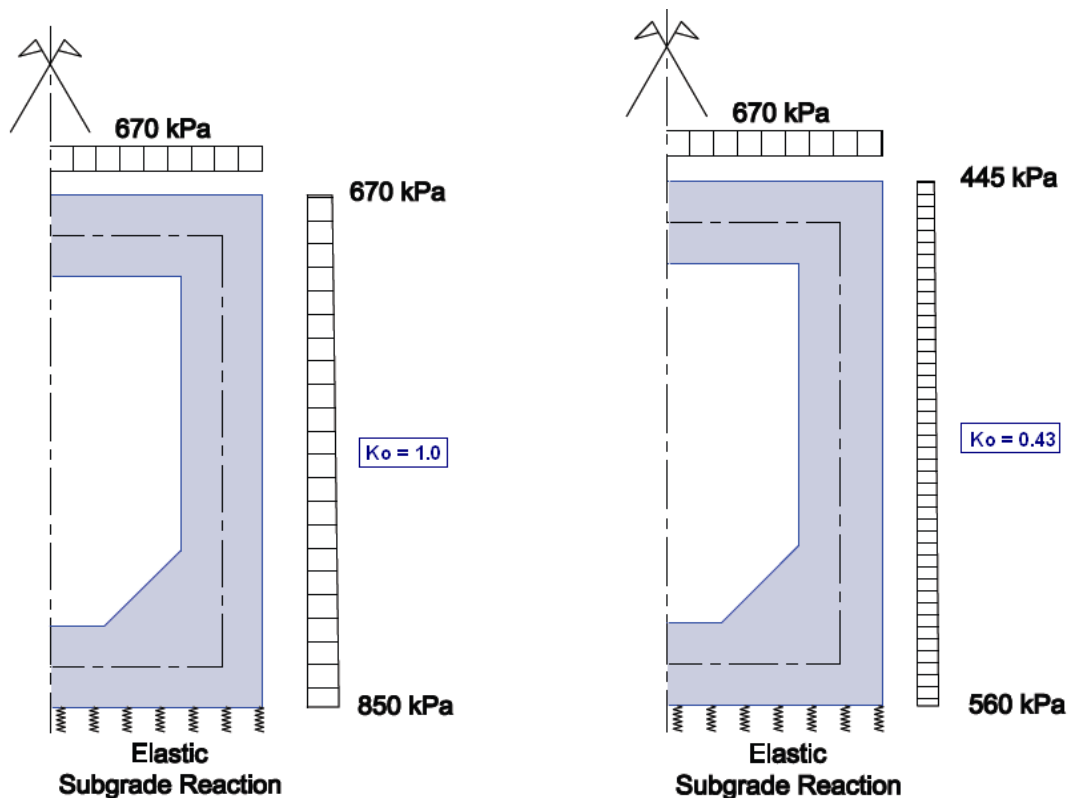


Figure 151: External pressures on the bottom outlet structure

Load Calculation

- Top of deck slab at elevation 1425.0 MASL
- Dam crest at elevation 1451.0 MASL
- Depth of fill above deck slab = 1451 MASL – 1425 MASL = 26m
- Depth of overtopping water above crest = 2m
- Unit weight of saturated fill = 25 kN/m³
- Unit weight of reinforced concrete = 25 kN/m³
- Gravity load on deck slab = 10 (26+2) + 15 (26) = 670 kPa

Two limiting values for K_o are used to find the most onerous internal forces:

- $K_o = 1.0$ is the expected value from FEA above. This will give the maximum bending moment in the side walls, but minimum moment in the slabs.
- $K_o = 0.43$ is the min possible value according to elastic analysis. This will give maximum bending moment on the slabs, but minimum moment on the side walls.

Figure 151 shows the external loads acting on the bottom outlet in both cases of K_o , in addition to the self weight of the structural elements (not shown). All loads are *at service level* as explained in the design criteria.

The 2D model by Abaqus and the Finite Element analysis results for the case of $K_o = 1.0$ are shown in Figure 152, Figure 153 and Figure 154.

The deformed shape under the applied external pressure is shown in Figure 153. It is clear that the side walls

deform with a greater magnitude than the deflection of the deck and base slabs.

The corresponding stress distribution for the normal stress components S11, S22 and the shear stress S12 are shown in Figure 152 and Figure 153. Of note is the stress concentration around the inner upper corner as shown in Figure 154, for which the normal stress distribution is non-linear. Otherwise, the mid-span sections in the side wall and base slab show a linear distribution of normal stresses. The top slab is under a nearly constant compression. The stress distribution on the critical sections as defined in Figure 155 is shown in Figure 156 and Figure 157. The results use the following coordinate system for displacements and stresses. Compressive stresses are negative.

- x1 (x): Horizontal →
- x2 (y): Vertical upwards ↑
- u1: Horizontal displacement in x1 direction
- u2: Vertical displacement in x2 direction
- S11: Horizontal normal stress
- S22: Vertical normal stress
- S12: In-plane shear stress

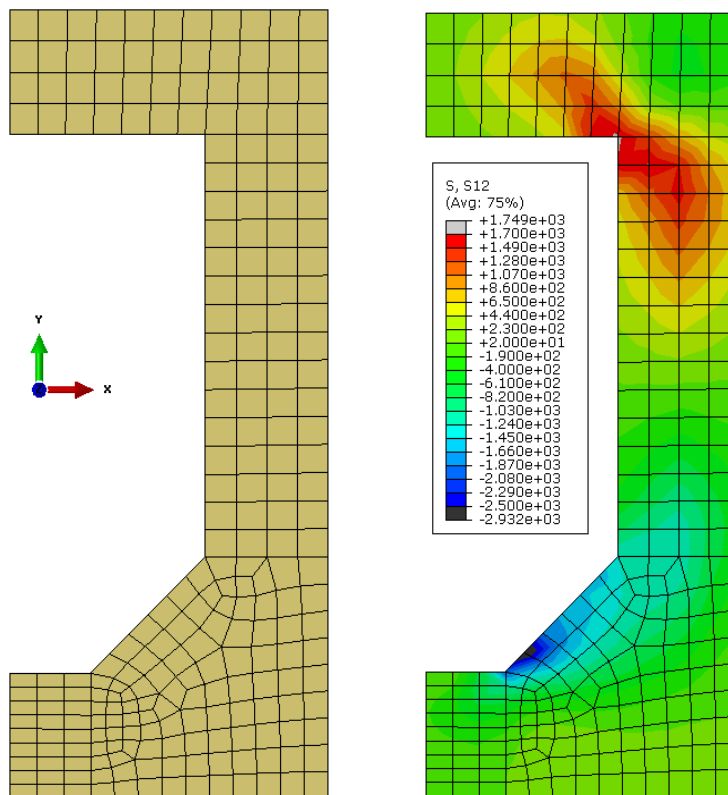


Figure 152: Abaqus model and in-plane shear stresses for $K_o = 1.0$

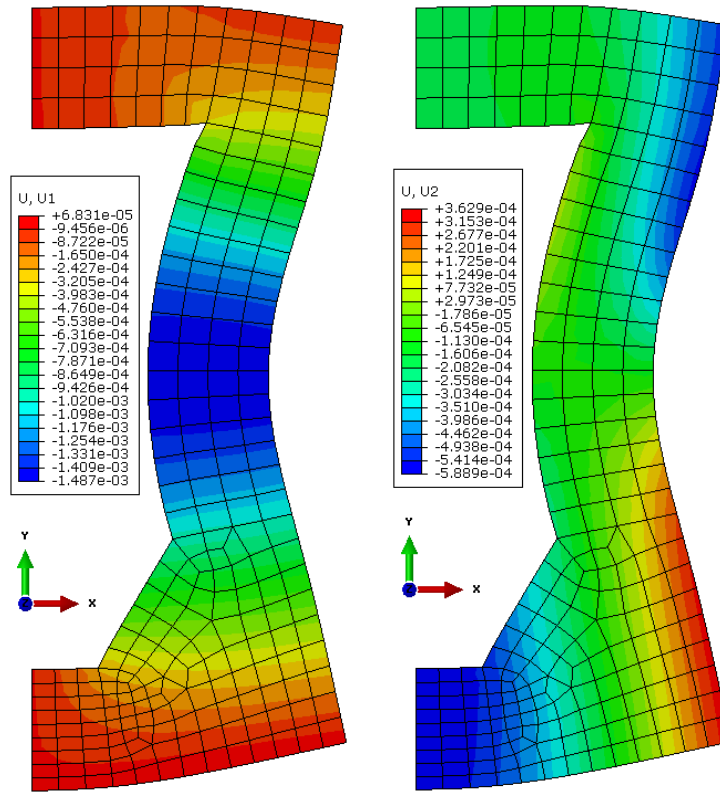


Figure 153: Deformed shape and distribution of displacements u_1 & u_2 for $K_o = 1.0$ [m]

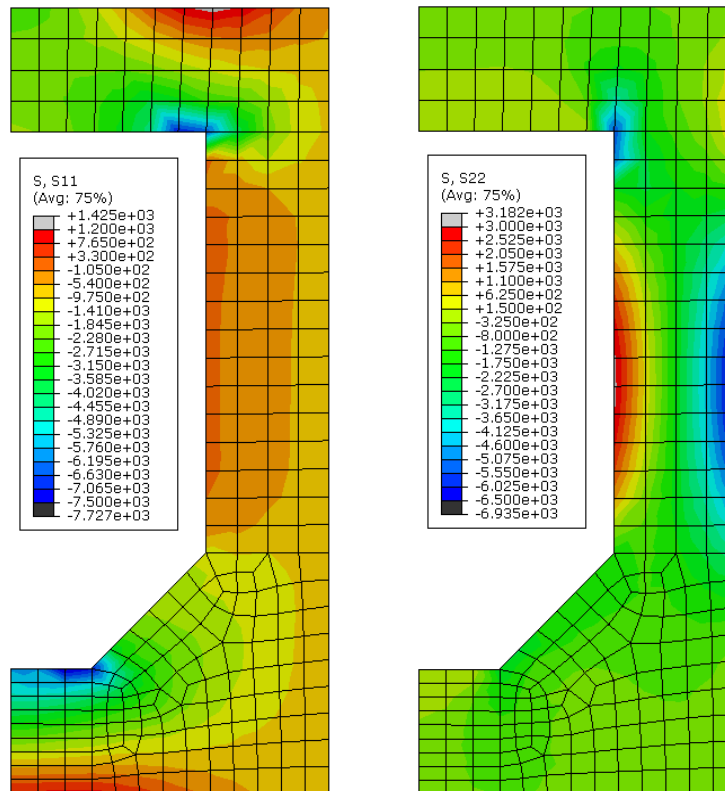


Figure 154: Normal stresses S11 & S22 for $K_o = 1.0$ [kPa]

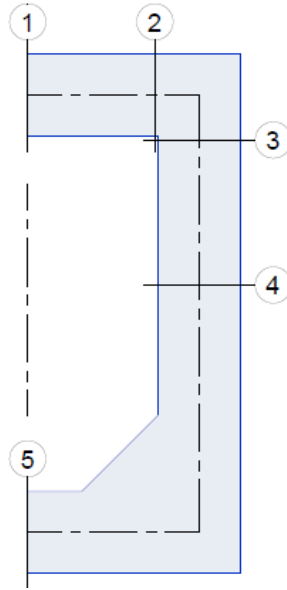


Figure 155: Critical sections for reinforced concrete design of the BOS

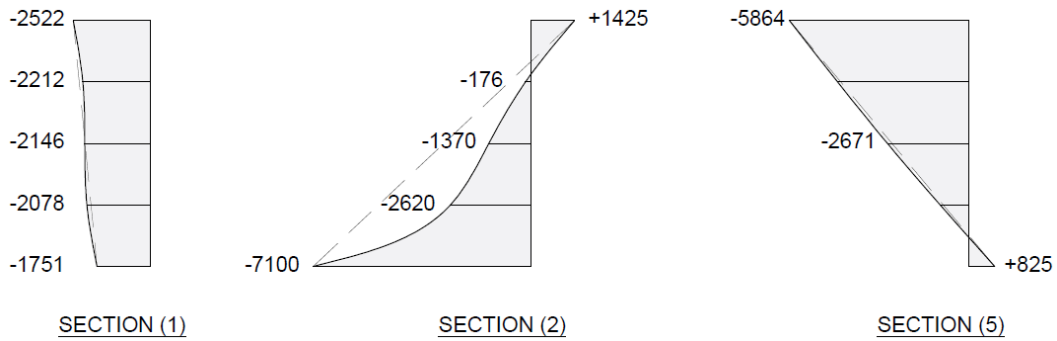


Figure 156: Stress distribution from the 2D model on the BOS base slab and deck slab sections

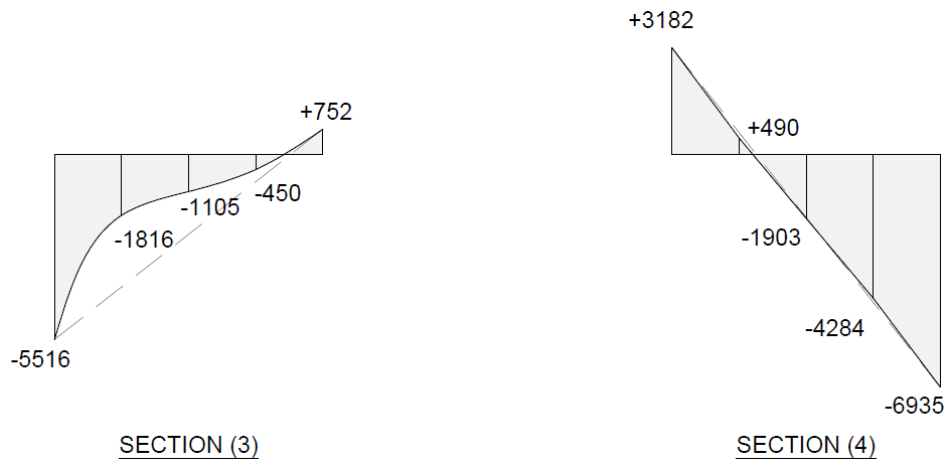


Figure 157: Stress distribution from the 2D model on the BOS sidewall sections

The integration of the normal stresses on the sections with nearly linear stress distribution (1, 4, 5) gives the following normal forces and bending moments

Section (1) $N = -2,367 \text{ kN/m}$ and $M = 81 \text{ kN.m/m}$

Section (4) $N = -2,064 \text{ kN/m}$ and $M = 1,020 \text{ kN.m/m}$

Section (5) $N = -2,771 \text{ kN/m}$ and $M = 675 \text{ kN.m/m}$

11.01.03 Internal Forces by 1D Model

An equivalent frame model was used to calculate the internal forces and moments under the same loading shown in Figure 151 for the case of $K_o = 1.0$. The results of this model are directly accessible for verifying the strength and crack width on the different sections. This analysis accounts for the deformations due to shear strain, which play a significant role in structures with small span-to-depth ratio, unlike the case of slender beams.

Section properties of elements with constant thickness have been considered according to the actual geometry, while those in the chamfer or corner zones have been modified to obtain results close to those of the 2D model. The results of the frame model are shown in Figure 158.

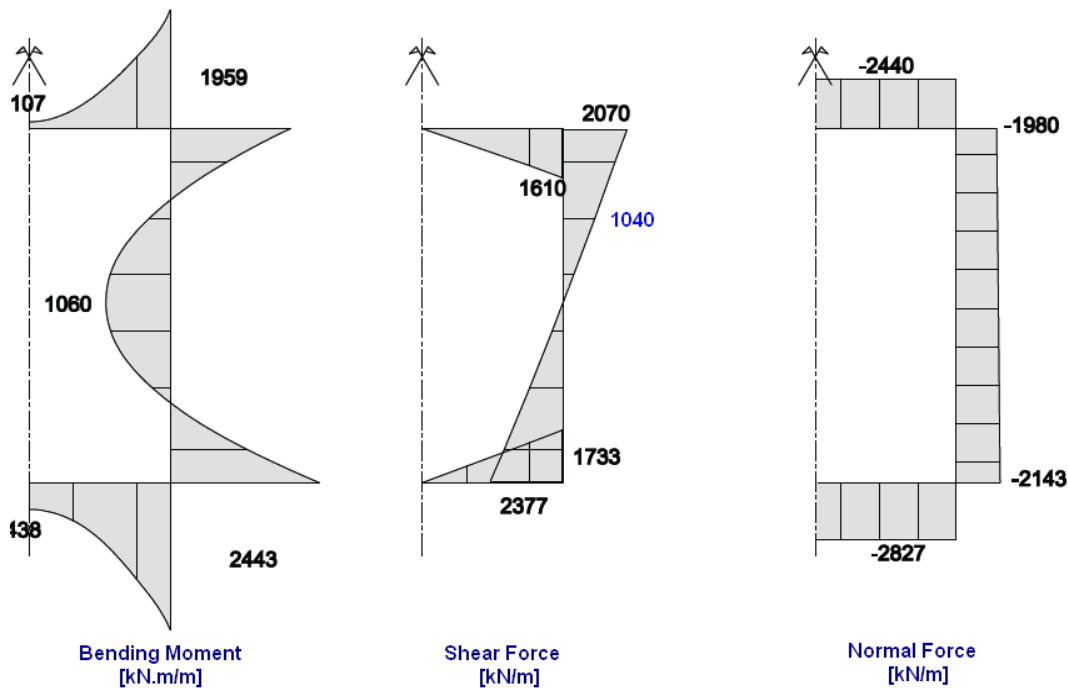


Figure 158: Internal forces and moments from the frame model

11.01.04 Acting Forces and Moments

Table 79 shows the internal forces from the 2D and 1D model. Good agreement can be seen between the results of both models, which do not differ by more than 5%. However, section (1) shows a difference in sign of the bending moment, which is small in all cases. This difference has no effect on the structural design of sections.

Table 79: Acting forces and moments on the bottom outlet structure

	2D Plane Stress Model		1D Frame Model	
	N [kN/m]	M [kn.m/m]	N [kN/m]	M [kn.m/m]
Section (1)	-2,367	+81	-2,440	-107
Section (2)			-2,440	-1,179
Section (3)			-1,995	-925
Section (4)	-2,064	+1,020	-2,050	+1,060
Section (5)	-2,771	-675	-2,827	-438

11.01.05 Structural Design of Critical Sections

Flexure

Sections with significant bending moment (2, 3 & 4) have been analysed for steel stresses and crack widths. The calculation reports are shown in Appendix K. Steel stress at Serviceability Limit State (SLS) is generally below 120 MPa and crack width is below 0.2mm.

All sections have been checked for the Ultimate Limit State (ULS) using the interaction diagrams shown in Appendix K. Wall sections have a reasonable margin of safety.

Shear

The critical section for shear is in the upper part of the side wall at distance d_v below the underside of the deck slab (face of support). This section is checked according to CAN/CSA A23.3-14-11.3.

The internal forces acting on this section at SLS and ULS are:

Normal force $N = -2,020 \text{ kN/m}, \quad N_f = -3030 \text{ kN/m}$

Shear force $V = 1,030 \text{ kN/m}, \quad V_f = 1,545 \text{ kN/m}$

Bending moment $M = 340 \text{ kN.m/m}, \quad M_f = 510 \text{ kN.m/m}$

The section is 1.0m x 1.1m and reinforced with 25M@200 each face.

$H = 1.1\text{m}, d = 1.1 - 0.07 = 1.03\text{m}$

$d_v = \max(0.9 d, 0.72 h) = \max(0.93, 0.79) = 0.93\text{m}$

$$V_c = \phi_c \cdot \beta \cdot \sqrt{f'_c} \cdot b \cdot d_v$$

Equation 30

where

$\phi_c = 0.65$

$f'_c = 35 \text{ MPa}$

$b = 1.0\text{m}$

$$d_v = 0.93\text{m}$$

Case of no transverse reinforcement and nominal maximum size of aggregate $\geq 20\text{mm}$:

$$\beta = 230 / (1,000 + 930) = 0.119 \text{ (small)}$$

Assuming min transverse reinforcement $\rightarrow \beta = 0.18$

Axial compression has a major effect on the shear resistance provided by concrete.

$$s_z = d_v = 930\text{mm}$$

$$s_{ze} = (35 \cdot s_z) / (15 + a_g) = (35 \cdot 930) / (15 + 20) = 930\text{mm}$$

$\epsilon_x = -9.3\text{E-}05$ from stress calculation at ULS

$$\beta = (0.4 \cdot 1,300) / [(1 + 1,500 \epsilon_x) \cdot (1,000 + s_{ze})] = 0.31$$

$$V_c = 0.65 \cdot 0.31 \cdot \sqrt{35} \cdot 1.0 \cdot 0.93 = 1,120 \text{ kN/m} < V_f$$

Transverse reinforcement is required. Use 10M @ 200 x 500

$$\theta = 29 + 7,000 \cdot \epsilon_x \approx 29^\circ$$

$$V_s = (\phi_s \cdot A_v \cdot f_y \cdot d_v) \cot \theta / s = 0.85 \cdot 200 \cdot 400 \cdot 930 \cdot \cot 29^\circ / 200 = 570 \text{ kN/m}$$

$$\rightarrow V_r = V_c + V_s = 1120 + 570 = 1,670 \text{ kN/m} > V_f$$

Transverse reinforcement 10M @ 200 x 500 is sufficient to carry shear at the critical section.

11.02 Cut-Off Wall

As seen in the dam cross-section on drawing LTMM CC-DAM-504, the central cut-off wall consists of

- A secant pile wall in the alluvial deposits, extending from 1m to 2m below the top of bedrock to the top of the alluvial deposits (current ground surface). The secant pile wall is equipped with a capping beam.
- The monolithic concrete seal wall, extending from top of the capping beam of the secant pile wall to the dam crest at an elevation of 1451.00 MASL.

Both elements were included in the analysis of dam stability and deformations using finite element analysis. Results are discussed in chapter 10.04 of the design report, calculation reports are shown in Appendix K.

11.02.01 Secant Pile Wall

The secant pile wall consists of bored piles 1.25m in diameter, spaced at 0.9m (see the figure below). Only the secondary piles are reinforced. The intercutting between primary and secondary piles is 0.35m.

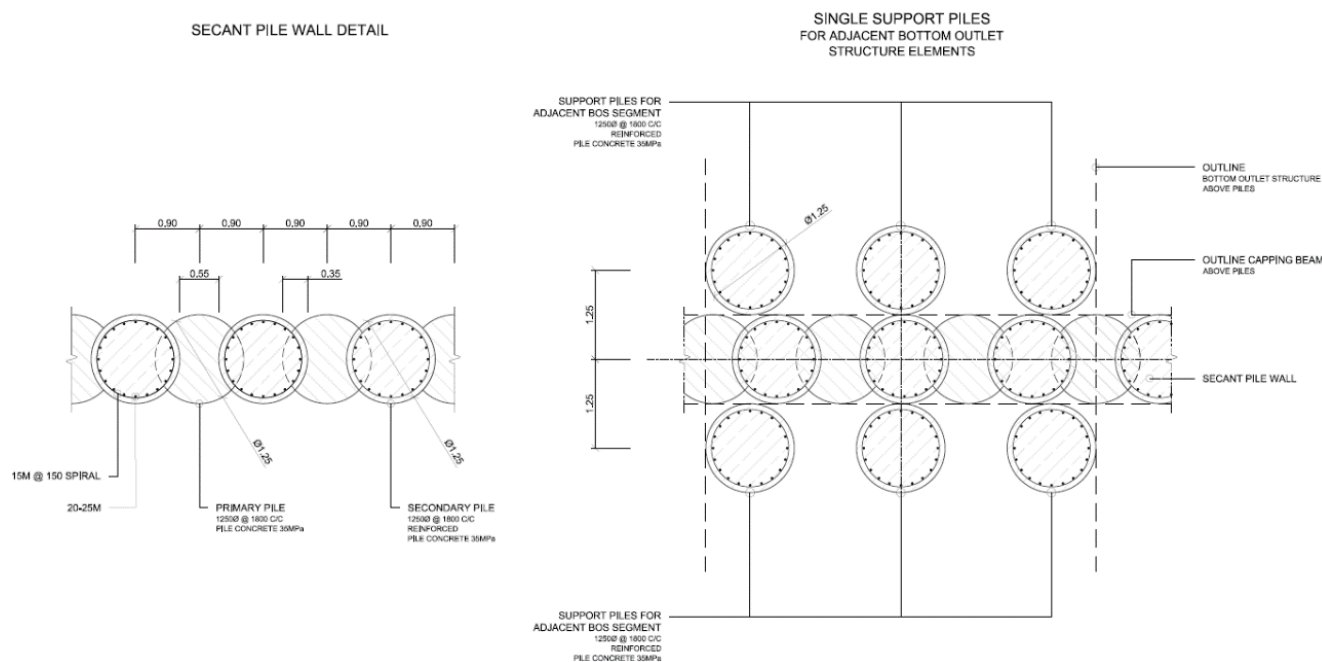


Figure 159: Construction scheme of the secant pile wall and adjacent support piles for the BOS (see Drawing LTMM CC-DFG-404 R00)

From FEA results, the design values for the secant piles are the following:

Normal force $N = -1,800 \text{ kN/m}$, $N_f = -1,800 \text{ kN/m}$

Shear force $V = 250 \text{ kN/m}$, $V_f = 375 \text{ kN/m}$

Bending moment $M = 400 \text{ kN.m/m}$, $M_f = 600 \text{ kN.m/m}$

Only the reinforced secondary piles carry the internal forces over a length = 1.8m. A load factor = 1.5 is used for M and V since these values are due to lateral earth pressure. On the other hand, a load factor = 1.0 is used for the axial force N, which is a result of uncertain skin friction with neighboring soil. It is more conservative to reduce the effect of axial compression on the laterally loaded pile. Furthermore, the unreinforced primary

piles could as well carry the axial force, which means that the axial force per secondary pile is to be multiplied by an effective length = 0.9m.

Accordingly, the forces per reinforced pile are then:

Normal force	$N = -1,620 \text{ kN},$	$N_f = -1,620 \text{ kN}$
Shear force	$V = 450 \text{ kN},$	$V_f = 675 \text{ kN}$
Bending moment	$M = 720 \text{ kN.m},$	$M_f = 1,080 \text{ kN.m}$

The interaction diagram for the reinforced secondary pile (see Appendix K) indicates a sufficient margin of safety.

Design of Monolithic Concrete Seal Wall

The seal wall is 0.5m thick and reinforced with 20M @ 200 each face, vertical and horizontal. The internal forces are generally small on the seal wall (see 10.05.03).

The design values are:

Normal force	$N = \text{neglected (conservative to neglect small compressive force)}$	
Bending moment	$M = 80 \text{ kN.m/m},$	$M_f = 120 \text{ kN.m/m}$

The interaction diagram in the appendix indicates sufficient flexural capacity of the seal pile wall. Check of SLS gives a steel stress = 136 MPa and crack width = 0.2mm. More information on crack control can be found in Appendix K.

There will be no expansion or contraction joints in the seal wall, for durability reasons. Since the wall will be more than 100m long, shrinkage will be an important design parameter. To mitigate the effect of shrinkage, two precautions are provided:

- Use of shrinkage-compensating (Type K) cement.
- Providing shrinkage reinforcement. According to ACI 350-01-7-12-2.1, the minimum shrinkage reinforcement in walls with movement joints arranged at spacing greater than 12m will be 0.5% of the gross area. This gives $25\text{cm}^2/\text{m}$ area of steel, to be distributed on both faces. The provided reinforcement of 20M @ 200 each side gives a total area of $30\text{cm}^2/\text{m}$.

11.03 Lining of the Downstream Slope

Because the complete width of the downstream slope of the structure is acting as a spillway, it is lined with a reinforced concrete slab of 0.8m minimal thickness, armored with grouted stone pitching of heavy rock riprap specified with a nominal diameter of 1,000mm (100% greater than 800mm and non greater than 1,200mm).

Under loading conditions (impoundment), the downstream slope and the lining, will follow the movements of the embankment under lateral water pressure. However, these movements are not expected to create significant curvatures in the lining as it is detached from the rock abutments. The reinforcement in the lining is provided to satisfy minimum shrinkage requirements in concrete walls and mats without movement joints. Following ACI 350-01-7-12-2.1, the minimum shrinkage reinforcement will be 0.5% of the gross area. In addition, the reinforcement for each side is to be calculated for a maximum thickness of 300mm. This gives $15\text{cm}^2/\text{m}$ area of steel on each side. Provided are 20M @ 200 for each wall as well as for top and bottom resulting in a grade of reinforcement of $15\text{cm}^2/\text{m}$.

11.04 Spillway Training Walls

The downstream lining is equipped with monolithic reinforced concrete sidewalls, arranged on both sides of the downstream slope, to confine the overtopping flow to the lined part of the spillway and to detach the downstream lining from the rock abutments. As such, internal forces in the downstream lining due to contact with the rock abutments are excluded.

The sidewalls are 0.5m thick and have a clear vertical height of 2m above the stone pitched surface and a height perpendicular to the slope of 1.74. Backfill of heavy rock riprap blend class M1 to 2 is placed between the side walls and the rock abutment (see drawing LTMM CC-DAM-506).

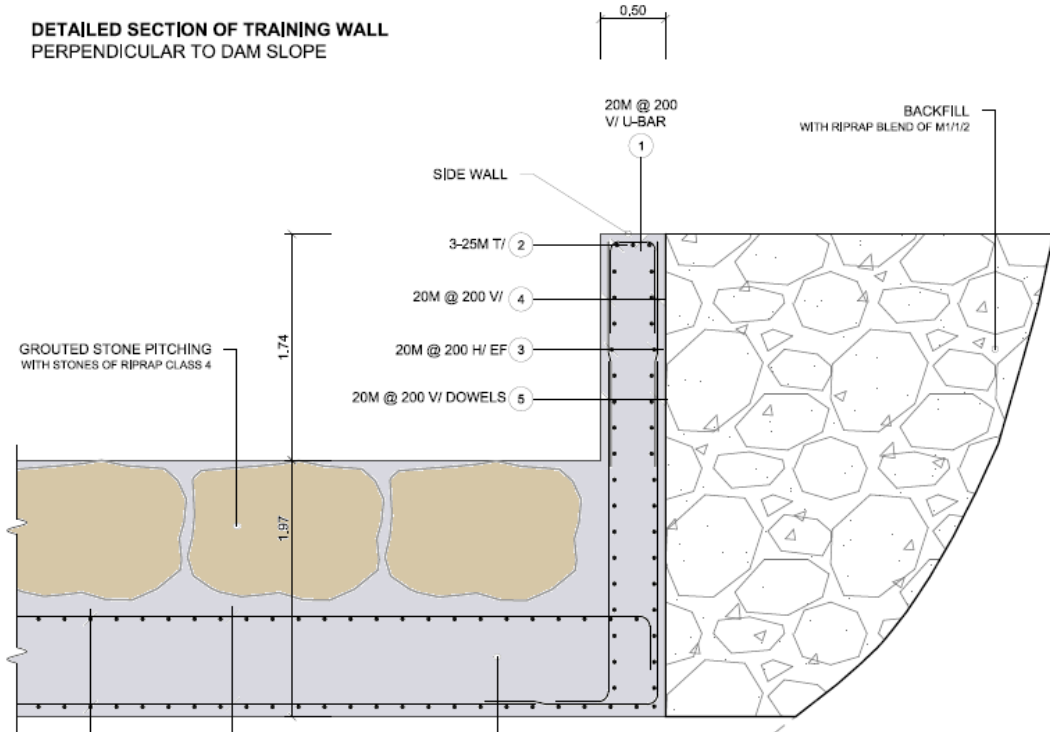


Figure 160: Detail of downstream lining and spillway-training walls (section is normal to the slope - see Drawing LTMM CC-DAM-506)

Accordingly, the side-walls are designed for internal and external lateral pressure as follows:

- Internal water pressure on the water side for a conservative height of 3m. The corresponding bending moment will be $M = 10 \cdot (3)^3 / 6 = 45 \text{ kN.m/m (SLS)}$
- External earth pressure on the fill side. Using a dry unit weight of fill = 23 kN/m^3 and an active earth pressure coefficient $K_a = 0.33$ for the backfill, the corresponding bending moment will be $M = 0.33 \cdot 23 \cdot (3)^3 / 6 = 35 \text{ kN.m/m (SLS)}$.

The crack control for the governing case of internal water pressure in Appendix K shows a low steel stress = 76 MPa and crack width = 0.114mm. The wall thickness and reinforcement are oversized for the lateral pressures, but are adequate for long-term durability under consideration of diverse impacts during spillway floods (e.g. wooden logs).

11.05 Intake Box

11.05.01 Loads, Acting Forces and Moments

The intake box consists of two triangular sidewalls with max height of 15m, in addition to the face wall and the 10m wide base slabs. The front wall and sidewalls act as retaining walls to support the fill behind. Under full

impoundment, the water pressure on the inside and outside faces will be balanced so that there will be no differential water pressure. A horizontal strut is planned between both side walls as an additional support as shown in Figure 161. Figure 162 shows a longitudinal section through the intake and the connected outlet structure. The deformations and internal forces under the applied loads are calculated by a 3D finite element shell model using Abaqus. Figure 163 and Figure 164 show the geometry, wall thickness and element mesh of the FE model representing the northern half of the intake box, utilizing symmetry. The model does not include the horizontal strut shown in Figure 161, to check its efficacy.

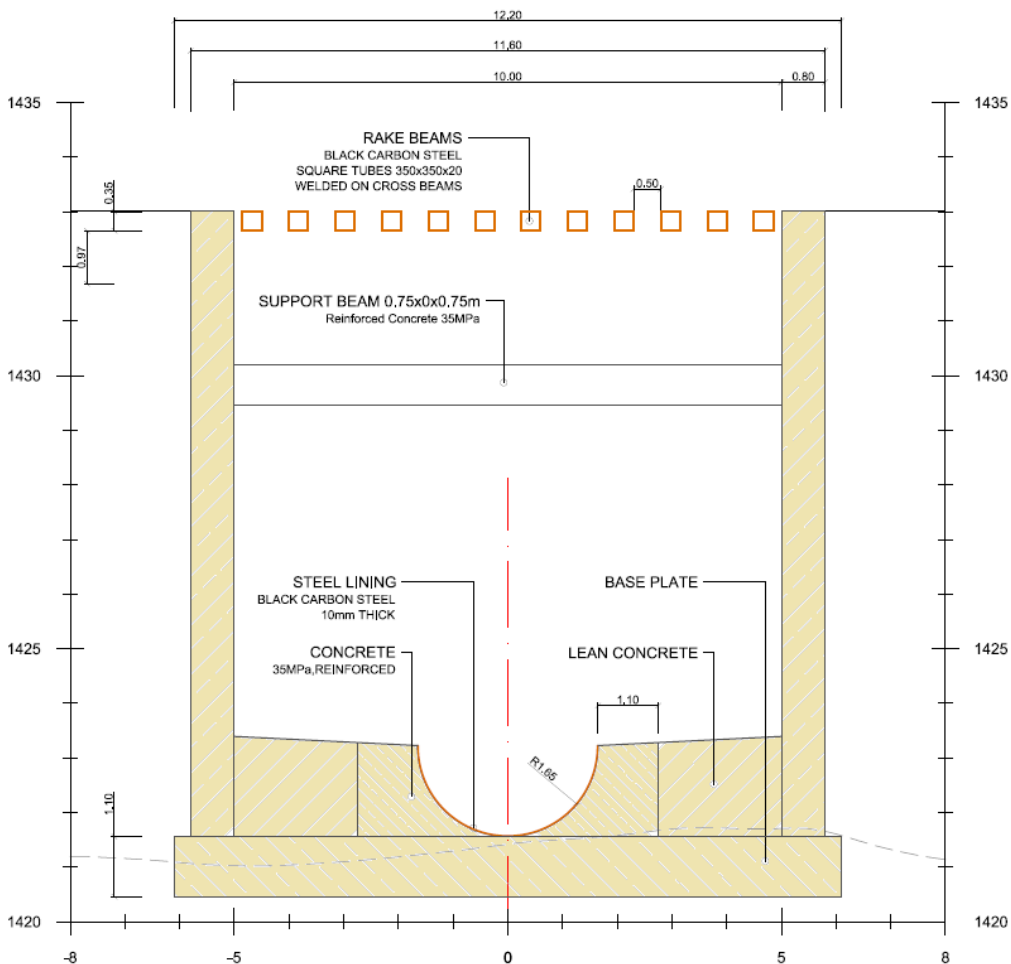


Figure 161: Cross section of the intake box

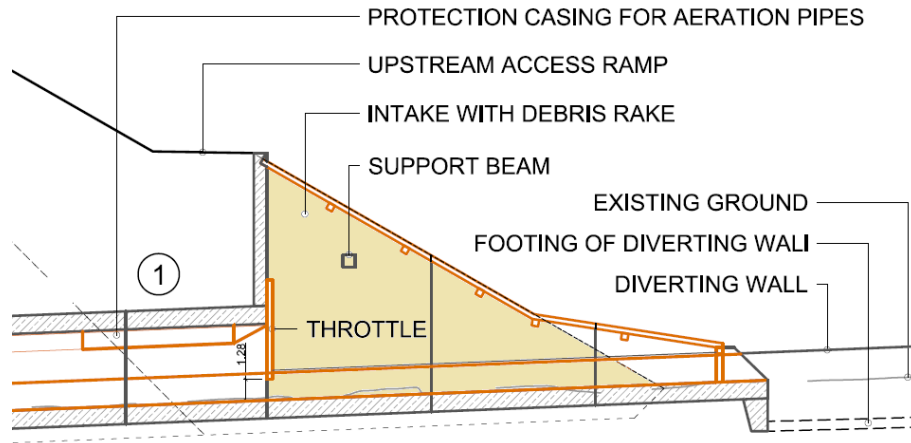


Figure 162: Longitudinal section of the intake box

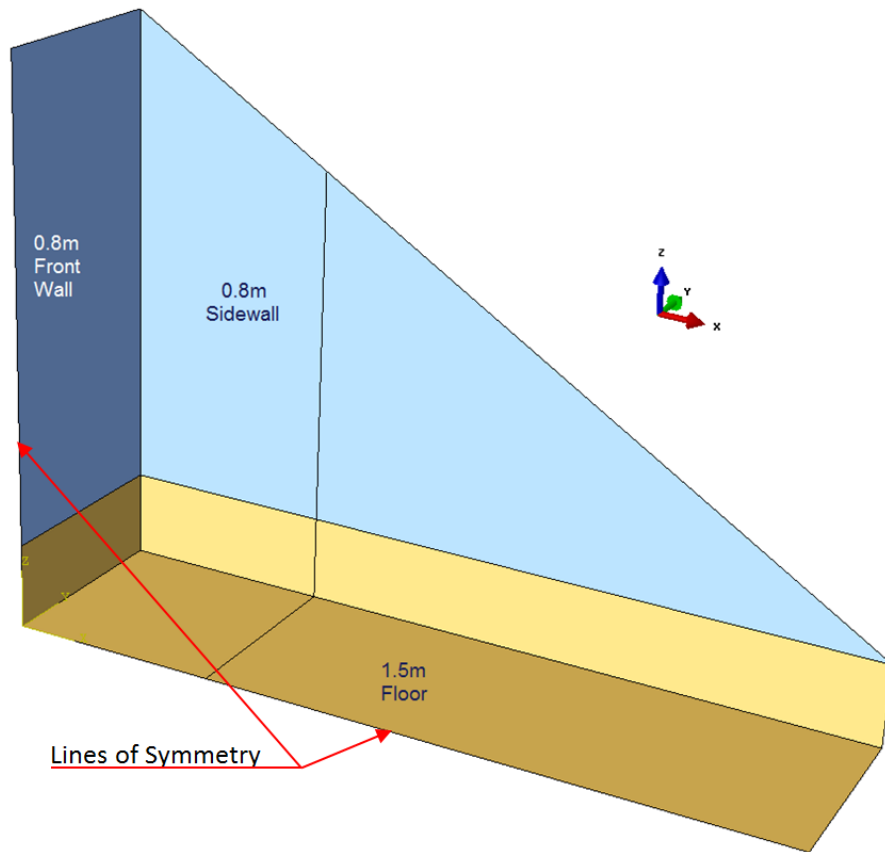


Figure 163: Shell model of the northern half, utilizing symmetry

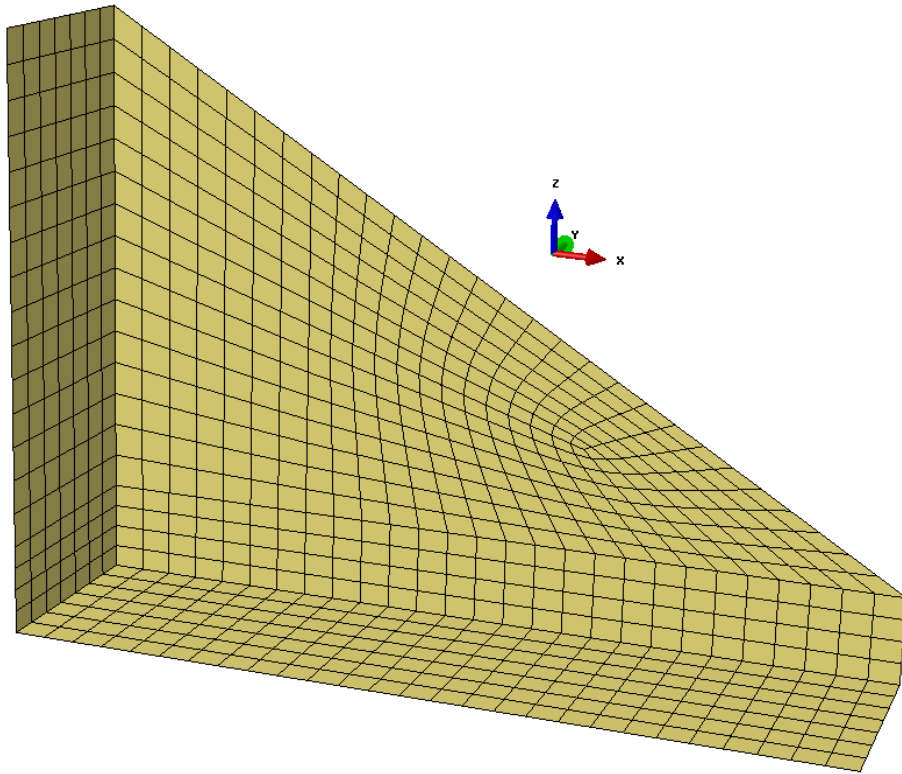


Figure 164: Finite element mesh

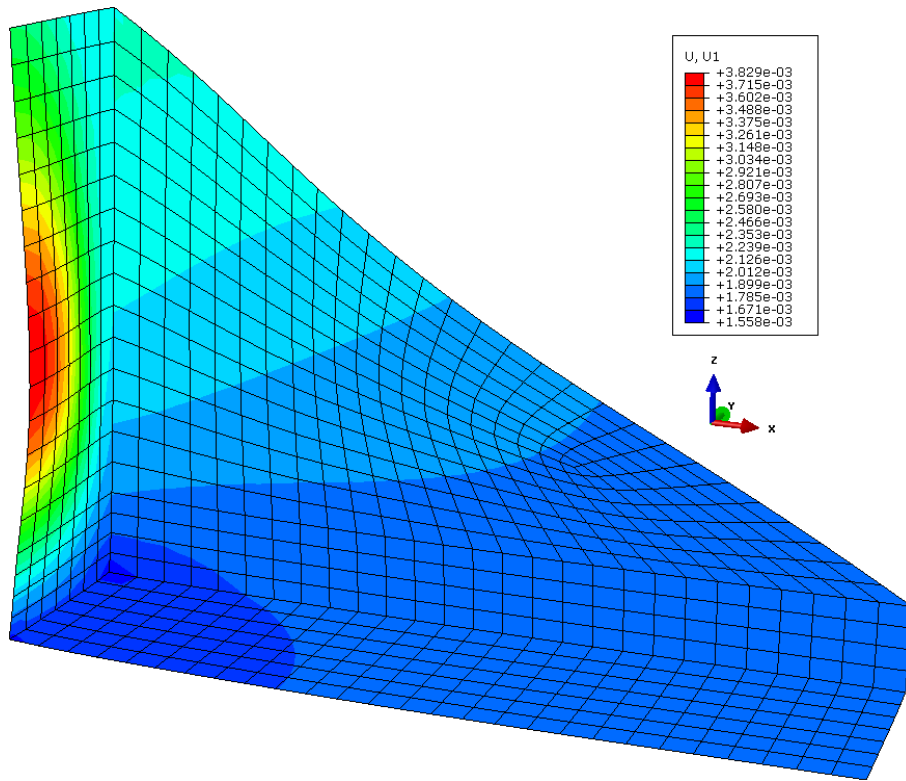


Figure 165: Deformed shape and contour lines of u1 displacement in longitudinal direction [m]

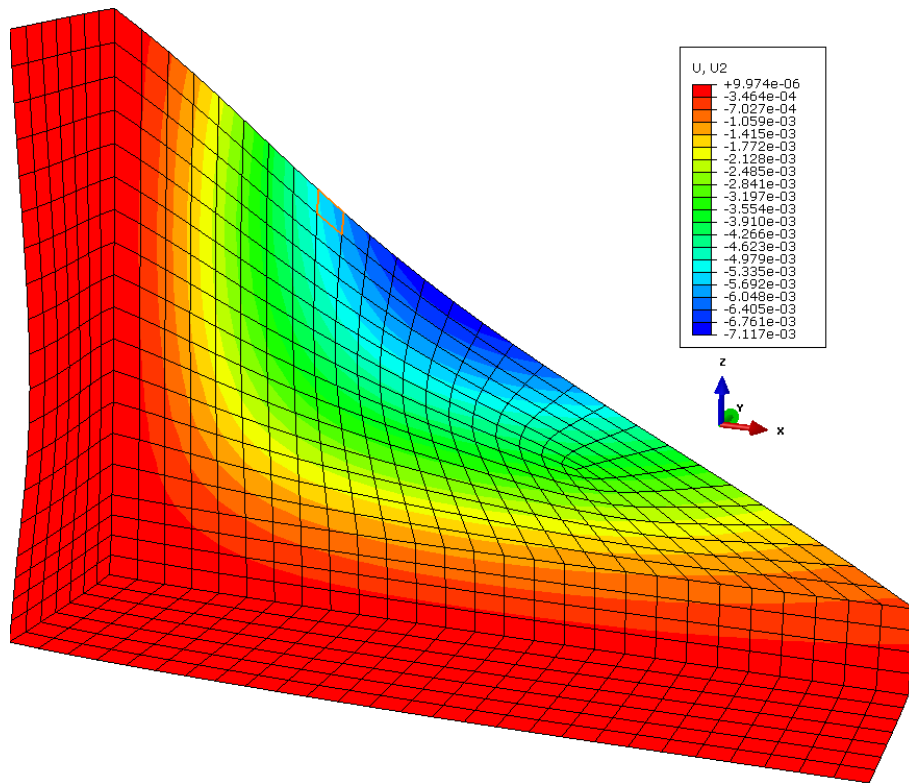


Figure 166: Deformed shape and contour lines of u_2 displacement in transverse direction [m]

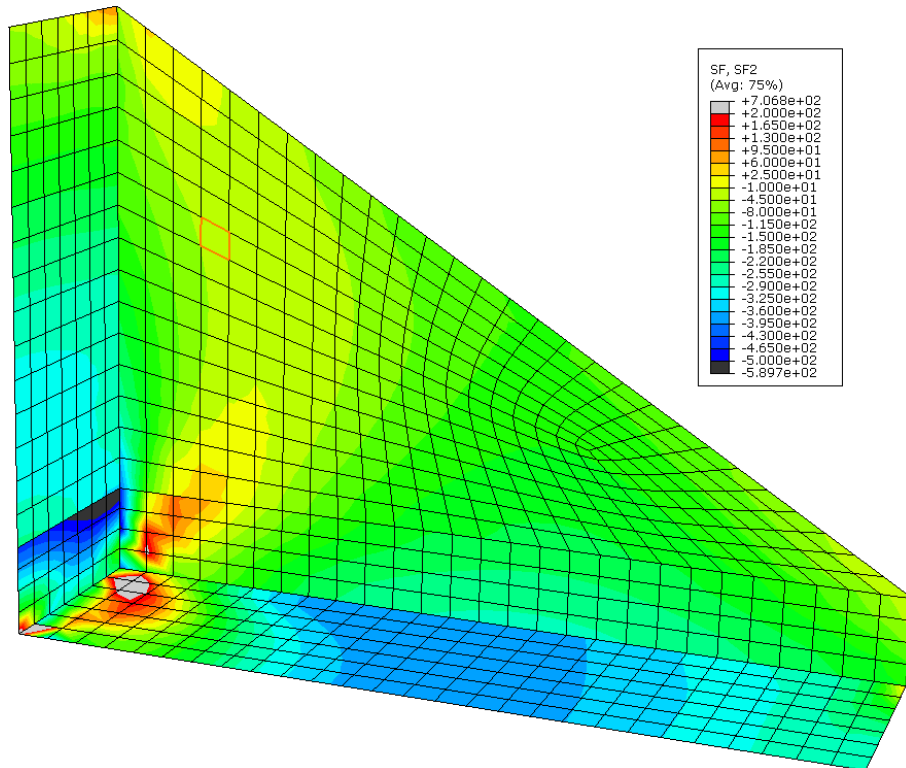


Figure 167: Membrane force SF_2 in transverse direction [kN/m]

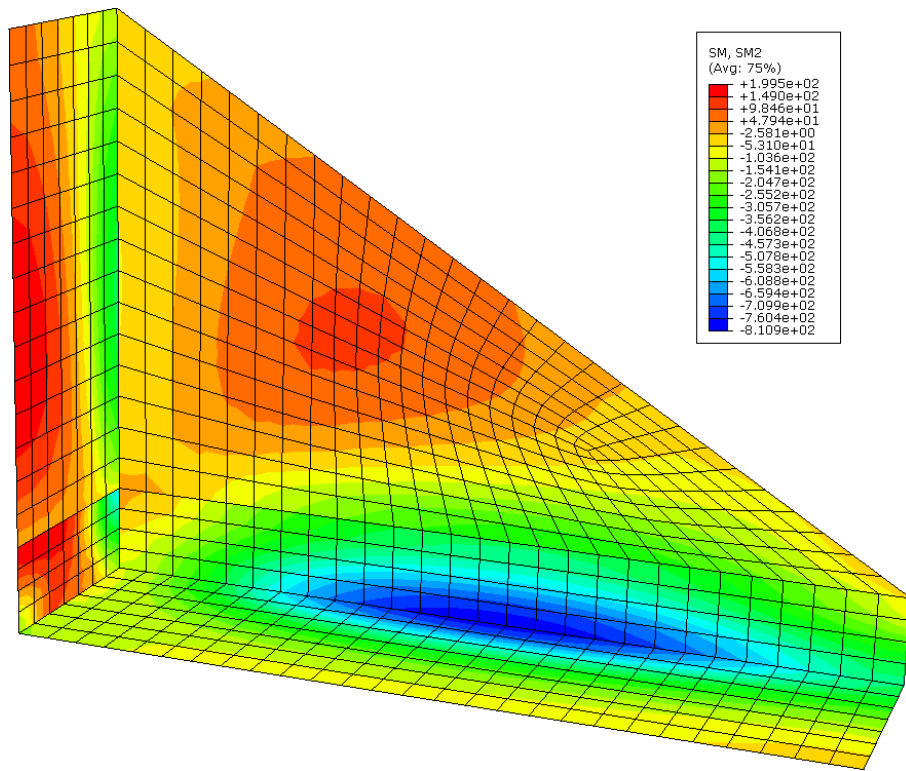


Figure 168: Transverse bending moment SM2 [kN.m/m]

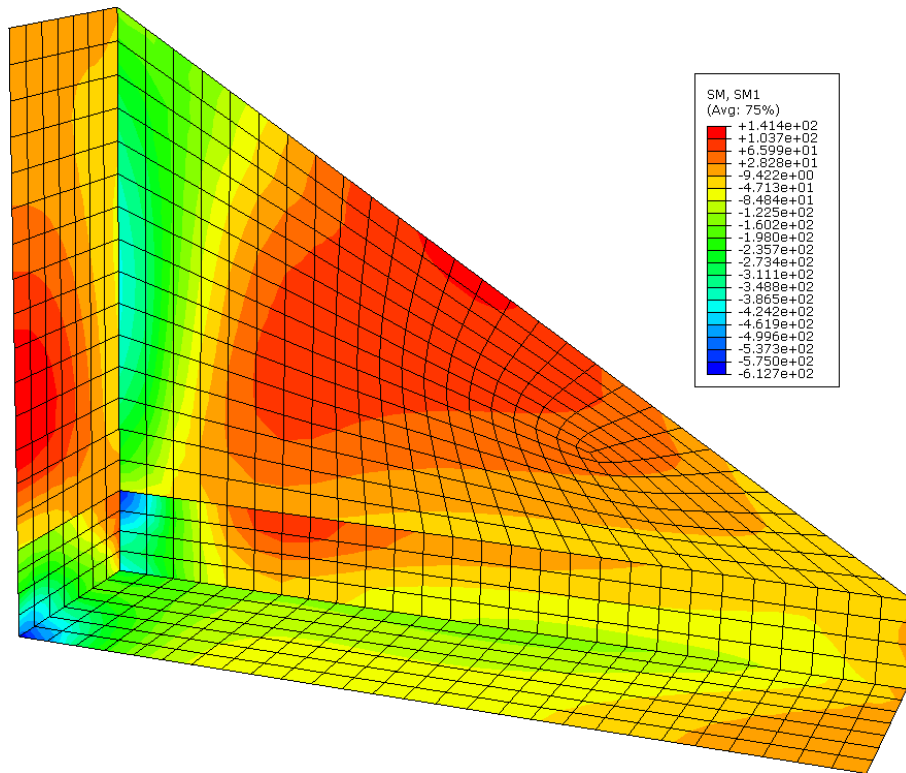


Figure 169: Longitudinal bending moment SM1 [kN.m/m]

The light blue color in Figure 163 designates the 0.8m thick sidewalls, ending at top of the concrete floor. A

rigid vertical arm (in golden color) connects the walls to the mid-surface of the floor slab. The critical sections for wall design are at the lower ends of the light blue zone (face of support).

The applied loads consist of its own weight and the lateral earth pressure in dry conditions. All loads are applied at service level (without load factors). The resulting deformations and internal forces are shown in Figure 165 to Figure 169 according to the following definitions:

- Global x-axis (x1) points in longitudinal direction toward the upstream
- Global y-axis (x2) points in transverse direction northwards
- Membrane force SF2 and transverse bending moment SM2 act in the cross sectional plane of the intake box.
- Positive membrane force indicates tension.

All forces and moments are at SLS level.

11.05.02 Design of Critical Sections

The critical section for the side wall is at face of support (top of base slab). The acting forces are:

- Normal force $N = -180 \text{ kN/m}$ (due to own weight of the 0.8m thick wall)
- Bending moment $M = 300 \text{ kN.m/m}$

The wall is 0.8m thick and reinforced with 25M @ 200 vertical.

Check of the SLS by the spreadsheet shown in Appendix K shows a steel stress of 145MPa and crack width of 0.2mm.

The critical section for the base slab is under the lowest point of the armoring steel plate (min. thickness at centerline). The acting forces are:

- Normal force $N = -380 \text{ kN/m}$ (from lateral earth pressure)
- Bending moment $M = 100 \text{ kN.m/m}$

The slab wall is 0.8m thick and reinforced with 20M @ 200 top (min reinforcement).

Check of the SLS by the spreadsheet shown in Appendix K shows a small tensile steel stress and negligible crack width.

12 DAM INSTRUMENTATION AND DATA TRANSMISSION

Dam instrumentation is designed to allow subsequent checks and maintenance or replacement. All sensors are accessible and removable.

12.01 Site Command Post (SCP)

The person in charge manning the Site Command Post the structure in case of unusual operation and/or emergencies. The responsible staff will be informed about present conditions and critical states. The person in charge will support the Local Emergency Operations Centre and performs initial notifications as described in the Fan-Out Procedures (see EPP). The SCP is located at a platform above the access road, safe from flooding.

12.02 Permanent Survey Points for Tachymeter Survey

Permanent survey points will consist of stainless steel measuring pins on which a surveying prism can be mounted. Observation is proposed to be done on a yearly basis. The measurement will be done daily during a test storage. During a flood event, tachymeter survey must not be conducted.

Permanent survey points will be arranged (a) along the dam crest; (b) inside the sealing of the bottom outlet structure at each end of each block segment; (c) along three dam crossing alignments at the upstream and the downstream slope; (d) at two points at each upper edge of the intake and the outflow structure.

12.03 Inclinometer Gauges

Four inclinometer gauges will be installed on the downstream face of the seal-wall (see Drawing LTMM CC-DAM-520 and LTMM CC-DAM-505). The inclinometer pipes will be bored through the alluvium into the bedrock and extended up to the crest. They will be mounted onto the wall with a special mounting clamp. All gauges are equipped with a screwable cover to avoid detachment during overtopping. Data is collected by manual inclinometer survey in every year, and daily during a test storage. In the alluvium, the inclinometer pipes shall be equipped with perforated sections that they can be used as ground water observation wells as well.

12.04 Piezometers inside the Dam Structure

For pore water pressure detection in the downstream embankment close to the footing of the concrete seal wall, four piezometers will be installed at the capping beam of the secant pile wall. The piezometers are installed in vertical plastic pipes reaching up to the crest of the dam. The pipes are equipped with a screwable cover. Data will be transmitted to a Town of Canmore server for remote monitoring.

12.05 Piezometer for Detection of Height of Impoundment

For detection of impoundment height, two piezometers will be installed at the intake. The piezometers are installed in steel protection pipes, reaching down to the bottom of the intake structure. Data will be transmitted to a Town of Canmore server for remote monitoring.

12.06 Flow Height Gauge at the Outlet Structure

For detection of flow height at the outlet structure, a radar gauge will be installed at the outlet structure. Data will be transmitted to a Town of Canmore server for remote monitoring.

12.07 Discharge Monitoring at all Drainage Pipes

All drainage pipes will be monitored by means of a combination of piezometers and Thomson weirs installed in according shafts, allowing the unhindered inflow and outflow of water. Data will be transmitted to a Town of Canmore server for remote monitoring.

12.08 Web Camera

A web camera for remote controlled visual inspection of conditions at the structure, and in particular at the retention basin, is planned to be installed at the right or left abutment, safe from flooding and rock-fall.

13 ACCESS RAMP

From the gravel road aligned along the creek, a ramp provides access to the structure's crest and to the observation and maintenance platform. Vehicles will only be allowed to access the crest backwards, under constant guidance. A turning bay is located at the right abutment only.

On the downstream side, predominantly cutting into the right creek flank of bedrock is required. The pavement will be a 60cm thick compacted aggregate of well-graded angular gravel of 32mm minus, placed directly on bedrock.

From the crest to the retention basin, the ramp is integrated in the embankment slope and forms inclined terraces. Bends are constructed by rock cuts in the bedrock. Ramp sections located on the embankment slope require geotextile for layer separation between the embankment material and the road pavement material.

Construction of the access ramp shall be done by a contractor familiar with forestry road construction in steep slopes and requires guidance by experienced forestry road engineers.

Unstable sections will require slope stabilization such as rock-bolts, anchored wire mesh or, for stabilizing larger potential slope detachments, anchored support beams of reinforced concrete.

14 OPERATION AND SERVICE FACILITIES

As defined within the Dam Safety Guidelines (CDA, 2007), Section 3.4.3, the operating procedures for normal, unusual and emergency operations have to be determined. However, as Cougar Creek debris flood retention structure is built for flood retention, it needs to be considered differently than other type of dams, e.g. built for power generation. As mentioned in chapters above, the retention structure is designed to withstand full impoundment as well as overtopping scenarios. Therefore, full impoundment of the structure is considered as a normal loading condition. Operating procedures (see the OMS Manual, section 04.03.02, 04.03.03, 04.03.04), which require supervision and monitoring of the structure for different levels of impoundment, do not correlate to the loading conditions of the dam.

Operating procedures are listed in the OMS Manual and comprise of regular observation of the structure by visual inspection, supported by monitoring of dam instrumentation facilities, and extra procedures and checks in case of unusual or extreme operation conditions. No specific facilities, other than dam instrumentations discussed above, are required for operating the structure.

15 INVESTIGATION OF FREEZING

15.01 Purpose of Investigation of Freezing

Because seepage cut-off measures will lead to groundwater upwelling, freezing at the intake could occur during the cold season, potentially resulting in blockage of the intake and leading to unintended impoundment. To estimate the expected conditions, under consideration of the embankment dam structure, a thermometric analysis was conducted using the FE analysis tool WinTube (see chapter 10.04.01.02).

15.02 Methodology

As described in the Canadian Foundation Engineering Manual (CGS, 2006), chapter 13.4, thermal conduction is the dominant mechanism of heat transfer in soil and rock. Heat flow in the ground follows Fourier's law of conduction described by a term accounting for the release or absorption of latent heat of water during phase change. Heat transfer by mechanisms other than conduction are a factor in porous soils where groundwater flow occurs. Water velocities generally must exceed 10^{-4} cm/s before convective heat flow starts to become significant. This can be expected at Cougar Creek as the alluvium has a considerably high water permeability. However, the convective heat transfer has been neglected in the calculation to ensure conservative results. Release of latent heat during phase change of water has been neglected for the same reason.

The calculation method used is based on the thermodynamic principle mentioned above and as shown in Equation 31. Fourier's law is inserted in the energy conservation law (see Equation 32) which gives Equation 33, the basic equation for thermal analysis.

$$\underline{y} = -Kt \cdot \text{grad}T \quad \text{Equation 31}$$

$$\text{div } \underline{y} = q - \rho \cdot c_p \frac{\delta T}{\delta t} \quad \text{Equation 32}$$

$$\text{div}(-Kt \cdot \nabla T) = q - S \cdot \frac{\delta T}{\delta t} \quad \text{Equation 33}$$

Where

Kt	tensor of conductivity with conductivity being dependent on flow direction [W/K m]
gradT	temperature gradient [K/m]
\underline{y}	vector of heat fluxes [W/m ²]
q	power of sources or sinks [W/m ³]
ρ	unit weight [kg/m ³]
c_p	specific thermal capacity [Ws/K kg]
S	specific storage coefficient [J/K m ³]

As described by Hillel (1982) the response of soil regarding air temperature changes is dampened and shifted progressively over time and depth (see Figure 170). Because of this effect, governed by latent heat of the soil, daily air temperature fluctuation mostly influences the soil temperature of the near-surface soil. The annual air temperature wave penetrates the ground to maximum depth of 15m due to heat flow from the crust produced by uranium fission in minerals. From a depth of 15m and beyond, ground temperature gradient is approximately 1°C per 35m.

The influence of air temperature fluctuation on the structure was modeled by multiple stages with varying duration. Based on available data as listed in chapter 15.03 and aspects mentioned above, the following sequence was modeled:

- 1) The initial state was set to a soil temperature of 4.5°C at a depth of 50m and a mean annual air temperature of 3.375°C at the surface;

- 2) After modeling the initial state, the air temperature was set to 0°C for 20 days;
- 3) The following sequences were set according to Figure 173 to demonstrate conditions as recorded in January and February 2016;
- 4) For investigating extreme conditions, a seven day lasting period with an air temperature of -40 °C was modeled. This setting shall represent conditions according to the map for extreme minimum temperature zones of parts of Central and Western Canada as shown in Figure 174 (NRC, 2014).
- 5) For investigating the situation assuming the blockage of the outlet structure and impoundment of 2m in height, scenarios with air temperatures down to -40°C were modelled as well.

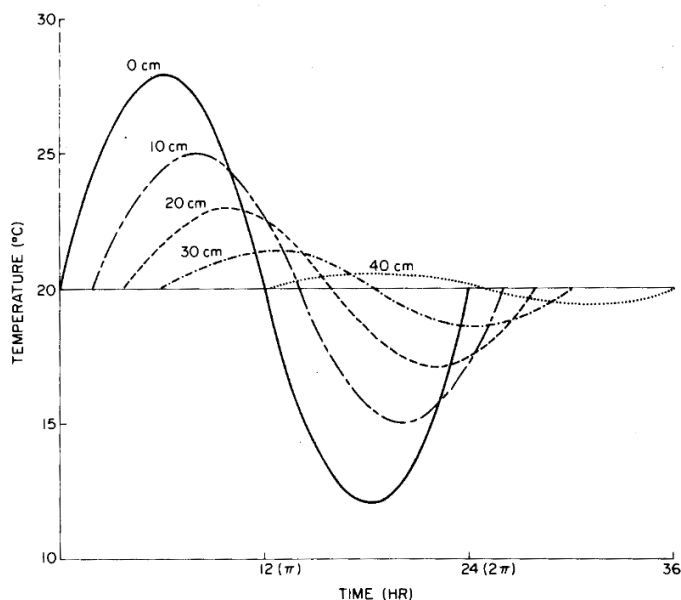


Figure 170: Idealized variation of soil temperature with time for various depths (Hillel, 1982)

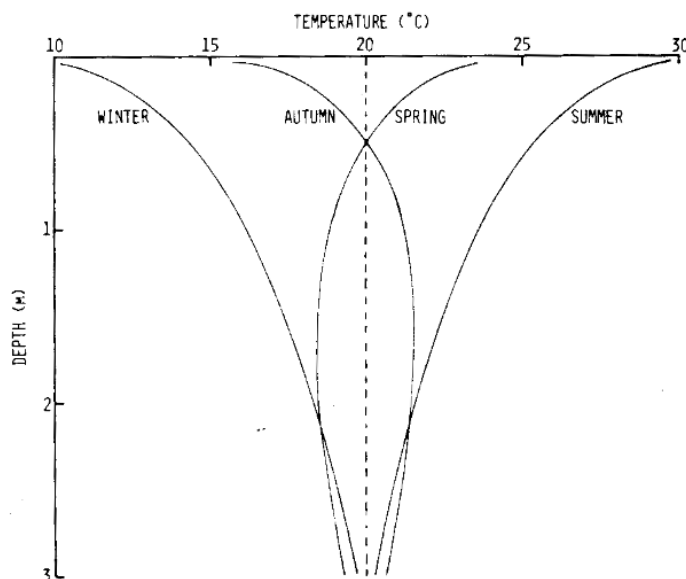


Figure 171: Example of a soil temperature profile as it varies from season to season (Hillel, 1982)

15.03 Basic Data

For a rough estimation of on-site conditions regarding ground response to air-temperature changes, the main well TP14-3 which was used for pumping tests in August 2015, was equipped with a temperature sensor at a depth of 2m below ground. Recorded data for the available time span is shown in Figure 172. Noted is that water temperature did not fall below 0.5°C independent from air temperature falling down to -22°C. This shows the effect of ground water recharge in combination with heat transfer from the deep ground as explained in chapter 15.02.

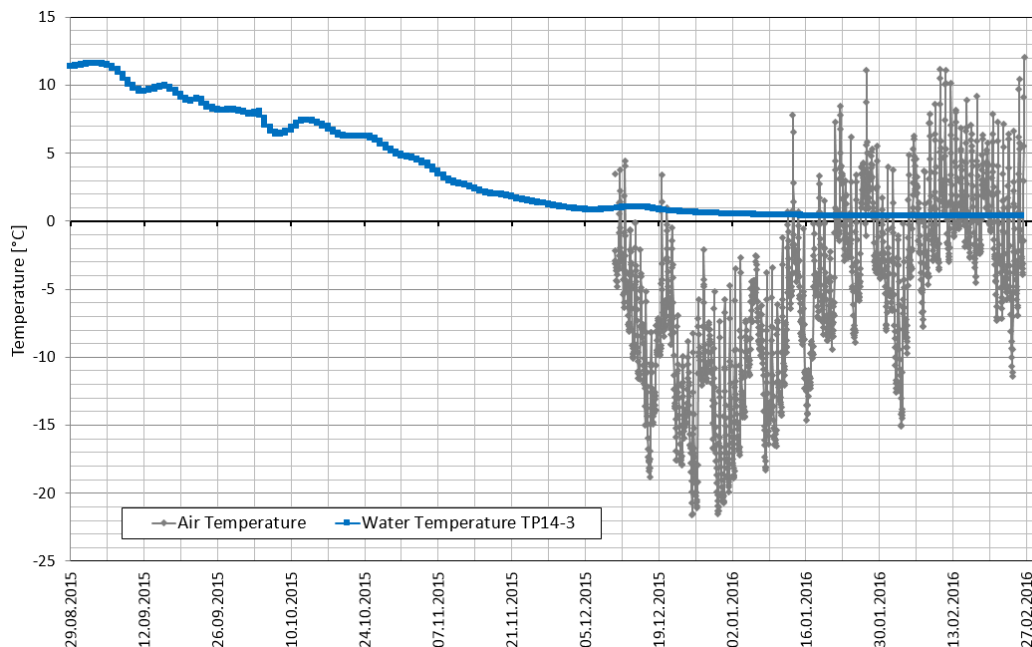


Figure 172: Recorded air temperature and water temperature at the well TP14-3 at Cougar Creek

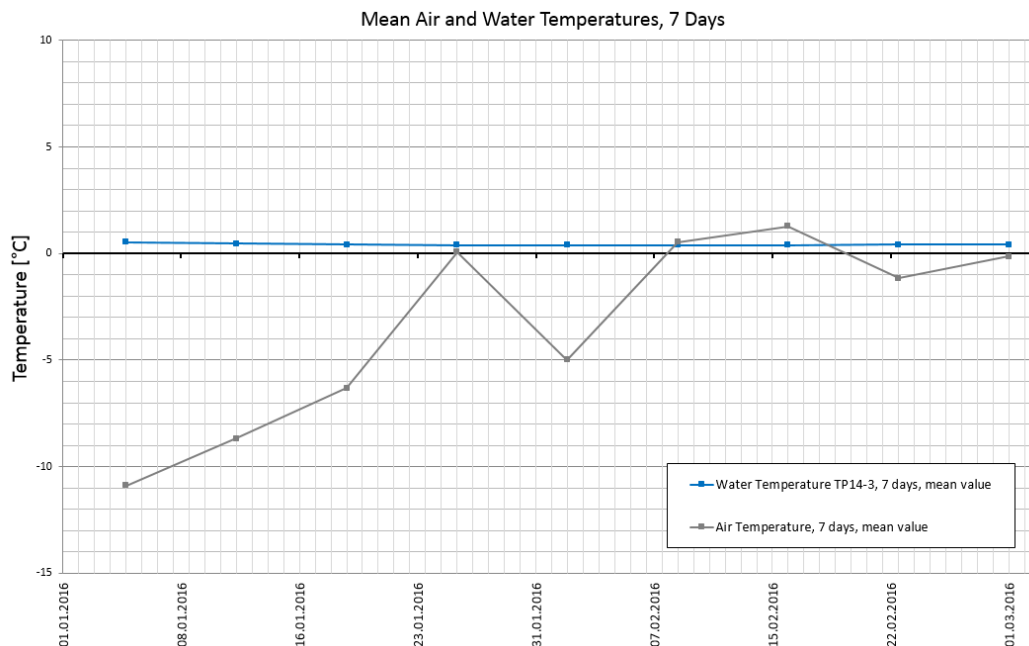


Figure 173: Example of mean weekly air and water temperature during winter, based on the temperature log at Cougar Creek (see Figure 172)

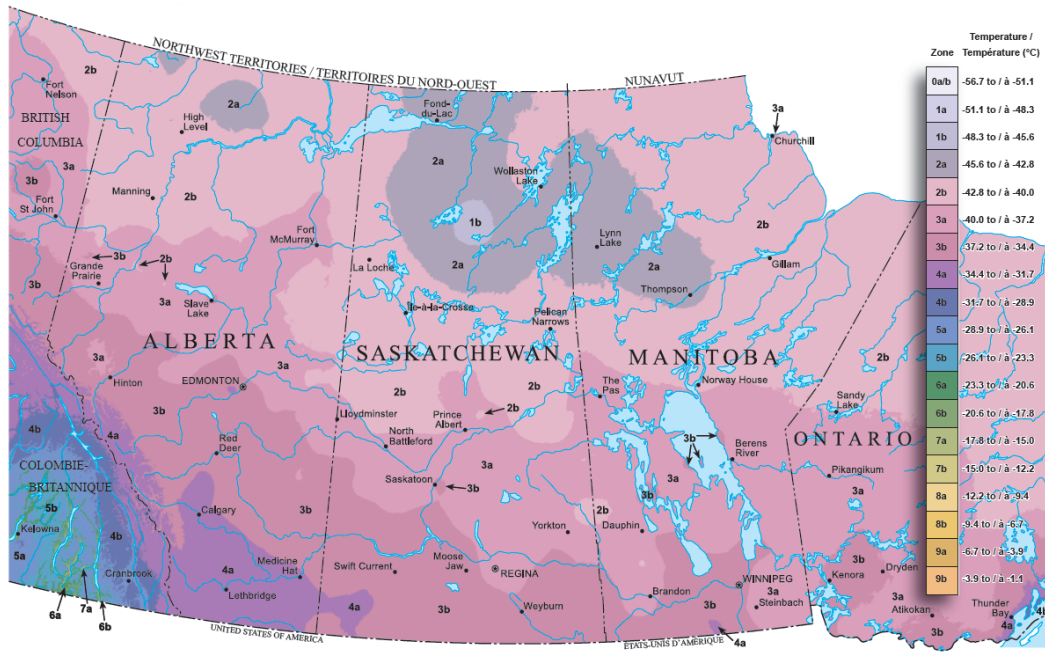


Figure 174: Extreme minimum temperature zones of parts of Central and Western Canada (NRC, 2014)

15.04 Calculation Results

Parameters for heat flow calculation are listed below.

Table 80: Parameter used for the thermal analysis, (Hillel, 1982)

Soil Type	Thermal conductivity [W/k m]	Specific storage capacity [J/K m ³]
Alluvium, low moisture content	1.5	1*10 ⁶
Alluvium, Groundwater	2.7	1.94*10 ⁶
Bedrock	8.8	3*10 ⁶
Water	0.57	4.2*10 ⁶
Ice	2.2	1.9*10 ⁶

For the situation with no impoundment conditions are as listed in Table 81.

Table 81: Frost penetration depth, Frost lenses [m], groundwater no impoundment

Air temperature [°C]	-10.3	-8.7	-6.3	0.1	-5.0	0.5	1.3	-1.2	-0.1	-40.0	3.375	3.375
Duration [days]	7	7	7	7	7	7	7	7	7	7	14	28
Frost penetration depth [m]	2.1	2.6	2.9	0.1-3.0	3.0	0.3-2.9	1.8-2.4	1.9	1.4	3.3	0.6-4.6	1.7-4.3

Modelling the situation assuming the blockage of the outlet structure and impoundment of 2m high, the situation with -40°C air temperature gives results as listed in Table 82.

Table 82: Frost penetration depth, Frost lenses [m], 2m impoundment, ice

Air temperature [°C]	-10.3	-8.7	-6.3	0.1	-5.0	0.5	1.3	-1.2	-0.1	-40.0	3.375	3.375
Duration [days]	7	7	7	7	7	7	7	7	7	7	14	28
Thickness of ice cover at 2m of impoundment [m]	0.8	1.1	1.1	0.1-1.0	1.0	0.2-0.9	-	0.7	0.2	1.5	0.5-1.4	0.7-1.0

Summarizing the results as listed in Table 81 and in Table 82 as well as shown in Figure 175 to Figure 198, frost at -40°C air temperature is expected to penetrate the ground to a depth of approximately 3.3m if there is no impoundment. This corresponds to the estimate of the maximum frost penetration depth of 2.9m according to calculations as listed in chapter 04.05.

In case of impoundment due to blockage, upwelling groundwater and heat transfer lead to thawing at the base of the intake. The calculated thickness of the ice cover, by neglecting release of latent heat due to phase change, is 1.5m at -40°C air temperature. It can be assumed, that at higher unintended impoundment levels, the ice cover is of the same thickness, or thinner.

These results show that freezing in winter is likely but substantial impoundment during extreme air temperature conditions is not expected. Discharge of groundwater through the bottom outlet structure or the emergency bypass is still expected at extreme air temperatures.

15.04.01 Mean Annual Air Temperature of 3.374°C

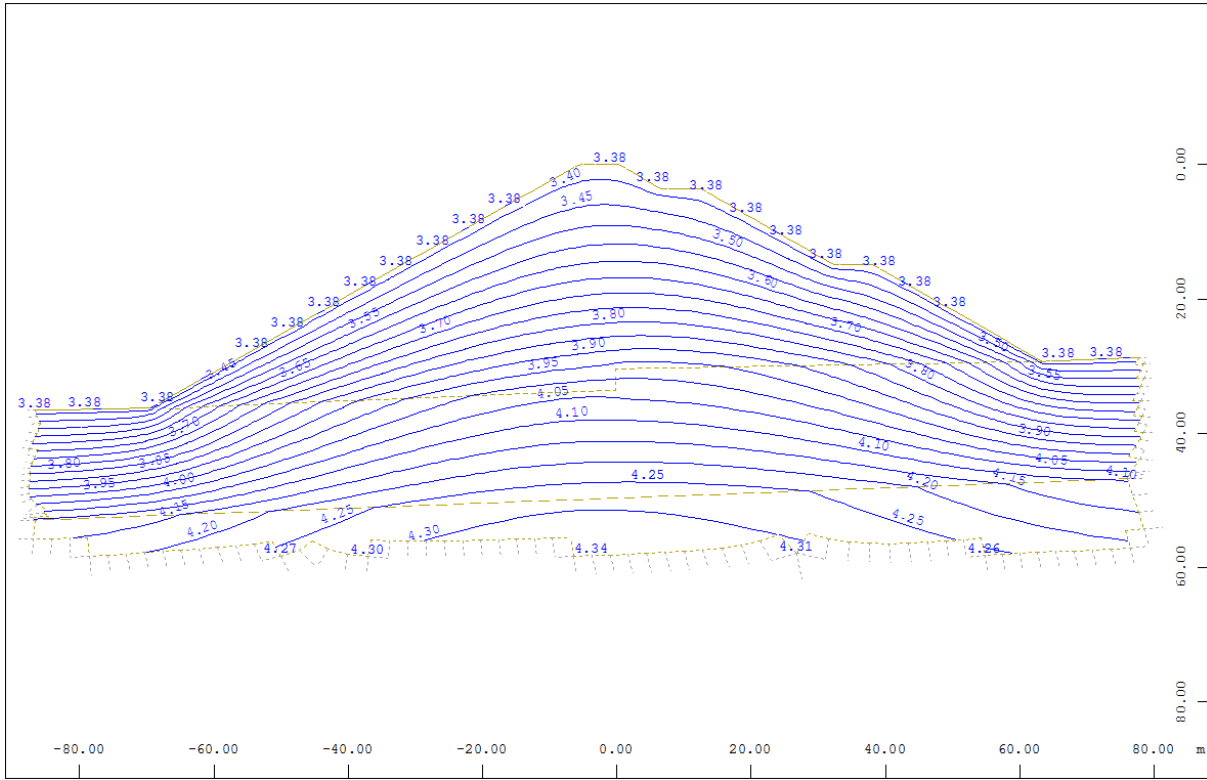


Figure 175: stationary temperature analysis in °C, mean annual air temperature 3.374 °C

15.04.02 Sequence of Mean Weekly Air Temperatures varying according to Records in Winter 2016

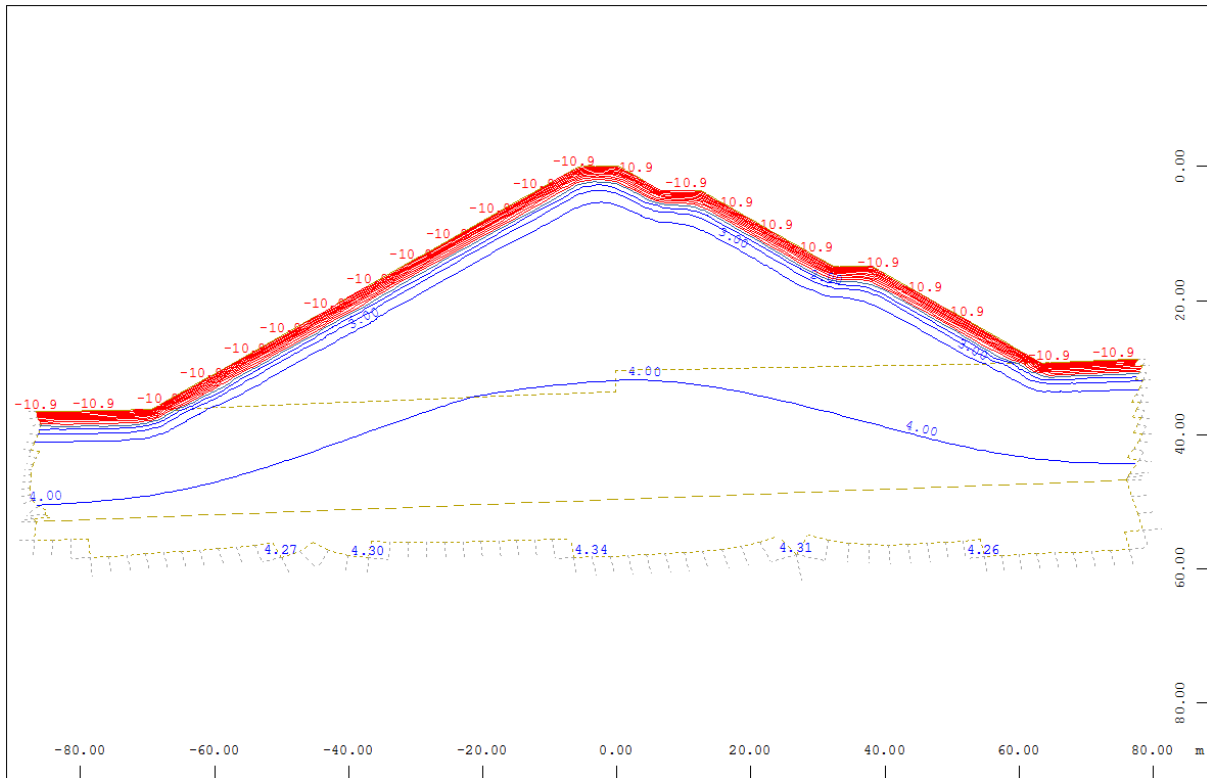


Figure 176: transient temperature analysis in °C mean weekly temperature -10.9 °C

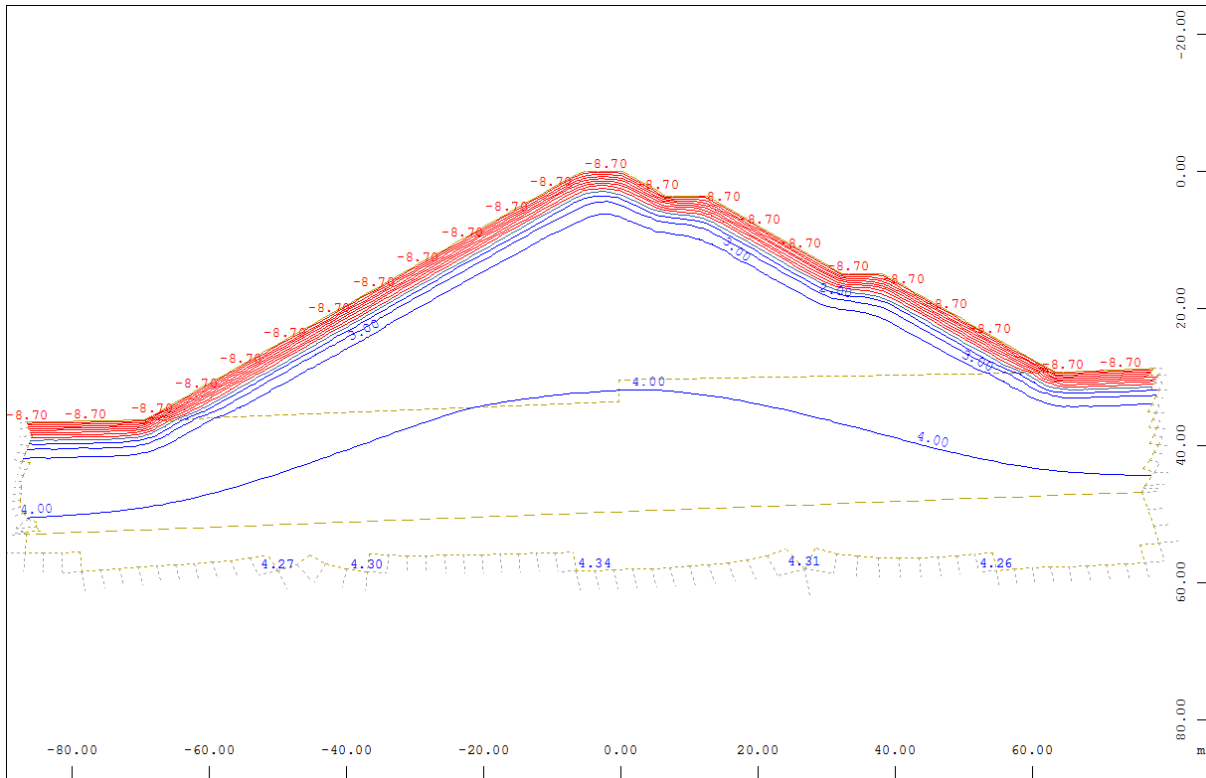


Figure 177: transient temperature analysis in °C mean weekly temperature -8.70 °C

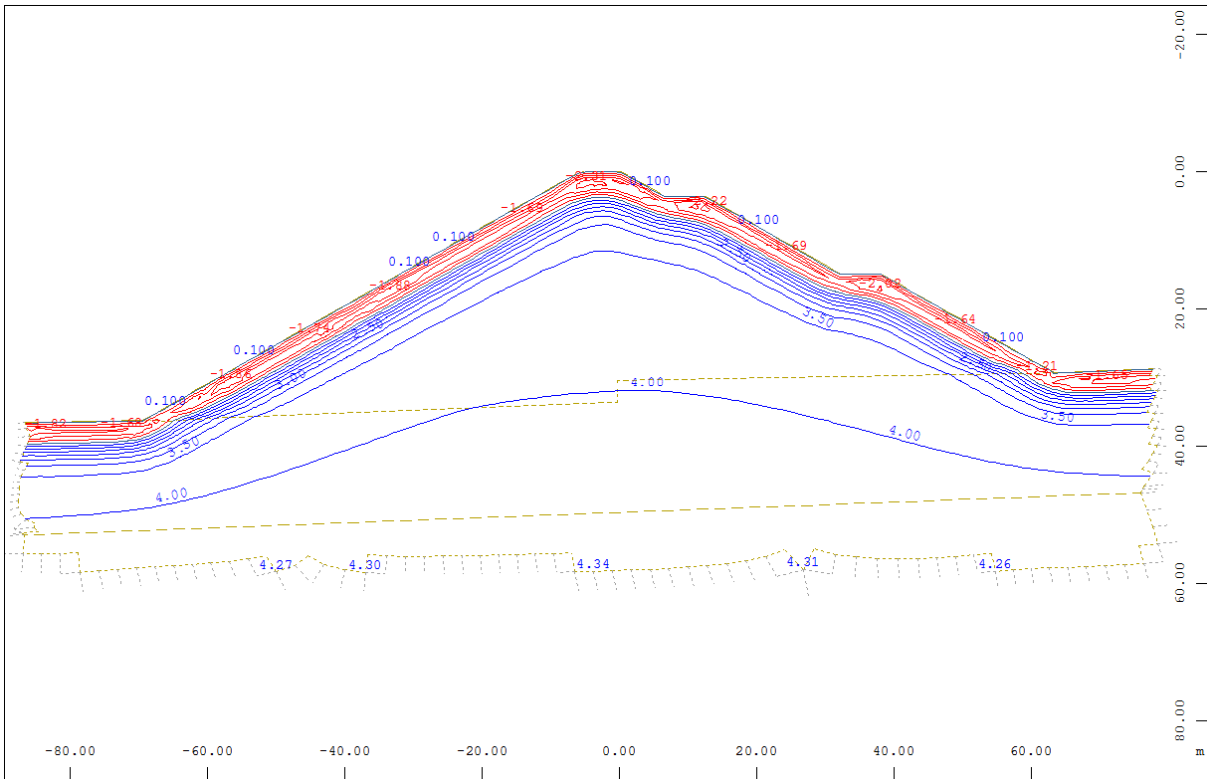


Figure 178: transient temperature analysis in °C mean weekly temperature 0.10 °C

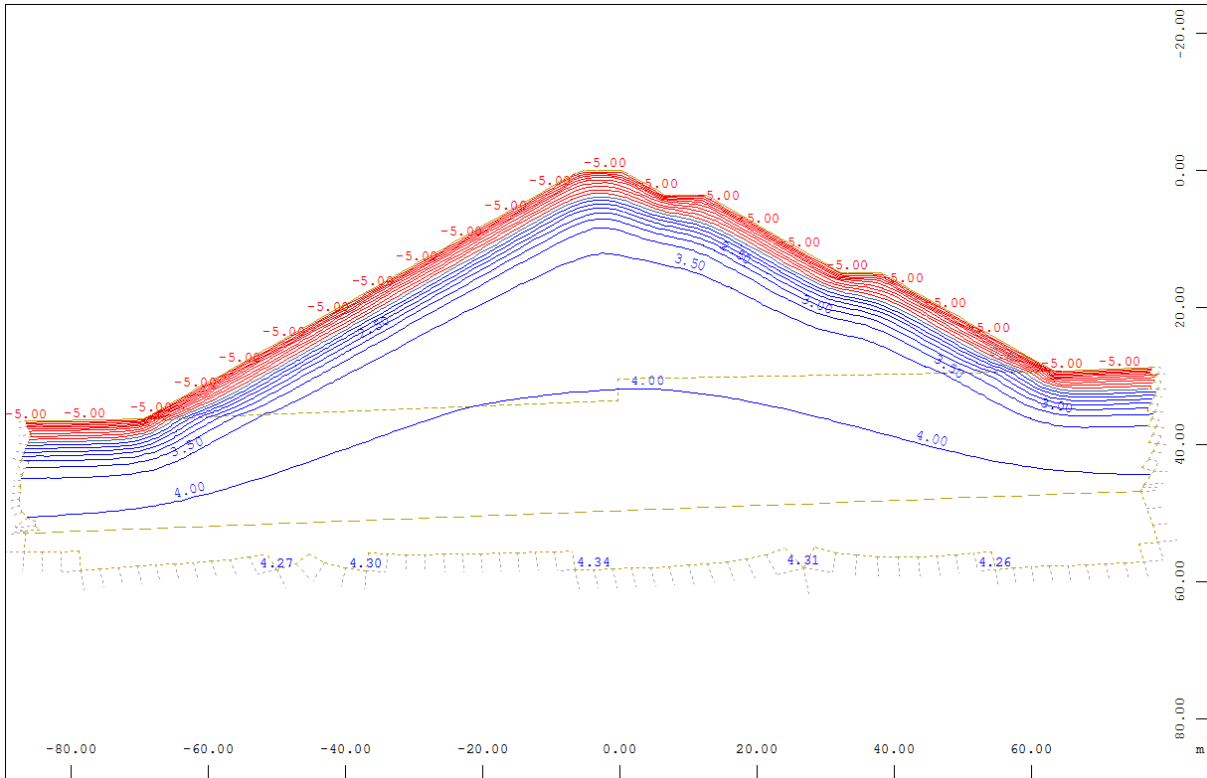


Figure 179: transient temperature analysis in °C mean weekly temperature -5.00 °C

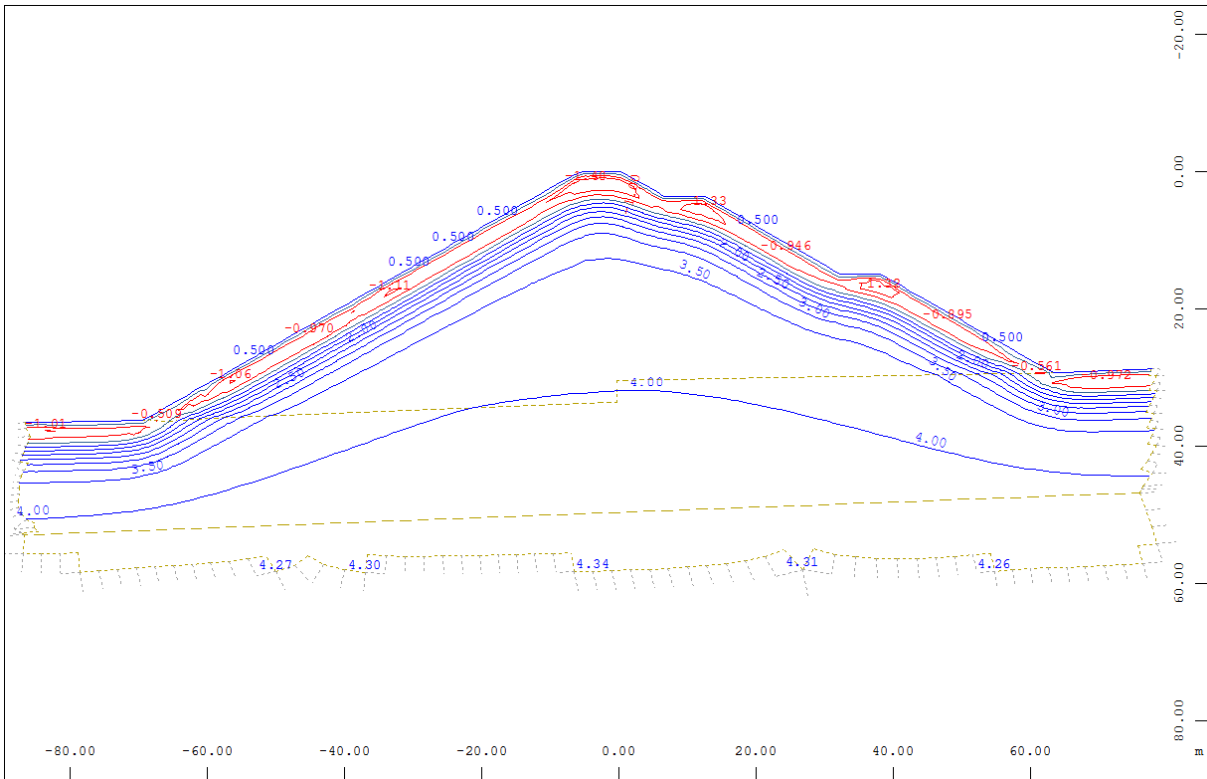


Figure 180: transient temperature analysis in °C mean weekly temperature 0.50 °C

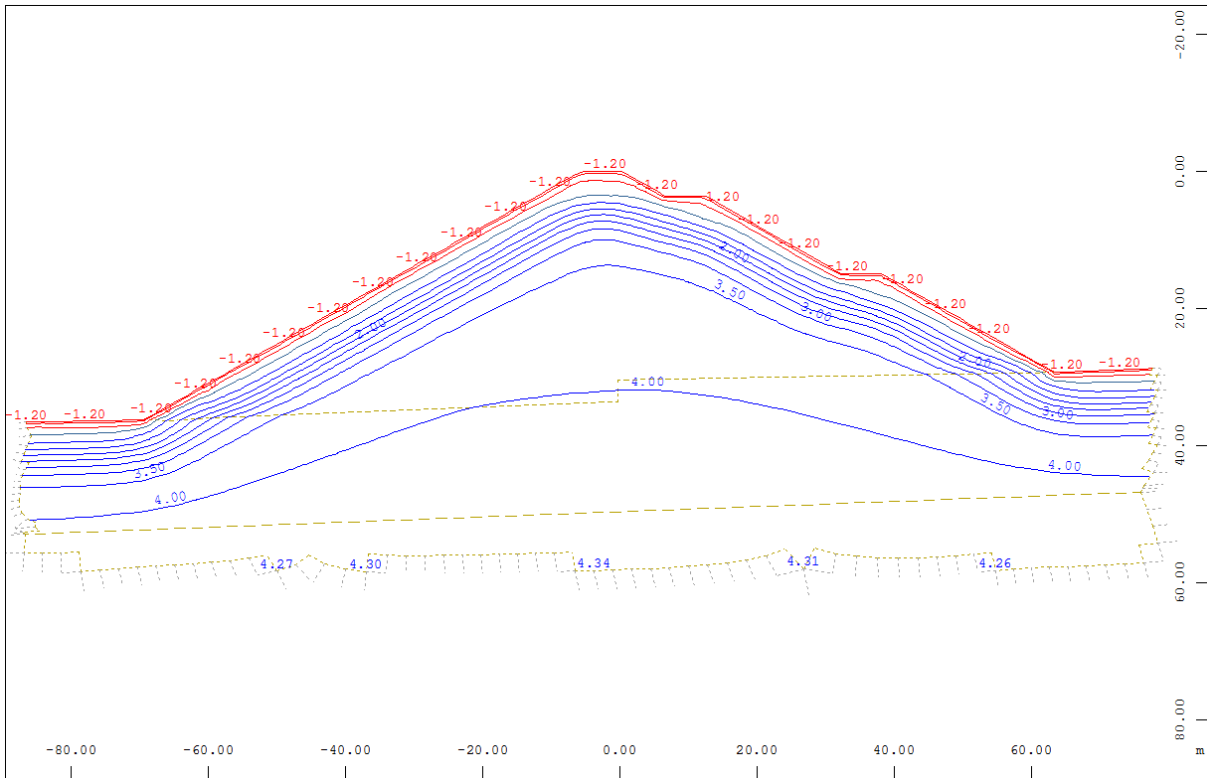


Figure 181: transient temperature analysis in °C mean weekly temperature -1.20 °C

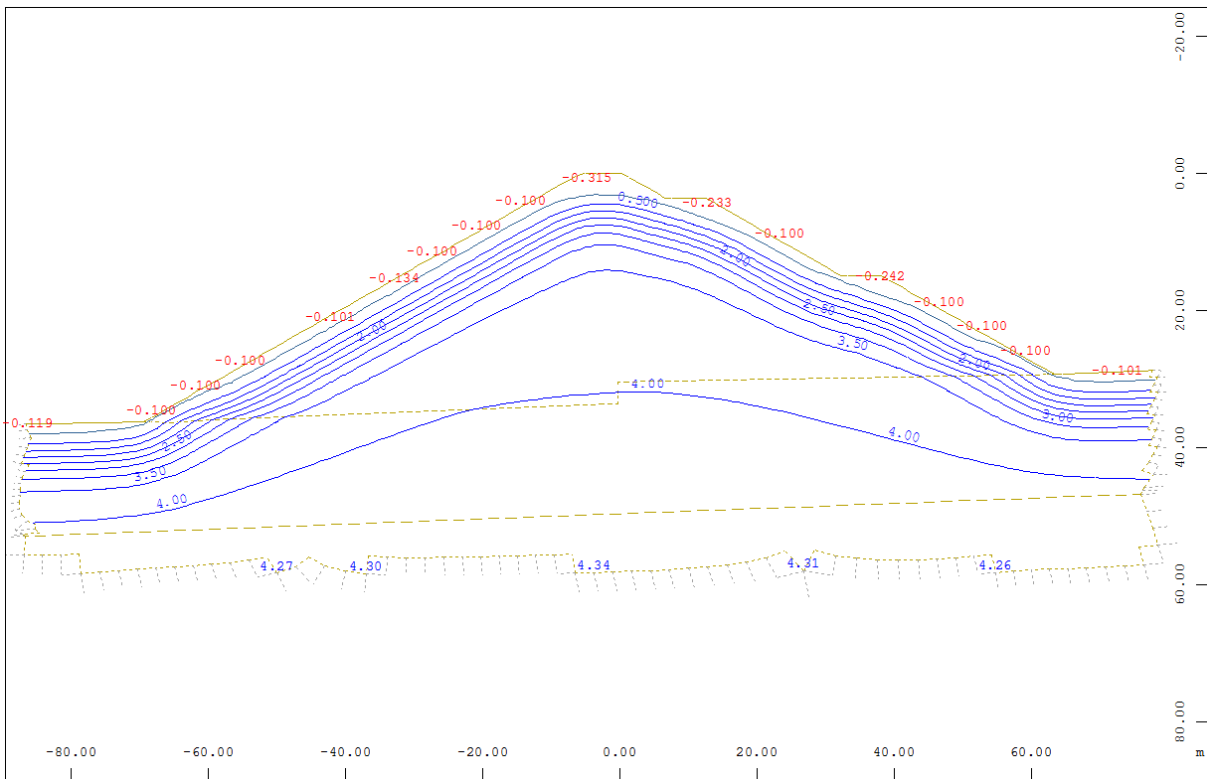


Figure 182: transient temperature analysis in °C mean weekly temperature -0.10 °C

15.04.03 Air Temperatures at -40°C for seven Days followed by mean annual air Temperature

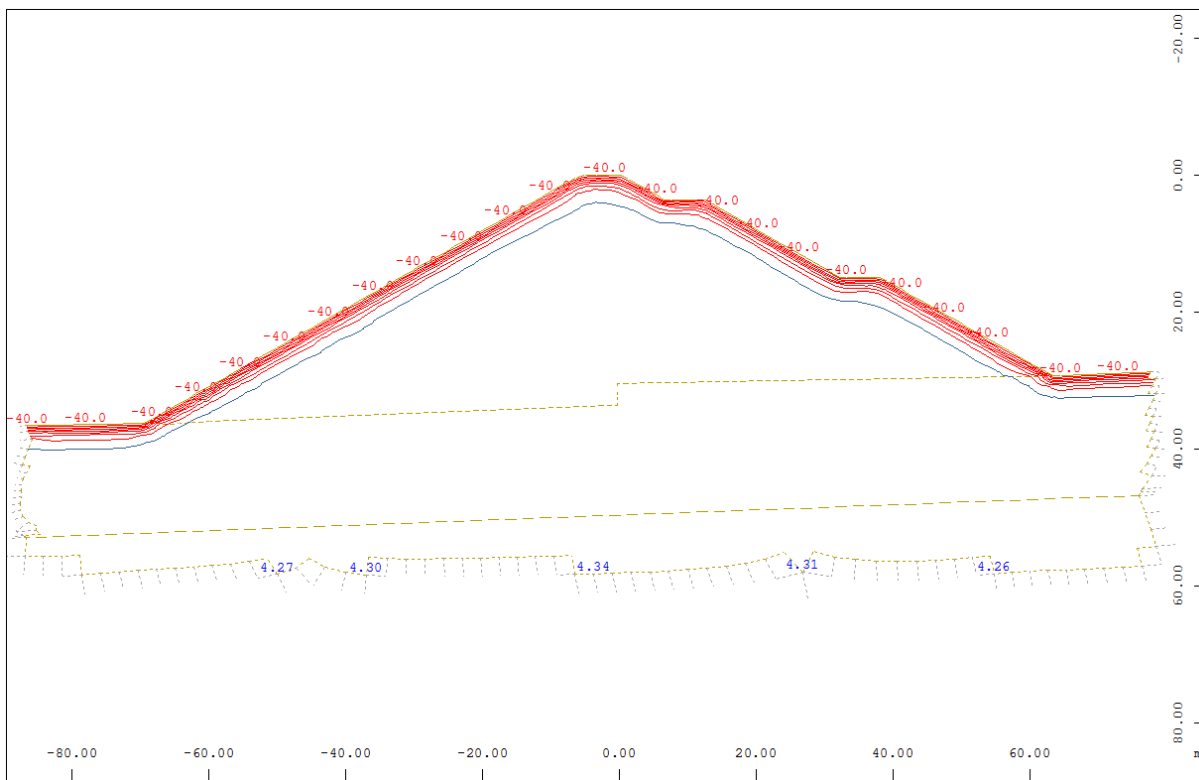


Figure 183: transient temperature analysis in °C, extreme minimum -40.0 °C for 7 days

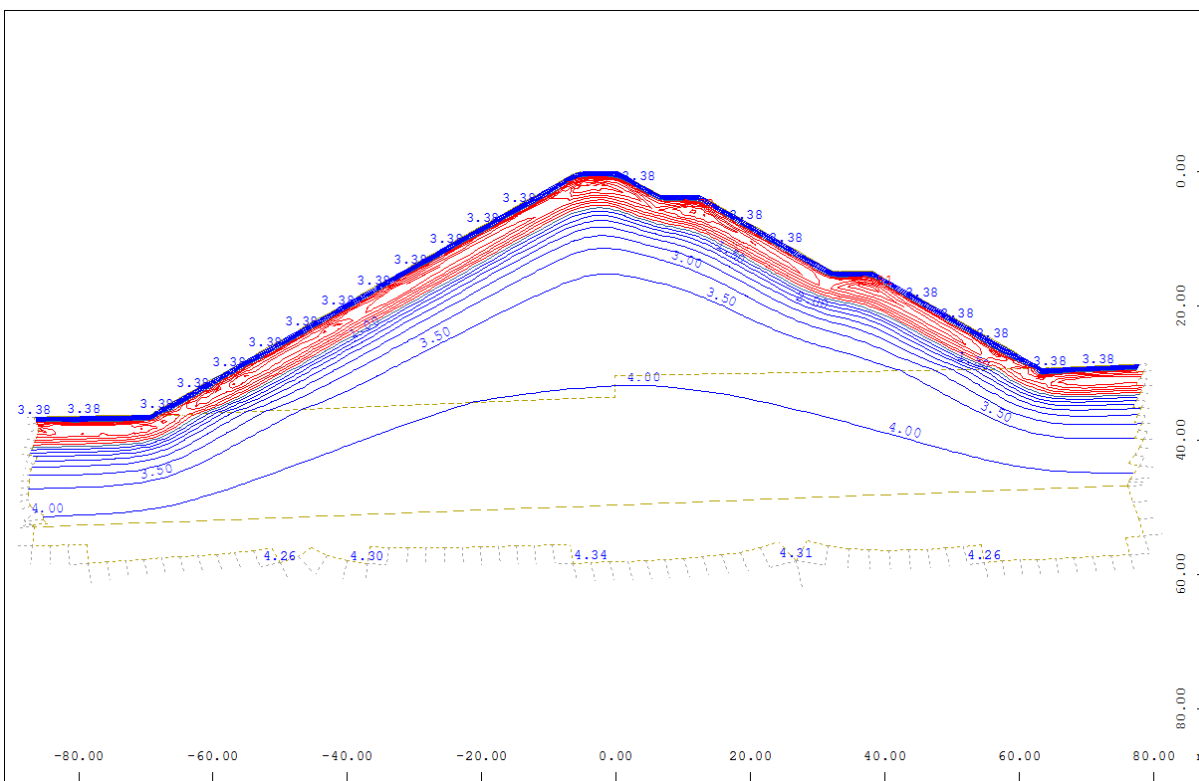


Figure 184: transient temperature analysis in °C, 14 days after extreme minimum, 3.375 °C

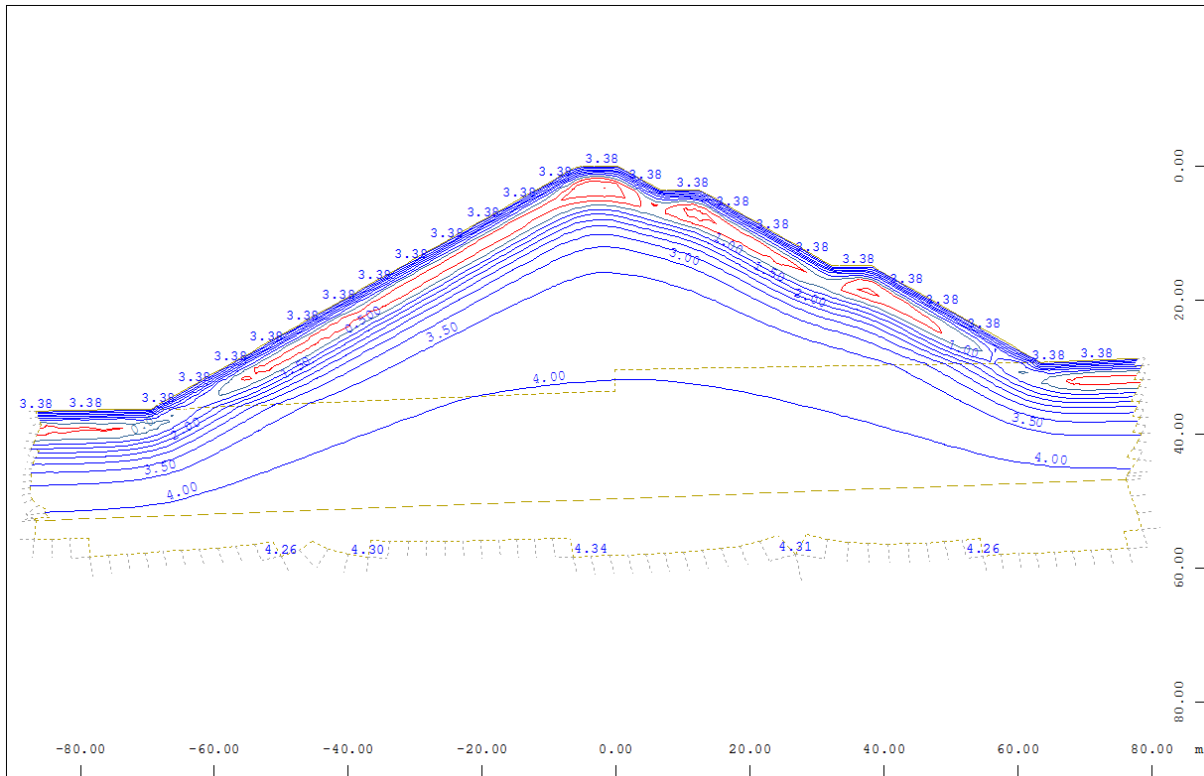


Figure 185: transient temperature analysis in °C, 28 days after extreme minimum, 3.375 °C

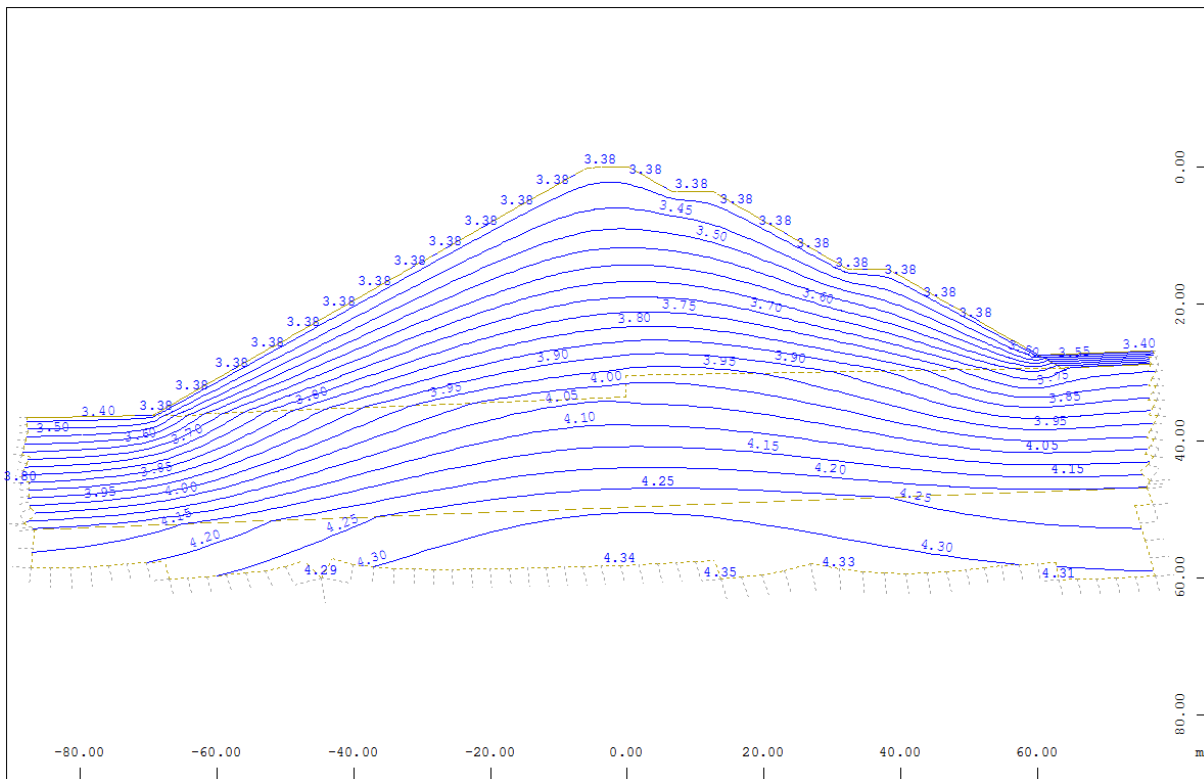


Figure 186: stationary temperature analysis in °C, mean annual air temperature 3.374 °C

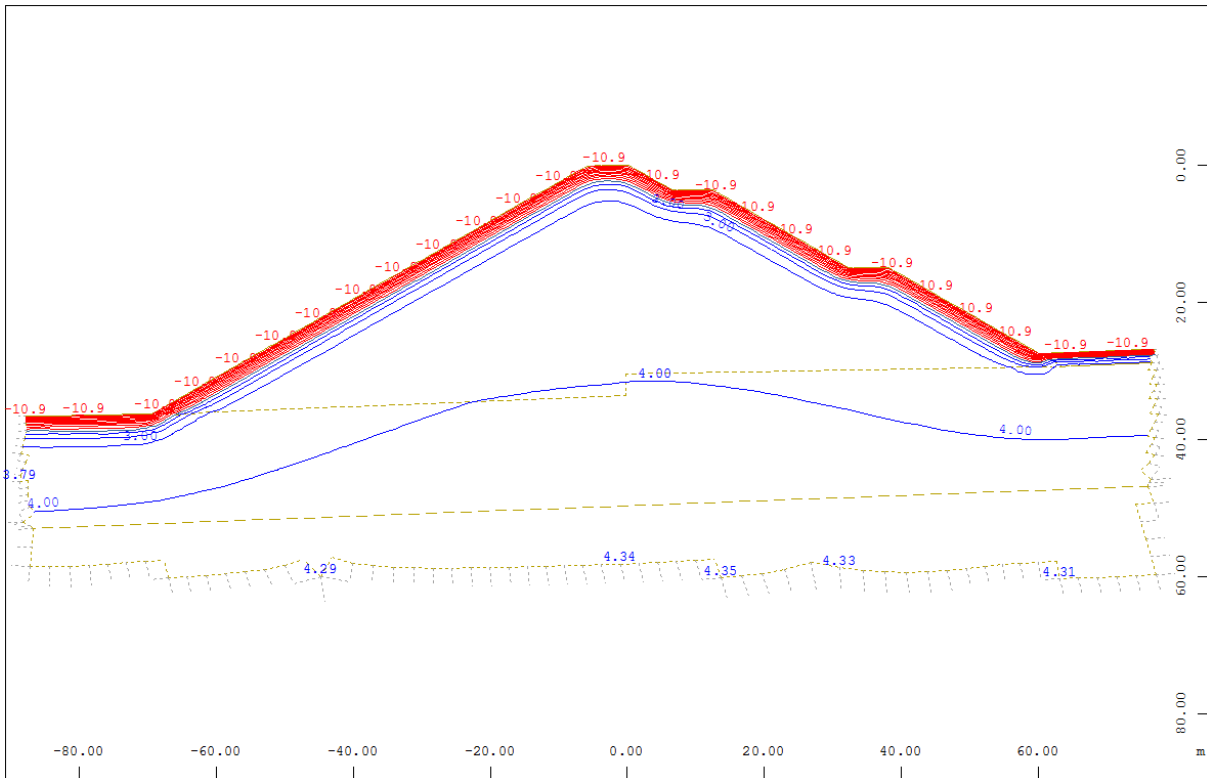


Figure 187: transient temperature analysis in °C mean weekly temperature -10.9 °C

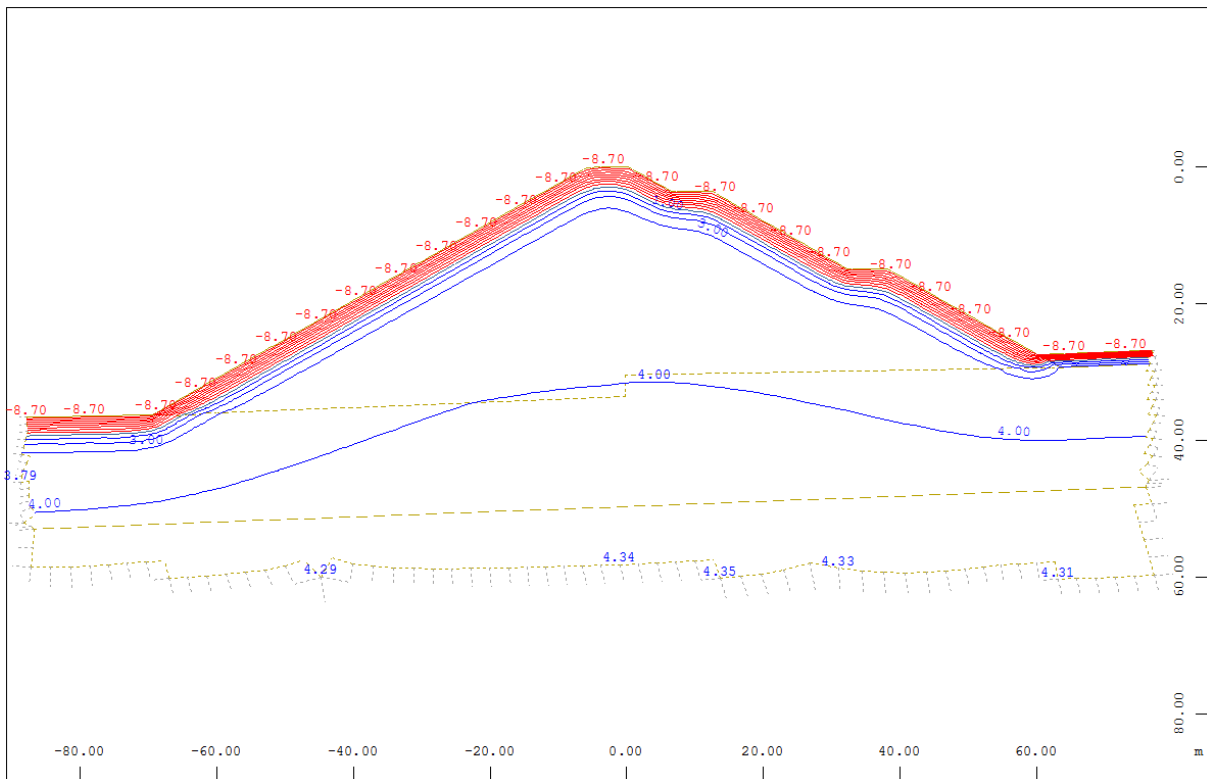


Figure 188: transient temperature analysis in °C mean weekly temperature -8.70 °C

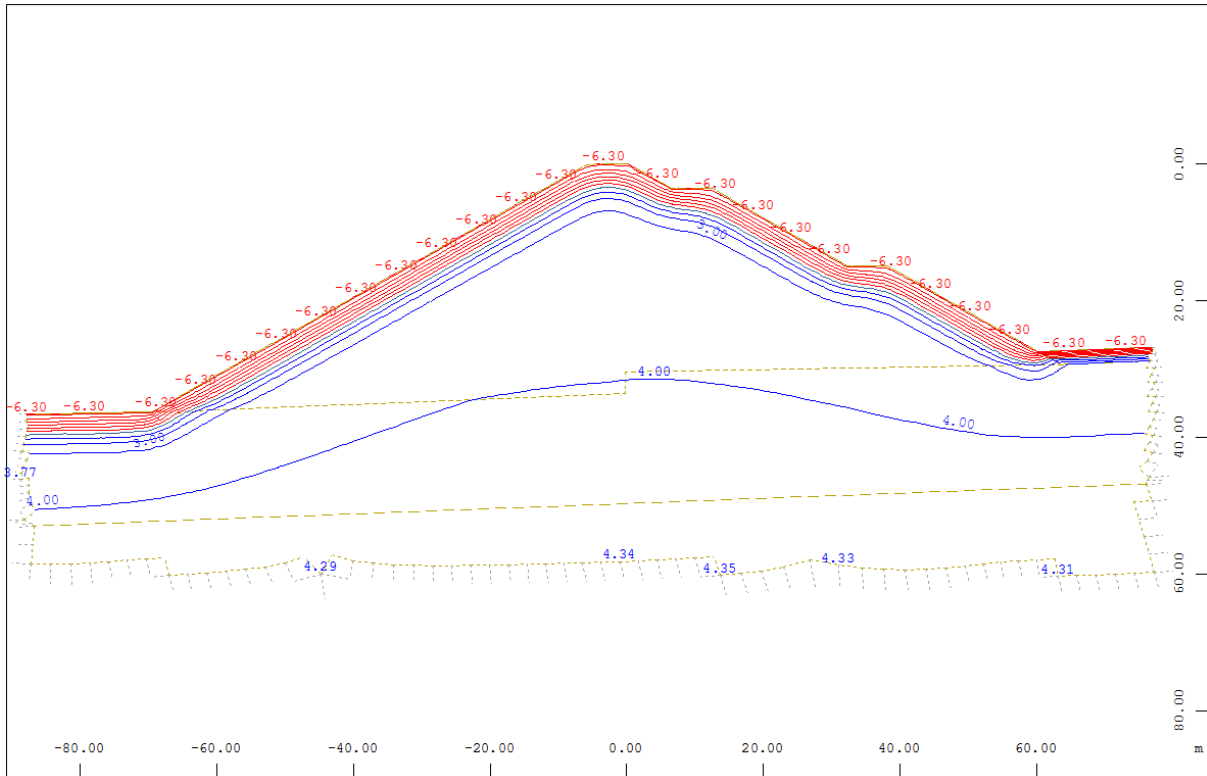


Figure 189: transient temperature analysis in °C mean weekly temperature -6.30 °C

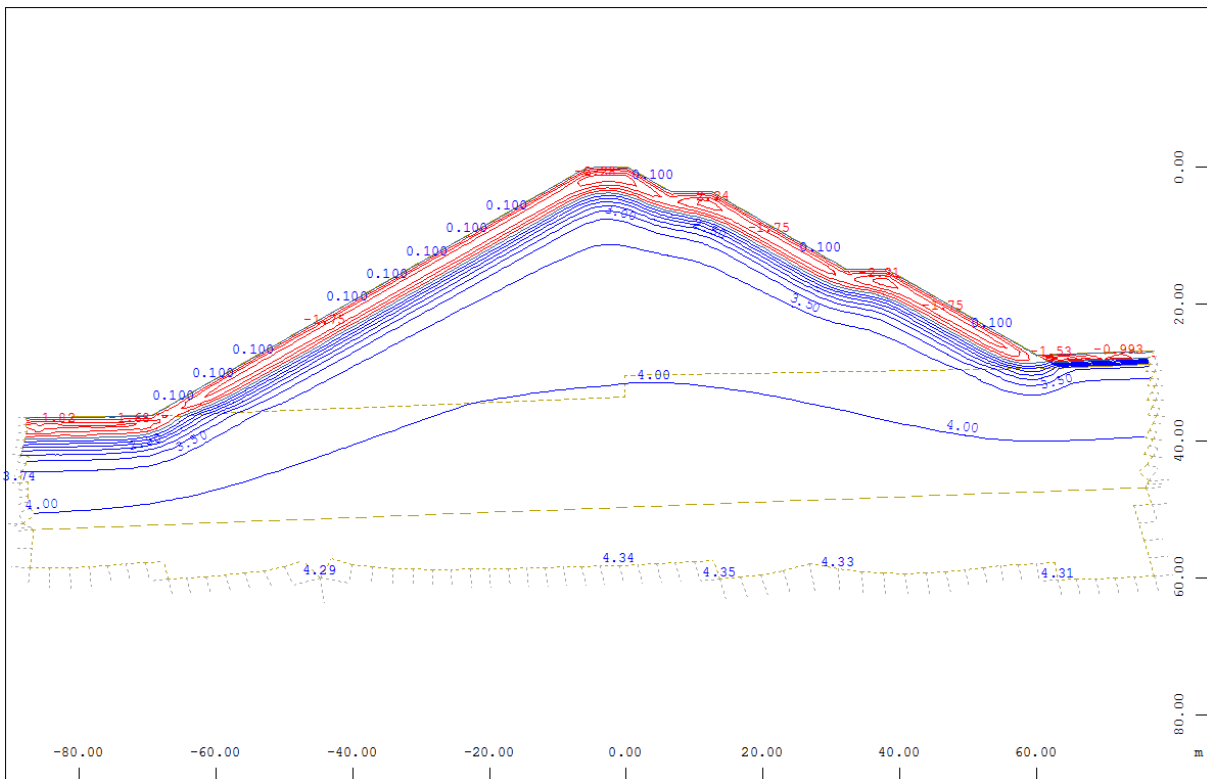


Figure 190: transient temperature analysis in °C mean weekly temperature 0.10 °C

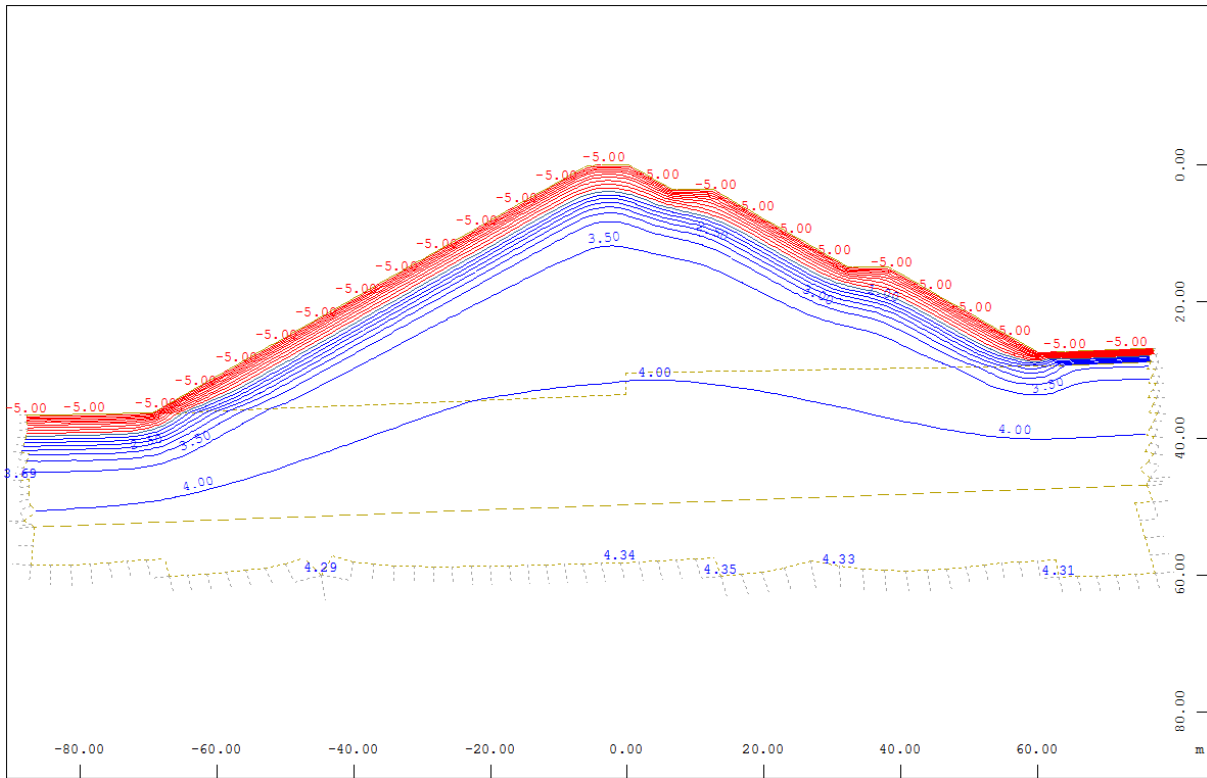


Figure 191: transient temperature analysis in °C mean weekly temperature -5.00 °C

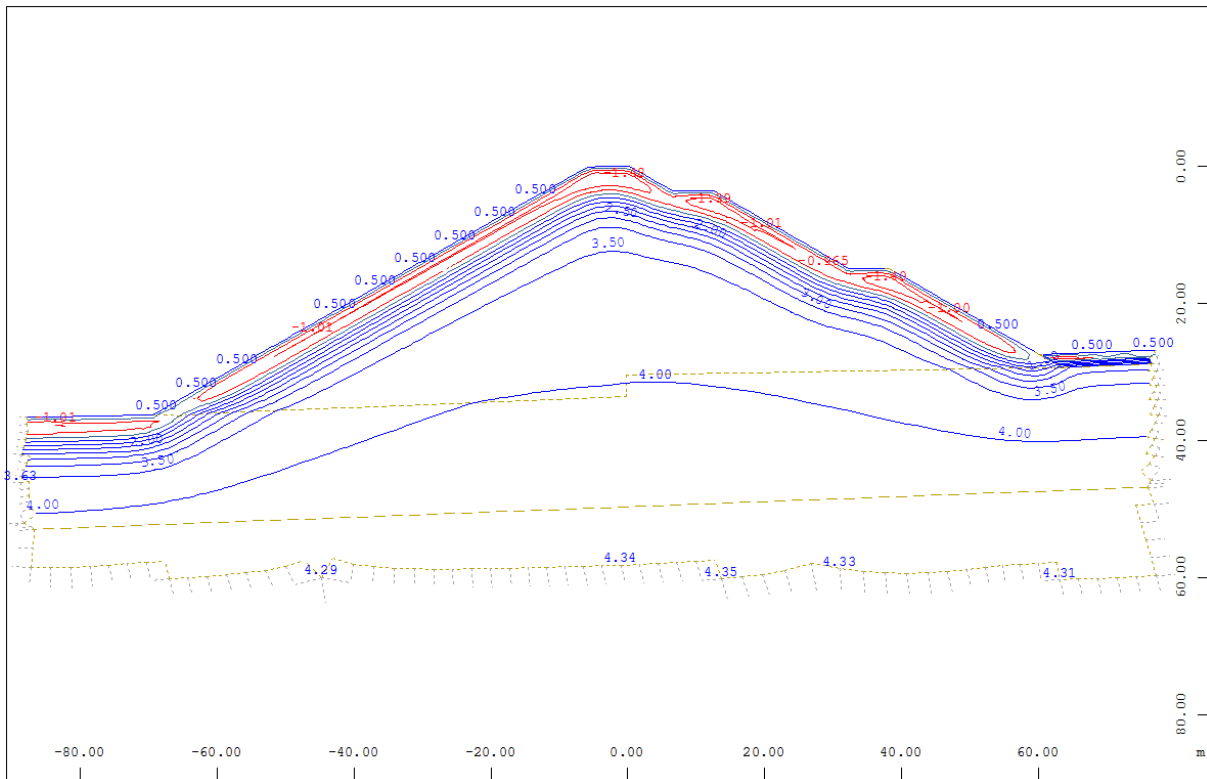


Figure 192: transient temperature analysis in °C mean weekly temperature 0.50 °C

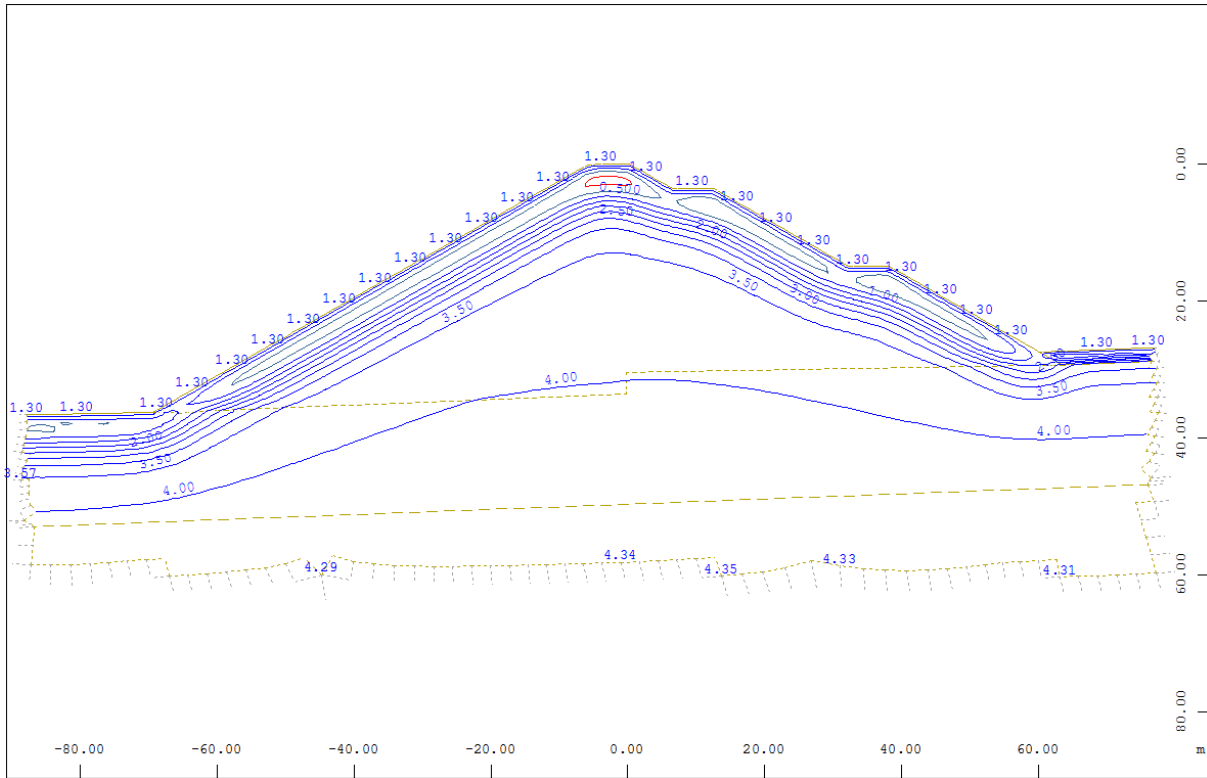


Figure 193: transient temperature analysis in °C mean weekly temperature 1.30 °C

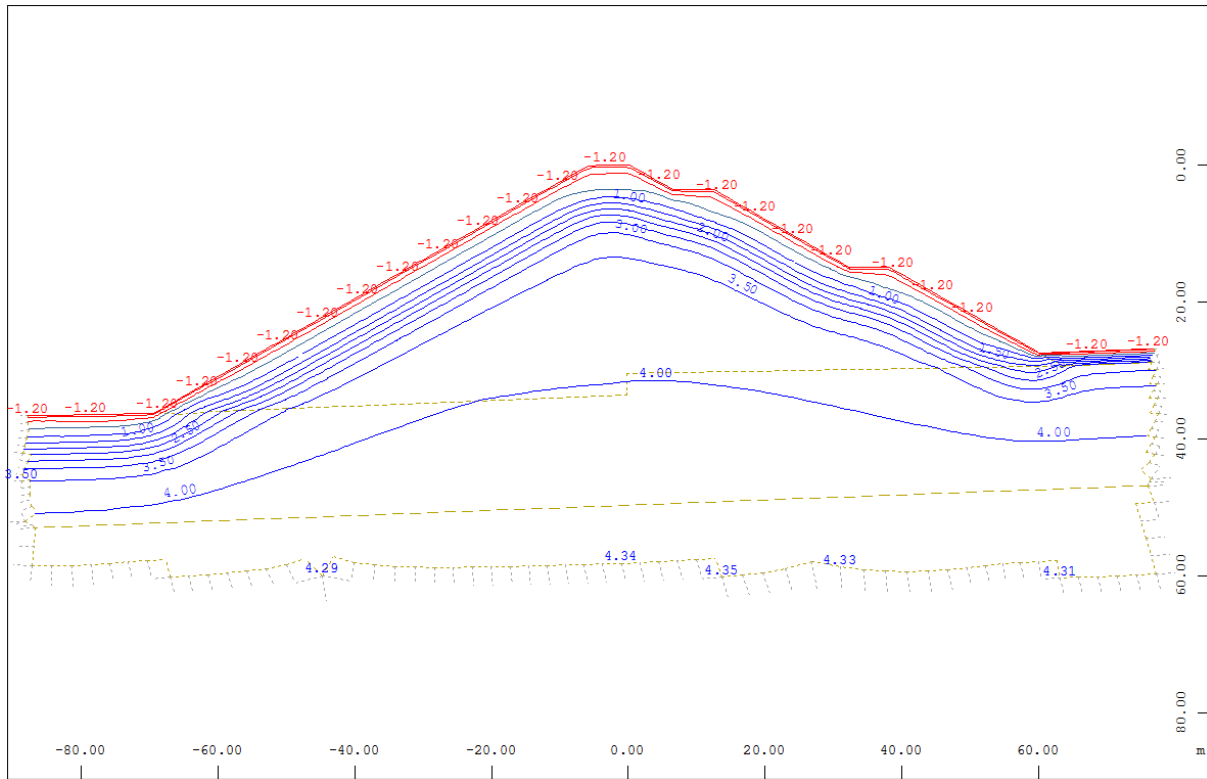


Figure 194: transient temperature analysis in °C mean weekly temperature -1.20 °C

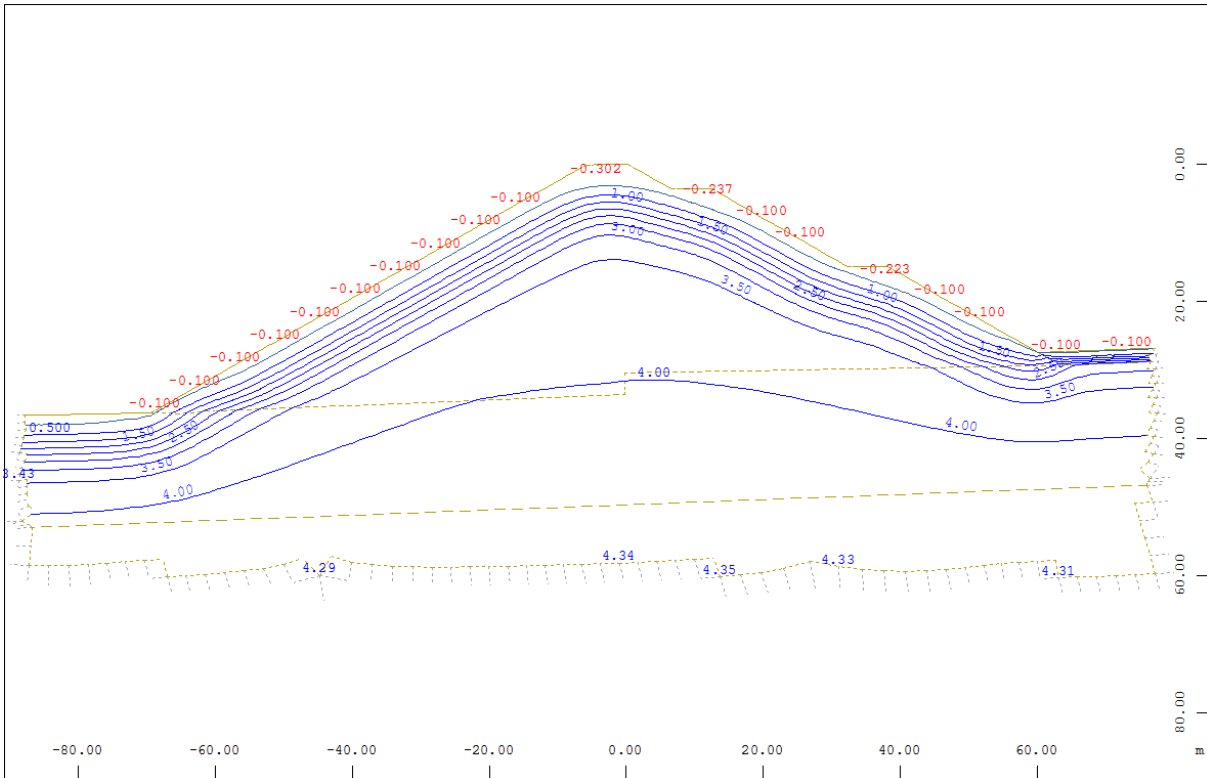


Figure 195: transient temperature analysis in °C mean weekly temperature -0.10° C

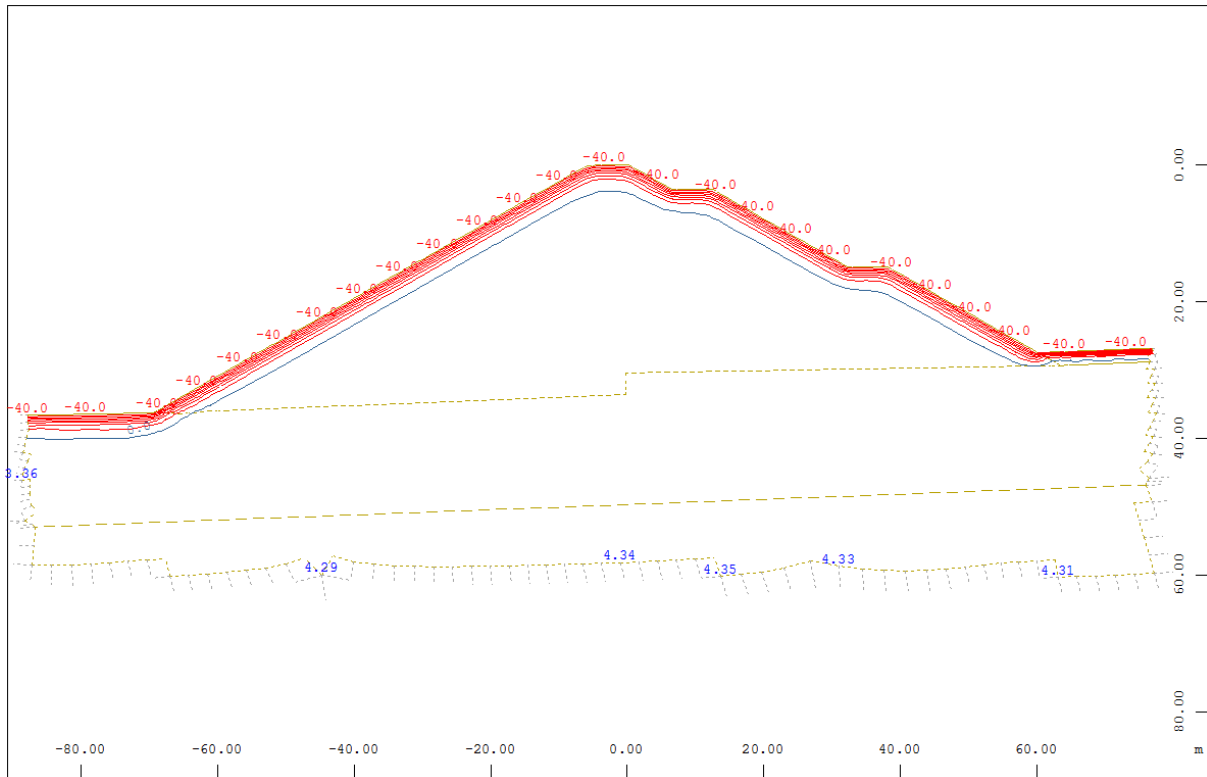


Figure 196: transient temperature analysis in °C, extreme minimum -40.0 °C, 7 days

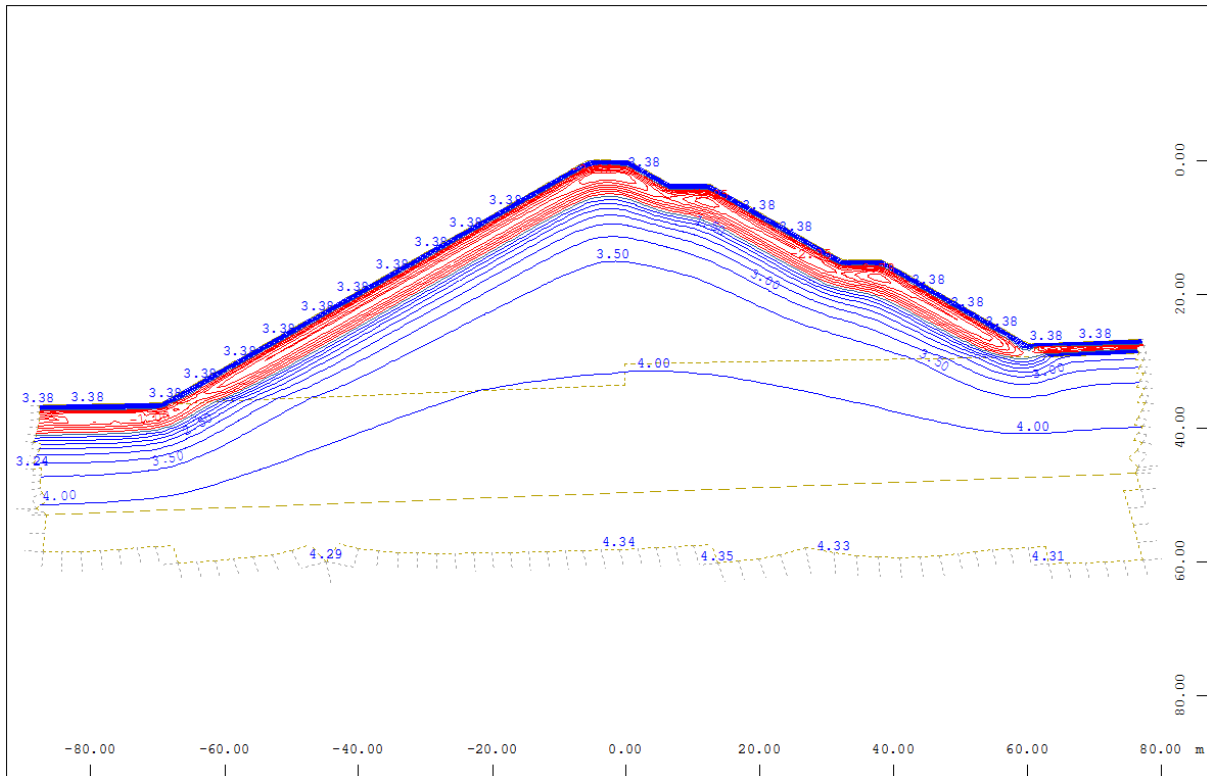


Figure 197: transient temperature analysis in °C, 14 days after extreme minimum, 3.375 °C

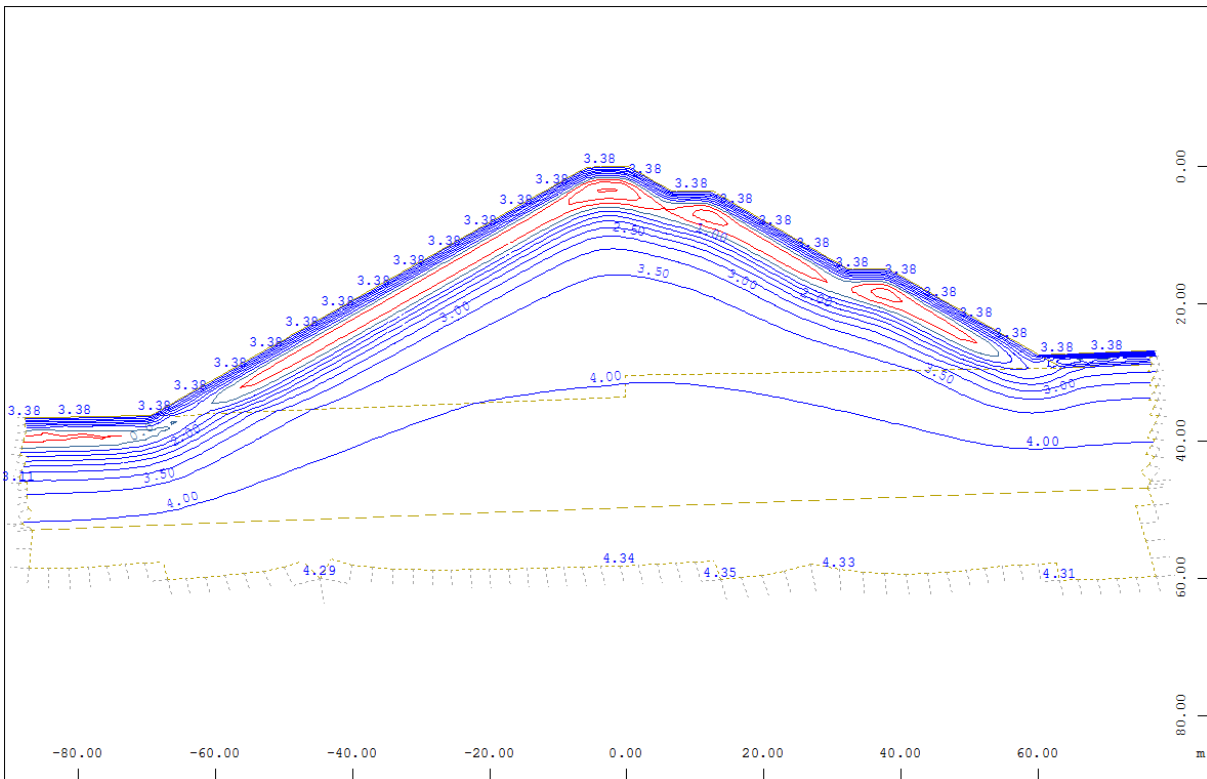


Figure 198: transient temperature analysis in °C, 28 days after extreme minimum, 3.375 °C

16 CONSTRUCTION

16.01 Preliminary and rough Construction Staging Concept

The construction of the entire structure is proposed to be carried out in the following major steps:

- 1) Preconstruction works possibly including the access road up to the right abutment.
- 2) Establishment of deep foundation elements for seepage cut-off measures with a secant pile wall as well as ground improvement below the bottom outlet structure.
- 3) Establishment of a grout curtain in the bedrock abutments and underneath the pile wall, including structural grouting at the interface between the secant pile wall and the bedrock as well as the secant pile wall and the capping beam.
- 4) Preparations for dam construction works:
 - a. Establishment of temporary water management measures by means of bypass pipes or a temporary channel;
 - b. Preparation of the pile heads of the secant pile wall for the construction of a capping beam;
 - c. Preparation of the rock abutments by cutting a trench into the grouted rock. The rock trench will be equipped with a flexible sleeve pipe for structural grouting after concreting of the foundation of the seal wall and backfilling to a certain height;
 - d. Preparation of the improved footprint of the bottom outlet structure;
 - e. Leveling and compacting of the footprint of the embankment dam;
- 5) Construction of the stilling basin which reaches underneath the downstream embankment including the baffles;
- 6) Concreting of the outlet structure, the intake box and the outflow;
- 7) Moving the water management back through the outlet structure;
- 8) Subsequent concreting and filling of the embankments including installation pipes for instrumentation facilities;
- 9) Construction of the armored downstream lining including the piers at the toe of the downstream slope;
- 10) Testing of the structure by means of a test storage, 10m in height followed by a controlled draw down;
- 11) Installation of the throttle;
- 12) Installation of the debris rake;
- 13) Landscaping.

16.02 Description of Grout Works and Deep Foundation Works

16.02.01 Deep Foundation

Deep foundation works are required for the construction of the secant pile wall and the ground improvement underneath the bottom outlet structure, which is planned to be done by means of jet grouting.

16.02.01.01 Secant Pile Wall and Adjacent Support Piles for the BOS

The design provides a 52m long, straight aligned secant pile wall where secondary piles are reinforced and cut into the primary piles, which are not reinforced. Piles are socketed into bedrock with a minimum depth of 1m. The selected pile diameter is 1.25m to compensate for axial deviations during drilling (structurally required

diameter is 1m). A spacing of 0.9m and an intersecting length of 0.35m results in a nominal wall thickness of 0.87m and a minimum wall thickness of approximately 0.5m considering deviations during drilling. Connection reinforcement for structural connection to a reinforced cast in place capping beam is integrated in the reinforcement cage of the secondary piles. Sleeve pipes are provided for structural grouting at the interface between the seal wall and the secant pile wall. In addition, the interface between pile wall and seal wall is covered with impervious material placed upstream of the core structure (see chapter 10.01).

Piling will be done from the existing terrain formed from alluvial deposits, which will be leveled and compacted prior to pile works. Water management will be established prior to piling and needs to be rearranged for piling the section where water management is located first. Piling and improvement of the section where the bottom outlet structure is located allows to concrete the BOS as soon as possible and to establish water management through the BOS in an early stage.

The following construction requirements are to be considered for piling in the alluvial deposits:

- Cased Drilling;
- Use of optimized concrete mix for minimizing loss and excessively consumption of concrete during pulling back of casing;
- Detailed monitoring of concrete volume consumption during pulling back of casing;
- Boring, chiseling, grabbing, embedment into bedrock formed by reverse circulation drill or other methods.

16.02.01.02 Jet Grouting for Ground Improvement

Ground improvement for the bottom outlet structure shall be performed by means of jet grouting. Independently working drill- and grout rigs can establish columns along the BOS-axis.

The process is to drill with a string of jet grouting rods into the alluvium and for approximately 1m into the bedrock by a rotary drilling rig. The lower end of the drill string is fitted to a nozzle holder and a laterally mounted jet grouting nozzle. In a second step a cement based grout slurry is pumped through the drill string to the jet grouting nozzle at high pressures. The resulting high-velocity "cutting jet" erodes the soil from its natural position and mixes it with the grout slurry. The erosion distance of the jet is determined by the density and the type of soil. By rotating and simultaneously retracting the jet grouting drill string, the trace of the cutting jet forms a tightly-spaced helix in the soil, resulting in a column-shaped space filled with grout slurry and soil.

There are several techniques available for improving ground by means of jet-grouting such as cutting the soil directly with the grout slurry, and adding air into the slurry (air shrouding) for obtaining greater diameters, applied in granular and coarser soils. Other techniques with water cutting are for cohesive soils and therefore not applicable here.

Ahead of the production of columns, test columns will be grouted, excavated and tested for homogeneity and strength to inform the detailed jet-grouting parameters. Final drill and jet-grouting pattern and shape of columns need to be determined based on the real-scale jet-grouting tests. This forms a mandatory part of jet-grouting works.

Jet grouting requires a slurry management consisting of a high turbulence mixer, an agitator and pumps. Occurring backflow of grout slurry needs to be managed accordingly, disposed off-site or used for improving the footprint of the embankment structure.

16.02.02 Rock Grouting

16.02.02.01 Purpose of Rock Grouting

Because high transmissivity was observed during water pressure tests conducted in test drill-holes underneath the footprint and at the lower abutments, which indicated Lugeon values of up to 150 [l/m/min], substantial seepage through the bedrock is expected under loading conditions. This can result in internal erosion in the embankment fill as well as in the alluvial deposits, and subsequently in the development of piping and dam destabilization.

Rock grouting shall reduce the transmissivity in the bedrock to an acceptable value of 10 Lugeon. The extension of the grout curtain is shown in drawing no. LTMM CC-DFG-403. The initial preliminary grout holes pattern for primary and secondary holes is shown in drawing no. LTMM CC-DFG-401.

16.02.02.02 Description of Grout Works

Execution of Grout Works under the Direction of the Owner

Drilling, water pressure testing, and grouting shall be performed under the technical direction of the Owner and its technical representative, an experienced grouting engineer. This direction includes the determination of grout pressures and flow rates as well as advices regarding the grout mix design and grouting sequence in general and per grout hole.

Grouting Equipment

The following grouting equipment is required amongst others:

- Drill rigs capable of drilling through the alluvium and through piles into the bedrock (partly cased drillings);
- Drill rigs for drilling on steep creek slopes, including securing of rigs for precise drill hole geometry;
- Fully electronic working water pressure testing equipment for Lugeon tests with single packers and double packers;
- Acoustic and optical bore hole imaging equipment;
- Cement containments for ordinary Portland cement as well as for fine cement.
- Grout mix plant containing a high turbulence mixer, agitator, slurry storage, at least 4 double piston pumps fully electronic controlled and implemented into an electronic grout control;
- Grout packers, valves and pressure gauges at the borehole mouth for transient pressure analysis;
- Plastic sleeve pipes and equipment for mounting geotextile packers for multi packer sleeve pipes;
- Water supply;
- Service and maintenance container.

Commissioning and Proof of Functionality of Equipment

Prior to the work it will be proved that all equipment mobilized to site is fully functional and calibrated. This includes:

- Generators, light plants, material storage, waste management etc.;

- Drill rig condition, sufficient spare parts, drill rod and grout pipe handling capabilities, drill bit condition, proof of ability to drill in the alluvium and in the bedrock;
- Grout mixing plant condition, setup, containment of cement, grout pump condition, batching capability, cleaning and maintenance;
- Grout header condition, flow control setup, grout hose lengths and diameters, initial calibration checks on all flowmeters and pressure transducers, condition and adequacy of valves and connections, whip checks for high pressure lines, test run of water through system, cleaning and maintenance;
- Maintenance record of the drill rigs to be used for the project;
- Adequacy of the real-time data acquisition system for monitoring water pressure testing and pressure grouting operations;
- Packer inflation and deflation methods as well as leakage allowance past the packer; double packer setup for water pressure testing;
- Adequacy of grout mix testing equipment;

General Grouting Sequence

It is planned to establish a three-row grout curtain whereas the upstream grout curtain shall be established first, the downstream grout curtain second and the central curtain last. In general, grouting shall be done bottom up and at the creek axis first.

Upstage Working

In general it is planned to work upstage which comprises drilling the grout hole to full depth, washing and cleaning the hole, setting the packer at the top of the lowest stage, and then grouting that stage. If the target injection pressure and/or grout volume is reached, grouting may be continued by placing the packer at the next stage above. If the target pressure or volume is not reached under application of the design grouting parameters, then intervention is required. For poor pressure development this can be e.g.:

- (a) Stopping for 10 to 20 minutes for the development of filtration in the fissure and restarting grouting work;
- (b) Change of mix to a lower water binder ratio or change to another general mix design;

For poor grout take e.g.:

- (a) Rising of pressure limited with 90% of fracking pressure;
- (b) Change of mix to a higher water/binder ratio or admixture of plasticizer;

Split Spacing

For progressively closing the grout curtain, drilling and grouting is conducted on an initial pattern for primary holes. The secondary holes will subsequently be drilled and grouted at intermediate positions between the primary holes. The detailed spacing of holes may vary depending on conditions encountered during grouting. Generally, secondary holes are located half way between primary holes. For tertiary holes and quaternary holes, the same scheme is applied.

Grouting of Contact between alluvium and Bedrock

Grouting of the contact between the alluvium and bedrock will comprise of drilling and grouting of the curtain using MPSP grouting technique.

General Description of Grout Mixes

In general simple and stable cement based grout mixes shall be applied. For stable grout mixes (bleeding is limited to a maximum of 2% after two hours) the water/binder ratio for an Ordinary Portland Cement (OPC) based mix shall be below 0.9 (0.8). Stabilizers and plasticizers shall be limited to a minimum required. If required for grouting of fine fissures the water/cement ratio for OPC mixes may be of up to 1.1 by using bentonite based stabilization, which requires admixture of plasticizers. Fine cement mixes shall be designed under consideration of the same principles. The grout mix design, grouting parameters as well as intervention and stop criteria shall be established within grout tests ahead of construction of the grout curtain.

The grout mix shall be tested for the following parameters:

- Bleeding
- Pressure Filtration Coefficient
- Marsh Value
- Yield Stress
- Specific Weight
- Compressive Strength

Monitoring of Grouting

As grouting will be directed by the Owner, monitoring of ground response during grouting is required. Measurements of grout injection pressure needs to be done within 2m of the hole collar. Flow rate is measured at the pumps. Pressure, injected volume and grouting Lugeon data shall be recorded automatically. Records shall be made available as single, time synchronized ASCII text files (*.csv) at a scanning frequency of at least 1 Hz for each grout hole and each grout section. All other grout parameters such as the grout mix currently being applied and incidences shall be recorded and time stamped as well.

Control of Grout Success

The grout success will be subsequently monitored and analyzed by recoding and evaluating the grout parameters and application of the grouting Lugeon Value (GuL – see Equation 34).

$$Gul = \text{Flow rate} \left(\frac{L}{m} \right) \cdot 10\text{bar/MPa}/P_{\text{eff}}(\text{bar})/m_{\text{stage length}} \cdot \frac{V_{\text{Marsh Grout}}}{V_{\text{Marsh Water}}} \quad \text{Equation 34}$$

Additionally, selected grout holes will be tested with water pressure tests for the determination of the remaining transmissivity at certain grout stages. For completion of grout works the Lugeon value determined at a number of at least five grout holes, which are accordingly arranged along and inside the grout curtain, must not be higher than 10 [l/min/m]. If values are exceeding 10 Lugeon the grouting works will continue.

16.03 Description of Earthworks

16.03.01 Footprint

The footprint will be leveled and compacted prior to construction. Cohesive or soft soil layers as well as sand lenses will be removed and soil exchange is applied. Compaction of the footprint shall be done with a vibratory roller compactor with a total weight of at least 15tonnes. The footprint construction needs to be inspected, tested for loading capacity (stiffness) and approved by the geotechnical site engineer. Minimum required loading capacity is to be defined within the final stage of the design.

16.03.02 Embankment Fill

The embankments will be constructed by filling and compacting zone 1 and 2 material in lifts of 60cm thickness. Zone 3, as well as Zone 6, shall be filled and compacted ahead of adjacent fill by at least 1.2m. Zone 3, as well as Zone 6, which are located downstream of the seal wall, shall be filled and compacted in lifts with a maximum thickness of 30cm each. This sequence prevents the seal wall from damages by larger components.

The seal wall shall not be poured higher than approximately 5m ahead of filling.

The height difference between the upstream and downstream embankment within the course of construction has to be limited to 1.0m to limit unilateral loads to the concrete core.

A lateral excess of at least 1m has to be filled and compacted accordingly to assure complete compaction of the nominal support body. Lateral excess material shall be profiled after completion of embankment filling. Additionally completed and profiled slopes shall be compacted using an adequate vibratory roller compactor.

The compaction of single lifts has to be carried out with a vibratory roller compactor with a minimum required weight of 15tonnes. The conformity of lifts shall be monitored using continuous compaction control as well as independent checks of loading capacity. After construction of any five lifts, loading capacity shall be verified at selected test spots, using plate loading tests or other adequate testing procedures.

No individual construction criteria for the drainage material is defined. However, it has to be guaranteed that drainage material is placed with a smooth and even surface and according to design. Drainage layers must not be accessed by dirty construction machines. Drainage layers must not be contaminated neither with other fill material, cement slurry or dirt.

16.03.03 Construction Equipment

The following equipment is required for the construction of the embankments:

- Rock Trucks;
- Bulldozers;
- Excavators equipped with bucket of varying size and shape as well as with hydraulic hammers;
- Sheep foot vibratory roller compactors with a minimum total weight of 10t for Zone 3 material;
- Vibratory roller compactors with a minimum required weight of 15t;
- Trench roller compactor for compacting the protection layer adjacent to the concrete core with a minimum total weight of 10t;

Further equipment is required for on-site material processing such as:

- Crusher and Screen for processing material to the required grading;
- Excavator for filling the screen and/or the crusher and for loading rock trucks;

16.03.04 Quality Control

Quality control shall be done according to the guideline of the US Federal Emergency Management Agency – Filters for Embankment Dams (FEMA, 2011).

For a minimum of required quality control of earth works, the following aptitude tests and checks shall be performed:

- Grain size distribution;
- Large direct shear box tests as well as triaxial tests;
- Proctor tests;

- Water permeability tests;
- Determination of unit weight of built in and compacted fill;
- Check of loading capacity / stiffness of fill layers.

Test for Zone 3 material:

- Sieve and hydrometer analysis;
- Atterberg limits;
- Water permeability;
- Standard proctor density;
- Determination of unit weight of built in and compacted fill;
- Check of loading capacity / stiffness of fill layers.

Fill and Compaction Tests ahead of Construction:

For confirmation of the suitability of the construction process, a test field shall be established on site to determine the following parameters:

- Number of compaction passes required for each class of material;
- Suitability of the deployed compaction equipment and definition of settings of the roller compactors such as for the eccentric and frequency;
- Determination if final grain size distribution of fill material after compaction for refinement of grading for supplied fill material;
- Calibration of continuous compaction control using static and dynamic plate loading tests or other adequate testing procedures;

Extend of Quality Control during Filling for all fill materials except Zone 3 Material:

- Three large direct shear box tests and one triaxial test per 10,000m³ of filled volume;
- In situ test of water permeability by infiltration tests per 5,000 m³ of filled volume;
- Evaluation of the uniformity and conformity of compaction for each lift using continuous compaction control;
- Plate loading tests or other adequate testing per 5,000m³ of filled volume.

Extend of Quality Control during Filling for Zone 3 Material:

- Sieve and hydrometer analysis per 2,500m³;
- Atterberg Limits per 2,500m³;
- Water permeability per 2,500m³;
- Loading Capacity / stiffness per 5,000m³;

17 TESTING AND COMMISSIONING

For the evaluation of installed dam instrumentation, a check of water tightness of sealing measures, as well as for a check of other seepage control measures and the emergency bypass, a test storage shall be performed. After reaching the target impoundment elevation, a controlled draw down shall be commenced. During the test storage, the emergency preparedness plan shall be executed for initial training.

The intended target storage level is 10m above the elevation of the invert at the throttle. To achieve this impoundment level, the opening at the throttle shall be equipped with a winding gate able to regulate discharge for emptying the retention basin after testing. For safety reasons, explosives shall be affixed at the gate, in case of troubles during the initiation of the drawdown.

The target impoundment level of 10m above the invert at the throttle section shall be achieved and maintained for at least 10 days. During the testing procedure, the impoundment level shall be kept stable by controlling the winding gate. The discharge during drawdown shall be limited to 10m³/s and the response of the downstream channel shall be monitored.

The following sequence is intended to be executed:

- 1) Terrestrial detail survey of all construction elements of the structure, in particular the top of the seal wall, the crest of the embankment, the intake structure, the outlet structure of the bottom outlet, the heads of pipes encasing inclinometers and piezometers and the stilling basin;
- 2) Check of all dam instrumentation facilities, data transmission equipment and accessibility and visualization tools of monitoring data;
- 3) Installation of winding gate including explosives;
- 4) Closing of the winding gate;
- 5) Impoundment until target impoundment level is reached;
- 6) Controlling the winding gate for a stable test storage level;
- 7) Observation of monitoring data and visual inspection three times a day including photo documentation;
- 8) Recording of web camera pictures in a frequency of at least 1hour;
- 9) Holding the storage level for 10 days;
- 10) Opening of the winding gate and initiation of the controlled drawdown;
- 11) Visual inspection of all elements of the structure and photo documentation, as well as complete terrestrial survey of tachymeter survey points;
- 12) Repair works as required;
- 13) Installation of the throttle and start of normal operation.

18 CREEK SLOPE STABILITY ASSESSMENT

18.01 General

18.01.01 Purpose of the Analysis

For the assessment of potential rock-slope instabilities within the retention basin that may be affected by impoundment, subsequent drawdown, and resulting joint water pressure, a geomorphic and geotechnical analysis of rock slopes was conducted. The analysis comprises the following:

- Mapping of geomorphic phenomena focusing on slope instabilities;
- Analysis of geologic structures by means of kinematic analysis of planar sliding and wedge sliding using the software tool Dips (Rocscience Inc.)
- Semi-static analysis for wedge sliding considering ground movement using the software tool Swedge (Rocscience Inc.)

Results are shown in chapters 18.02, 18.03 and 18.04 as well as corresponding drawings and maps as listed in Table 83.

Table 83: Overview of chapters and drawings for the Creek Slope Stability Assessment

Chapter	Assessment	Corresponding Drawings			
		Drawing Number	Type	Scale	Content
18.02	Mapping of Geomorphic Phenomena	LTMM CC-GEN-020 R00	Plan View	1:5,000	Geomorphic Map General Overview
18.03	Kinematic analysis of planar and wedge sliding	LTMM CC-CSSA-110 R01	Plan View	1:2,500	Slope Gradient Map Construction Site Creek Slope Stability Assessment
		LTMM CC-CSSA-111 R01	Stereo Plot	N/A	Kinematic Analysis Sector 1 Creek Slope Stability Assessment
		LTMM CC-CSSA-112 R01	Stereo Plot	N/A	Kinematic Analysis Sector 1 Creek Slope Stability Assessment
		LTMM CC-CSSA-113 R01	Stereo Plot	N/A	Kinematic Analysis Sector 2 Creek Slope Stability Assessment
		LTMM CC-CSSA-114 R01	Stereo Plot	N/A	Kinematic Analysis Sector 3 Creek Slope Stability Assessment
		LTMM CC-CSSA-115 R01	Stereo Plot	N/A	Kinematic Analysis Sector 4 Creek Slope Stability Assessment
		LTMM CC-CSSA-116 R01	Stereo Plot	N/A	Kinematic Analysis Sector 5 Creek Slope Stability Assessment
		LTMM CC-CSSA-117 R01	Stereo Plot	N/A	Kinematic Analysis Sector 6 Creek Slope Stability Assessment
		LTMM CC-CSSA-118 R01	Stereo Plot	N/A	Kinematic Analysis Sector 7 Creek Slope Stability Assessment
18.04	Semi-static sliding wedge analysis	LTMM CC-CSSA-119 R01	Stereo Plot	N/A	Kinematic Analysis Sector 8 Creek Slope Stability Assessment
		LTMM CC-CSSA-120 R00	Stereo Plot	N/A	Wedge Stability Analysis Sector 9 Creek Slope Stability Assessment
		LTMM CC-CSSA-121 R00	Stereo Plot	N/A	Wedge Stability Analysis Sector 2 Creek Slope Stability Assessment
		LTMM CC-CSSA-122 R00	Stereo Plot	N/A	Wedge Stability Analysis Sector 3

Chapter	Assessment	Corresponding Drawings			
		Drawing Number	Type	Scale	Content
					Creek Slope Stability Assessment
		LTMM CC-CSSA-123 R00	Stereo Plots	N/A	Wedge Stability Analysis Sector 4 Creek Slope Stability Assessment
		LTMM CC-CSSA-124 R00	Stereo Plot	N/A	Wedge Stability Analysis Sector 5 Creek Slope Stability Assessment
		LTMM CC-CSSA-125 R00	Stereo Plot	N/A	Wedge Stability Analysis Sector 6 Creek Slope Stability Assessment
		LTMM CC-CSSA-126 R00	Stereo Plot	N/A	Wedge Stability Analysis Sector 7 Creek Slope Stability Assessment
		LTMM CC-CSSA-127 R00	Stereo Plot	N/A	Wedge Stability Analysis Sector 8 Creek Slope Stability Assessment
		LTMM CC-CSSA-128 R00	Stereo Plot	N/A	Wedge Stability Analysis Sector 9 Creek Slope Stability Assessment

18.01.02 Summary

As shown by the geomorphic mapping, the rock slopes adjacent to the retention basin of the Cougar Creek debris flood retention structure primarily feature steep cliffs with local potential rock-fall detachments, accompanied by numerous scree. No substantial larger slope instabilities, potentially endangering the retention basin, have been identified. Inside the retention basin a total of 9 relevant sectors with slope gradients equal to or greater than 50° (see Figure 199) were further selected for a detailed kinematic as well as sliding wedge analysis.

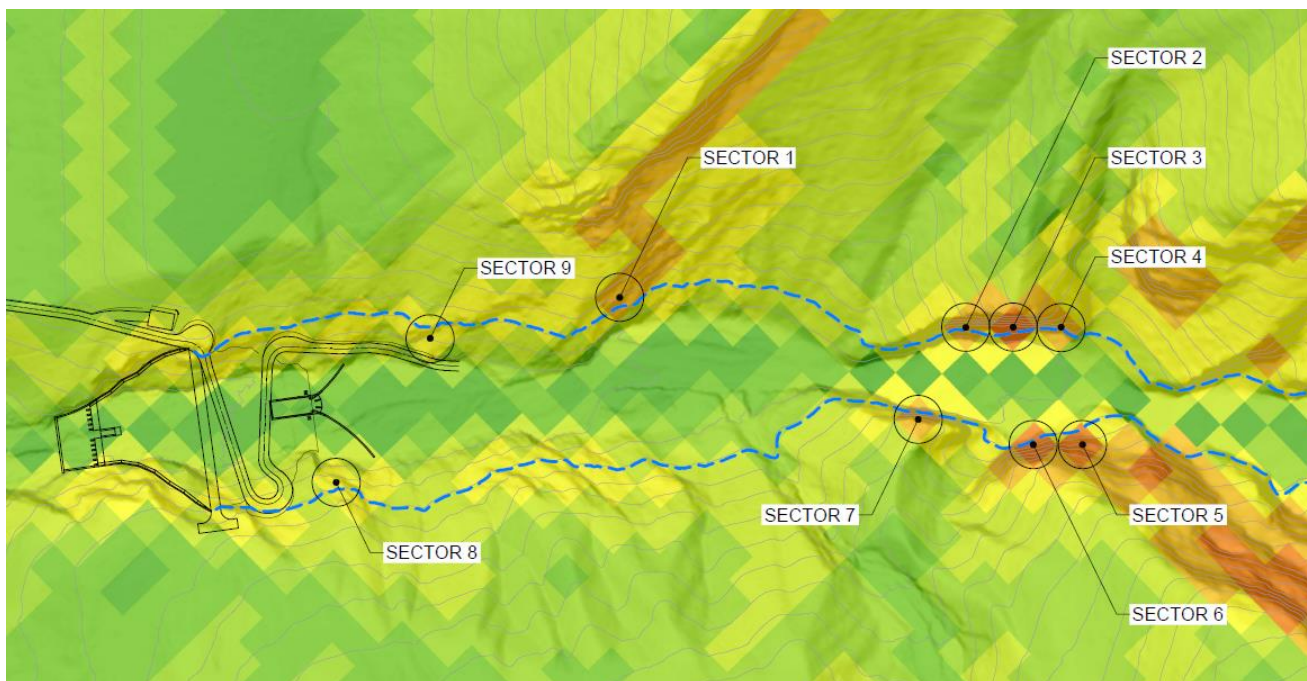


Figure 199: Slope gradient map with selected sectors for the kinematic and sliding wedge analysis, according to drawing LTMM CC-CSSA-110 R01

Based on available data of terrain and geologic discontinuities, the kinematic analysis shows that there is no significant risk for planar and/or wedge sliding of creek slopes. For nearly all investigated wedges, the calculations give a factor of safety greater than 1, for both dry conditions as well as for partially water filled fissures, even by applying conservative shear values.

Therefore, as shown by the assessment, no major instabilities of creek slopes within the retention basin could be identified. Although minor and local wedge detachments, as well as rock-fall related processes, have to be considered, the effects of these phenomena do not affect the capacity and safety of the Cougar Creek debris flood retention structure.

18.02 Geomorphic Phenomena

For a comprehensive analysis of the landscape and terrain, the geomorphic phenomena within the project area were mapped, based on the available digital terrain model. Moreover, multiple field surveys were undertaken by CHT in 2014 and 2015, and a surveying flight of the entire Cougar Creek watershed, focusing on rock slopes, conducted by BGC Engineering Ltd. and the Town of Canmore in 2014.

During the analysis, the following geomorphic phenomena were identified:

- general morphological phenomena;
- rock-fall related phenomena;
- fluvial phenomena.

The mapping of these phenomena is presented in the corresponding drawing LTMM CC-GEN-020. The area downstream of the fan apex is dominated by synglacial kame terraces, forming an irregularly shaped hill landscape. During the formation of these terraces, glacial meltwater shaped the drainage paths parallel to the Bow River valley, most likely partly occupied by a glacier. Closer to the active stream of Cougar Creek, this fossil and synglacial terrain has been superimposed by postglacial processes in form of erosional scarps, gullies as well as bank erosion and ridges, which all together with Cougar Creek and its channel form No Man's Land.

Upstream of the fan apex, the sediment layer covering the surface thins out and rock outcrops emerge. Beyond the limits of fossil deposits left and right of the creek, these outcrops form scarps and ridges accompanied by shallow gully erosions. Within the limits of fossil deposits and closer to the creek channel, the sediment layer has almost vanished and rock outcrops form numerous steep cliffs with potential rockfall detachments. These rockfall detachments are accompanied by a large amount of scree, which build a potential sediment source for debris flows and debris floods.

Starting approximately 400m upstream of the fan apex, multiple gullies and trenches lead into the creek bed of Cougar Creek, predominantly at an angle of 45° relative to the active stream and following the general orientation of the thrust belt. Therefore, the terrain is, to a certain degree, tectonically influenced. At the orographic right side of Cougar Creek, periglacial solifluction lobes were identified that are related to freeze-thaw activity and have been superimposed by ridges and gully erosion.

18.03 Kinematic Analysis

18.03.01 Methodology

A kinematic analysis was carried out for the creek slopes of Cougar Creek valley upstream of the proposed location of the debris flood retention structure.

Data from the discontinuity survey (Thurber Engineering Ltd., 2015a) and from borehole logs (Thurber Engineering Ltd., 2015b) were used for the kinematic analysis. The kinematic analysis output was plotted on stereonet using the software tool Dips version 7.004 stereographic projection analysis software, developed by Rocscience Inc.

The orientation data shows the symbolic pole plots of discontinuity types using the Equal Angle and Lower Hemisphere projection. Terzaghi Weighting was not applied to the contour plots. In the stereo plots the crescent shaped and red highlighted zones show the (primary) critical zones for planar or wedge sliding. The secondary critical zone for wedge sliding is highlighted in yellow (see Figure 200 and Figure 201).

The general orientation data of the creek slope sectors were derived from the existing digital terrain model. For this analysis, sectors with critical slope sectors steeper than 50° were considered.

Two potential failure modes – planar sliding and wedge sliding – were selected for the stability analysis. For both modes the symbolic pole plots of the discontinuity planes were combined with the major planes of the creek slopes for nine sectors in total. An estimated overall friction angle of 38 degrees for the local bedrock was superimposed for the analysis.

No lateral limits were used for planar sliding, meaning the planar sliding analysis considers the entire daylight envelope of each sector as a kinematic valid sliding zone.

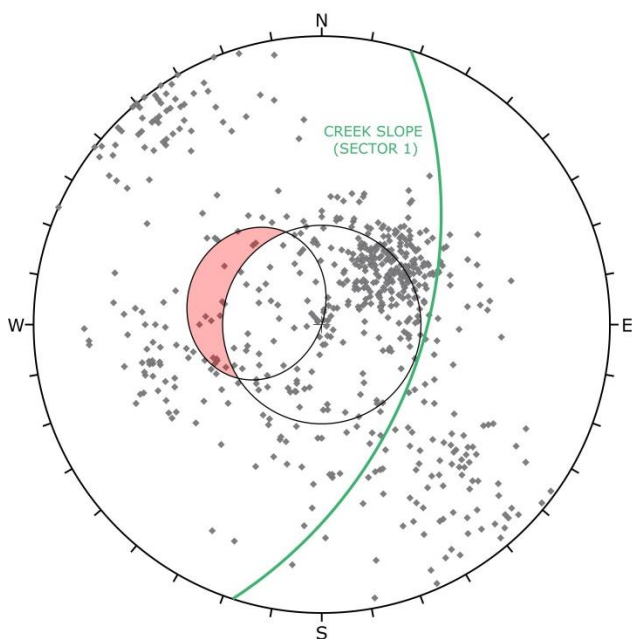


Figure 200: Example of the stereo plot with the critical zone for planar sliding (red)

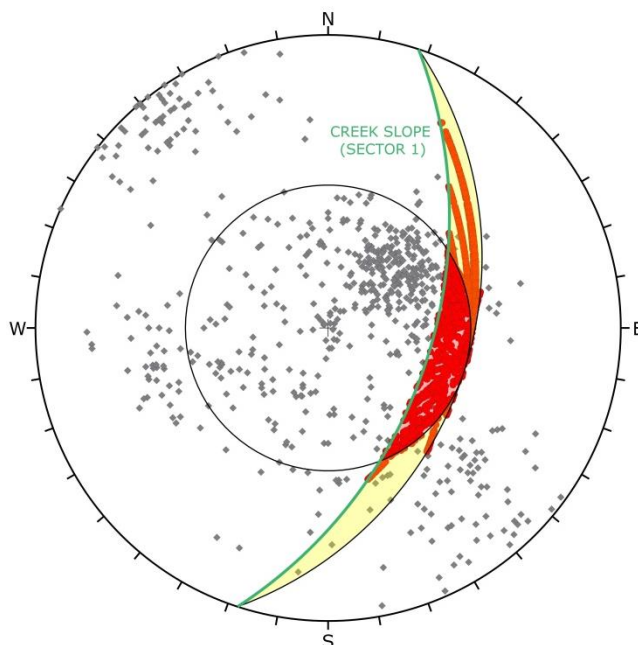


Figure 201: Example of the stereo plot with the primary (red) and secondary (yellow) critical zones for wedge sliding

18.03.02 Results and Assessment

The resulting probabilities of wedge and planar sliding according to the kinematic analysis are shown in Table 84 as well as in the corresponding drawings LTMM CC-CSSA-111 to LTMM CC-CSSA-117.

Table 84: Results from the Kinematic Analysis for Planar and Wedge Sliding (No. of Entries: 642)

	Sector						
	1	2	3	4	5	6	7
Probability of Planar Sliding [%]	2.18	3.89	4.83	2.96	6.70	6.85	2.49
Probability of Wedge Sliding [%]	0.98	2.26	3.01	1.60	4.75	5.92	1.58

The analysis shows that there is no significant risk for planar and/or wedge sliding of creek slopes for slope gradients equal to or greater than 50° within the retention basin.

The indication of planar sliding or wedge sliding does not necessarily mean that failure will occur, since factors other than kinematics and friction angle may work to increase stability (e.g. joint cohesion, joint persistence etc.).

18.04 Sliding Wedge Analysis

18.04.01 Methodology

A sliding wedge analysis was carried out using the software tool Swedge (version 6.012) by Rocscience Inc. for potentially relevant slopes identified by the kinematic analysis (see section 18.03). Swedge evaluates the geometry and stability of surface wedges in rock slopes that are defined by two intersecting discontinuity planes, the slope surface and a potential tension crack (see Figure 202) and subsequently calculates the factor of safety for each specific wedge.

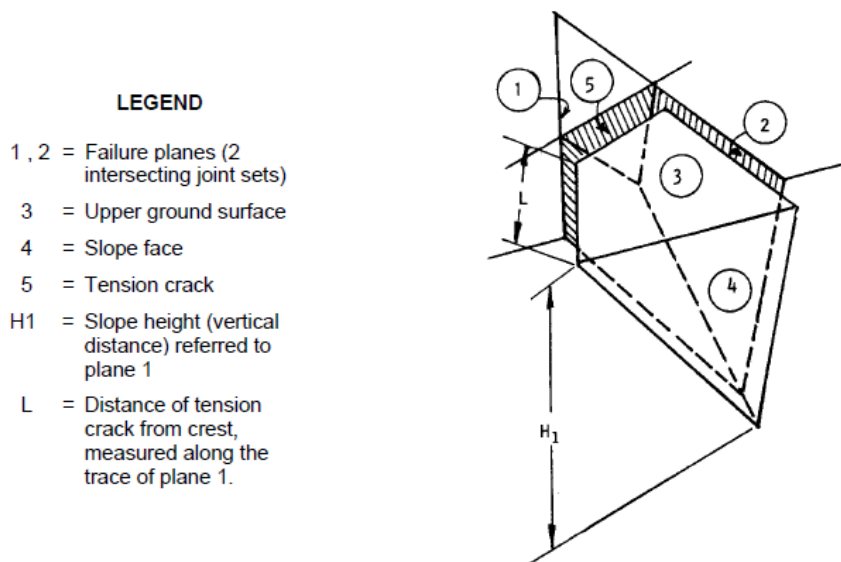


Figure 202: Typical wedge geometry for the Sliding Wedge analysis (Rocscience Inc., 2016)

For the analysis of potentially relevant sliding wedges of creek slopes within the retention basin of the Cougar Creek debris flood retention structure, data from the discontinuity survey (Thurber Engineering Ltd., 2015a) and from borehole logs (Thurber Engineering Ltd., 2015b) were used to identify discontinuities. The orientation of surface slopes (dip and dip direction) was derived from the available digital terrain model.

As a global input parameter, waviness, which accounts for undulations of a joint surface, was set to 2°. Shear strength was calculated using the Mohr-Coulomb model by assuming a cohesion of 2kN/m² and a friction angle of 35°. According to a photo documentation of creek slopes during a field survey by CHT in 2015, the bank height for potential wedges was set to 2m. Each wedge was analyzed for dry conditions, combined with a seismic coefficient factor for a 1/2,475 year return period earthquake, as well as for partially wet conditions, where 33% of rock fissures are filled with water, combined with a seismic coefficient factor for a 1/100 year return period earthquake.

Input data for the sliding wedge analysis is listed in Table 85.

Table 85: Input Data for Sliding Wedge Analysis

	Slope		Upper Face		Bank Height [m]	Waviness [°]	Cohesion [kN/m ²]	Friction Angle [°]	Soil Class
	Dip	Dip Dir	Dip	Dip Dir					
Sector 1	51	108	35	237	2	2	2	35	A
Sector 2	57	135							
Sector 3	61	135							
Sector 4	54	125							
Sector 5	61	313							
Sector 6	61	304							
Sector 7	50	328							
Sector 8	42	316							
Sector 9	41	139							

18.04.02 Results

Even by applying conservative values for the shear strength model (cohesion and friction value), only a single wedge indicates unstable conditions with a factor of safety smaller than 1. The calculations for all the other potentially relevant rock wedges resulted in factors of safety greater than 1, for both dry conditions as well as with partially water filled fissures. However, these results do not rule out potential detachments of local rock wedges. However, inside the retention basin area the size of potentially detaching wedges are limited with the height of beddings which is approximately 2m. The results of sliding wedge analysis are listed in Table 86 to Table 94. Graphics are shown in the corresponding drawings LTMM CC-CSSA-120 to LTMM CC-CSSA-128.

Table 86: Sliding Wedge Analysis and resulting Factor of Safety for Sector 1

	Joint 1		Joint 2		Water filled Fissures [%]	Seismic Coefficient	Volume [m ³]	Weight [kg]	Factor of Safety
	Dip	Dip Dir	Dip	Dip Dir					
Wedge 1-1	48	187	62	077	33	0.007 ($\pm 1/100$ yr)	0.099	263	2.8
					0	0.042 ($\pm 1/2,475$ yr)	0.099	263	2.7
Wedge 1-2	44	094	89	336	33	0.007 ($\pm 1/100$ yr)	0.024	65	3.9
					0	0.042 ($\pm 1/2,475$ yr)	0.024	65	3.8
Wedge 1-3	47	138	61	059	33	0.007 ($\pm 1/100$ yr)	0.081	215	2.4
					0	0.042 ($\pm 1/2,475$ yr)	0.081	215	2.3
Wedge 1-4	43	070	50	129	33	0.007 ($\pm 1/100$ yr)	0.442	1,121	1.8
					0	0.042 ($\pm 1/2,475$ yr)	0.442	1,121	1.7

Table 87: Sliding Wedge Analysis and resulting Factor of Safety for Sector 2

	Joint 1		Joint 2		Water filled Fissures [%]	Seismic Coefficient	Volume [m³]	Weight [kg]	Factor of Safety
	Dip	Dip Dir	Dip	Dip Dir					
Wedge 2-1	41	190	51	129	33	0.007 ($\pm 1/100\text{yr}$)	0.126	333	2.3
					0	0.042 ($\pm 1/2,475\text{yr}$)	0.126	333	2.2
Wedge 2-2	48	187	78	085	33	0.007 ($\pm 1/100\text{yr}$)	0.065	173	2.4
					0	0.042 ($\pm 1/2,475\text{yr}$)	0.065	173	2.4
Wedge 2-3	50	129	63	077	33	0.007 ($\pm 1/100\text{yr}$)	1.584	4,179	1.3
					0	0.042 ($\pm 1/2,475\text{yr}$)	1.584	4,179	1.2
Wedge 2-4	79	165	43	070	33	0.007 ($\pm 1/100\text{yr}$)	0.011	30	5.3
					0	0.042 ($\pm 1/2,475\text{yr}$)	0.011	30	5.1

Table 88: Sliding Wedge Analysis and resulting Factor of Safety for Sector 3

	Joint 1		Joint 2		Water filled Fissures [%]	Seismic Coefficient	Volume [m³]	Weight [kg]	Factor of Safety
	Dip	Dip Dir	Dip	Dip Dir					
Wedge 3-1	41	208	46	151	33	0.007 ($\pm 1/100\text{yr}$)	0.186	510	2.8
					0	0.042 ($\pm 1/2,475\text{yr}$)	0.186	510	2.6
Wedge 3-2	78	086	48	184	33	0.007 ($\pm 1/100\text{yr}$)	0.370	1,019	1.6
					0	0.042 ($\pm 1/2,475\text{yr}$)	0.370	1,019	1.5
Wedge 3-3	50	129	62	078	33	0.007 ($\pm 1/100\text{yr}$)	5.416	14,373	0.9
					0	0.042 ($\pm 1/2,475\text{yr}$)	5.416	14,373	0.8
Wedge 3-4	42	071	79	165	33	0.007 ($\pm 1/100\text{yr}$)	0.112	298	2.4
					0	0.042 ($\pm 1/2,475\text{yr}$)	0.112	298	2.3

Table 89: Sliding Wedge Analysis and resulting Factor of Safety for Sector 4

	Joint 1		Joint 2		Water filled Fissures [%]	Seismic Coefficient	Volume [m³]	Weight [kg]	Factor of Safety
	Dip	Dip Dir	Dip	Dip Dir					
Wedge 4-1	63	078	51	129	33	0.007 ($\pm 1/100\text{yr}$)	0.414	1,121	2.7

	Joint 1		Joint 2		Water filled Fissures [%]	Seismic Coefficient	Volume [m³]	Weight [kg]	Factor of Safety
	Dip	Dip Dir	Dip	Dip Dir					
					0	0.042 ($\pm 1/2, 475\text{yr}$)	0.414	1,121	2.6
Wedge 4-2	50	129	43	070	33	0.007 ($\pm 1/100\text{yr}$)	0.003	8	18.8
					0	0.042 ($\pm 1/2, 475\text{yr}$)	0.003	8	18.1
Wedge 4-3	47	190	64	094	33	0.007 ($\pm 1/100\text{yr}$)	0.072	192	2.6
					0	0.042 ($\pm 1/2, 475\text{yr}$)	0.072	192	2.5

Table 90: Sliding Wedge Analysis and resulting Factor of Safety for Sector 5

	Joint 1		Joint 2		Water filled Fissures [%]	Seismic Coefficient	Volume [m³]	Weight [kg]	Factor of Safety
	Dip	Dip Dir	Dip	Dip Dir					
Wedge 5-1	43	235	61	325	33	0.007 ($\pm 1/100\text{yr}$)	0.076	202	2.9
					0	0.042 ($\pm 1/2, 475\text{yr}$)	0.076	202	2.8
Wedge 5-2	55	356	60	265	33	0.007 ($\pm 1/100\text{yr}$)	0.780	2,039	1.3
					0	0.042 ($\pm 1/2, 475\text{yr}$)	0.780	2,039	1.3
Wedge 5-3	57	340	50	242	33	0.007 ($\pm 1/100\text{yr}$)	4.048	10,703	1.4
					0	0.042 ($\pm 1/2, 475\text{yr}$)	4.048	10,703	1.3
Wedge 5-4	63	073	48	325	33	0.007 ($\pm 1/100\text{yr}$)	0.120	318	1.8
					0	0.042 ($\pm 1/2, 475\text{yr}$)	0.120	318	1.8

Table 91: Sliding Wedge Analysis and resulting Factor of Safety for Sector 6

	Joint 1		Joint 2		Water filled Fissures [%]	Seismic Coefficient	Volume [m³]	Weight [kg]	Factor of Safety
	Dip	Dip Dir	Dip	Dip Dir					
Wedge 6-1	41	231	67	322	33	0.007 ($\pm 1/100\text{yr}$)	0.061	162	3.3
					0	0.042 ($\pm 1/2, 475\text{yr}$)	0.061	162	3.2
Wedge 6-2	57	340	48	246	33	0.007 ($\pm 1/100\text{yr}$)	4.822	12,742	1.3
					0	0.042 ($\pm 1/2, 475\text{yr}$)	4.822	12,742	1.3

	Joint 1		Joint 2		Water filled Fissures [%]	Seismic Coefficient	Volume [m³]	Weight [kg]	Factor of Safety
	Dip	Dip Dir	Dip	Dip Dir					
Wedge 6-3	46	020	70	067	33	0.007 ($\pm 1/100\text{yr}$)	0.006	16	8.1
					0	0.042 ($\pm 1/2,475\text{yr}$)	0.006	16	7.8
Wedge 6-4	59	256	55	357	33	0.007 ($\pm 1/100\text{yr}$)	0.221	612	1.8
					0	0.042 ($\pm 1/2,475\text{yr}$)	0.221	612	1.7

Table 92: Sliding Wedge Analysis and resulting Factor of Safety for Sector 7

	Joint 1		Joint 2		Water filled Fissures [%]	Seismic Coefficient	Volume [m³]	Weight [kg]	Factor of Safety
	Dip	Dip Dir	Dip	Dip Dir					
Wedge 7-1	59	256	55	356	33	0.007 ($\pm 1/100\text{yr}$)	0.035	92	3.4
					0	0.042 ($\pm 1/2,475\text{yr}$)	0.035	92	3.2
Wedge 7-2	43	360	47	296	33	0.007 ($\pm 1/100\text{yr}$)	1.396	3,670	1.5
					0	0.042 ($\pm 1/2,475\text{yr}$)	1.396	3,670	1.4
Wedge 7-3	63	073	45	335	33	0.007 ($\pm 1/100\text{yr}$)	0.047	124	3.7
					0	0.042 ($\pm 1/2,475\text{yr}$)	0.047	124	3.6
Wedge 7-4	47	332	54	238	33	0.007 ($\pm 1/100\text{yr}$)	6.279	16,616	1.5
					0	0.042 ($\pm 1/2,475\text{yr}$)	6.279	16,616	1.5

Table 93: Sliding Wedge Analysis and resulting Factor of Safety for Sector 8

	Joint 1		Joint 2		Water filled Fissures [%]	Seismic Coefficient	Volume [m³]	Weight [kg]	Factor of Safety
	Dip	Dip Dir	Dip	Dip Dir					
Wedge 8-1	50	253	56	356	33	0.007 ($\pm 1/100\text{yr}$)	0.007	19	7.3
					0	0.042 ($\pm 1/2,475\text{yr}$)	0.007	19	7.0
Wedge 8-2	42	347	61	262	33	0.007 ($\pm 1/100\text{yr}$)	0.024	64	4.7
					0	0.042 ($\pm 1/2,475\text{yr}$)	0.024	64	4.5
Wedge 8-3	43	360	43	305	33	0.007	0.025	66	6.5

	Joint 1		Joint 2		Water filled Fissures [%]	Seismic Coefficient	Volume [m³]	Weight [kg]	Factor of Safety
	Dip	Dip Dir	Dip	Dip Dir					
						($\cong 1/100\text{yr}$)			
					0	0.042 ($\cong 1/2,475\text{yr}$)	0.025	66	6.2

Table 94: Sliding Wedge Analysis and resulting Factor of Safety for Sector 9

	Joint 1		Joint 2		Water filled Fissures [%]	Seismic Coefficient	Volume [m³]	Weight [kg]	Factor of Safety
	Dip	Dip Dir	Dip	Dip Dir					
Wedge 9-1	48	187	63	078	33	0.007 ($\cong 1/100\text{yr}$)	0.012	31	6.0
					0	0.042 ($\cong 1/2,475\text{yr}$)	0.012	31	5.8
Wedge 9-2	58	067	40	141	33	0.007 ($\cong 1/100\text{yr}$)	0.487	1,325	6.3
					0	0.042 ($\cong 1/2,475\text{yr}$)	0.487	1,325	6.1

19 REFERENCES

- Alberta Environment and Sustainable Resource Development. (2015). *June 19-22, Storm Event*. Retrieved 09 09, 2015, from Precipitation Maps: http://environment.alberta.ca/forecasting/data/precipmaps/event_Jun19_22.PDF
- Alberta Transportation. (n.d.). *PMP Mapping Issues - Alberta*. Retrieved 09 10, 2015, from Hydrotechnical Documents: <http://www.transportation.alberta.ca/Content/doctype30/Production/pmpmapissu.pdf>
- ALPINFRA Consulting & Engineering GmbH. (2014). *Option Analysis, Mountain Creek Hazard Mitigation Measures, Design of Mitigation Measures Cougar Creek (Doc. No. 16494_REP03_R03_20141213)*.
- Association of Professional Engineers and Geoscientists of British Columbia (APEGBC). (2010). *Guidelines for Legislated Landslide Assessments for Proposed Residential Developments in British Columbia*.
- Beyer, W. (1964). *Zur bestimmung der Wasserdurchlässigkeit von Kiesen und Sanden aus der Kornverteilung [On the determination of hydraulic conductivity of gravels and sands from grain size distribution]*. *Wasserwirtschaft-Wassertechnik* 14, pp. 165-169.
- BGC Engineering Ltd. (2014, 2015). *Risk Reduction Optimization and Risk Reduction Optimization Phase 2*.
- BGC Engineering Ltd. (2013). *Cougar Creek, 2013 Forensic Analysis and Short-Term Debris Flood Mitigation (Doc. No. TC13-004)*.
- BGC Engineering Ltd. (2014a). *Cougar Creek Debris Flood Risk Assessment (Doc. No. TC14-001)*.
- BGC Engineering Ltd. (2014b). *Cougar Creek Debris Flood Hazard Assessment (Doc. No. TC13-010)*.
- BGC Engineering Ltd. (2014c). *Cougar Creek Forensic Analysis. Hydroclimatic Analysis of the June 2013 Storm (Doc. No. TC13-005)*.
- BGC Engineering Ltd. (2014c). *Cougar Creek Forensic Analysis. Hydroclimatic Analysis of the June 2013 Storm (Doc. No. TC13-005)*.
- Bray, J., & Travasarou, T. (2007). Simplified Procedure for Estimating Earthquake-Induced Deviatoric Slope Displacements. *Journal of Geotechnical and Geoenvironmental Engineering*, 133(4), pp. 381-392.
- Bureau of Reclamation & U.S. Army Corps of Engineers. (2012). *Best Practices in Dam and Levee Safety Risk Analysis*.
- Campbell, F. B., & Guyton, B. (1953). Air demand in Gated Conduits. *Proceedings of the 5th Congress on the International Association of Hydraulic Research*. Minneapolis.
- Campen, F. (2002). Modernisierung des Westharz-Talsperrensystems. Beispiel Sösetalsperre - Ersatz der Grundablässe. *Internationales Symposium; MODERNE METHODEN UND KONZEPTE IM WASSERBAU*. Zürich: ETH Zürich.
- Canadian Dam Association. (2013). *Dam Safety Guidelines 2007 (2013 Edition)*. Toronto: Canadian Dam Association.
- Carman, P. (1937). *Fluid flow through granular beds*. Transactions, Institution of Chemical Engineers, London, 15: 150-166.
- CDA. (2007). *Dam Safety Guidelines*. Canadian Dam Association.
- CDA. (2007). *Dam Safety Guidelines*. CDA, Canadian Dam Association.
- Century Wireline Services. (2015). *Borehole scan raw data*.
- CGS. (2006). *Canadian Foundation Engineering Manual and actual Errata*. The Canadian Geotechnical Society.

- CH2M Hill Engineering Ltd. (1994). *Cougar Creek Flood Risk Mapping Study (Doc. No. CGY\25182\999.R)*.
- Comité Nacional de Grandes Presas (SPANCOLD). (1997). *Guía Técnica de Grandes Presas n°5: Aliviaderos y Desagües, Anejo n°2 Aireación*.
- CSA. (2014). *A23.3-14 Design of Concrete Structures*. CSA Group.
- CSA. (2014). *S16-14 Design of Steel Structures*. CSA Group.
- CSA. (2014). *S6-14 Canadian Highway Bridge Design Code*. CSA Group.
- CSA. (2015). *S832-14 Seismic risk reduction of operational and functional components (OFCs) of buildings*. CSA Group.
- Dow Chemical Canada ULC. (2008). *Calculating Insulation Needs to fight Frost Heave by comparing Freezing Index and Frost Depth*. Calgary.
- Engineers, U. A. (2004). *General Design and Construction Considerations of Earth and Rock-Fill Dams*.
- Erbisti, P. (2004). *Design of Hydraulic Gates*. CRC Press.
- Federal Energy Regulatory Commission (FERC). (2006). *Engineering Guidelines for the Evaluation of Hydropower Projects*. Office of Hydropower Licensing.
- FEMA. (2011). *Filters for Embankment Dams. Best Practices for Design and Construction*. USA.
- Franke, P. (2001). *Dams in Germany. Deutsches Talsperrenkomitee, Verlag Glückauf GmbH*.
- Fredlund, D., & Radhardjo, H. (1993). *Soil Mechanics for Unsaturated Soils*. New York: John Wiley and Sons Ltd.
- Frizell, K. W. (2004). *Hydraulic Model Studies of Aeration Enhancements at the Folsom Dam Outlet Works: Reducing Cavitation Damage Potential*.
- Golder Associates . (2015a). *Preliminary results of laboratory test on soil samples*.
- Golder Associates. (2015b). *Report on triaxial compression test* .
- Gutiérrez Serret, R. M. (1995). *Aireación en las estructuras hidráulicas de las presas: aliviaderos y desagües profundos*. Universidad Politécnica de Madrid, Ingenieros de Caminos.
- Hazen, A. (1892). *Some Physical Properties of Sands and Gravels, with Special References to their Use in Filtration*. Annual Report, Massachusetts State Board of Health, Boston, pp.539-556.
- Hillel, D. (1982). *Introduction to Soil Physics*. Department of Plant and Soil Science, University of Massachusetts.
- Hynes-Griffin, M., & Franklin, A. (1984). *Rationalizing the Seismic Coefficient Method*. Vicksburg, MS: Miscellaneous Paper GL-84-13, United States Army Engineers, WES.
- ISL Engineering Ltd. (2013). *Cross Sections for Channel Bank Protection (Doc. No. 344 SO)*.
- Johnston, G. (1981). *Permafrost Engineerign, Design and Construction*. Associate Committee on Geotechnical Research, National Council of Canada, John Wiley & Sons, Toronto, New York, 540.
- Kalinske, A. A., & Robertson, J. M. (1943). Air entrainment in Closed Conduits Flow. *Transactions of the American Society of Civil Engineers*, 108, pp. 1435-1516.
- Kersten, M. (1949). *Thermal Properties of Soils*. University of Minnesota, Engineering Experiment Station, Bull. 28, 227.
- Kozeny, J. (1927). *Über kapillare Leitung des Wassers im Boden [On capillary flow of water in soil]*. Vienna: vol 136. Sitz Ber Akad Wiss Wien.

- Levin, L. (1965). Calcul Hydraulique des Conduits d'aeration des Vindages de Fond et Dispositifs Deversants. *La Houille Blanche*, 2.
- M. J. O'Connor & Associates Ltd. (1980). *Geotechnical Evaluation Proposed Canmore Residential Subdivision and Highway Commercial Area (Doc. No. 10-038)*.
- Makdisi, F., & Seed, H. (1978). *Simplified procedure for estimating dam and embankment earthquake-induced deformations*. Journal of Geotechnical and Environmental Engineering, ASCE, Vol 104, No 4 , pp 381-392.
- Makdisi, F., & Seed, H. (1978). *Simplified procedure for estimating dam and embankment earthquake-induced deformations*. Journal of Geotechnical and Environmental Engineering, ASCE, Vol 104, No 4 , pp 381-392.
- Melo, C., & Sharma, S. (2004). *Seismic Coefficients for Pseudostatic Slope Analysis*. Vancouver, B.C., Canada: 13th World Conference on Earthquake Engineering.
- Melo, C., & Sharma, S. (2004). *Seismic Coefficients for Pseudostatic Slope Analysis*. Vancouver, B.C., Canada: 13th World Conference on Earthquake Engineering.
- Ministry of Transportation and Infrastructure of British Columbia. (2012). *Geotechnical Design Specifications and Subdivisions*. Engineering Branch Publications, Geotechnical and Pavement Engineering Publications.
- Morgenstern, N., & Price, V. (1965). *The analysis of the stability of general slip surfaces*. Géotechnique, 15(1), 79-93.
- NRC. (2010). *National Building Code of Canada*. National Research Council of Canada, Canadian Commission on Building and Fire Codes.
- NRC. (2014). *Extreme Minimum Temperature Zones of Parts of Central and Western Canada*. Retrieved 06 30, 2016, from <http://www.planthardiness.gc.ca/>
- Oñate, E., Idelsohn, S. R., Celigueta, M. A., & Rossi, R. (2008). Advances in the particle finite element method for the analysis of fluid-multibody interaction and bed erosion in free surface flows. *Computer Methods in Applied Mechanics and Engineering*, 19-20, pp. 1777–1800.
- Osher, S., & Fedkiw, R. (2001). Level set methods: an overview in some recent results. *Journal of Computational Physics*, 169, pp. 463-502.
- Preissler, B. (2000). *Technische Hydromechanik. Band 1, 5. Auflage*. Wien: Verlag für Bauwesen.
- Reiter. (2014). *A revised crustal stress orientation database for Canada*. Tectonophysics.
- Rocscience Inc. (2016). *Swedge - 3D Surface Wedge Analysis for Slopes. Online Help*. Retrieved 06 13, 2016, from <https://www.rocscience.com/help/swedge/webhelp/Swedge.htm>
- Safavi, K., Zarrati, A. R., & Attari, J. (2008). Experimental Study of air demand in high head gated tunnels. *Proceedings of the Institution of Civil Engineers - Water Management*, 161(2), pp. 105-111.
- Salazar, F., Morán, R., Rossi, R., & Larese, A. (2011). Numerical modeling of the hydraulic performance of Oliana Dam spillway using Kratos. *XI Benchmark Workshop on Numerical Analysis of Dams*. Valencia (Spain), October 20-21.
- Sanger, F., & Sayles, F. (1978). *Thermal and Rheological Computations for Artificially Frozen Ground Construction*. Engineering Geology, Elsevier, Vol. 13, 311-337.
- Scheickl, M., Fieger, S., & Ribitsch, R. (2015, 11). Hochwasserschutz Lankowitzbach, eine multidisziplinäre

Herausforderung. *Journal for Torrent, Avalanche, Landslide and Rockfall*.

- Schober, W. (1987). Der Staudamm Bockhartsee. *Mitteilungen des Institutes für Bodenmechanik, Felsmechanik und Grundbau der Universität Innsbruck*.
- Seed, H. (1979). *Considerations in the earthquake-resistant design of earth and rockfill dams*. Geotechnique, Vol 29, No 3, p 215-263.
- Seed, H. (1979). *Considerations in the earthquake-resistant design of earth and rockfill dams*. Geotechnique, Vol 29, No 3, p 215-263.
- Sharma. (1976).
- Sharma, H. R. (1976). Air-Entrainment in High Head Gated Conduits. *Journal of the Hydraulics Division*, 102(11), pp. 1629-1646.
- Sherard, J. L., & Dunnigan, L. P. (1985). *Filters and Leakage Control in Embankment Dams*.
- Sofistik. (2014). *HYDRA Manual, Seepage and Thermal Analysis with Finite Elements*. Sofistik AG.
- Sofistik. (2014). *TALPA Manual, 2D Finite Elements in Geotechnical Engineering*. Sofistik AG.
- Spencer, E. (1967). *A method of analysis of the stability of embankments assuming parallel interslice forces*. Géotechnique, 17(1), 11-26.
- Terzaghi, K. (1922). *Der Grundbruch an Stauwerken und seine Verhütung. (The failure of dams by piping and its prevention.)*. Die Wasserkraft, Vol 17, 445-449.
- Terzaghi, K., & Peck, R. (1964). *Soil Mechanics in Engineering Practice*. New York: Wiley.
- Thurber Engineering Ltd. (2014a). *Cougar Creek Long Term Debris Flood Mitigation, Initial Geotechnical Field Investigation (Doc. No. 19-598-440A)*.
- Thurber Engineering Ltd. (2014b). *Cougar Creek Long Term Debris Flood Mitigation, Geotechnical Investigation for Phase 1 Option Analysis (Doc. No. 19-598-440)*.
- Thurber Engineering Ltd. (2015a). *Cougar Creek Long Term Mitigation Project Phase 2A Geotechnical Investigation (Doc. No. 19-598-440B)*.
- Thurber Engineering Ltd. (2015a). *Cougar Creek Long Term Mitigation Project Phase 2A Geotechnical Investigation (Doc. No. 19-598-440B)*.
- Thurber Engineering Ltd. (2015b). *Cougar Creek Long Term Debris Flood Mitigation Project. Phase 2B Geotechnical Investigation*.
- Town of Canmore. (2015). *Option Analysis Summary Report, Cougar Creek Long Term Mitigation* .
- U.S. Army Corps of Engineers. (1964). Hydraulic Design Criteria, Air Demand, Regulated Outlet Works. *Sheet 050-1*.
- USBR. (1987). *Design of Small Dams*. United States Department of the Interior, Bureau of Reclamation.
- Vetsch, D., Siviglia, A., Ehrbar, D., Facchini, M., Gerber, M., Kammerer, S., . . . Faeh, R. (2015). *System Manuals of BASEMENT, Version 2.5*. Laboratory of Hydraulics, Glaciology and Hydrology (VAW). ETH Zürich.
- Vischer. (1993). *Wasserbau Hydrologische Grundlagen*. Springer Verlag.
- Vukovic, M., & Soro, A. (1992). *Determination of Hydraulic Conductivity of Porous Media from Grain-Size Compositions*. Littleton Colorado: Water Resources Publications.
- Waterline Resources Inc. (2015). *Cougar Creek Debris Flood Mitigation - Production Well Testing Program*

Results. Technical Memorandum.